# UNCLASSIFIED

| AD NUMBER |
|---|
| AD378805 |

| CLASSIFICATION CHANGES |
|---|

TO:          unclassified

FROM:          confidential

| LIMITATION CHANGES |
|---|

TO:

Approved for public release, distribution
unlimited

FROM:

Distribution authorized to U.S. Gov't.
agencies and their contractors; Critical
Technology; DEC 1966. Other requests shall
be referred to US Air Force Rocket
Propulsion Laboratory, Attn: RPPR-STINFO,
Edwards AFB, CA 93523.

| AUTHORITY |
|---|

31 Dec 1972, per document marking; AFRPL
ltr 7 May 1973

# THIS PAGE IS UNCLASSIFIED

# GENERAL DECLASSIFICATION SCHEDULE

## IN ACCORDANCE WITH
### DOD 5200.1-R & EXECUTIVE ORDER 11652

# THIS DOCUMENT IS:

Subject to General Declassification Schedule of

Executive Order 11652-Automatically Downgraded at

2 Years Intervals. DECLASSIFIED ON DECEMBER 31, 1972

## BY
Defense Documentation Center
Defense Supply Agency
Cameron Station
Alexandria, Virginia 22314

# SECURITY

# MARKING

The classified or limited status of this report applies
to each page, unless otherwise marked.
Separate page printouts MUST be marked accordingly.

(Unclassified Title)

# DEVELOPMENT AND TEST
# OF HIGH ENERGY
# SOLID PROPELLANTS

FINAL TECHNICAL REPORT, APRIL 1966

DECEMBER 1966

## HERCULES INCORPORATED
### BACCHUS WORKS      MAGNA, UTAH

AIR FORCE ROCKET PROPULSION LABORATORY
RESEARCH AND TECHNOLOGY DIVISION
AIR FORCE SYSTEMS COMMAND

# CONFIDENTIAL

(Unclassified Title)

DEVELOPMENT AND TEST OF
HIGH ENERGY SOLID PROPELLANTS

FINAL TECHNICAL REPORT

December 1966

HERCULES INCORPORATED
BACCHUS WORKS, MAGNA, UTAH

In addition to security requirements which must be met,
this document is subject to special export controls and
each transmittal to foreign governments or foreign
nationals may be made only with prior approval of
AFRPL (RPPR-STINFO), Edwards, Calif 93523.

AIR FORCE ROCKET PROPULSION LABORATORY
RESEARCH AND TECHNOLOGY DIVISION
AIR FORCE SYSTEMS COMMAND
UNITED STATES AIR FORCE
EDWARDS, CALIFORNIA

# CONFIDENTIAL

# CONFIDENTIAL

# CONFIDENTIAL

## FOREWORD

This is the final report under Contract AF 04(611)-10754. This report was prepared by the Propellant Development Group, Bacchus Works, Chemical Propulsion Division, Hercules Incorporated. The report was written by R. F. Keller with contributions by J. L. Judkins (Ballistic Testing), G. R. Gibson (Laboratory Formulation), and J. M. Trowell (Laboratory Analytical Support). Major contributions were also made by Dr. B. Brown, Dr. K. P. McCarty, and J. W. Schowengerdt in analyzing the impulse efficiency losses associated with beryllium and LMH-2 propellants and by J. W. Schowengerdt in formulation design. The AP and wax LMH-2 posttreatments were initially developed by Dr. H. C. Dehm and D. F. Mellow under an IR&D program. This report was approved by Dr. K. P. McCarty and Dr. R. L. Schaefer.

Preparation of this report is authorized under Contract AF 04(611)-10754, in accordance with line item 6 of "Contractor Data Requirement List," Form DD 1423. The report is classified confidential to protect a compilation of information, or a complete analysis of the subject, from individually unclassified items of information.

The cognizant Air Force Officers are F. W. Joffs and R. Miller, First Lieutenants, RPMCP, Edwards Air Force Base, California.

ii

# CONFIDENTIAL

## CONFIDENTIAL ABSTRACT

The objective of this contract was to conduct theoretical and experimental investigations resulting in the demonstration of beryllium hydride (LMH-2) solid propellants delivering in excess of 280 lbf-sec/lbm at standard conditions. The program consisted of three tasks: Task I, Analysis and Data Correlation; Task II, Formulation and Ballistic Evaluation; and Task III, Advanced Concepts.

LMH-2 fueled, double-base propellants having theoretical specific impulse values up to 314 lbf-sec/lbm were developed. LMH-2 loadings as high as 19 percent were achieved at 60 percent total volume solids loadings. These propellants gave delivered specific impulse values in 15-pound-charge (15PC) motors in the range of 280 to 282 lbf-sec/lbm; the first demonstration of the original ARPA Project PRINCIPIA goal. The developed propellants were characterized for sensitivity, thermal stability, processibility, mechanical properties, and explosive classification. Satisfactory processing characteristics were obtained by using surface treatments and grinding to improve bulk density of LMH-2.

Seventy beryllium (Be) and thirty-five LMH-2 15PC motors were fired to develop efficiency correlations based on motor and propellant parameters. The efficiency of Be propellants was found strongly dependent on flame temperature and, to a lesser extent, oxidation ratio. For LMH-2 propellants, flame temperature, oxidation ratio, and motor residence time were controlling factors. Efficiency losses for LMH-2 propellants were related to surface agglomeration of unburned Be. A limited amount of testing indicated a fluorine-rich environment is beneficial for LMH-2 combustion.

# CONFIDENTIAL

# TABLE OF CONTENTS

## LIST OF FIGURES

## LIST OF FIGURES (Cont)

LIST OF FIGURES (Cont)

LIST OF FIGURES (Cont)

# LIST OF TABLES

xi

LIST OF TABLES (Cont)

## LIST OF ABBREVIATIONS

| Abbreviation | Meaning |
| --- | --- |
| 2-NDPA | 2-Nitrodiphenylamine |
| 5PC | 5-pound charge |
| 15PC | 15-pound charge |
| AL | Aluminum |
| AN | Ammonium nitrate |
| AP | Ammonium perchlorate |
| Be | Beryllium |
| BeO | Beryllium oxide |
| C5A | Pentyl fluoroalkyl acrylate |
| C7A | Fluorinated acrylate adhesive |
| C7M | Fluorinated acrylate adhesive |
| C9M | Nonylfluoroalkyl methacrylate |
| CMDB | Composite modified double-base |
| DTA | Differential thermal analysis |
| ESD | Electrostatic discharge |
| FAAV | 20 C7A, 60 C7M, 20 viton |
| FAV | 23 C5A, 67 C9M, 10 viton |
| FPC | 40-pound charge |
| HC | Polybutadiene type rubber (Thiokol) |
| HDP | Hydrazine diperchlorate |
| Hg | Mercury |
| HMX | Cyclotetramethylene tetranitramine |
| JANAF | Joint Army, Navy, Air Force |
| K | Kelvin |

LIST OF ABBREVIATIONS (Cont)

| Abbreviation | Meaning |
|---|---|
| LI | Lithium |
| LIP | Lithium perchlorate |
| LMH-2 | Beryllium hydride |
| MG | Magnesium |
| NFPA | 1, 2-bis (Difluoramino) propyl acetate |
| NG | Nitroglycerin |
| NP | Nitronium perchlorate |
| PNC | Plastisol nitrocellulose |
| P-K-r | Pressure-K-burning rate |
| RES | Resorcinol |
| SI | Silicon |
| TA | Triacetin |
| TAGN, TAGNO$_3$ | Triaminoguanidine nitrate |
| TAZ | Triaminoguanidine azide |
| TDI | Toluene diisocyanate |
| TFLN | Teflon |
| TVOPA | Hexakis (Difluoramino) vinoxy propane |
| VCP | Be/HMX propellant formulation |
| VITON | Viton rubber |
| ZR | Zirconium |

## SECTION I

## INTRODUCTION

### A. OBJECTIVE

Solid propellants containing beryllium hydride (LMH-2) have a theoretical specific impulse (Isp) up to 30 sec greater than that of Be-fueled propellants. In the past, firings of test motors containing LMH-2 propellants had not yielded the expected gain in delivered specific impulse. Motor and propellant parameters of chamber temperature, chamber pressure, mass-flow rate, expansion ratio, oxidation ratio, oxidizer particle size, hydride content, metal/hydride ratio, and total metal content were investigated under various government contracts. Although much was learned about LMH-2 propellants during this period, the high Isp promised by the hydride was still not realized.

The objective of this program was to conduct theoretical and experimental investigations resulting in the demonstration of LMH-2 solid propellant delivering an Isp in excess of 280 lb-sec/lb at standard conditions, and thus significantly advance the performance levels obtained from LMH-2 propellants.

### B. SCOPE

The program is a three task effort. In Task I, the results of previous Be and LMH-2 firings were correlated to define the parameters important for higher delivered impulses. The results of this effort were applied in Task II to formulate and test candidate high-performance propellant systems. In Task III advanced formulation techniques were studied to improve LMH-2 combustion.

## SECTION II

### TASK I - ANALYSIS AND DATA CORRELATION

#### A.  SCOPE

The objective of this task was to evaluate and correlate available Be and LMH-2 motor firing data. Particular emphasis was placed on the correlation of motor efficiency with motor and formulation variables. Theoretical Isp calculations were conducted on a wide variety of formulations to establish the relationship between propellant parameters and theoretical performance of Be and LMH-2 propellants. Based on the correlations and theoretical performance calculations, formulations were designed which were predicted to deliver Isp values capable of meeting the program objectives. Six candidate LMH-2 formulations were selected for motor evaluation. In addition to the advanced formulation effort, Be formulations were investigated to confirm the validity of the developed correlations and, where necessary, to extend their useful range. In particular, the performance of Be systems containing high metal levels equivalent to those of LMH-2 propellants having high theoretical performance potential were investigated. These results were combined with earlier correlations and those obtained on concurrent related programs to allow accurate predictions to be made for Be and LMH-2 propellants and to gain some insight into the possible causes of performance losses.

#### B.  INITIAL DATA CORRELATIONS

The following discussion describes the data analysis and correlations developed from a review of the available Be and LMH-2 motor data at the start of this program.

The basic assumption was made that LMH-2 decomposes to the parent metal at temperatures of approximately 300° C.[1] With this assumption, the factors affecting impulse efficiency of Be propellants become important for LMH-2 propellants for determining expected LMH-2 performance levels. As a consequence, a large amount of effort was expended establishing correlations for Be propellants. However, it has been suggested by various workers[2] that as LMH-2 decomposes, a cloud of hydrogen surrounds the metal particle, suppressing final conversion to the oxide. Thus, some basic differences in the correlations between Be and LMH-2 can be expected. To gain possible insight into the performance of metallized propellants in general, a limited comparison was made between Be and Al efficiencies.

The following parameters were considered of prime importance in defining the performance efficiency of Be and LMH-2 propellants:

(1)  Motor parameters

(a)  Chamber pressure

---

[1,2]Refer to List of References

        (b)  Characteristic length (L*)

        (c)  Mass flow rate

        (d)  Expansion ratio

        (e)  Nozzle geometry

    (2)  Propellant parameters

        (a)  Chamber temperature

        (b)  LMH-2 content and particle size

        (c)  Total Be metal content

        (d)  Oxidation ratio $\dfrac{\text{Moles O}}{\text{Moles C + moles metal}}$

        (e)  Oxidizer particle size

        (f)  Binder type

        (g)  Oxygen source

A literature survey was conducted to accumulate data from recent major propellant contracts on all of the above listed parameters. Since performance data was obtained by the various contractors over a wide range of test conditions and motor configurations, initial emphasis was placed on developing scaling curves for each propellant. This allowed comparison on a common motor basis for evaluation of propellant parameters and determination of the effect of propellant parameters on motor scaling. In addition, theoretical performance calculations were performed on the Bacchus Free Energy Program for all propellants used in the final correlations. This eliminated differences in theoretical calculations among contractors and allowed for updating of JANAF thermochemical data.

All Isp efficiencies, unless otherwise stated, were calculated by dividing the delivered impulse by the theoretical equilibrium flow impulse, calculated at the actual chamber pressure and expansion half angle. All reported $\text{Isp}\vert_{1000}^{15}$ values were calculated by multiplying the theoretical impulse at standard conditions by the efficiency determined at the actual firing conditions.

## 1. Motor Parameters

The majority of data on the motor efficiency of Be propellants has been obtained under Air Force contracts. The Air Force programs performed by Atlantic Research Corporation, Aerojet-General Corporation, Thiokol Chemical Corporation, and Hercules Incorporated were reviewed. Priority for selection of propellants for correlations was given to those

propellants which had been tested at a wide variety of motor conditions and, preferably, in motors of propellant weight greater than 30 lb. Only those propellants for which the final performance could be reasonably predicted at large motor conditions were used in the final correlations. Table I contains a summary of the propellants selected for the final correlations.

Figure 1 shows the effect of mass-flow rate for 5-, 15-, 40-, and 400-lb motors containing Be-fueled VCP propellant and is typical of the motor scaling curve found for efficient Al and Be propellants. Figure 1 also shows effeciency as a function of chamber pressure for 15-, 40-, and 400-lb motors and indicates no loss in efficiency down to 400 psia. Atlantic Research has also shown scaling curves for various Be propellants as presented in Figure 2. A strong dependence of mass-flow rate on efficiency for each motor size is also indicated in this figure. This phenomenon may be explained by considering scaling equations such as those developed by Rohm and Haas, where for constant heat flux, thermal efficiency, and mass-flow rate, heat losses are proportional to the internal area exposed. Decreased particle lag with the larger nozzles used at high-mass flow is probably also important.

For the Hercules 40-lb charge (FTC) motor, the Rohm and Haas scaling equation predicts an insignificant loss in efficiency for mass-flow rates in the 5- to 10-lb/sec region. Data obtained from four Hercules propellants are plotted in Figure 3. These data show a significant loss in efficiency when the mass-flow rate is decreased from 10 lb/sec to 5 lb/ sec for two of the propellants, whereas no loss in efficiency is shown for the other two. The primary difference between the two pair of propellants is a significantly higher oxidation ratio for the group showing no efficiency loss with decreasing chamber pressure for the lower-oxidation-ratio propellants. The decrease in efficiency for the lower-oxidation-ratio curve is characteristic of that reported by other contractors for losses in efficiency with decreasing pressure. One possible explanation for this efficiency loss is insufficient residence time for combustion with propellants containing little excess oxygen. This possibility is illustrated in Figure 4, where efficiency is plotted as a function of residence time in terms of the characteristic chamber length (L*). This figure shows that L* correlates as well with efficiency as chamber pressure. Unfortunately, the two effects cannot be separated.

Figures 5 through 7 illustrate pressure and scaling effects on efficiency for several Atlantic Research propellants. Of particular interest are Figures 5 and 6, which show the effect of pressure on efficiency for Arcocel propellants 319 and 191 where mass-flow rate was kept essentially constant (keyed points). Little pressure effect on efficiency was observed; however, the constant mass-flow rate was maintained at low pressure by a considerable increase in L*. The increased L* values may explain the lack of efficiency loss with decreasing pressure. Figure 7 shows pressure and mass-flow effects on efficiency for Arcocel 333E. A sharp decrease in efficiency for both decreasing mass-flow rate and pressure was observed in 50-lb motors.

4

## TABLE I

### SUMMARY OF PROPELLANTS SELECTED FOR FINAL
### EFFICIENCY CORRELATIONS

| Designation | Company* | Type Formulation** | Binder Level (Wt %) | AP (Wt %) | HMX (Wt %) | Bu (Wt %) | Al (Wt %) | Other (Wt %) | $I_{sp}$ 1000/14.7 A | $I_{sp}$ 1000/14.7 B | $T_c$ (°R) A | $T_c$ (°R) B | Oxidation Ratio A | Oxidation Ratio B |
|---|---|---|---|---|---|---|---|---|---|---|---|---|---|---|
| VTP | HPC | DB | 52 | 9 | 29 | 10 | -- | -- | -- | 283.0 | -- | 3835 | -- | 1.210 |
| VOR | HPC | DB | 63.6 | 5.9 | 17.5 | 13 | -- | -- | -- | 283.9 | -- | 3895 | -- | 1.060 |
| VHE | HPC | DB | 63.6 | 7.4 | 17.0 | 12 | -- | -- | -- | 283.0 | -- | 3870 | -- | 1.10 |
| VHH | HPC | DB | 63.6 | 5.9 | 20.5 | 10 | -- | -- | -- | 281.8 | -- | 3773 | -- | 1.100 |
| VHC | HPC | DB | 32.0 | -- | 54.0 | 8 | -- | -- | -- | 285.4 | -- | 3783 | -- | 1.170 |
| VOG | HPC | DB | 48.0 | 20.5 | -- | 12 | -- | 19.5 (TAE) | -- | 291.2 | -- | 3874 | -- | 1.02 |
| EJC | HPC | DB | 51.0 | 5.0 | 26.0 | -- | 18.0 | -- | -- | 278.4 | -- | 3285 | -- | 1.19 |
| 317 | ARC | DB | 60.0 | -- | 27.0 | 13.0 | -- | -- | 281.2 | 283.1 | 3637 | 3767 | 1.067 | 1.067 |
| 319M | ARC | DB | 50.0 | 12.3 | 26.2 | 11.5 | -- | -- | 286.4 | 286.6 | 3369 | 3649 | 1.02 | 1.02 |
| 191 | ARC | DB | 50.0 | 36.0 | -- | 14.0 | -- | -- | 280.1 | 281.2 | 3702 | 3852 | 1.08 | 1.008 |
| 333M | ARC | DB | 65.0 | 22.0 | -- | 13.0 | -- | -- | 281.9 | 283.0 | 3599 | 3659 | 1.080 | 1.086 |
| 365 | ARC | DB | 42.29 | 26.36 | -- | 11.55 | -- | 19.80 (TAE) | 289.1 | 290.2 | 3481 | 3131 | 1.08 | 0.998 |
| ANP-2991-ModlA | AGC | HPU | 26.0 | 60.0 | -- | 14.0 | -- | -- | 280.5 | 283.2 | 3459 | 3646 | 1.030 | 1.007 |
| ANB-3212 | AGC | CTPB | 13.0 | 72.5 | -- | 14.5 | -- | -- | 284.5 | 285.2 | -- | 3842 | -- | 0.988 |
| XP-93 | AGC | CTPB | 15.0 | 72.0 | -- | 13.0 | -- | -- | 285.6 | 286.1 | -- | 3462 | -- | 0.992 |
| XP-96 | AGC | CTPB | 13.0 | 74.0 | -- | 13.0 | -- | -- | 284.0 | 283.1 | -- | 3129 | -- | 1.08 |
| XP-112 | AGC | CTPB | 14.0 | 73.0 | -- | 13.0 | -- | -- | 284.9 | 283.8 | -- | 3569 | -- | 1.006 |
| TP-H-3108 | TCC | CTPB | 14.0 | 74.0 | -- | 12.0 | -- | -- | 282.1 | 282.0 | 3566 | 3341 | 1.10 | 1.000 |
| 532 | ARC | PU | -- | -- | -- | -- | -- | -- | 282.5 | -- | 3457 | -- | 1.00 | -- |
| 2AE | AGC | PU | -- | -- | -- | -- | -- | -- | 279.1 | -- | 3383 | -- | 1.20 | -- |

*Company:
  HPC - Hercules Powder Company
  ARC - Atlantic Research Corporation
  TCC - Thiokol Chemical Corporation
  AGC - Aerojet-General Corporation

**Type Formulation:
  DB  = Double Base
  HPU = Nitroplasticized Polyurethane
  CTPB = Carboxyterminated Polybutadiene
  PU  = Polyurethane

A - Reported by Contractor
B - Hercules Calculations
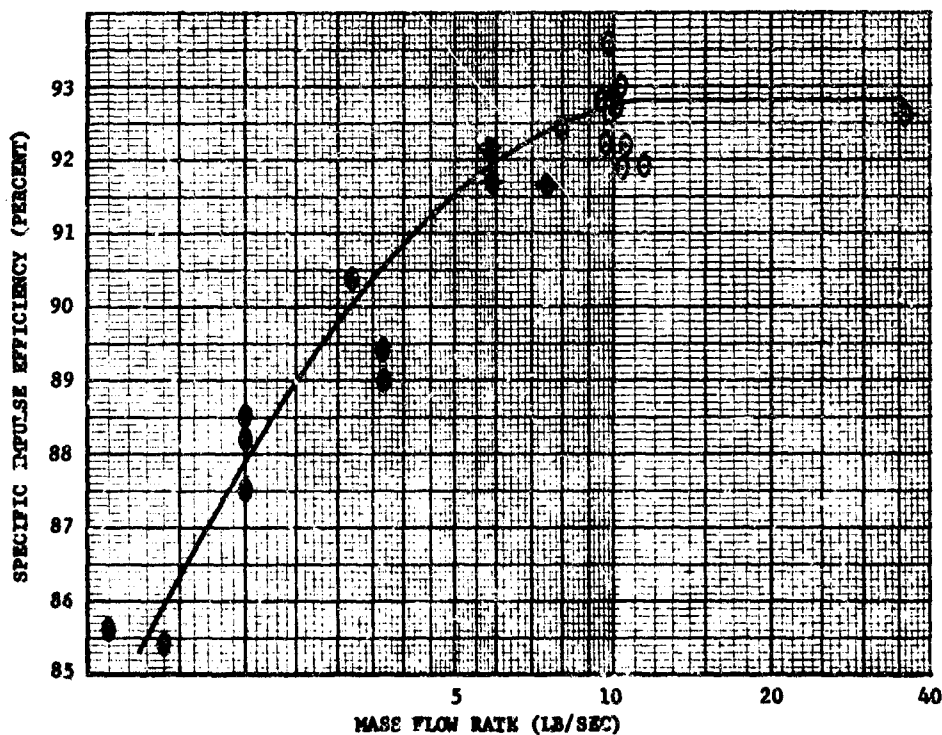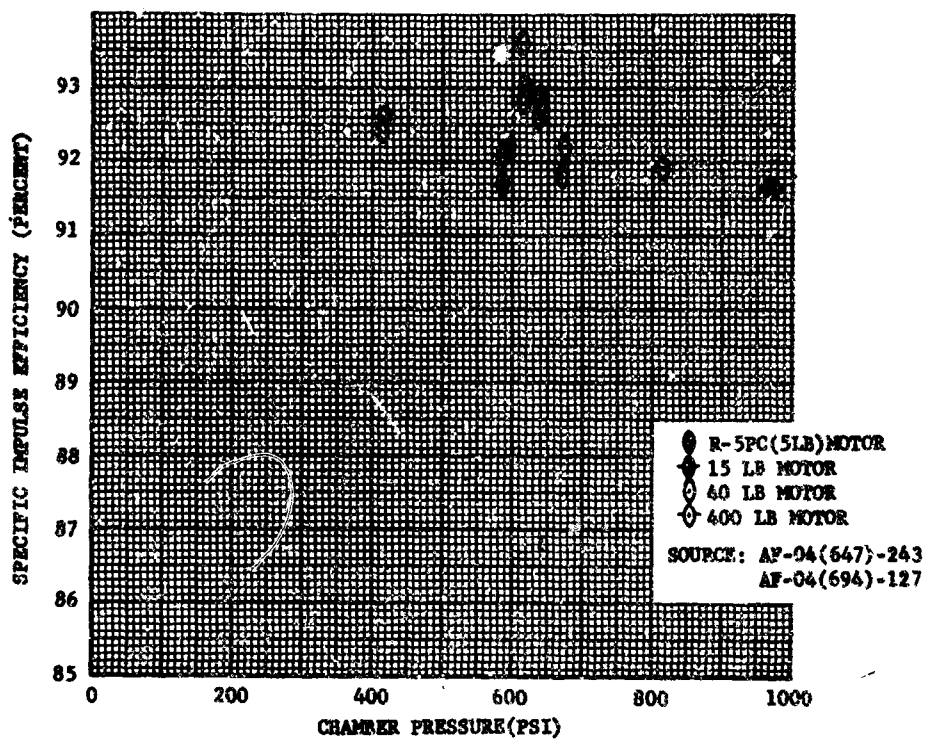
Figure 1. Effect of Chamber Pressure and Mass-Flow Rate on Specific Impulse Efficiency of VCP

6
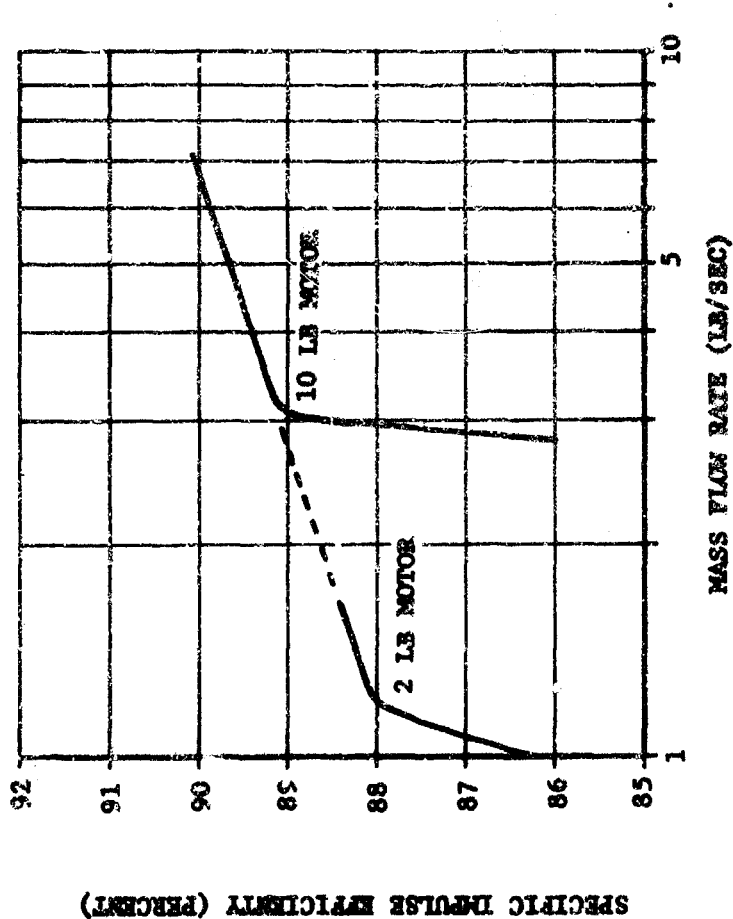
Figure 2. Effect of Mass-Flow Rate on Specific Impulse Efficiency for Four Atlantic Research Corporation Propellants
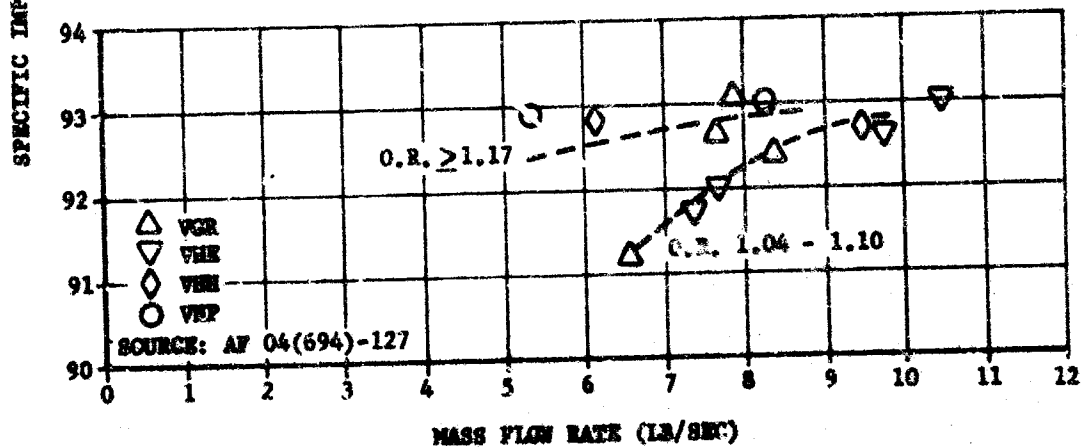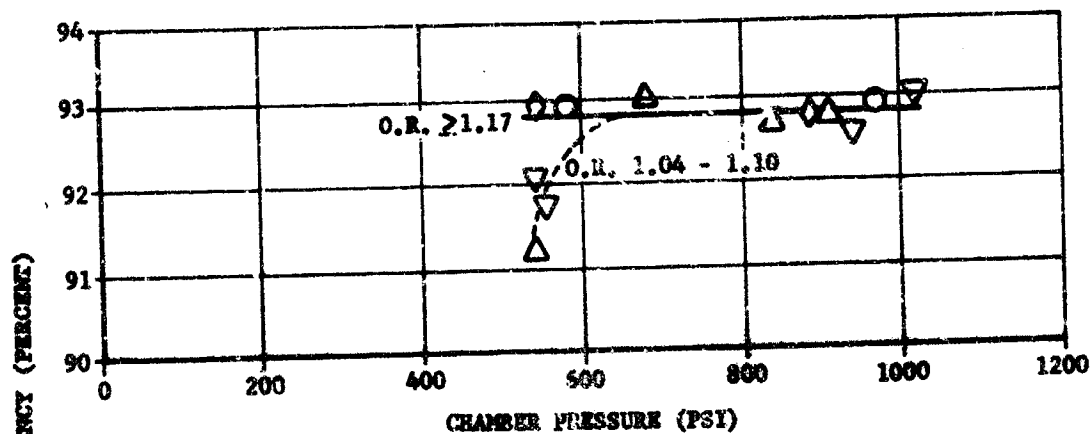
Figure 3. Effect of Chamber Pressure and Mass-Flow Rate on Specific Impulse Efficiency for Four Hercules Be Propellants

8
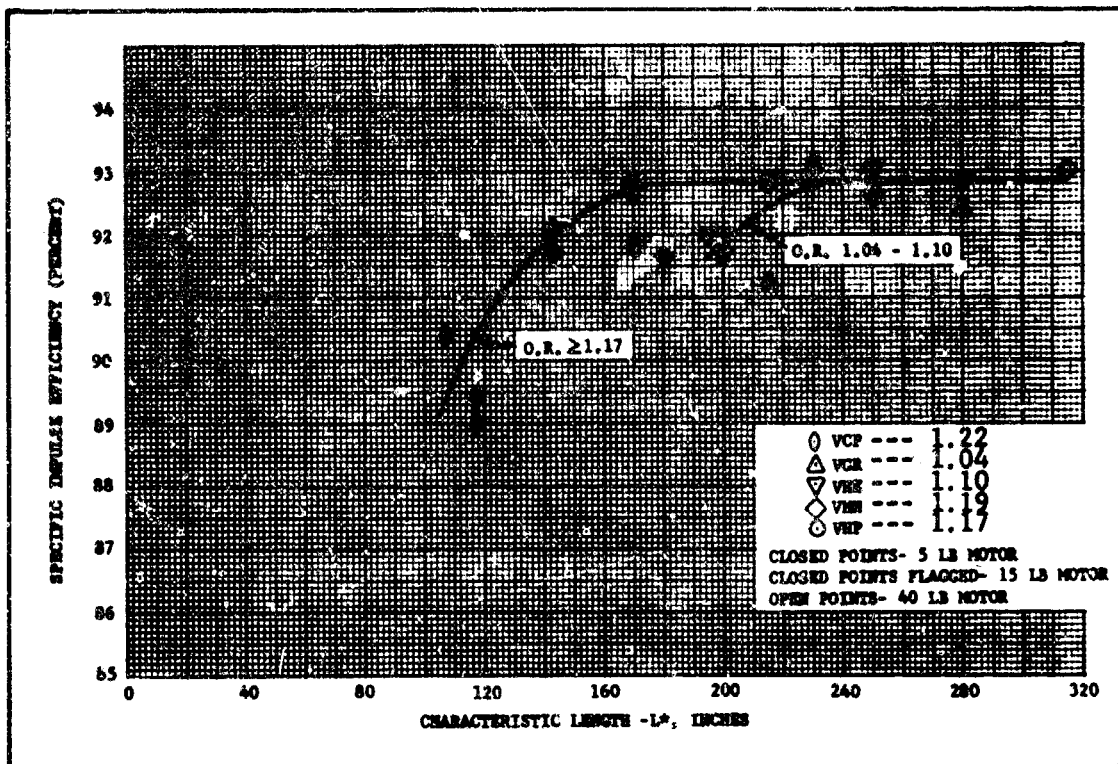
Figure 4. Effect of L* on Specific Impulse Efficiency for
Five Hercules Be Propellants

Figures 8 and 9 show a comparison of Be propellants on the basis of mass-flow rate and L*. The following trends appear:

(a) Beryllium propellants with high flame temperatures (>3700° K) and high oxidation ratios show the highest impulse efficiencies.

(b) Beryllium propellants showing no L* effect above 200 for a given motor also show no pressure effect on impulse efficiency.

(c) Beryllium propellants with low flame temperatures and low oxidation ratios require large L* values and high mass-flow rates to approach good impulse efficiencies.
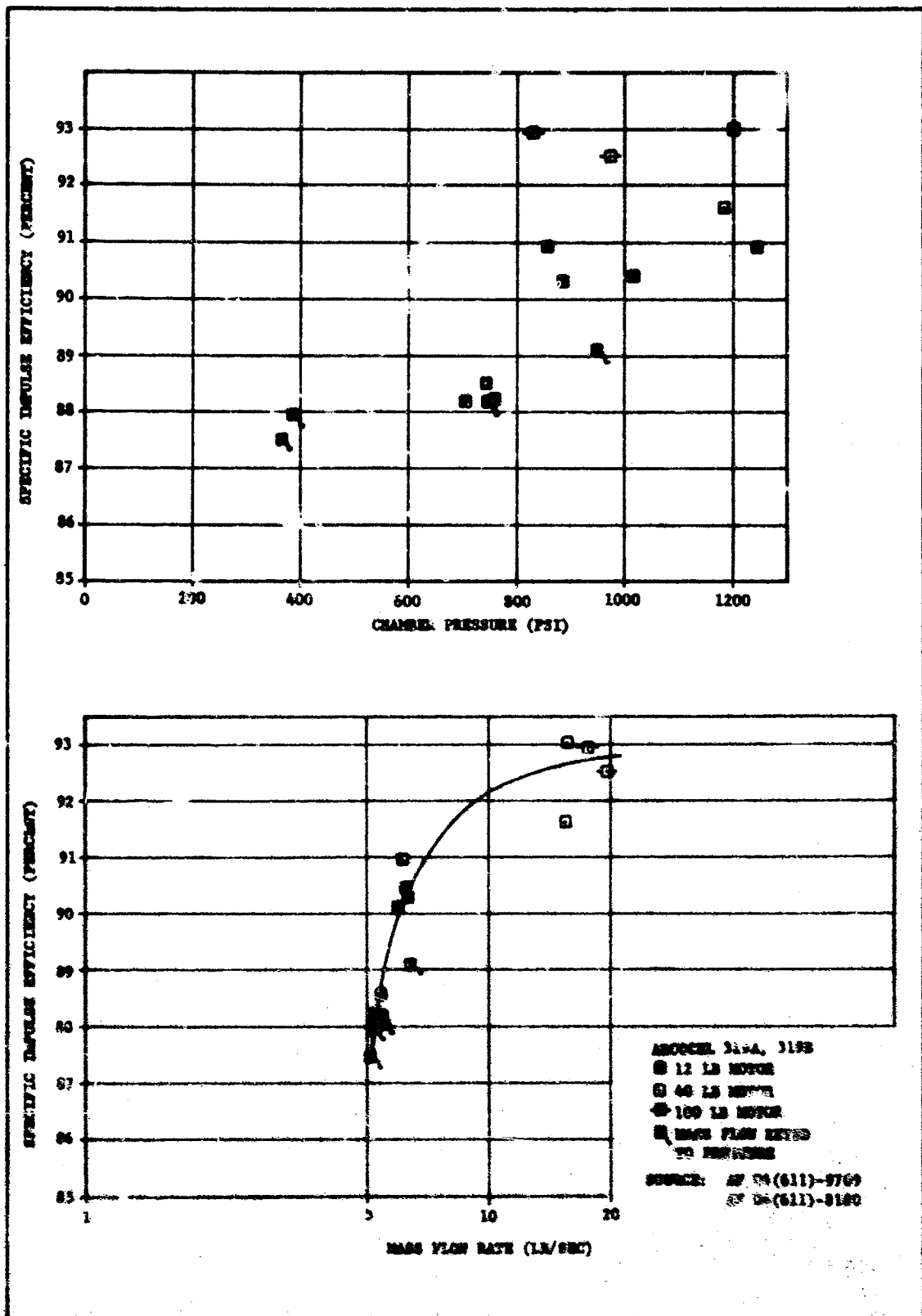
Figure 5. Effect of Chamber Pressure and Mass-Flow Rate on Specific Impulse Efficiency of Arcocel 319

10
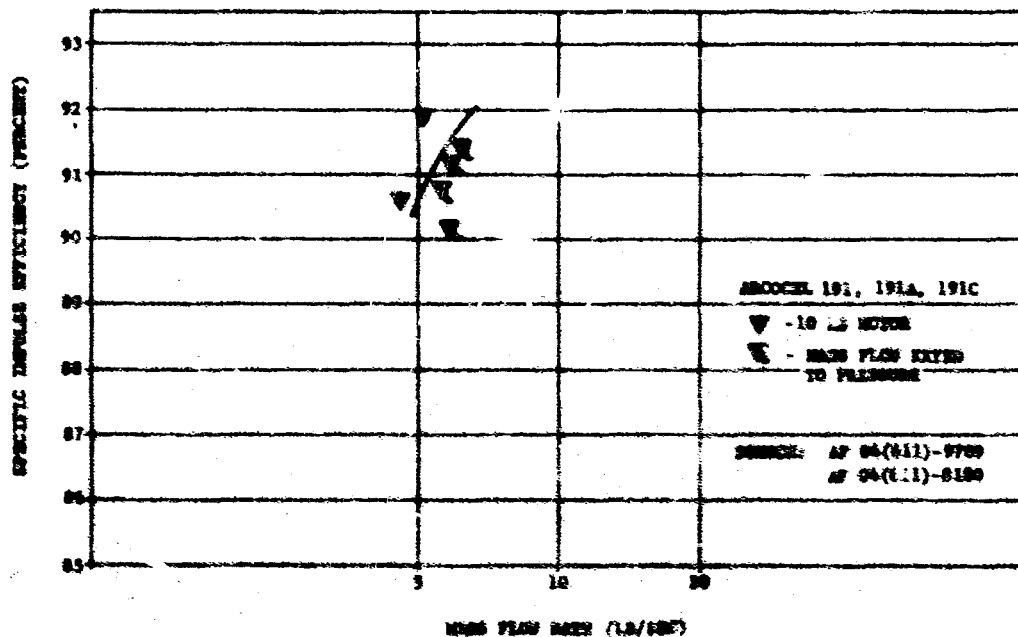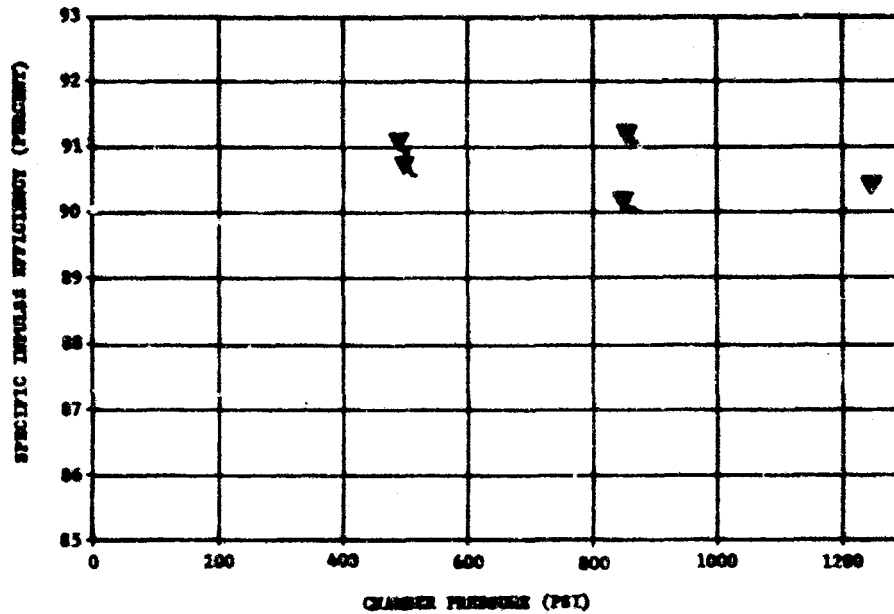
Figure 6. Effect of Chamber Pressure and Mass-Flow Rate on Specific
Impulse Efficiency of Arcocel 191
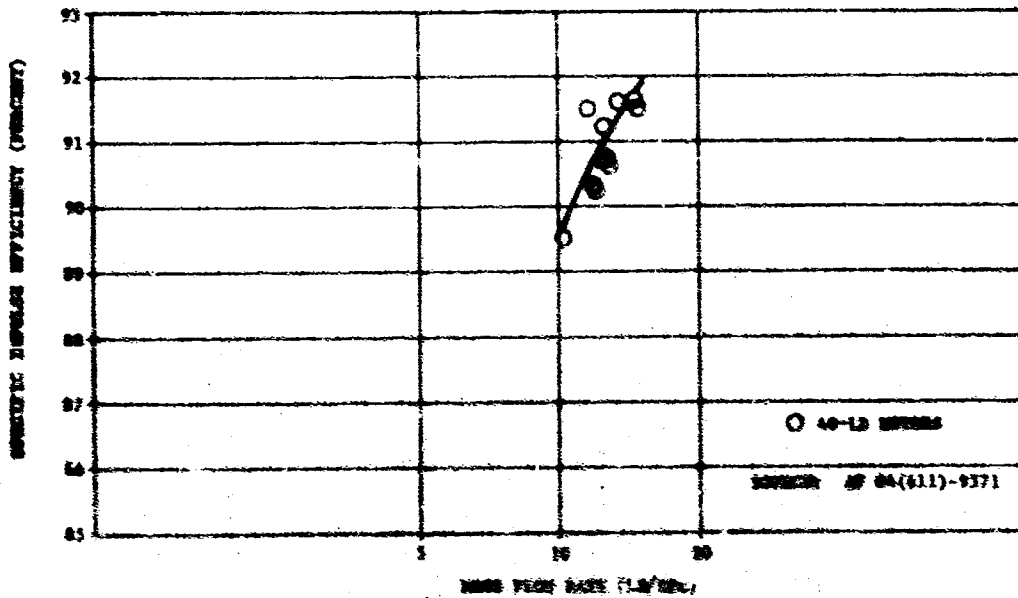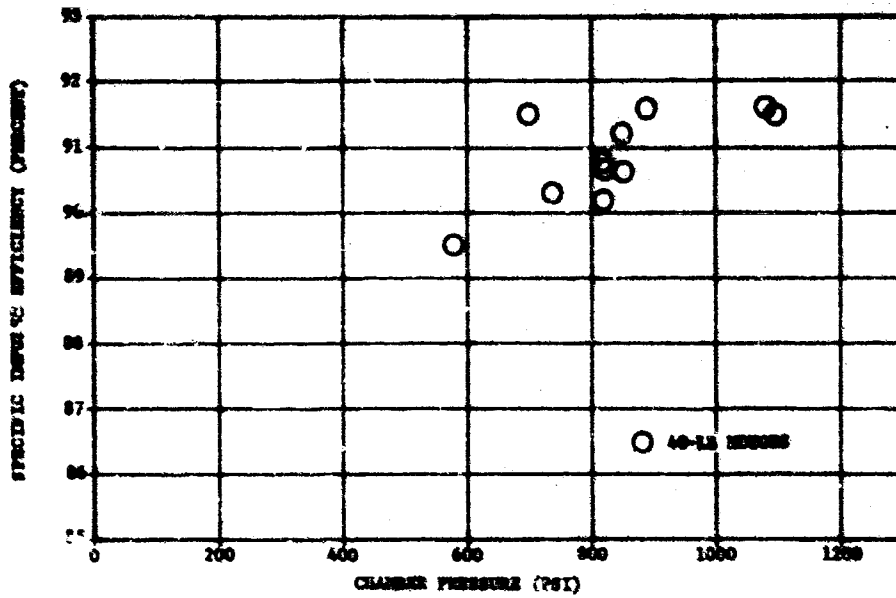
Figure 7. Effect of Chamber Pressure and Mass-Flow Rate on Specific
Impulse Efficiency of Arcocel 333
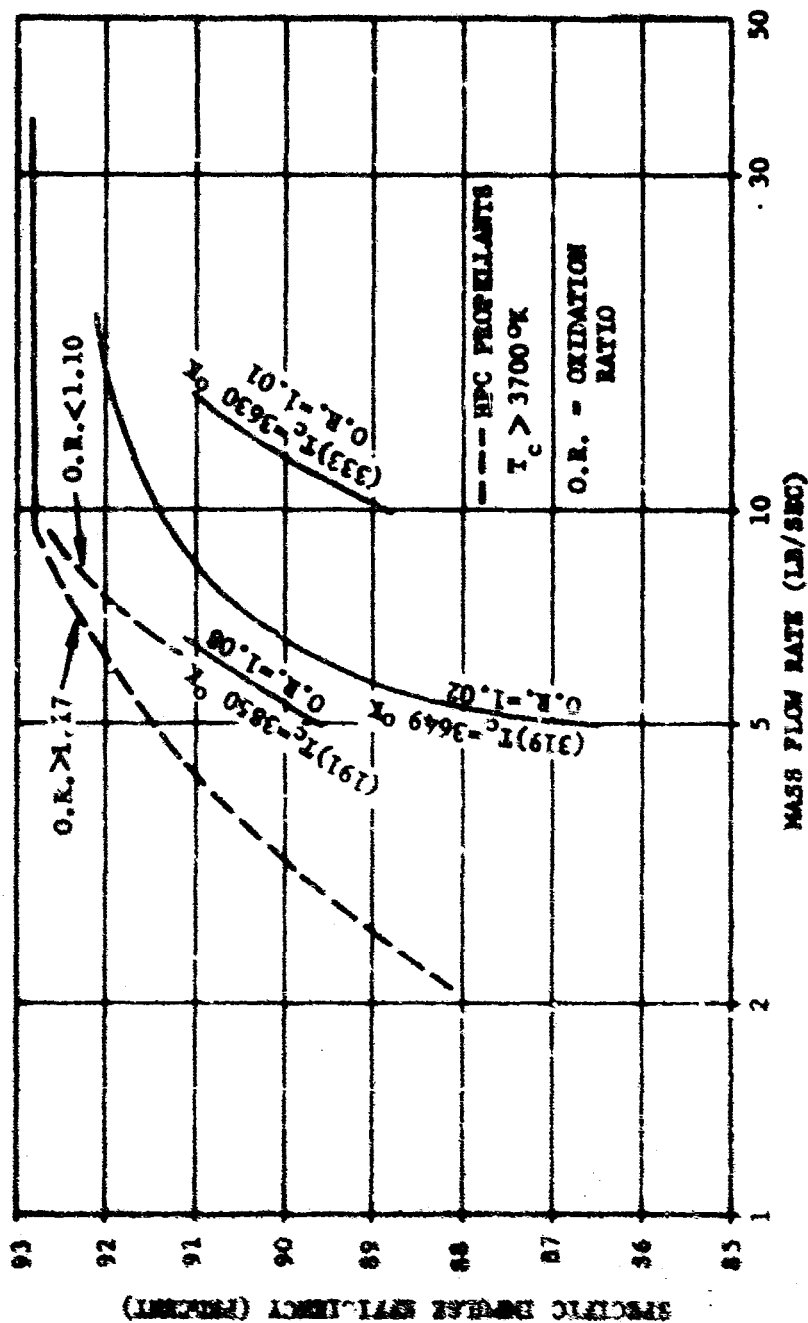
Figure 8. Effect of Motor Scaling on Specific Impulse Efficiency of Selected Propellants
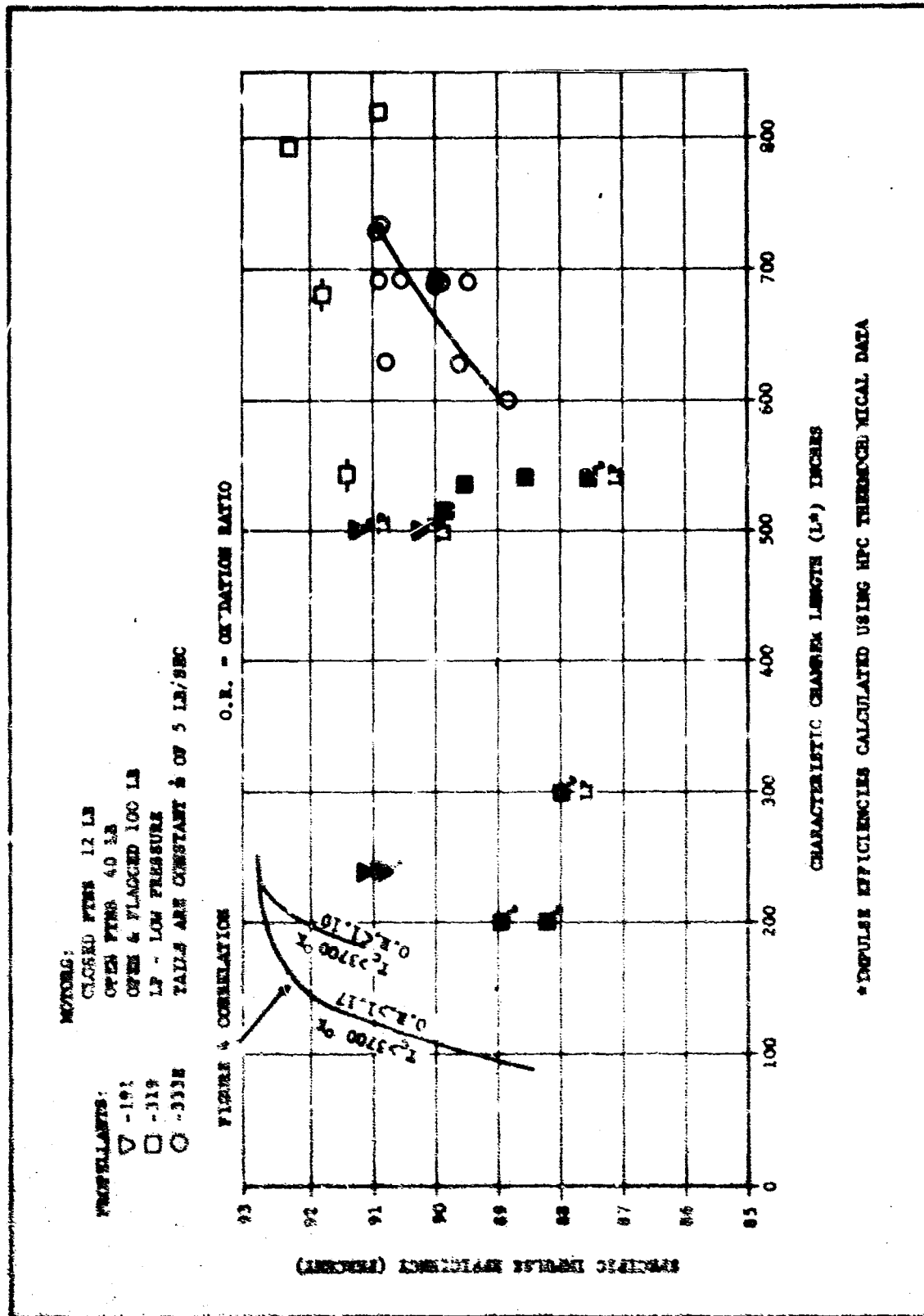
Figure 9. Effect of L* on Specific Impulse Efficiency of Selected Propellants

These trends are not absolute and additional testing is required for confirmation.

A comparison of the Be mass-flow rate curves at high and low temperatures to those of several LMH-2 propellants is shown in Figure 10. The majority of the LMH-2 mass-flow-rate curves follow those of a low-temperature Be propellant. It is also significant that Arcocel 340A (oxidation ratio of 1.0) is less efficient than the higher oxidation ratio propellants. Figure 10 also shows the effect of chamber pressure on efficiency for Arcocels 332 and 332A. No loss in efficiency occurred down to 450 psia. The results of Atlantic Research firings of a variety of propellants show a trend toward increased efficiency with increased L*, although other factors tend to obscure the correlation. Increased efficiency with increased flame temperature and higher oxidation ratio is also apparent in Figure 11.

The nozzle expansion ratio can influence efficiency by:

    (a)   Particle lags (velocity and thermal)

    (b)   Failure of gas phase reactions to reach completion

    (c)   Increased boundary layer friction losses occasioned by increased nozzle surface area

    (d)   Metal oxide fusion lag

    (e)   Errors in thermochemical data

    (f)   Heat exchange between gas and nozzle wall

Data showing the effect of increased expansion ratio on efficiency of Al propellants have been collected and are plotted on a common basis in Figure 12. All data appear to exhibit a consistent downward trend with increasing expansion ratio, although a leveling off at high expansion ratios is indicated for some propellants.

The effects of enthalpy loss from the gas stream to the nozzle wall and corresponding entropy decrease of the gas have been discussed in an Atlantic Research report.[3] Results of this calculation for Arcane 24, based on a 10-lb motor, predict a 1-percent Isp loss at an expansion ratio of 10, and 2-percent loss at an expansion ratio of 190. The data indicate a loss of over 3 percent between expansion ratios of 1 and 100; thus heat loss explains only part of the total loss.

Data for the effect of expansion ratio on efficiency of Be and LMH-2 propellants as determined by Hercules and Atlantic Research are summarized in Figure 13. The line through the Al data of Figure 12 is replotted for comparison. A distinct drop in efficiency with increasing expansion ratio is noted for all propellants. The efficiency loss is largest at the lower pressure. When data are recalculated assuming frozen flow, the low-temperature propellants, Arcane 24 and Arcane 53, show essentially

_____
[3] Refer to List of References
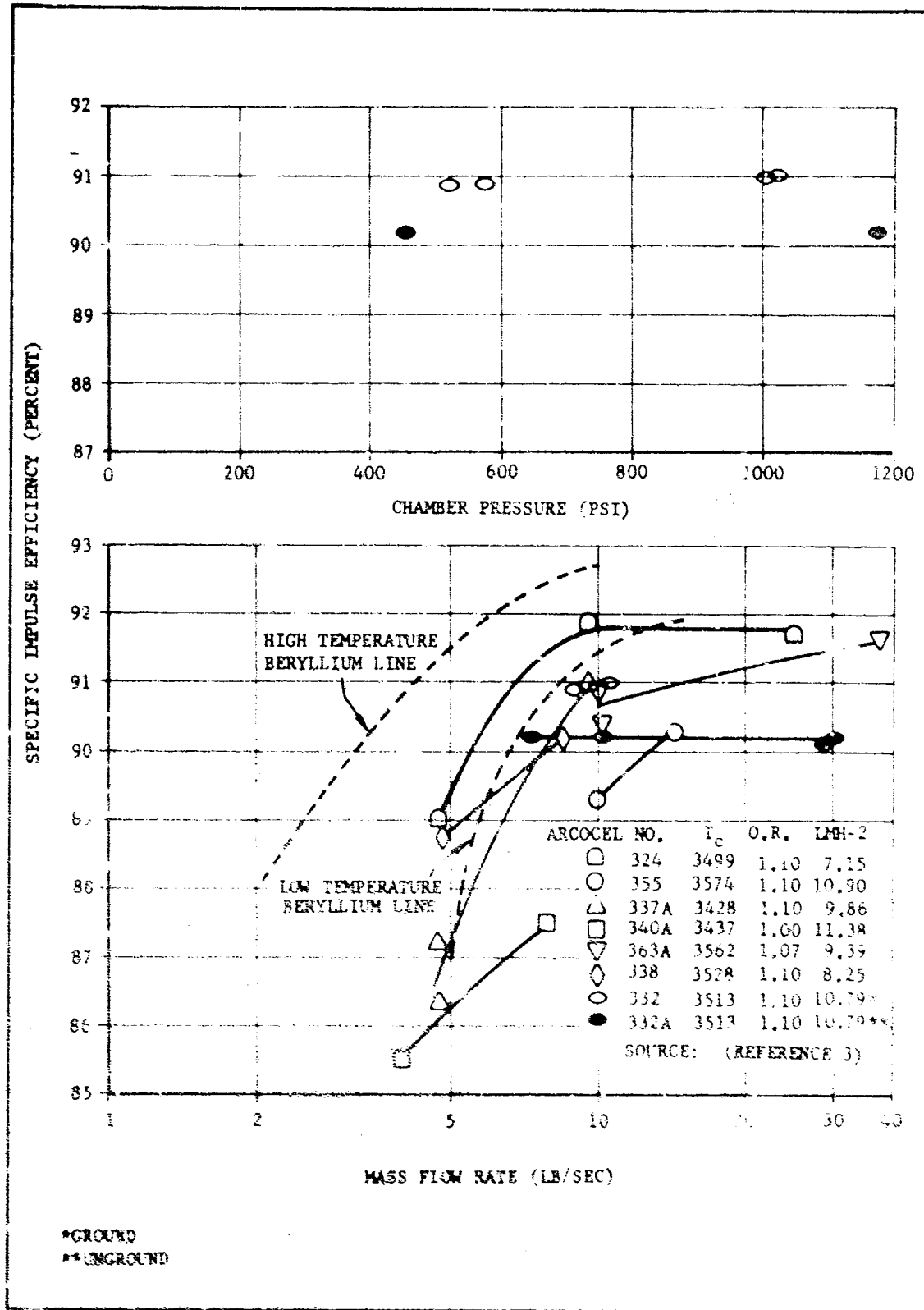
Figure 10. Effect of Chamber Pressure and Mass-Flow Rate on Specific Impulse Efficiency of LMH-2 Propellants
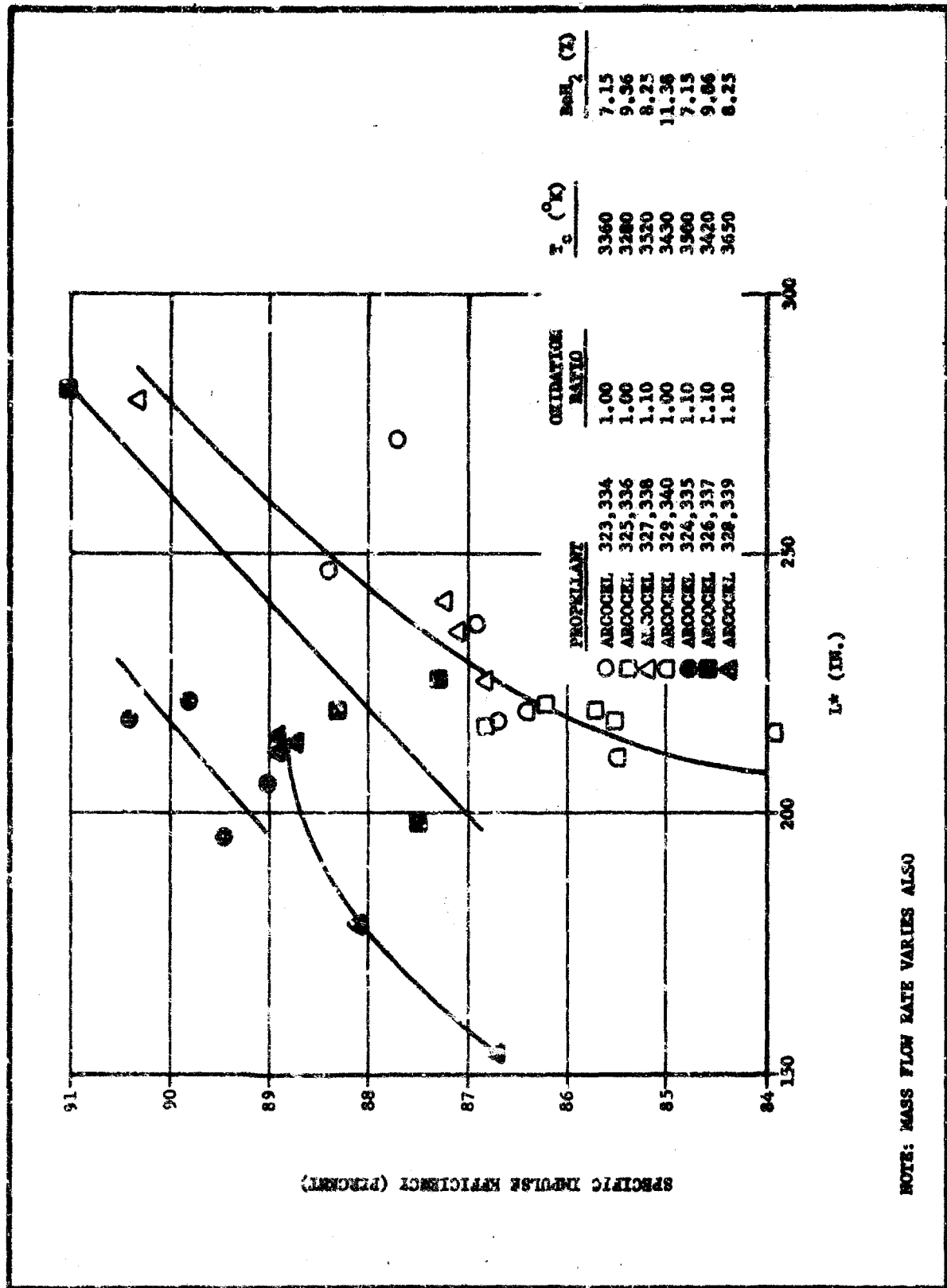
Figure 11.  Effect of Residence Time (L*) on Specific Impulse
Efficiency
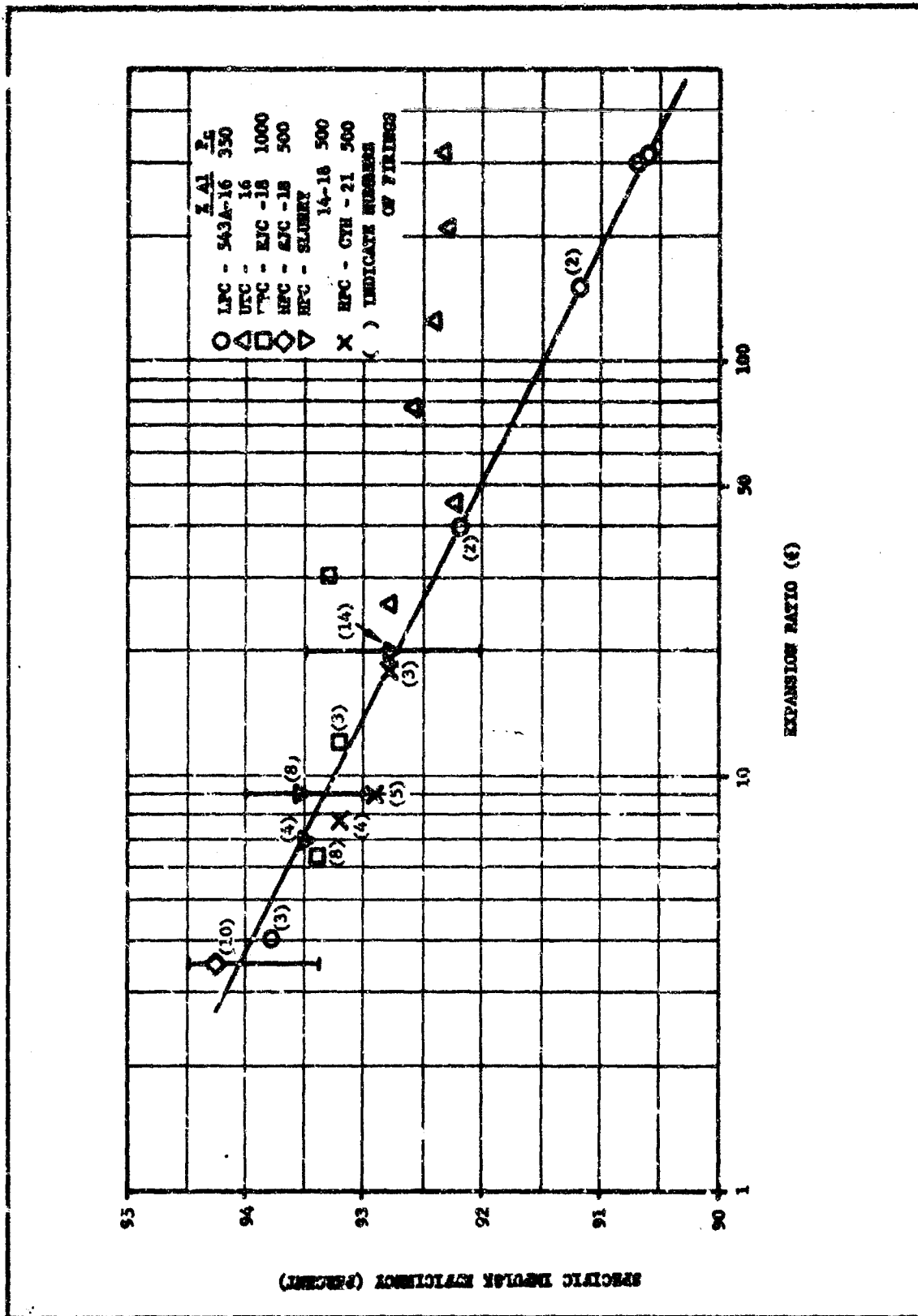
Figure 12.  Effect of Expansion Ratio on Specific Impulse Efficiency of Al Propellants

constant efficiency, indicating possible frozen-flow behavior for these formulations. Arcocel 191 shows an apparent increase in efficiency with expansion ratio, followed by constant efficiency at higher expansion ratios, indicating equilibrium flow for exit temperatures above approximately 2000° K and frozen flow thereafter. These correlations do not prove frozen flow, since other effects (items (a) and (b) above) could give similar results.

All three LMH-2 propellants for which data are available exhibit the same type efficiency behavior with expansion ratio as do the Be formulations. All three are intermediate in flame temperature, and all three contain considerable Be in addition to the LMH-2. The data are insufficient for definite conclusions at this time. Arcane 24 shows 1.5-percent efficiency loss between expansion ratios of 10 and 100, not greatly different from the loss predicted from considering heat transfer to the nozzle wall. All the other Be and LMH-2 propellants show at least 2-percent loss, indicating that another loss is also operative.

One important facet of obtaining good impulse efficiencies with metalized propellants is the minimization of velocity lag. This becomes increasingly important at high-metal levels, since the efficiency losses due to velocity lag can be expected to be proportioned to the percentage of condensables present. Thus, particularly at high-metal loadings, nozzle geometry must be optimum in order to achieve good efficiencies. Of particular importance is a good approach contour. Figures 14 and 15 show the effect of nozzle contouring on impulse efficiency as given by B. Brown.[4] Minimizing the approach angle and use of a large approach contour radius are shown to be necessary for good efficiency. In small motors, however, these factors must be balanced against increased heat losses for the longer nozzle. As a consequence, the present Hercules 15-lb-charge (15PC) motor has an approach angle of 30 degrees with a contour radius equal to the throat diameter; whereas the FPC motor has a 15 degree approach with the same contour radius ratio.

Design of these contours was based on experience with aluminized propellants and may not be optimum for LMH-2 propellants or the high Be analog formulations. There is some evidence to indicate that the 15 degree approach for FPC motors may not be optimum for even the low-metal VCP formulation. For example, FPC-motor, sea-level firings of VCP at Bacchus with the 15 degree approach consistently give efficiencies of 92.4 percent. But, several FPC altitude firings of VCP at Arnold Center with a 5 degree approach have given efficiencies of 93 percent. These data are also plotted in Figure 15. This reversal of the expected decrease in efficiency with increasing expansion ratio may have been due to the shallow approach angle. Nozzle approach contouring as a means of improving impulse efficiency at high metal loadings was therefore included in the program.

---

[4]Refer to List of References
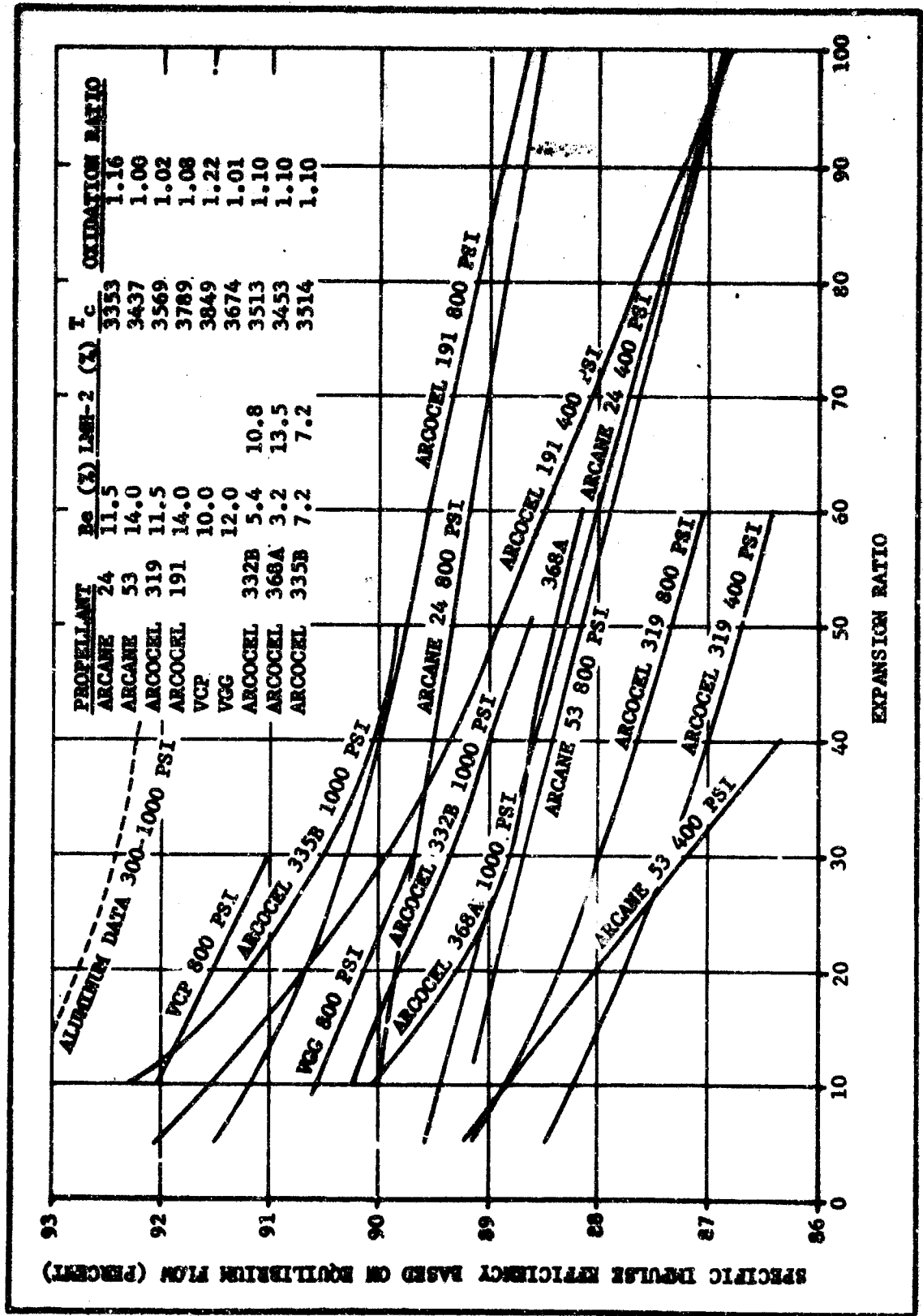
Figure 13.  Effect of Expansion Ratio on Efficiency of Be and LMH-2 Propellants
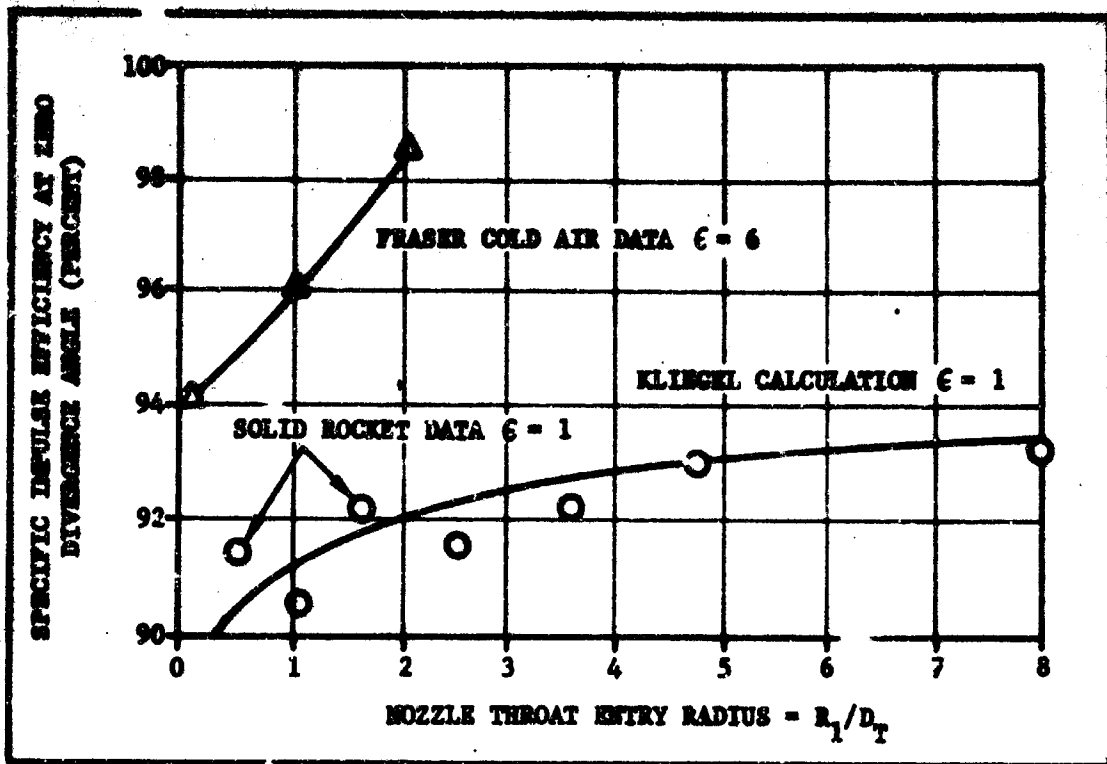
Figure 14. Effect of Nozzle Throat Contour on Efficiency

## 2. Propellant Parameters

The available data has demonstrated that motor efficiency is decreased at low combustion temperatures. This effect has already been noted in the discussion of L* and mass-flow rate. The following discussion shows that a chamber temperature of about 3700° K is required for efficient combustion of Be or LMH-2 propellants.

Figure 16 shows efficiency as a function of flame temperature for Be propellants. As shown, two distinct lines can apparently be drawn: one for hydrocarbon propellants (AP sole oxygen source) and one for nitrasol propellants. The hydrocarbon line shows a higher efficiency at a given flame temperature. However, this line is based on data from Aerojet, obtained in progressive 100-lb motor firings. A round-robin series of firings conducted between Hercules and Aerojet[5] has shown a 1-percent bias between the Aerojet motor and the Hercules FFC motor. As a consequence, 1 percent was subtracted from the Aerojet data. The same data is corrected for this bias in Figure 17 and shows little effect of oxygen source (AP versus nitrasol binders) on impulse efficiency. Attempts to remove the scatter from this data by combining flame temperature with total metal were unsuccessful. However, when Figure 17 is replotted with parameters of constant oxidation ratio (Figure 18), a trend toward higher efficiencies with higher

[5] Refer to List of References
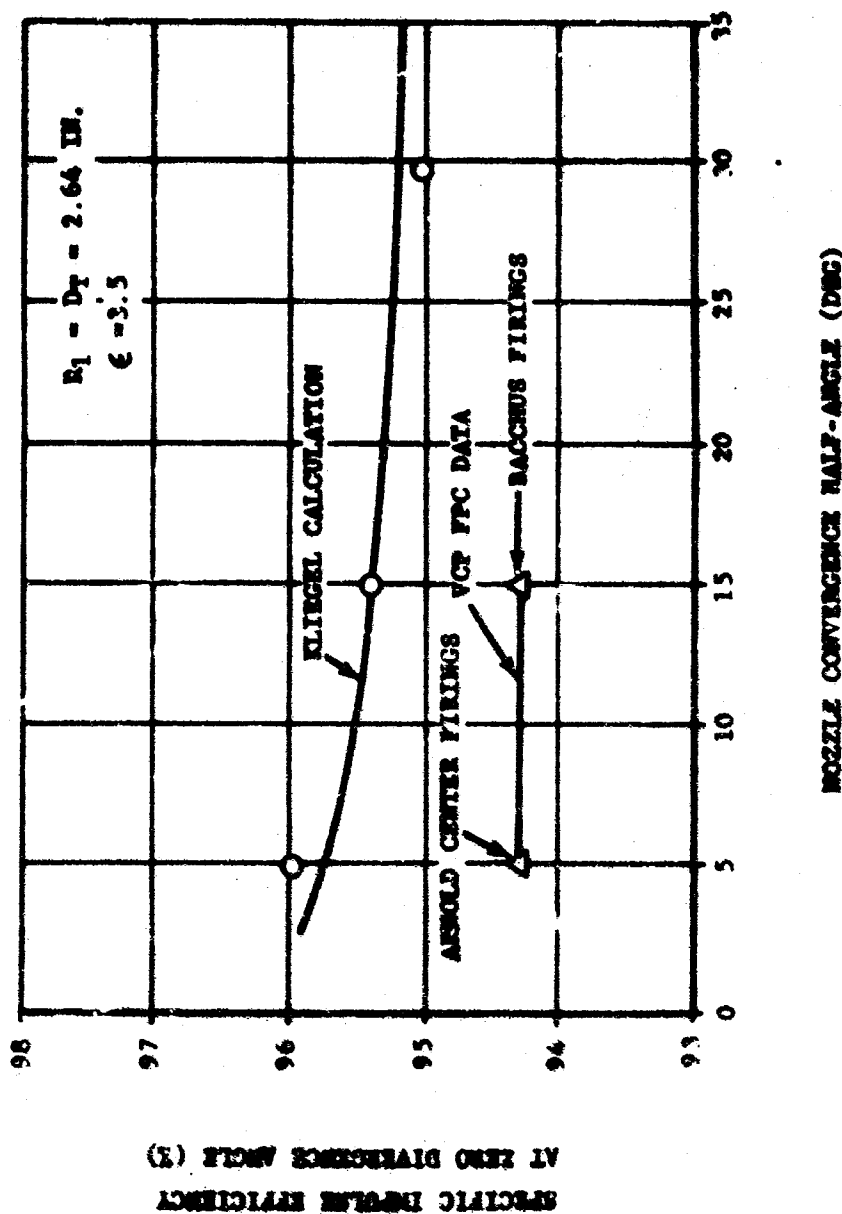
Figure 15. Effect of Convergence Angle on Nozzle Efficiency
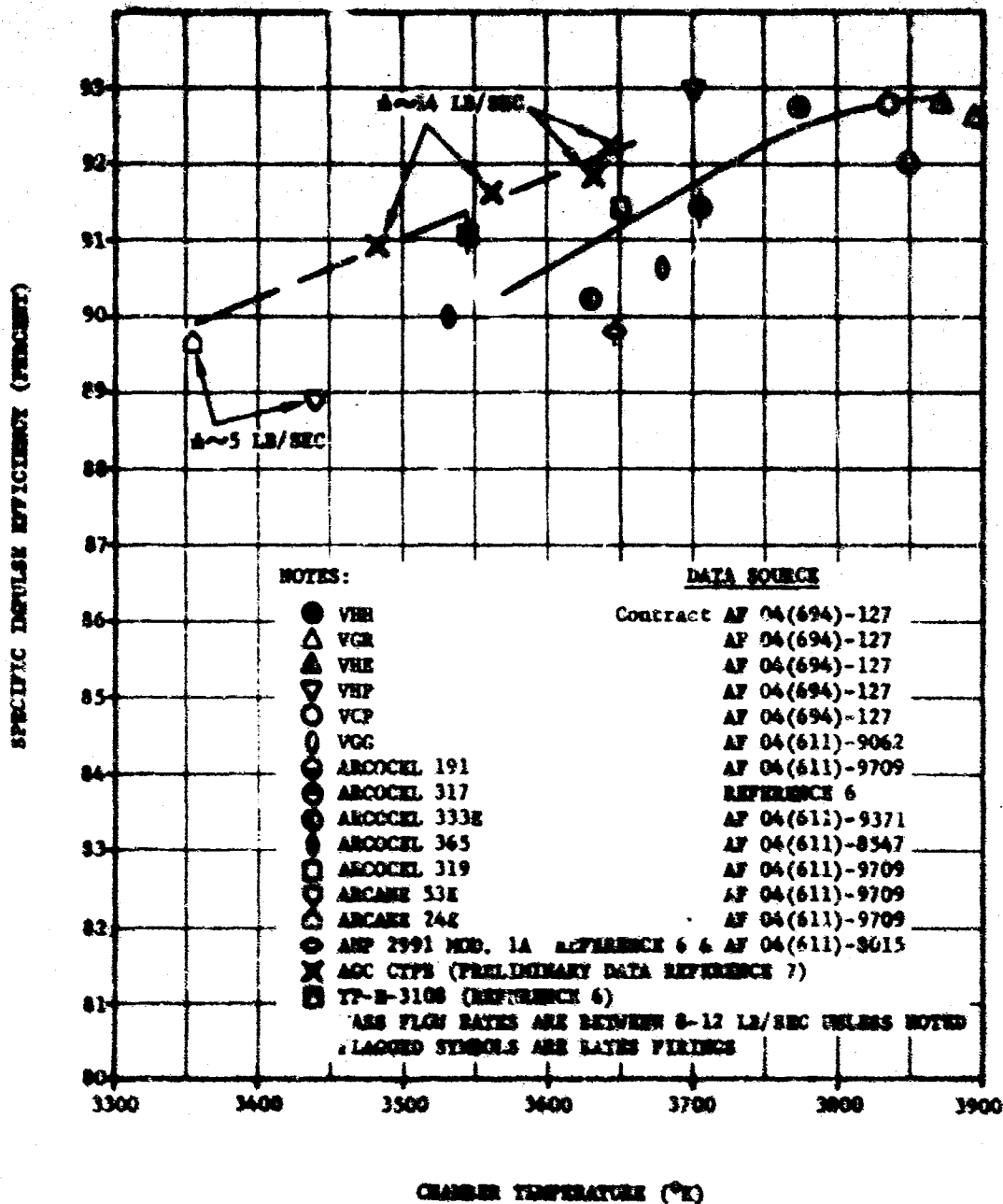
Figure 16. Effect of Chamber Temperature on Specific Impulse
Efficiency of Selected Bn Propellants

[6,7] Refer to List of References

23
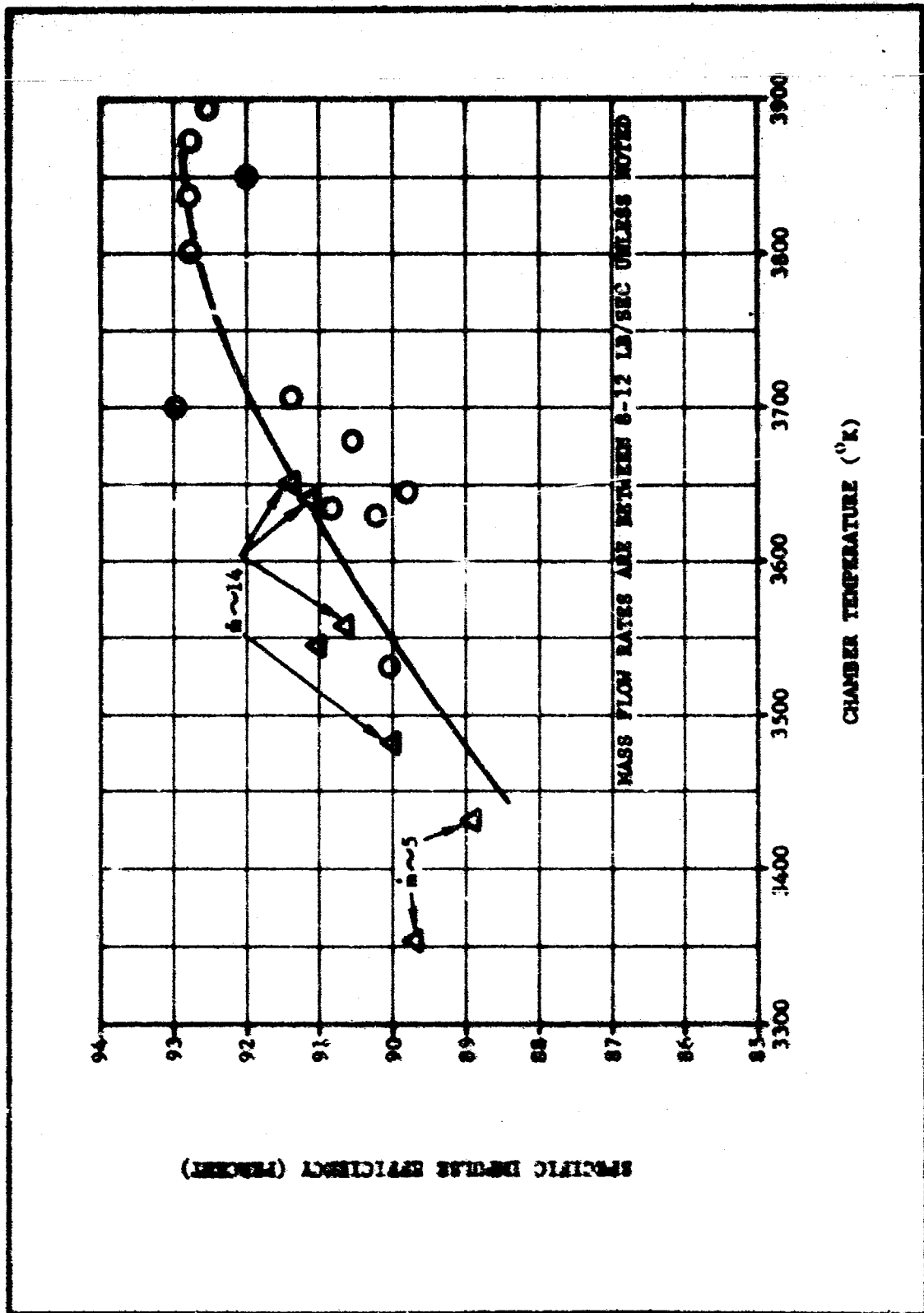
Figure 17. Effect of Chamber Temperature on Specific Impulse Efficiency (Corrected) of Selected Be Propellants
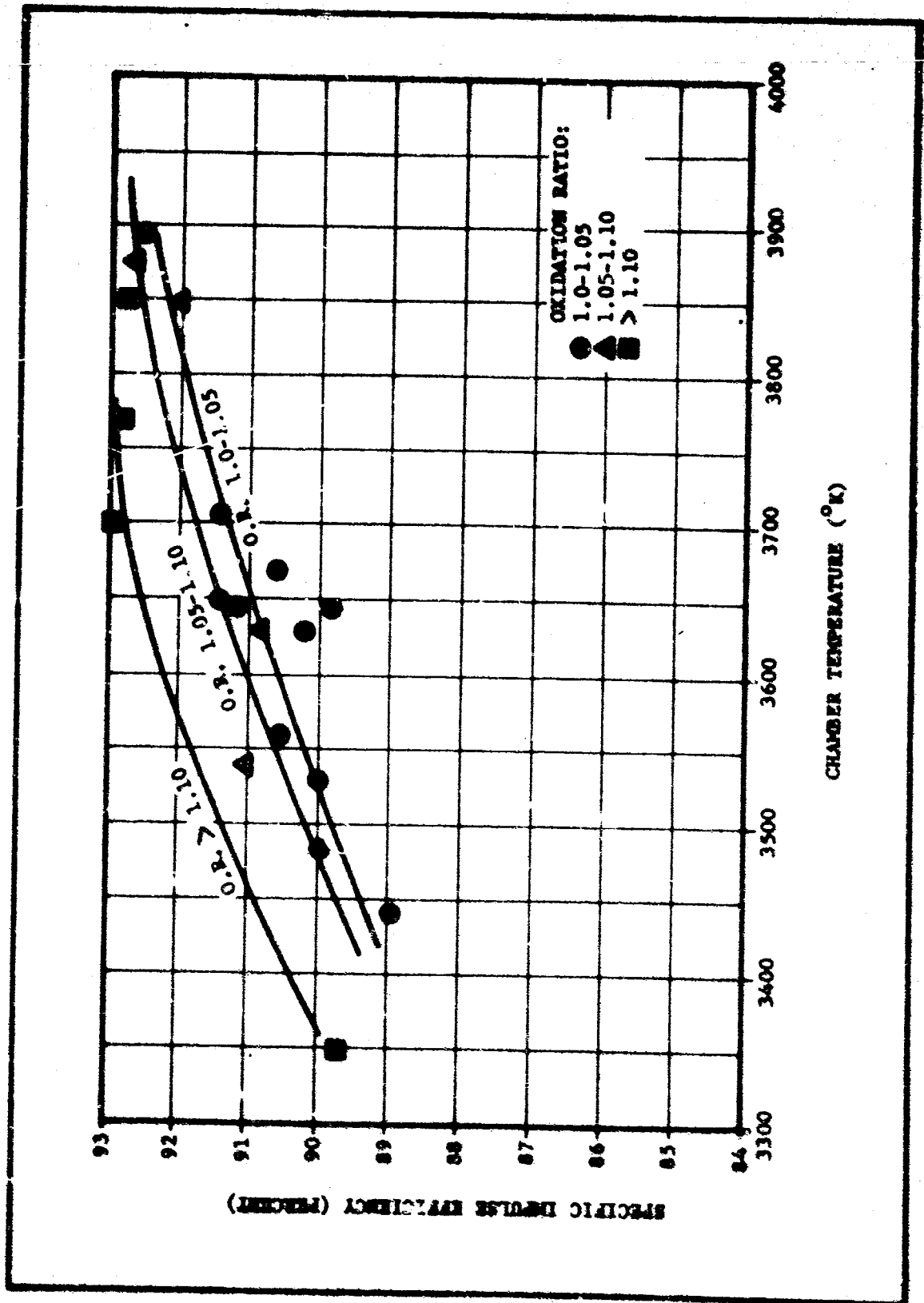
Figure 18.  Effect of Chamber Temperature and Oxidation Ratio on Specific Impulse Efficiency of Be Propellants

oxidation ratios at constant temperature appears. Unfortunately, data at high oxidation ratios for low-flame-temperature propellants is limited, and the correlation requires further investigation.

The substitution of HMX for AP affords the possibility of extending the range of the ratio AP/Be to zero. The effect on efficiency of varying this parameter is shown in Figure 19. A decrease in efficiency is evident. This decrease may be: (a) Due to decreased chamber temperatures at the higher AP/Be ratios; (b) an indication that the heat of formation of one or more of the Be-Cl species may be in error; and (c) an indication of an effect of oxygen source on combustion efficiency.

Extension of the Be temperature correlation to LMH-2 propellants is shown in Figure 20. A much larger scatter is noted with the Be line correlating only approximately 75 percent of the data within $\pm 1$ compared to 95 percent of the Be data. Based on the success of the Be-vs-temperature plot at constant oxidation ratio, the LMH-2 data was next correlated on this basis, as shown in Figure 21. However, no real trend as shown with Be propellants was observed. In order to compare the results of the success of this correlation with other correlations, an envelope of data points was constructed, as shown in Figure 21. This envelope accounted for approximately 85 percent of all the data points.

Attempts at correlating the data based on total metal and oxidation ratio met with less success. Figure 22 shows efficiency as a function of LMH-2 loading. Again the data is widely scattered, but shows a definite loss in efficiency at high LMH-2 loadings and is best shown by an envelope of data points. The effect of the ratio of the excess oxygen to weight percent LMH-2 on efficiency is shown in Figure 23. A trend toward higher efficiencies with excess oxygen is shown, but again only an envelope can be drawn. Based on these correlations it is observed that flame temperature influences LMH-2 efficiency more than any other parameter. Consequently, the extremes of the temperature envelope shown in Figure 21 were used to design formulations capable of meeting the program objective.

Three other factors have also been investigated, which show an effect on LMH-2 efficiency, two of which are related to the oxygen source. Atlantic Research has reported that both the ratio of AP/LMH-2 and the AP particle size affect LMH-2 efficiency. Figure 24 shows the effect of AP particle size on impulse efficiency for both Al and Be propellants. The LMH-2 data show a decrease in efficiency with increased AP particles size consistent with the Al propellant data. The third factor is LMH-2 particle size. Figure 10 compared pressure effects on efficiency for Arcocel 332A containing unground LMH-2 with Arcocel 332 containing ground LMH-2. The efficiency is 0.7 percent better with the ground LMH-2. All three of these factors point toward more intimate contact between LMH-2 and the primary oxidizer as a means of improving combustion efficiency of LMH-2.
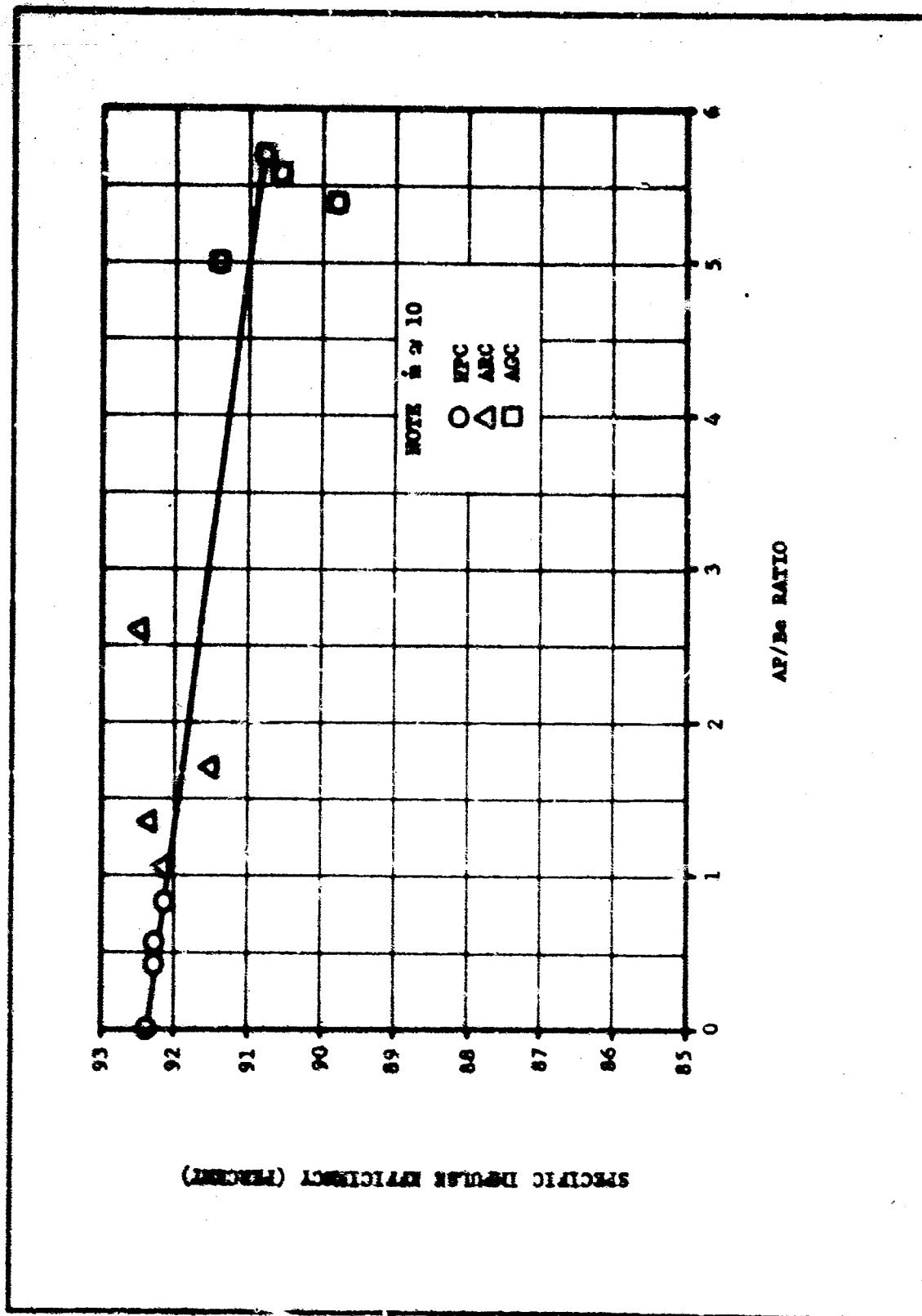
Figure 19. Effect of Oxygen/Oxidizer Source on Specific Impulse Efficiency
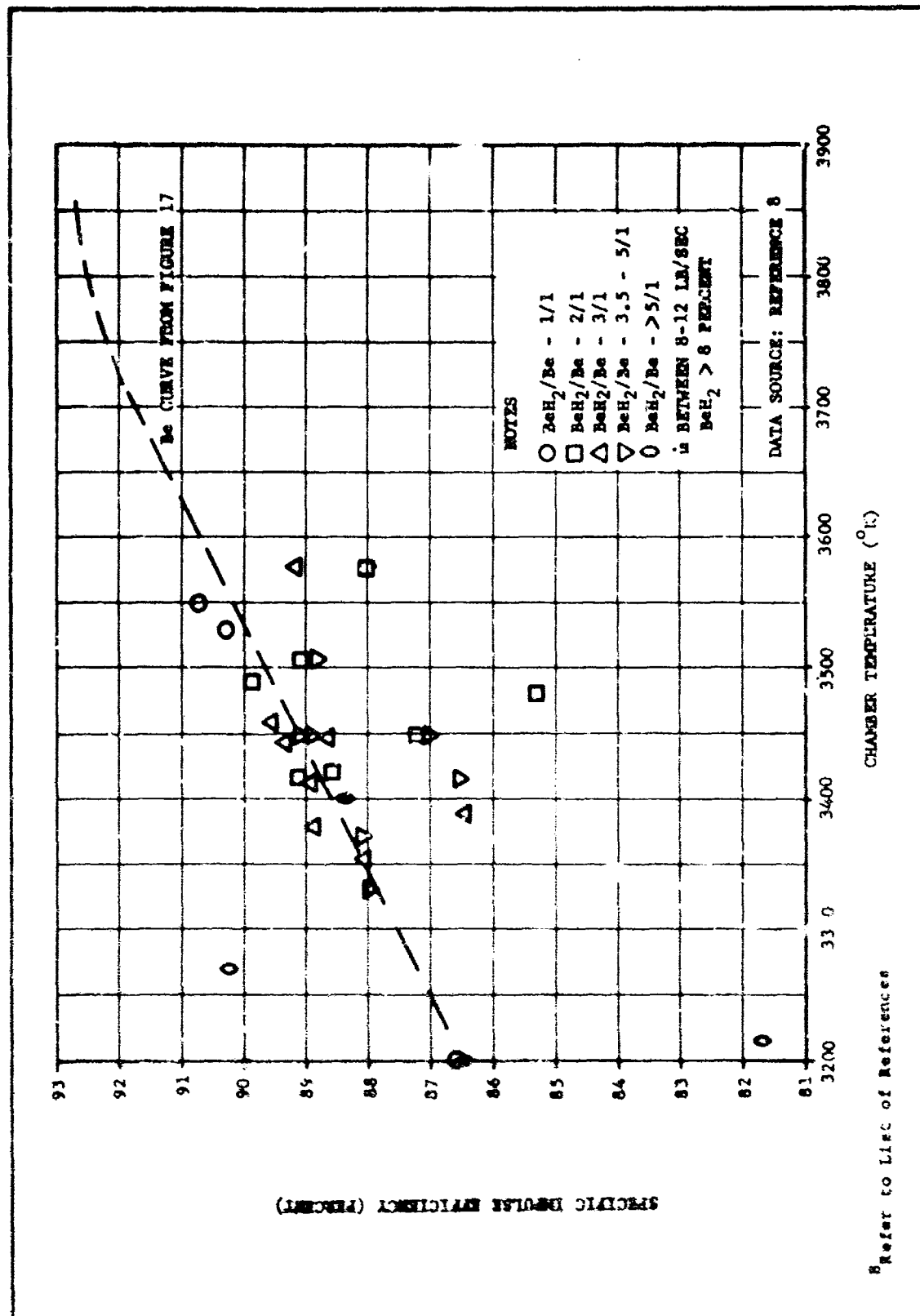
Figure 20. Effect of Chamber Temperature on Specific Impulse
Efficiency for LMH-2 Propellants

28
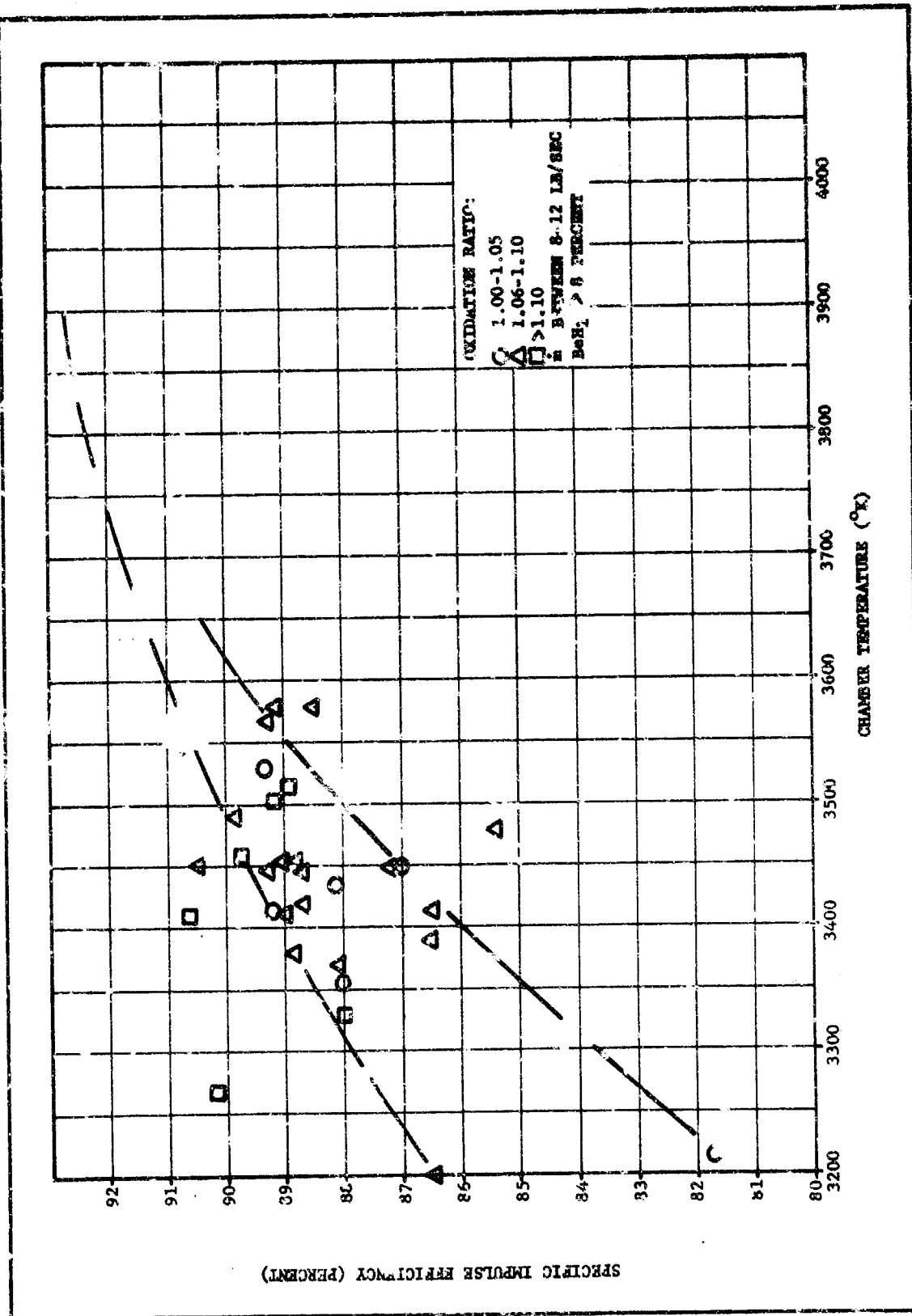
Figure 21. Effect of Chamber Temperature and Oxidation Ratio on Specific Impulse Efficiency of LMH-2 Propellants
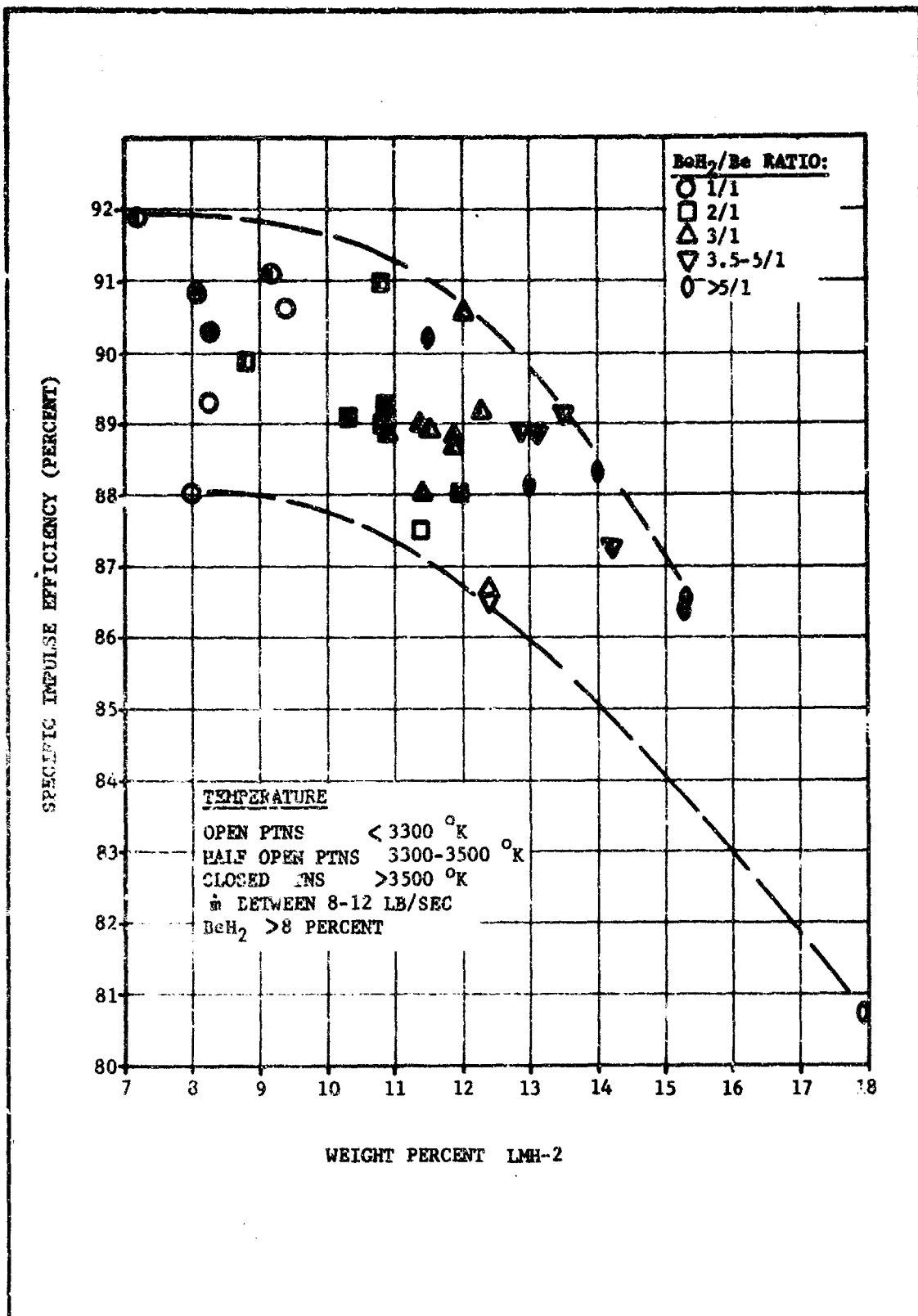
Figure 22. Effect of LMH-2 Content on Specific Impulse
Efficiency
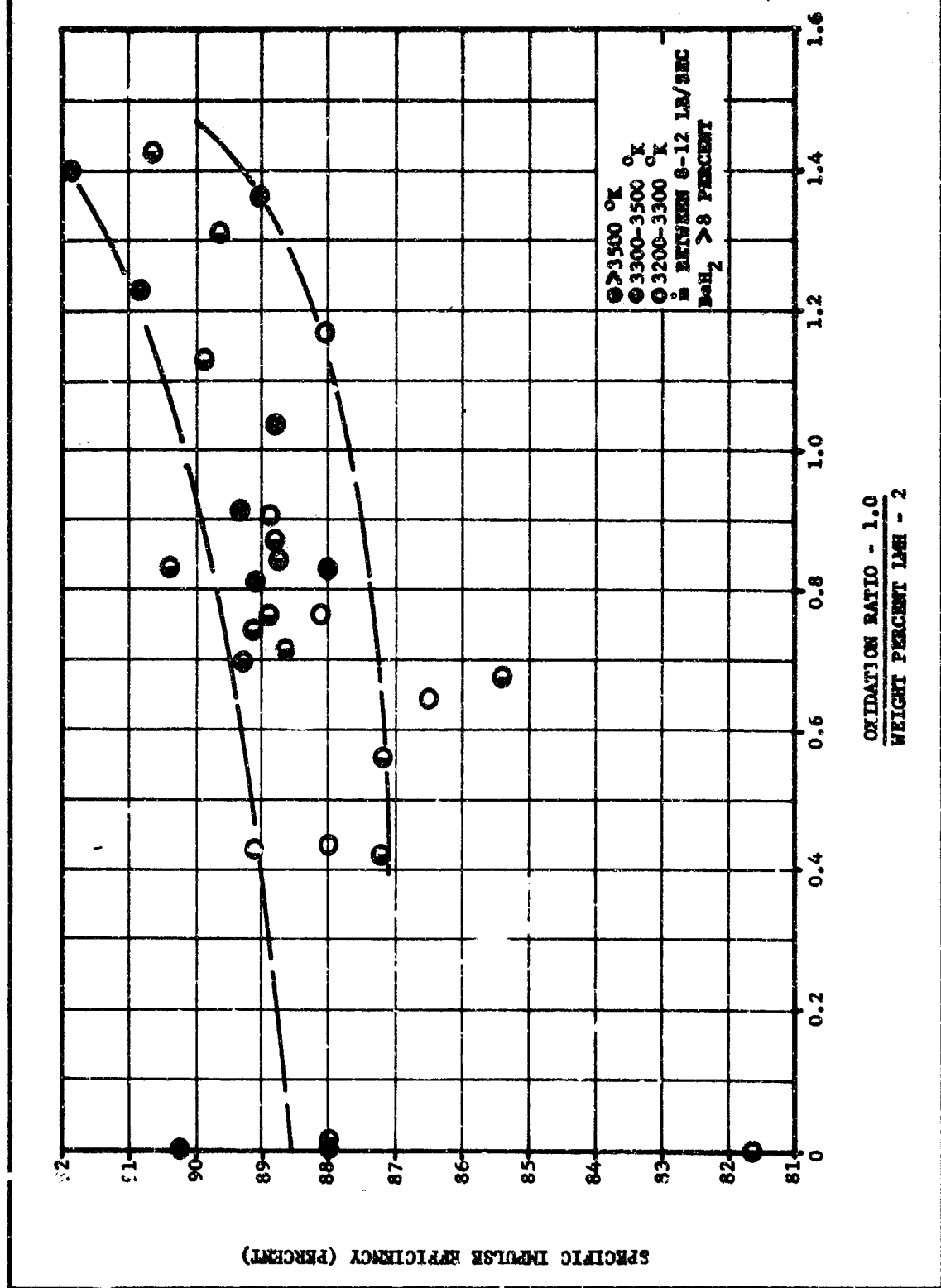
Figure 23.  Effect of Excess Oxygen/LMH-2 Ratio on Specific
Impulse Efficiency

31

**CONFIDENTIAL**
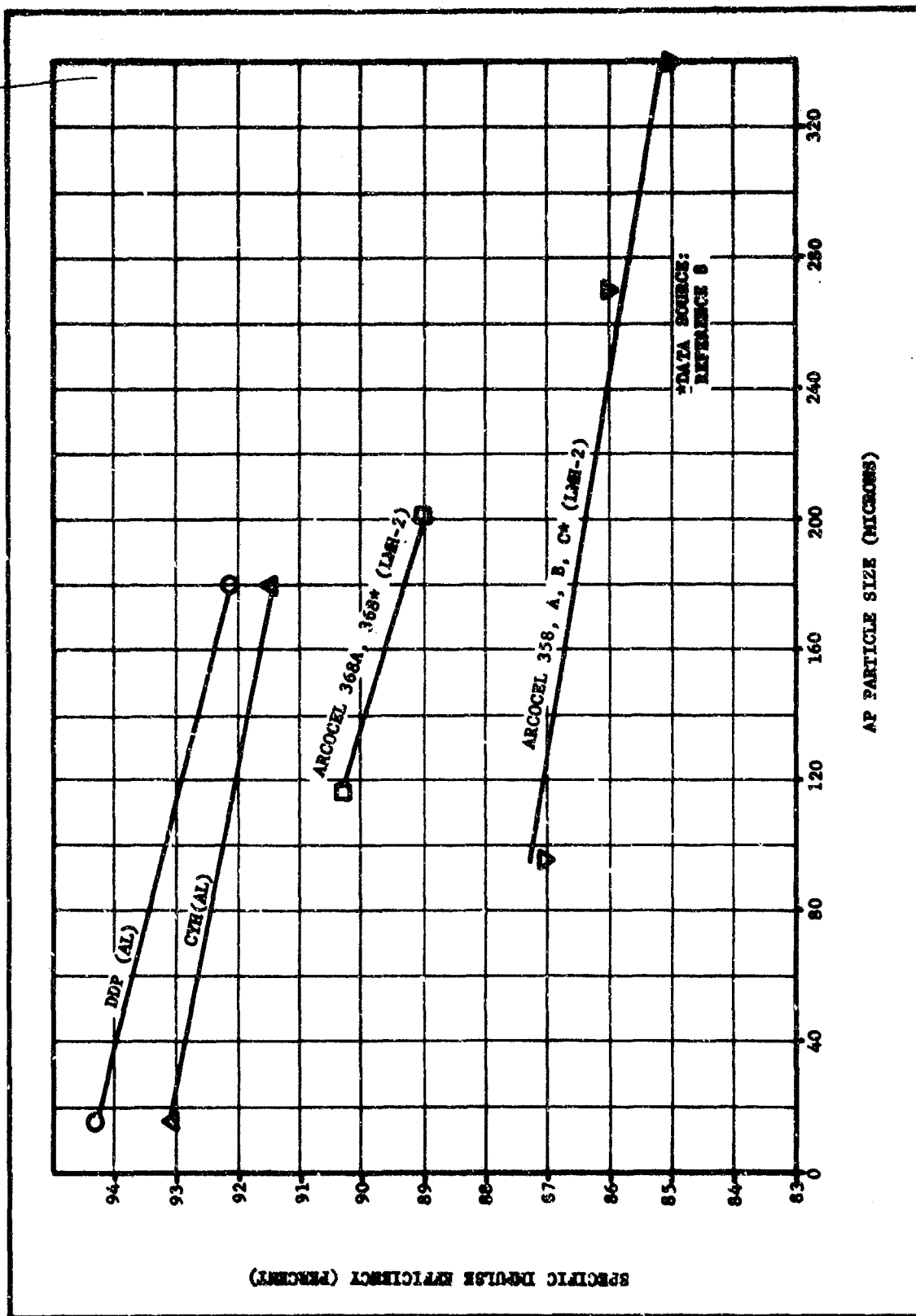
Figure 24. Effect of AP Particle Size on Specific Impulse Efficiency

Based on this preliminary analysis, the following factors influencing the motor efficiency of LMH-2 and beryllium propellants appeared to be important:

(a) High-flame-temperature and high-oxidation-ratio propellants show no loss in efficiency with decreasing pressure down to 500 psia.

(b) Low-flame-temperature and low-oxidation-ratio propellants show losses in efficiency with decreasing pressure. This effect could not be completely separated from mass flow or residence time effects on efficiency.

(c) Both Be and LMH-2 propellants show a strong dependence on high flame temperatures for good efficiency.

(d) Oxidation ratio has a strong effect on the efficiency of low temperature Be propellants. There is an indication that oxidation ratio is important for LMH-2 efficiency, but only a general trend could be obtained.

(e) Correlations based on total LMH-2 content show a loss in efficier y at high-hydride loadings (greater than 15 percent).

(f) More intimate contact of oxidizer and fuel in LMH-2 systems should improve efficiency based on efficiency effects of AP particle size, AP/LMH-2 ratios, and ground LMH-2.

## C. THEORETICAL SPECIFIC IMPULSE CALCULATIONS

Theoretical Isp calculations were made for a wide variety of systems containing Be and LMH-2 to support the formulation design effort. Details of these calculations are given in Appendix A. In summary, based on preliminary correlations it was found necessary to use as high an energy binder as practical with conventional oxidizers to ensure with reasonable confidence that specific impulse goals would be attained.

## D. FORMULATION AND TEST DESIGN

The correlations showed several areas in which further investigation was needed before reliable predictions could be made for the performance of both Be and LMH-2 propellants. In general, the Be correlations were significantly better than for LMH-2 systems. Additional Be testing was warranted in the following areas for further clarification of propellant parameters on impulse efficiency:

(1) High metal levels (15.5 percent) at high flame temperatures and oxidation ratios

# CONFIDENTIAL

(2) High metal levels and high flame temperatures at low
    oxidation ratios

(3) Evaluation of oxidizers different from AP and HMX,
    such as AN and $TAGNO_3$

(4) Additional testing at high oxidation ratios and
    high flame temperatures for determining the effect
    of AP particle size

Further testing was also needed in the following areas for clarification
of motor parameters:

(1) Optimization of nozzle geometry at high metal levels

(2) Increased L* studies for both efficient and inefficient
    Be propellants and LMH-2 propellants

For LMH-2 systems, the following testing was needed to clarify propel-
lant parameters:

(1) High LMH-2 loadings at flame temperatures in excess of
    $3600^\circ$ K and at high oxidation ratios

(2) Comparative evaluation of AP, AN, and HMX oxidizers

(3) More intimate contact between oxidizer and LMH-2

(4) Addition of fluorine to LMH-2 to aid combustion and to
    reduce two-phase flow losses.

The Task II and Task III effort was designed to clarify these areas
for Be and LMH-2 propellants.

Table II contains a list of the Be formulations chosen for testing to
better define the effect of propellant parameters on performance. VIH
propellant was designed to have the same metal level and oxidation ratio
as the proposed 19-percent LMH-2/AP formulation. VII was formulated to
show the effect of efficiency of the AP:Be ratio at a constant metal level,
flame temperature, and oxidation ratio. VIJ was also formulated with 45
and 180µAP to demonstrate the effect of AP particle size on impulse effi-
ciency thus providing the performance trade off between AP particle size
and LMH-2 loading necessary to optimize delivered impulse. The VIK, VIL,
VIM, and VIN propellants represent the Be analogs of the 17-percent LMH-2,
AP; 15-percent LMH-2, AP HMX; 19-percent LMH-2, AN; and 17-percent LMH-2,
AN formulations, respectively, in both metal level and oxidation ratio.
VIO was designed to determine the effect of oxidation ratio on efficiency at
low metal levels, and VIG was formulated to evaluate $TAGNO_3$ as an oxidizer.

TABLE II

BERYLLIUM PROPELLANTS FOR FORMULATION SCREENING

| Formulation | Be (wt %) | Oxidizer Type | $I_{sp}$ (sec) | $T_c$ (°K) | O.R.* | Number of Firings | | Purpose |
|---|---|---|---|---|---|---|---|---|
| | | | | | | 1000 psi | 500 psi | |
| VCP | 10 | HMX/AP | 283 | 3840 | 1.22 | 3 | 3 | Control |
| VIH | 15.5 | AP | 278 | 4173 | 1.17 | 3 | 3 | LMH-2 19% Analog with respect to TM and O.R. |
| VII | 15.5 | AP | 279 | 3971 | 1.05 | 3 | 3 | LMH-2 19% Analog with respect to TM; lower O.R. |
| VLJ | 15.5 | AP | 277 | 4145 | 1.17 | 3 | -- | Total AP effect |
| VIK | 14.0 | AP | 277 | 4109 | 1.27 | 3 | 3 | Analog with respect to TM and O.R. |
| VIL | 12.0 | HMX/AP | 281 | 4008 | 1.24 | 3 | 3 | LMH-2 15% Analog AP/HMX with respect to TM and O.R. |
| VIM | 15.5 | AN | 281 | 3820 | 1.17 | 3 | 3 | LMH-2 19% Analog with respect to TM and O.R. |

*, **, ***, See end of table

# TABLE II (Cont)

## BERYLLIUM PROPELLANTS FOR FORMULATION SCREENING

| Formulation | Be (wt %) | Oxidizer Type | $I_{sp}$ (sec) | $T_c$ (°K) | O.R.* | Number of Firings** 1000 psi | Number of Firings** 500 psi | Purpose |
|---|---|---|---|---|---|---|---|---|
| VIN | 14.0 | AN | 279 | 3744 | 1.28 | 3 | 3 | IMH-2 17% Analog with respect to TM and O.R. |
| VIO | 8.0 | HMX/AP | 281 | 3745 | 1.38 | 3 | -- | O.R. effect at low TM |
| VIG | 12.5 | TAGNO$_3$/AP | 291 | 3633 | 1.07 | 3 | -- | Evaluate TAGNO$_3$ |
| | | | | | | 30 | 21 | |

*O.R. = Oxidation Ratio

**Optimum expansion ratio at Bacchus ambient, number of firings originally scheduled

***TM = Total metal level

Based on the theoretical calculations and using the temperature correlation derived in Figure 21, six candidate LMH-2 formulations were chosen which were designed to confirm the expected efficiency envelope and to attain the program objective of a demonstrated $Isp \geq 280$ sec. Table III contains the LMH-2 propellants together with the theoretical and predicted performance values.

Additional testing to determine the effect of motor parameters on the performance of Be and LMH-2 propellants was also accomplished in Task II as follows:

| Motor Parameter | Formulation | Number of Firings |
|---|---|---|
| Nozzle Approach Angle | | |
| 15-degree Approach | VCP | 2 |
| 15-degree Approach | VIJ | 4 |
| 5-degree Approach | VCP | 2 |
| 5-degree Approach | VIJ | 3 |
| High L* | VCP | 2 |
| High L* | VII | 2 |
| High L* | VIY | 9 |

E.  PROGRAM DATA ANALYSIS

1.  Beryllium Firings

Data was available from the 70 Be firings on this program as outlined under Formulation and Test Design. Additional data was also available on three high-performance Be propellants (VIB, VID, and VIF) developed by Hercules under Contract AF 04(694)-127. Pertinent data on these formulations is given in Table IV.

A complete summary of the individual firings made on this program is given in Appendix B and additional details in Section III. Table V contains a summary of these data. A least squares analysis was performed on the Be efficiency firings for chamber pressure effects. (The data from this analysis are summarized in Table V.) This analysis allowed accurate comparison of all propellants tested at 1000 psia chamber pressure. In addition, efficiencies for the selected propellants specifically tested for pressure effects are summarized at 500 psia. Conclusions based on these data are contained in the following subparagraphs.

## TABLE III

## LMH-2 PROPELLANTS FOR FORMULATION SCREENING

| Propellant Type | Binder Level (wt %) | Oxidizer (wt %) | LMH-2 (wt %) | $I^0_{1000}$ (sec) | $T_c$ (°K) | O.R.* | Impulse Efficiency Range | Predicted $I_{sp}$ Del (H)** | Predicted $I_{sp}$ Del (L)*** |
|---|---|---|---|---|---|---|---|---|---|
| VIX | 62 | AP | 15 | 304 | 3678 | 1.34 | 90.7-91.6 | 279 | 276 |
| VIY | 62 | AP | 17 | 309 | 3679 | 1.22 | 90.7-91.6 | 283 | 280 |
| VIZ | 62 | AP | 19 | 314 | 3671 | 1.11 | 90.6-91.5 | 287 | 285 |
| --(1) | 62 | AP/HMX | 15 | 307 | 3636 | 1.23 | 90.2-91.2 | 280 | 277 |
| VJA | 61 | HMX | 15 | 309 | 3621 | 1.15 | 90.0-91.1 | 282 | 278 |
| --(1) | 62 | AN | 17 | 309 | 3529 | 1.25 | 88.6-90.4 | 279 | 274 |
| VJI | 61 | HMX | 17 | 314 | 3623 | 1.06 | 90.0-91.1 | 286 | 283 |
| VJL | 62 | AP/HMX | 17 | 313 | 3614 | 1.08 | 89.9-91.0 | 285 | 281 |

*Oxidation Ratio
**(H) High value expected from Figure 21
***(L) Low value expected from Figure 21

(1) The VJI and VJL formulations were substituted for these initial formulations

## TABLE IV

### ADVANCED Be PROPELLANTS

| Propellant Type | VIB | | VID | | VIF | |
|---|---|---|---|---|---|---|
| **Formulation (wt %)** | | | | | | |
| DB Binder | 44.0 | | 44.0 | | 45.0 | |
| AP | -- | | -- | | 6.0 | |
| HMX | 47.0 | | 44.0 | | 37.0 | |
| Be | 9.0 | | 12.0 | | 12.0 | |
| **Theoretical Performance** | | | | | | |
| Isp (1000/14.7) | 286.4 | | 289.1 | | 286.4 | |
| Tc ($^{\circ}$K) | 3780 | | 3885 | | 3897 | |
| Oxidation Ratio | 1.17 | | 1.02 | | 1.05 | |
| **Delivered Performance**[1] | | | | | | |
| Chamber Pressure (psia) | 488 | 846 | 518 | 911 | 381 | 754 |
| Mass Flow (lb/sec) | 5.5 | 7.8 | 5.7 | 7.8 | 6.3 | 8.8 |
| L* - VF/$A_t$ | 247 | 314 | 243 | 318 | 171 | 228 |
| $I_{sp1000}^{15}$ ($lb_f$-sec/lbm) | 264.8 | 267.7 | 268.9 | 267.9 | 267.0 | 267.6 |
| Efficiency | 92.5 | 91.9 | 93.0 | 92.7 | 93.2 | 93.5 |
| No. of Firings | 3 | 3 | 3 | 3 | 2 | 2 |

[1] Determined in FPC motor firings

Note: Data obtained from Contract AF 04(694)-127

TABLE V

BALLISTIC PERFORMANCE SUMMARY

| Formulation | Percent Me | Oxidizer | $T_c^1$ (°K) | $OR^2$ | $P_c^3$ (psia) | $\dot{m}^4$ | No. of Firings | Efficiency (%) | $Isp^{15}_{1000}$ (lbf-sec/lbm) | Efficiency vs $P_c$ |
|---|---|---|---|---|---|---|---|---|---|---|
| | | | | | Efficiency Studies | | | | | |
| VCP | 10.0 | AP/RDX | 3850 | 1.22 | 500 | 7.9 | 3 | 92.01 | 260.4 | 92.34 − 0.00065 $P_c$ |
| | | | | | 1000 | 8.2 | 3 | 91.69 | 259.5 | |
| VTJ | 15.5 | AP | 4145 | 1.17 | 500 | 8.2 | 3 | 92.27 | 236.0 | 91.67 + 0.00121 $P_c$ |
| | | | | | 1000 | 8.6 | 2 | 92.88 | 257.7 | |
| VTH | 15.5 | AP | 4173 | 1.17 | 1000 | 11.3 | 3 | 93.36 | 259.5 | 92.36 + 0.00100 $P_c$ |
| VTI | 15.5 | AP | 3971 | 1.05 | 900 | 6.9 | 3 | 90.71 | 252.8 | 89.87 + 0.00169 $P_c$ |
| | | | | | 1000 | 6.4 | 3 | 91.56 | 255.2 | |
| VLC | 14.0 | AP | 4109 | 1.27 | 500 | 11.3 | 3 | 92.84 | 256.7 | 92.08 + 0.00151 $P_c$ |
| | | | | | 1000 | 11.2 | 3 | 93.60 | 258.8 | |
| VTL | 12.0 | AP/RDX | 4008 | 1.24 | 500 | 12.0 | 3 | 92.99 | 261.4 | 93.43 − 0.00069 $P_c$ |
| | | | | | 1000 | 12.2 | 3 | 92.54 | 260.1 | |
| VTO | 8.0 | AP/RDX | 3756 | 1.38 | 1000 | 8.4 | 3 | 92.59 | 260.3 | 91.94 + 0.00065 $P_c$ |
| VTC | 12.5 | AP/TAGN | 3633 | 1.02 | 1000 | 6.8 | 3 | 88.50 | 257.3 | 88.79 − 0.00029 $P_c$ |
| VTM | 14.0 | AN | 3744 | 1.28 | 1000 | 6.2 | 4 | 90.50 | 253.5 | |
| | | | | | AP Particle Size | | | | | |
| VTJ-5421a | 15.5 | AP | 4145 | 1.17 | 810 | 6.8 | 3 | 92.19 | 255.7 | |
| VTJ-5031b | 15.5 | AP | 4145 | 1.17 | 800 | 8.2 | 2 | 92.70 | 257.1 | |
| VTJ-5041c | 15.5 | AP | 4145 | 1.17 | 760 | 9.0 | 2 | 93.24 | 257.4 | |
| | | | | | Nozzle Contouring | | | | | |
| VCPd | 10.0 | AP/RDX | 3850 | 1.17 | 970 | 7.7 | 2 | 92.28 | 261.2 | |
| e | | | | | 1050 | 8.2 | 2 | 92.36 | 261.4 | |
| f | | | | | 1000 | 8.2 | 3 | 91.69 | 259.5 | |
| VTJd | 15.5 | AP | 4145 | 1.17 | 970 | 8.0 | 3 | 93.77 | 260.1 | |
| e | | | | | 1040 | 8.4 | 3 | 93.41 | 259.1 | |
| f | | | | | 1000 | 8.6 | 2 | 92.53 | 257.7 | |

Notes:

1. $T_c$ = Chamber temperature
2. OR = Oxidation ratio $\left(\dfrac{\text{moles O}}{\text{moles C} + \text{moles metal}}\right)$
3. $P_c$ = Chamber pressure
4. $\dot{m}$ = Mass flow rate
5. Least squares analysis for pressure dependence
6. These firings showed a sharp decrease in efficiency with pressure; only high pressure data is shown

a = 180 μ AP
b = 90 μ AP normalized to 800 psia
c = 45 μ AP
d = 5° approach angle
e = 15° approach angle
f = 30° approach angle

60

a.  Be/AP/HMX Propellants - Temperature-Oxidation Ratio Effect

For Be/AP/HMX propellants, the highest efficiency at 1000 psia was 93.6 percent, which was obtained with the high-temperature (4109° K) and high-oxidation-ratio (1.27) propellant, VIK. Increasing the oxidation ratio to 1.38 with a decrease in metal level and flame temperature decreased efficiency to 92.6 percent (VIO firings). Decreasing the oxidation ratio to 1.05 at essentially constant flame temperature decreased the efficiency to 91.6 percent (VII firings). All of the Be/AP/HMX firings appeared to fit the same generalized temperature and oxidation ratio relationship with impulse efficiency shown in Figure 18. The effect of flame temperature and oxidation ratio on efficiency is shown in Figure 25. As noted from the VIO firings, high efficiencies can still be maintained at lower flame temperature by increasing the oxidation ratio. An extension of the data obtained from Task II firings along with the three propellants presented in Table IV to the previous temperature-oxidation-ratio correlation is shown in Figure 26. These firings are in good agreement with the earlier correlation and confirm that a strong temperature-oxidation effect does exist for Be propellants. However, the spread in data indicated other factors exert considerable influence on efficiency as well.

b.  Metal Level Effect

Particle lag considerations dictate that significant losses in impulse efficiency can occur as metal loadings are increased. It is significant, therefore, that the highest efficiencies obtained at 1000 psia were with the VIK and VII formulations having the highest metal levels (14- and 15.5-percent Be, respectively). Because of the interrelation between flame temperature, oxidation ratio, and metal level coupled with the strong efficiency-temperature effect it is impossible to separate metal level and oxidation ratio effects. For example, the data shown in Figure 25, correlated on the basis of temperature and oxidation ratio, can be correlated equally well on the basis of temperature and metal level. There is also a strong indication that metal level influences efficiency at high expansion ratios and is partially responsible for chamber pressure losses.

c.  VCP, VII, VIJ, VIK, and VIL Propellants - Pressure Effects

The five propellants, VCP, VII, VIJ, VIK, and VIL, were specifically tested for pressure effects. The correlations shown previously indicated the high-flame-temperature, high-oxidation-ratio propellants showed little or no efficiency loss with decreasing pressure. It was not possible in this initial correlation to separate the added effects of mass-flow rate and L*. In this program, the mass-flow rate was held essentially constant for a given propellant at two pressure levels. The effect of chamber pressure on impulse efficiency for the five propellants is shown in Figure 27. The three propellants, VII, VIJ, and VIK, showed efficiency losses ranging from 0.6 to 0.9 percent as the pressure was decreased from 1000 to 500 psia. In contrast the VCP and VIL propellants actually showed

41

Figure 25. Effect of Chamber Temperature and Oxidation Ratio on Specific Impulse Efficiency of Task II Be Propellants
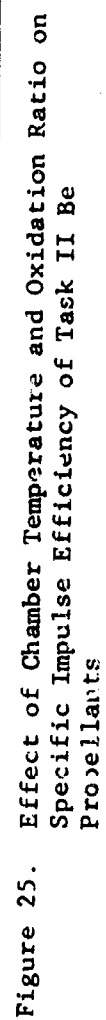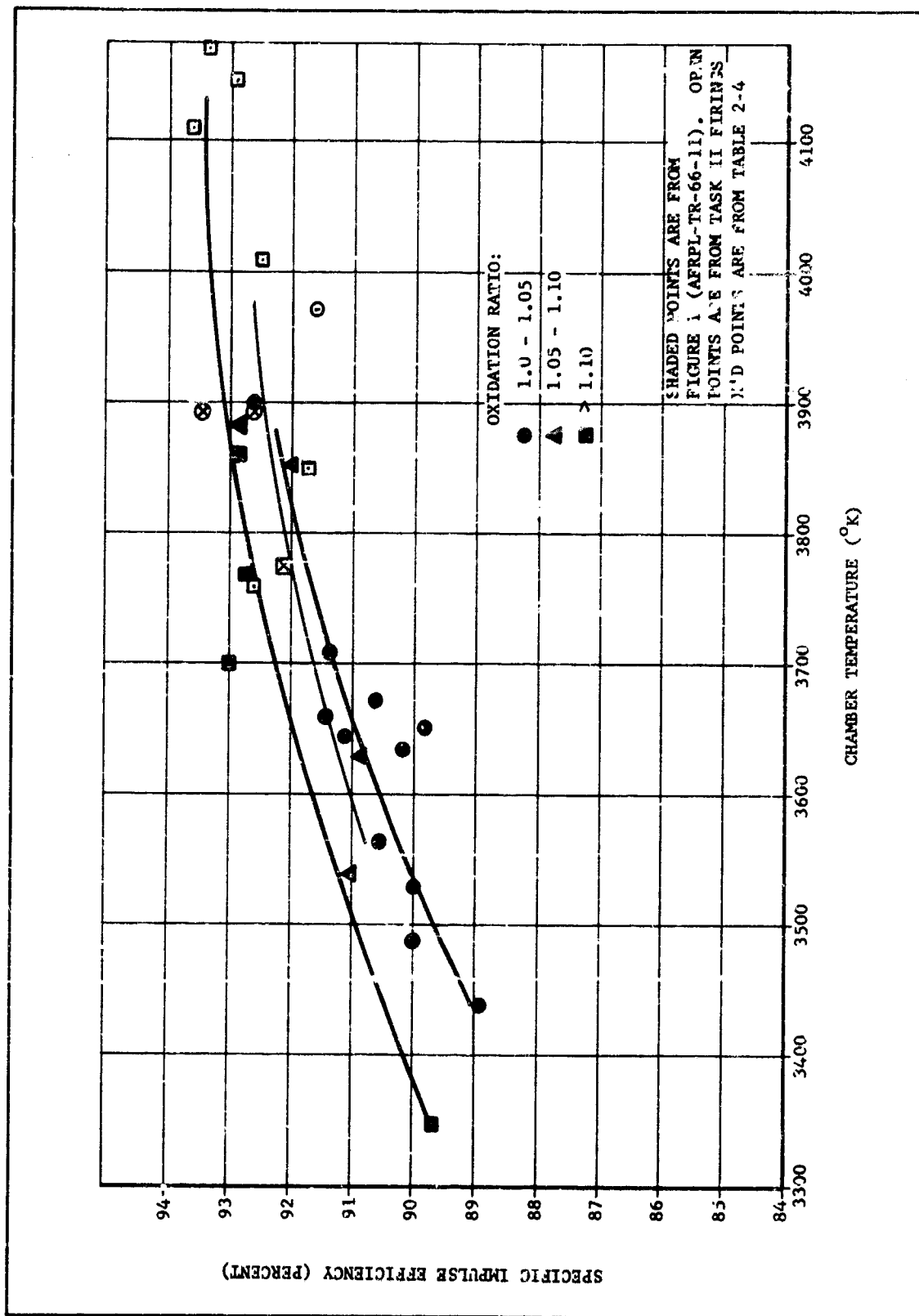
Figure 26. Effect of Chamber Temperature and Oxidation Ratio on Specific Impulse Efficiency of Fe Propellants (Revised)
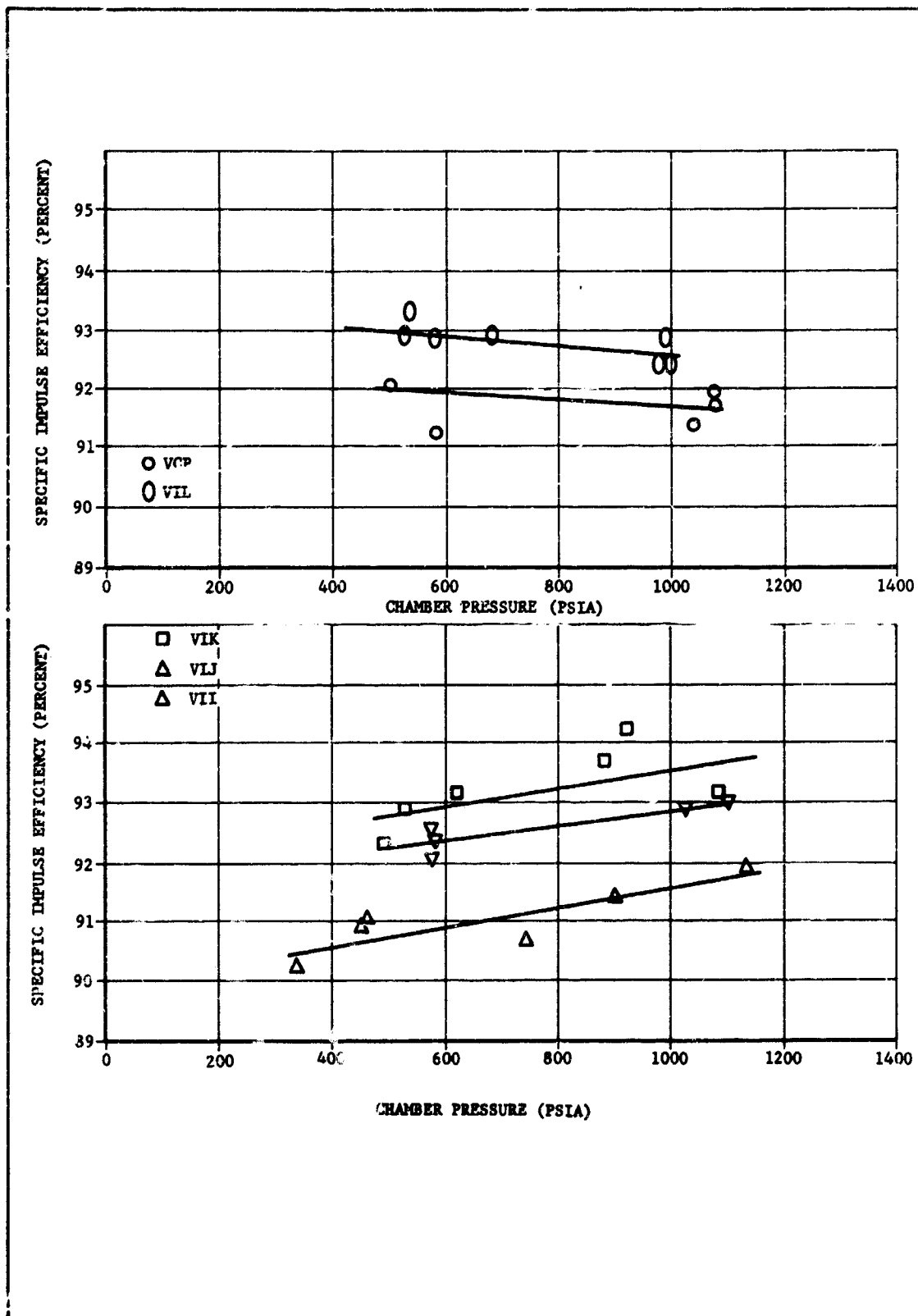
Figure 27.  Effect of Chamber Pressure on Specific Impulse
Efficiency of Be Propellants

a slight increase (0.3 to 0.5 percent) with decreasing pressure. A summary of the important propellant and motor parameters is contained in the following tabulation:

| Propellant | Oxidation Ratio | Tc | Be | Oxidizer | $m^{(1)}$ | $L*^{(1)}$ | $Eff^{(2)}$ |
|---|---|---|---|---|---|---|---|
| VCP | 1.22 | 3850 | 10.0 | AP/HMX | 6.7-8.4 | 130-180 | +0.3 |
| VIL | 1.24 | 4008 | 12.0 | AP/HMX | 9.1-12.1 | 100-150 | +0.5 |
| VIJ | 1.17 | 4145 | 15.5 | AP | 7.8-9.0 | 130-180 | -0.6 |
| VIK | 1.27 | 4109 | 14.0 | AP | 10.1-12.1 | 86-142 | -0.8 |
| VII | 1.05 | 3971 | 15.5 | AP | 6.0-8.0 | 170-260 | -0.9 |

(1) Mass flow and L* range covered

(2) Efficiency at 500 psia minus efficiency at 1000 psia

As shown, chamber temperature and oxidation ratio had no apparent effect on the pressure effects obtained. Mass-flow rates were maintained over a narrow range for a given propellant, and in addition mass-flow rates overlapped for most propellants. Thus, mass-flow rate is not considered a factor in the pressure effects. This leaves differences in metal level, oxygen source, and L* as possible reasons for the observed pressure effects. Data from other sources were correlated in an attempt to relate the above variables to the efficiency losses with decreasing pressure.

Table VI contains a summary of pertinent data on 15 propellants for which the effect of chamber pressure on efficiency was available. However, the motor and propellant parameters are so widely scattered that only general observations can be made. These formulations fall into two basic groups. All of the formulations containing more than 12-percent Be, with the exception of VGR, utilize AP as the sole solid oxidizer. With the exception of Arcocel 191, all these formulations show decreased efficiency with decreasing pressure. The Arcocel 191 data are also unique in that low pressure firings were made at twice the L* of high pressure firings. Increased residence time may well explain the lack of pressure dependence exhibited by this formulation. The largest efficiency loss was observed for the Arcocel 333E formulation, which had the lowest temperature and oxidation ratio. The properties of this propellant are such that a large portion of efficiency losses can be attributed to combustion inefficiencies. For the remainder of the propellants, there was no apparent trend with flame temperature, oxidation ratio, or metal level on efficiency losses with decreasing pressure.

TABLE VI

PROPELLANTS AND PERTINENT DATA FOR EVALUATION
OF EFFICIENCY LOSSES WITH CHAMBER PRESSURE

| Propellant | O.R.[1] | $T_c$ | Be | Oxidizer | $\dot{m}$ | L*[2] | Eff[3] |
|---|---|---|---|---|---|---|---|
| VLJ | 1.17 | 4145 | 15.5 | AP | 8-9 | 130-180 | -0.6 |
| VII | 1.05 | 3971 | 15.5 | AP | 6-8 | 170-260 | -0.9 |
| VIK | 1.27 | 4109 | 14.0 | AP | 10-12 | 86-142 | -0.8 |
| 191 | 1.08 | 3852 | 14.0 | AP | 6-7 | 500-240 | +0.4 |
| VGR | 1.04 | 3895 | 13.0 | AP/HMX | 7-9 | 230-280 | -0.9 |
| 333E | 1.01 | 3630 | 13.0 | AP | 10-15 | 600-720 | -2.4 |
| VIL | 1.24 | 4008 | 12.0 | AP/HMX | 9-12 | 100-150 | +0.5 |
| VIF | 1.05 | 3897 | 12.0 | AP/HMX | 6-9 | 170-230 | -0.3 |
| VID | 1.02 | 3885 | 12.0 | HMX | 6-8 | 243-318 | +0.3 |
| VFE | 1.10 | 3870 | 12.0 | AP/HMX | 8-10 | 200-250 | -0.8 |
| 319B | 1.02 | 3649 | 11.5 | AP/HMX | 5-7 | 540-200 | -1.0 |
| VCP | 1.22 | 3850 | 10.0 | AP/HMX | 7-8 | 130-180 | +0.3 |
| VHH | 1.19 | 3773 | 10.0 | AP/HMX | 6-9 | 215-250 | -0.4 |
| VIB | 1.17 | 3780 | 9.0 | HMX |  | 250-315 | +0.6 |
| VHP | 1.17 | 3703 | 8.0 | HMX | 5-8 | 280-320 | 0 |

(1) Oxidation ratio

(2) Mass flow and L* range covered

(3) Efficiency at 500 psia minus efficiency at 1000 psia

All the propellants presented in Table VI containing 12-percent Be or less utilized large percentages of HMX either as the sole solid oxidizer or in conjunction with AP. Efficiency losses in this group were in general much less than observed for the high metal group. Again, the formulation showing the greatest loss with decreasing chamber pressure had the lowest flame temperature and oxidation ratio (Arcocel 319ʳ). However, no trends of efficiency with temperature and oxidation ratio were apparent for the remainder of the propellants. It is interesting to note that efficiency did not decrease with decreasing pressure for any of the all-HMX-oxidized propellants.

Based on the above observations, it appears that high flame temperatures and oxidation ratios are beneficial in reducing efficiency losses at low chamber pressures. Additional factors such as metal level and oxygen source appear to exert some influence. Increased residence time appeared to improve efficiency for at least one formulation.

### d. Mass Flow and L* Effects

Figure 28 shows impulse efficiency as a function of mass-flow rate and L* for the propellants tested. All of the firings, with the exception of the low-burning-rate propellant (VIN containing AN), were conducted at mass-flow rates in excess of 6 lb/sec. The efficiency of the control propellant VCP, which shows no pressure effect, remained constant over a mass-flow range of 6 to 3 lb/sec. The efficiency data for the remainder of the propellants were widely scattered on the mass-flow plot with a general trend toward higher efficiencies at the higher mass-flow rates. However, if only high pressure firings are considered, no mass-flow effect is apparent.

The data shown on the L* plot in Figure 28 is also widely scattered. However, certain trends appear to exist. In particular, the three propellants, VIJ, VIK, and VII, which show pressure effects also show strong L* effects. A comparison of the data from this program with the L* relation previously developed (Figure 4) shows the higher temperature and oxidation ratio propellants, VIK and VIJ, maintain high efficiencies at relatively low L* values. In contrast, the high-temperature, low-oxidation-ratio propellant VII showed significant losses at relatively high L* values and approximated the low-temperature and low-oxidation curve, as shown. To further explore the effect of L* on efficiency, modifications were made to the standard 15PC to allow a large variation in L* to be made at constant pressure and mass-flow rate. Two Be propellants chosen for evaluation are presented in Table VII. VCP was chosen as the Be control propellant and previously showed no pressure effect or apparent L* effects. Propellant VII was chosen to determine if the efficiency of a high-temperature, low-oxidation-ratio propellant could be improved. Its demonstrated high pressure efficiency of 91.6 percent was considerably below that obtained with other propellants of equivalent temperatures but higher oxidation ratios. Combustion-bomb data also indicated its lower efficiency
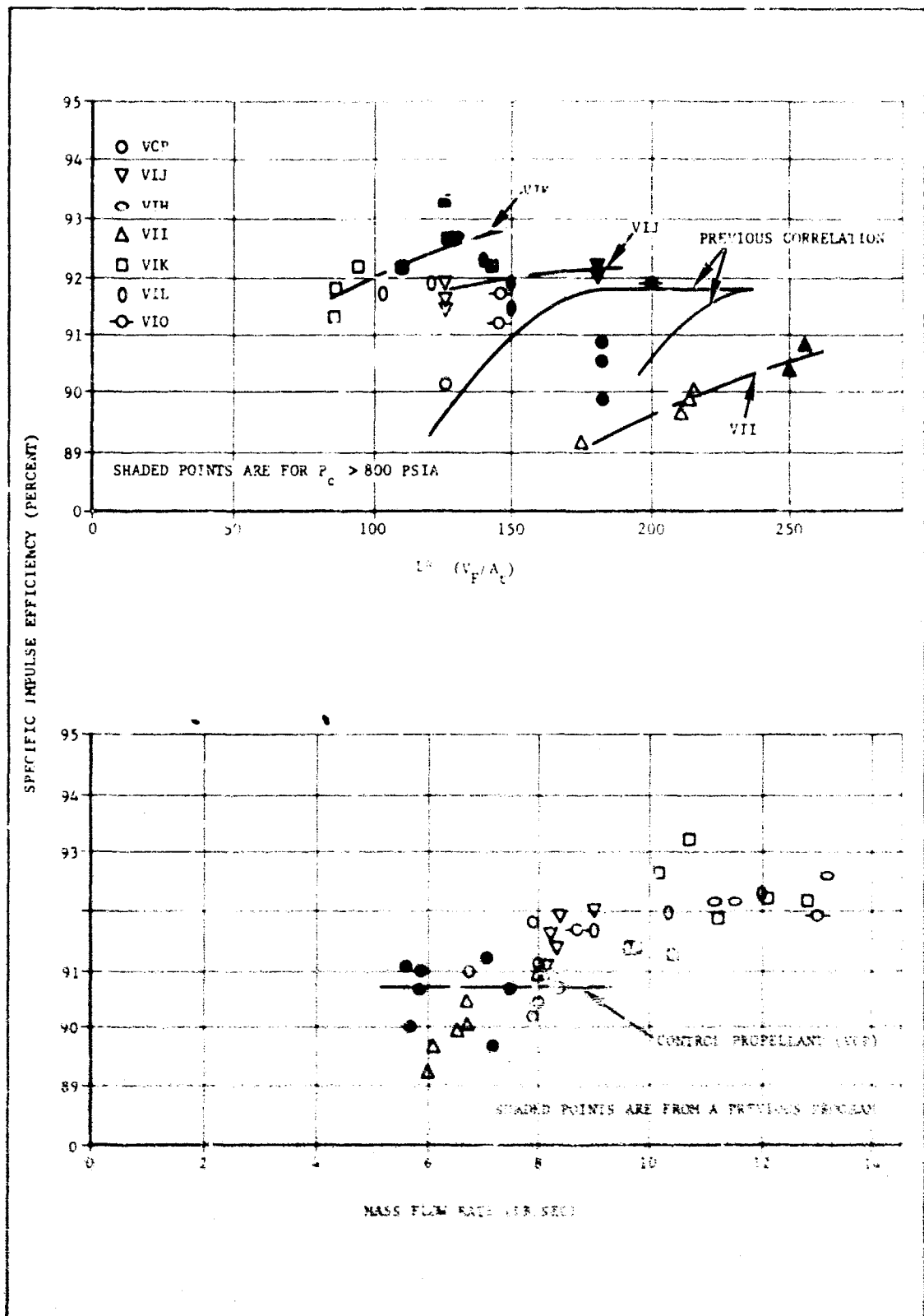
Figure 28. Effect of Mass-Flow Rate and L* on Specific Impulse
Efficiency of Task II Be Propellants

might be due to combustion ineffifiency. (Refer to Table VII.) Propellant VII also showed a significant efficiency decrease with decreasing pressure and L*.

All high L* firings were made at approximately 1000 psia, although a greater effect would be predicted at lower pressures for VII and VIY.

Figure 29 shows the effect of L* on efficiency for the two Be propellants, VCP and VII. A comparison of the efficiency values obtained previously from the least squares analysis of pressure effects with the efficiencies obtained at high L*'s is listed in the following tabulation:

| Propellant Type | VCP | | VII | |
|---|---|---|---|---|
| L* | 225 | 445 | 250 | 390 |
| $P_c$ | 1033 | 1033 | 920 | 920 |
| $\dot{m}$ | 8.2 | 8.0 | 6.4 | 6.7 |
| Efficiency | 91.67 | 91.67 | 91.43 | 91.81 |

As shown, only a marginal increase in efficiency was realized for either propellant. However, although the high L* motor provided more residence time, it also allowed more exposed surface for heat loss. The Minuteman Support Program[9] compared efficiency of various subscale motors and attempted to evaluate the losses due to increased exposed surface for heat loss. Based on their simplified assumptions, the heat loss is proportional to the internal area (other than propellant areas) exposed for thermal radiation and convection. The high L* motors should accordingly have about 60 percent more heat loss than the low L* motors. Assuming the low L* motors have a 1-percent efficiency loss due to heat loss, the high L* motors lose about 1.6-percent efficiency due to heat loss. Thus, some increase in efficiency was probably realized from the higher L* values, but was balanced by a corresponding decrease in efficiency due to heat loss.

e. Propellants with $TAGNO_3$ and AN

The propellants containing $TAGNO_3$ and AN were significantly less efficient than the Be/AP/HMX formulations. The average efficiency for firings of VIG propellant containing TAGNO was 88.5 percent at 1000 psia. For firings of VIN propellant containing AN, the average efficiency was 90.5 percent at 1000 psia. The VIN formulation also showed a 6.0 percent loss in efficiency with decreasing pressure from 1000 to 350 psia. Since the VIN formulation had both a reasonably high flame temperature and high oxidation ratio, the oxygen source is indicated as an important factor. Based on the poor performance of the VIN formulation, AN was eliminated from consideration for LMH-2 propellants. A comparison of oxygen sources is

---

[9] Refer to List of References

TABLE VII

PROPELLANTS FOR HIGH L* STUDY

| Propellant Type | VCP | VII |
|---|---|---|
| Formulation (wt %) | | |
| Binder | 52 | 52 |
| Be | 10 | 15.5 |
| LMH-2 | -- | -- |
| AP | 9 | 32.5 |
| HMX | 29 | -- |
| Theoretical | | |
| $T_c$ ($^\circ$K) | 3850 | 3970 |
| O.R. (1) | 1.22 | 1.05 |
| Ballistic performance | | |
| Motor efficiency (%) (2) | | |
| 1000 psia | 91.7 | 91.6 |
| 400 psia | 92.0 | 90.6 |
| Combustion-bomb efficiency (%) | | |
| 1000 psia | 100 | 98.0 |
| 400 psia | 100 | 91.0 |
| Window-bomb agglomerate size (mils) | | |
| 1000 psia | <1 | 1.91 |
| 400 psia | <1 | 2.53 |

(1) Oxidation ratio
(2) Determined in standard 15PC motor firings
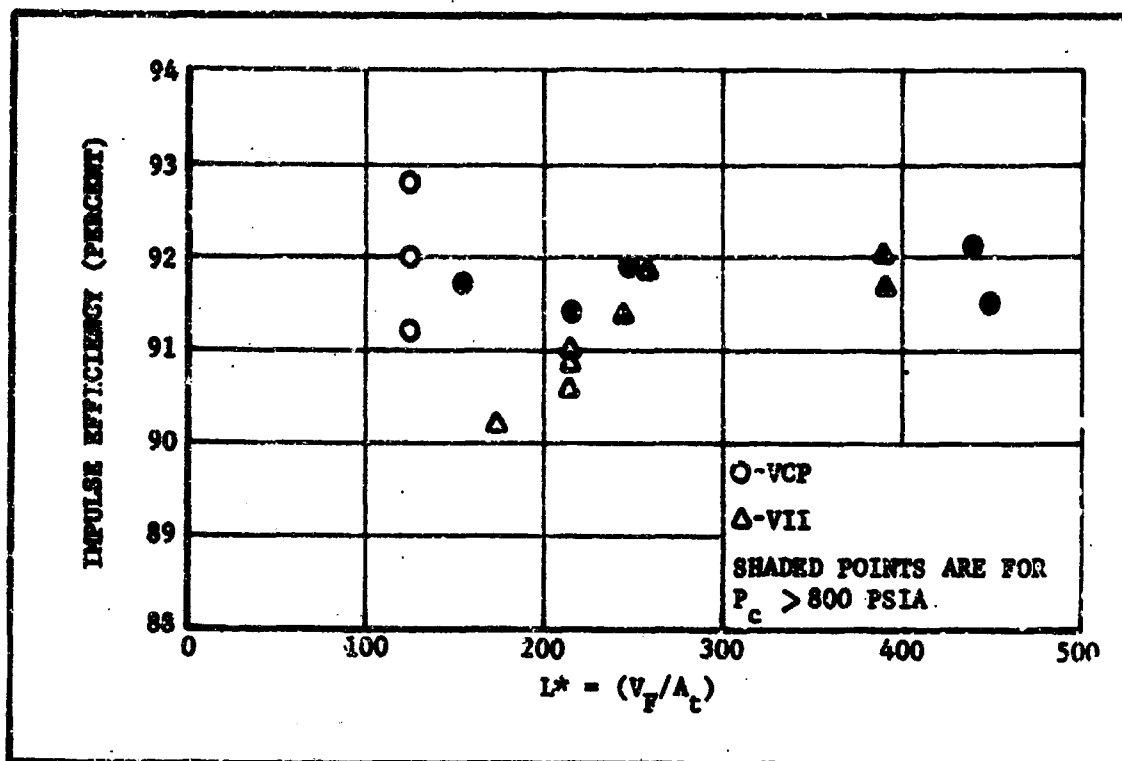
Figure 29. **Efficiency as a Function of L* For Be Propellants**

also available by comparing the VIJ formulation to VIH. Both formulations have the same oxidation ratio and equivalent flame temperatures. However VIH containing 5-percent NG in place of AP gave 0.5-percent higher efficiency. Bases on these results, a ranking of oxidizer effectiveness would be as follows: NG, AP, HMX, AN, and $TAGNO_3$.

### f. Nozzle Approach Contour Effect

The effect of nozzle approach contour cn efficiency for VCP and VIJ is shown in Figure 30. As shown, the efficiency increased 0.6 percent for VCP and 0.9 percent for VIJ when the approach angle was reduced from 30 to 5 degrees. Based on these data, the 15-degree approach appears near optimum and was used for the LMH-2 firings in the final characterization.

### g. AP Particle Size Effect

The effect of AP particle size on efficiency for the VIJ formulation is shown in Figure 31. The efficiency increased 1.0 percent, from $180\mu$ to $45\mu AP$. All of the LMH-2/AP formulations contained $90\mu AP$. These data indicate approximately 0.5-percent increase in efficiency could probably be realized with the LMH-2 formulations if $45\mu AP$ could be incorporated. Use of $45\mu AP$ in LMH-2 formulations was not possible due to processibility considerations.

51
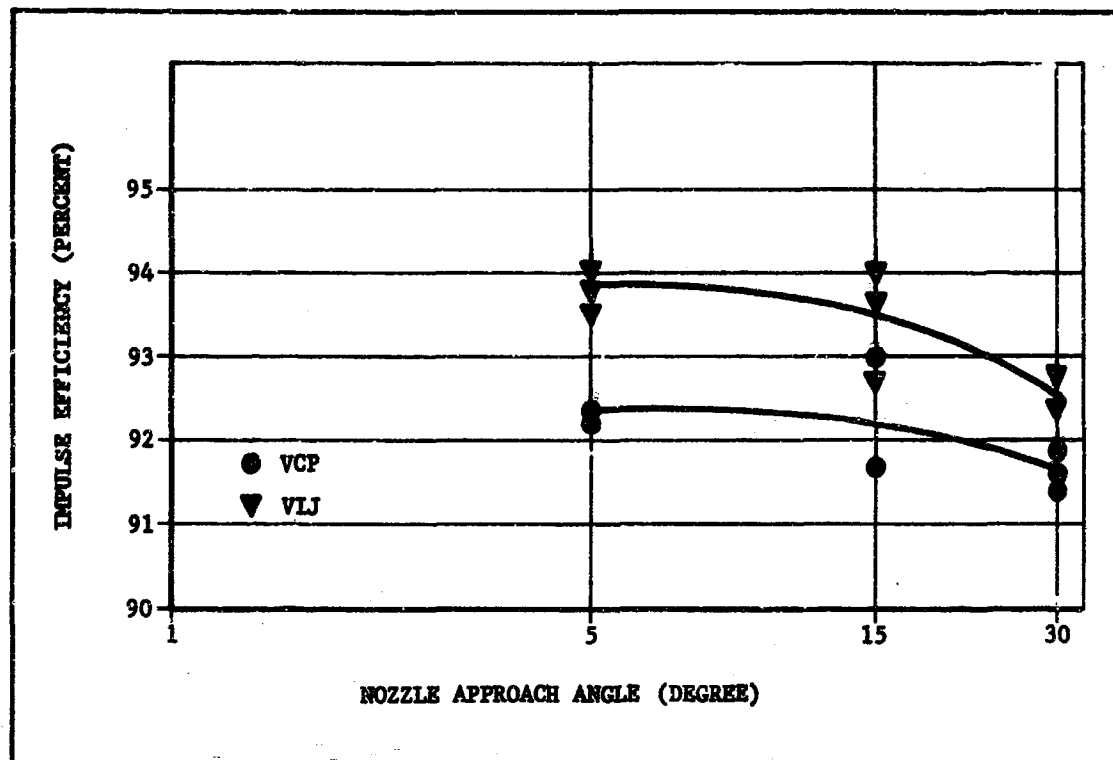
Figure 30. Impulse Efficiency as a Function of Nozzle Approach Angle
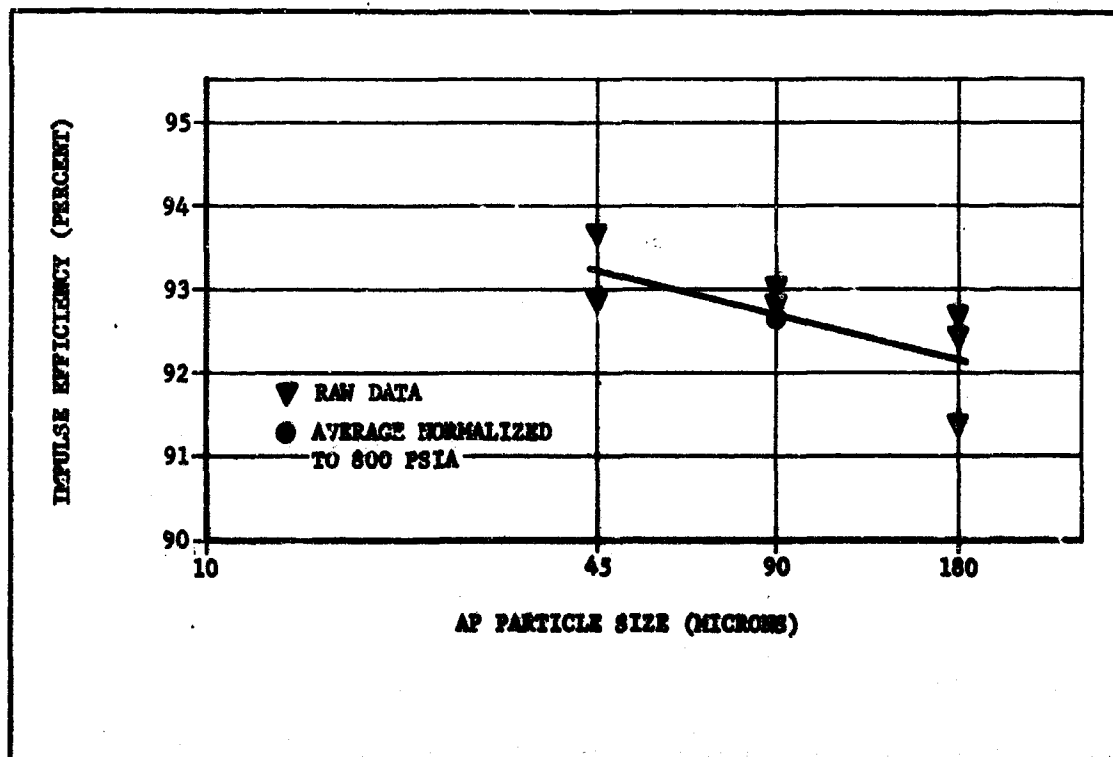


Figure 31. Impulse Efficiency as a Function of AP Particle Size in VLJ Formulations

52

2. LMH-2 Firings

Data from thirty-five 15PC firings of the six candidate formulations is presented in Table III. A complete summary of individual firings is contained in Appendix B, and formulation details are contained in Section IV.

Motor evaluation of the six candidate LMH-2 propellants began with an evaluation of the effect of L* on efficiency. The LMH-2 propellant selected for L* evaluation was VIY, containing wax-treated LMH-2, and VIY, containing AP-treated LMH-2. VIY was chosen because of its high impulse potential coupled with combustion-bomb data, indicating some combustion inefficiency could be expected, particularly with AP-treated material. A secondary purpose was to compare the effect of the two posttreatments on impulse efficiency.

In contrast to the Be results, the VIY firings (Figure 32) gave a significant increase in efficiency at the higher L* values. A summary of the impulse efficiency data is listed in the following tabulation:

| Propellant Type | VIY (Wax treated) | | VIY (AP treated) | |
|---|---|---|---|---|
| L* | 145 | 234 | 119 | 311 |
| Efficiency | 90.25 | 91.01 | 89.51 | 90.98 |
| $Isp^{15}_{1000}$ | 278.9 | 281.1 | 276.5 | 281.0 |

As shown, the efficiency of VIY containing wax-treated LMH-2 increased by 0.7 percent and for VIY containing AP-treated LMH-2 by 1.5 percent. The larger increase in efficiency with residence time for AP-treated LMH-2 is in agreement with the combustion-bomb results, which show the AP-treated material to be less efficient than the wax-treated material. Thus, residence time effects should be more significant for the AP-treated material.

Hardware limitations precluded additional exploration of the L* effect. All further LMH-2 firings were made with the high L* configuration.

A summary of ballistic data obtained from 15PC firings of candidate propellants is contained in Table VIII. As indicated, the first four propellants (VIX, VIY, VIZ, and VJA) met or exceeded the target impulse of 280 lbf-sec/lbm at standard conditions. The highest average delivered impulse of 281.8 lbf-sec/lbm for an efficiency of 89.8 percent was obtained with the AP-oxidized VIZ formulation containing 19-percent LMH-2. The highest efficiency of 92.2 percent was obtained with the AP-oxidized VIZ formulation containing 15-percent LMH-2. These firings gave the highest delivered Isp to date with LMH-2 solid propellants and demonstrated the excellent potential of this ingredient in high-energy systems.
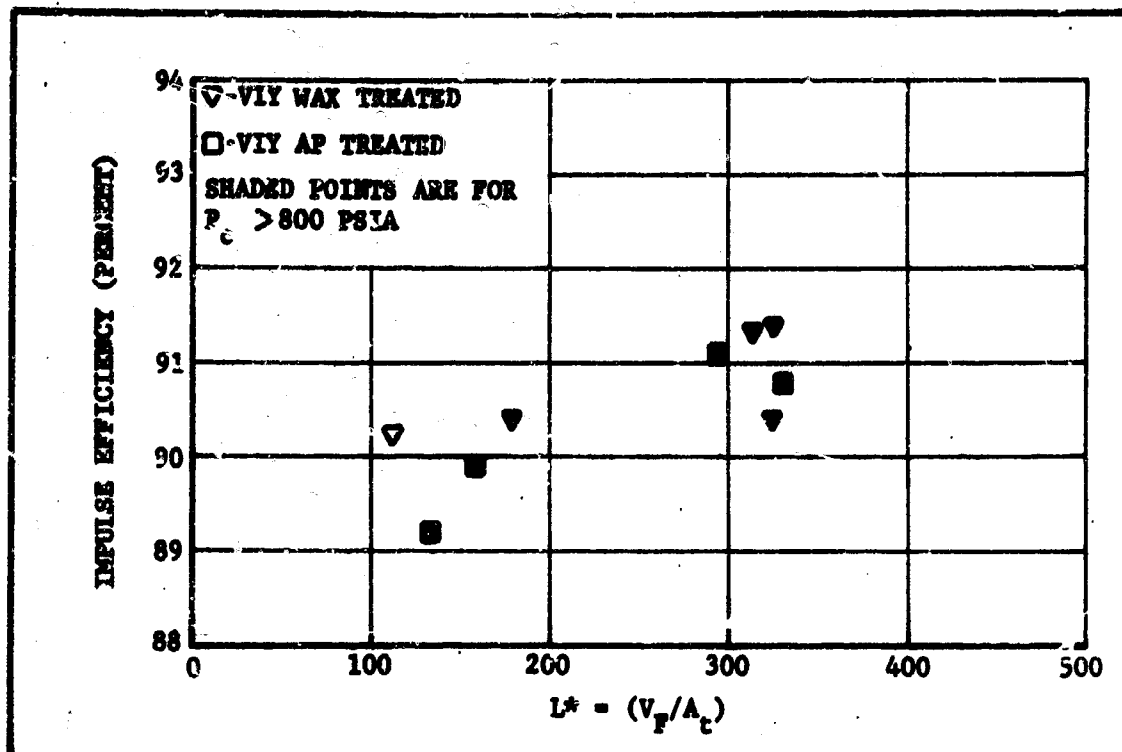
Figure 32. Efficiency as a Function of L* for LMH-2 Propellants

The remaining two LMH-2 candidate formulations (VJI and VJL) gave significantly lower performance than obtained with other formulations as presented in Table VIII. A comparison of the efficiency of candidate LMH-2 propellants tested with that of Be analog formulations on the basis of temperature and oxidation ratio is shown in Figure 33. The VIX, VJA, and Allegany Ballistic Laboratory FIQ formulations all appear to fit the same generalized curve as the Be propellants. However, some deviation of VIY and a major deviation of the remaining lower-oxidation-ratio LMH-2 propellants are apparent. This anomalous behavior is better illustrated in Figure 34, which shows a cross plot of Figure 33 of efficiency versus oxidation ratio at a temperature of approximately 3680° K for both Be and LMH-2 propellants. The efficiency of VIZ is approximately 1 percent below that predicted from the Be correlation. The data show that efficiencies of LMH-2 propellants are comparable to Be propellants for comparable temperature and oxidation ratios at LMH-2 loadings up to 15 to 17 percent and corresponding to oxidation ratios of greater than 1.15. At higher LMH-2 loadings and lower oxidation ratios, LMH-2 propellants appear to be unique.

## 3. Final LMH-2 Confirmation Firings

Based on the demonstrated high performance of VIY and VJA, these formulations were chosen for further ballistic characterization in 15PC firings. The test grid was designed to maintain as high a constant L* as possible while using the longer 15 degree approach and maintaining a mass-flow rate greater than 7 lb/sec. A summary of impulse and efficiency data
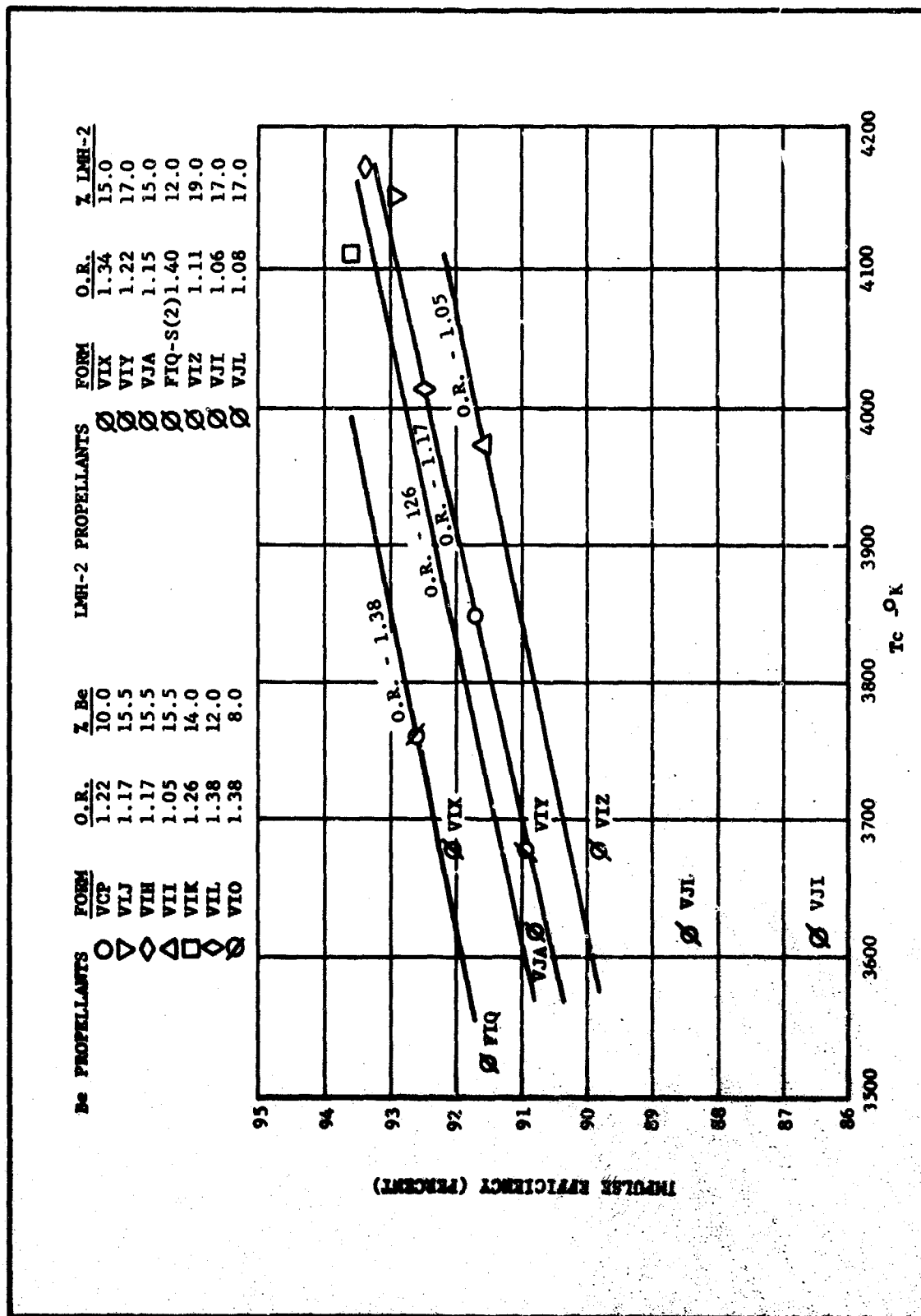
TABLE VIII

LMR-2 FIRING SUMMARY

Figure 53. Effect of Chamber Temperature and Oxidation Ratio on Specific Impulse Efficiency of Be and LMH-2 Propellants
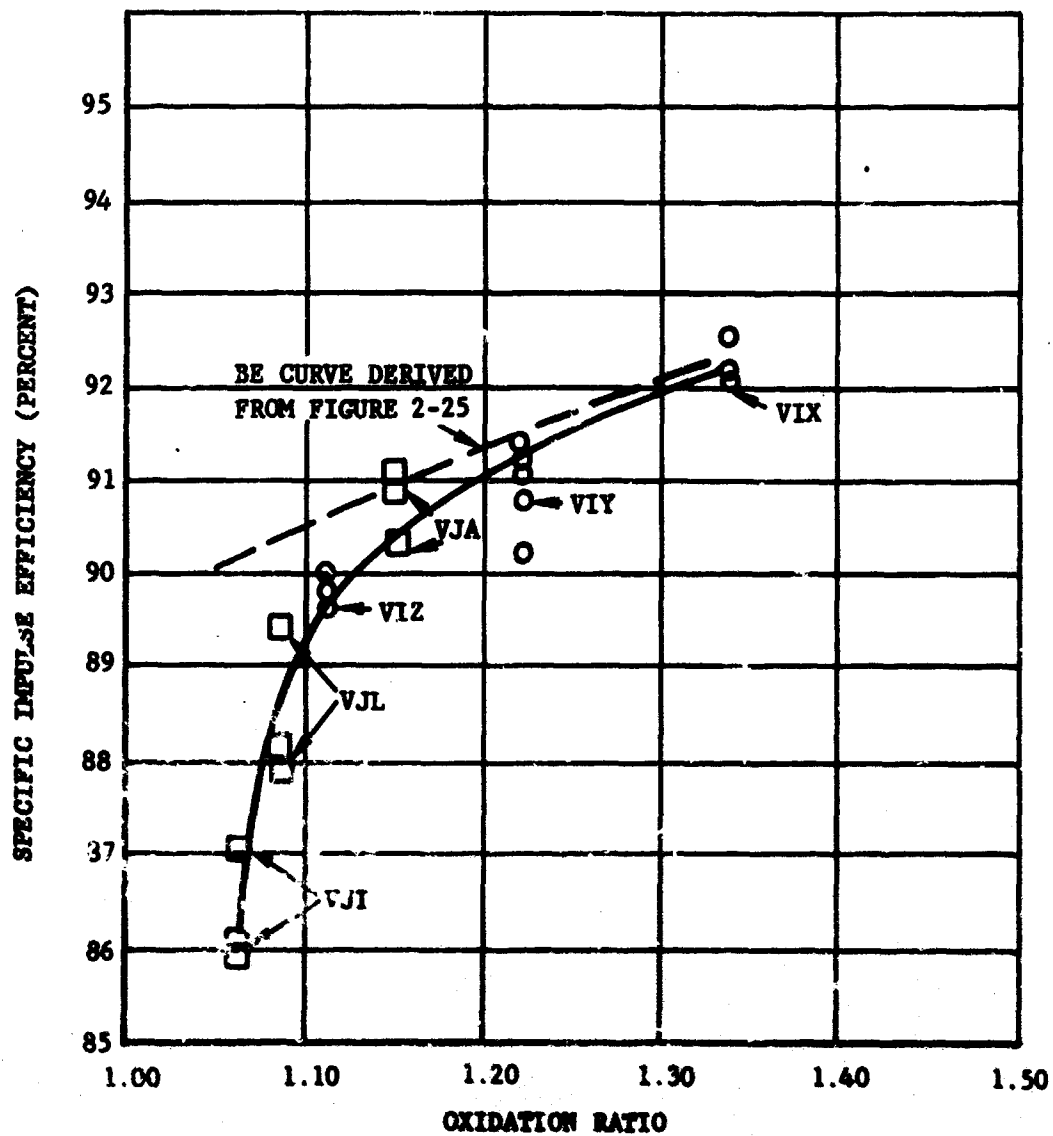
Figure 34.  Impulse Efficiency as a Function of Oxidation Ratio for Be and IRM-2 Propellants

obtained from VIY and VJA firings, along with the data previously obtained, is presented in the following tabulation:

| Formulation | VIY | | | VJA | | |
|---|---|---|---|---|---|---|
| $P_c$ | 641 | 930* | 1290 | 675 | 892* | 1140 |
| $\dot{m}$ | 7.1 | 7.3 | 8.9 | 7.2 | 8.1 | 7.1 |
| L* | 334 | 323 | 315 | 336 | 300 | 344 |
| Efficiency | 89.99 | 91.01 | 91.13 | 90.13 | 90.99 | 89.75 |
| $Isp^{15}_{1000}$ | 278.0 | 281.1 | 281.5 | 278.8 | 281.4 · | 277.6 |

*Data obtained from earlier firings

All of the confirmation firings, except the high-pressure, high-mass-flow-rate VIY firings, gave efficiencies 1 percent lower than previously obtained. These data show chamber pressure has little or no effect on the efficiency of VJA from 650 to 1150 psia. However, mass-flow rate appeared to significantly affect the efficiency of VJA with a 1-percent loss obtained by decreasing the mass-flow rate from 8 to 7 lb/sec. It should be pointed out that the longer 15 degree approach and corresponding greater heatsink may be a contributing factor to the apparent mass-flow effect. For VIY it was impossible to seperate the effects of mass-flow rate and chamber pressure on impulse efficiency. The lower mass-flow rate is suspected to be the major cause of the 1-percent lower efficiency obtained at the lower pressure level. Figure 35 shows the effect of mass-flow rate on efficiency for VJA and VIY appeared comparable at equivalent mass-flow rates with little performance penalty expected for chamber pressure down to 600 psia at high mass-flow rates.

Figure 36 shows efficiency as a function of mass flow for all of the LMH-2 propellants at high L* values compared to the VCP mass-flow curve. As shown, VIX follows the VCP scaling curve, whereas the VIY, VJA, and VJL formulations show a much more severe scaling curve. The VIZ and VJL formulations are less efficient than the VIY and VJA formulations and undoubtedly follow still more severe scaling curves. The apparent tendency of VJL to follow the VIY and VJA scaling curve leaves hope for good performance of this propellant at higher mass-flow rates. Since VJL has a 3-sec higher theoretical impulse than VIY and VJA, the delivered impulse of this propellant may well be higher than either VIY and VJA at high mass-flow rates.

These firings point out the limitations of optimizing performance of LMH-2 propellants in small motors by optimizing motor and propellant parameters. Of the three motor parameters considered--mass-flow rate, L*, and nozzle approach angle--optimization of one parameter can be made only at the expense of the other two parameters within the present hardware limitations. Based on these firings, mass-flow rate appears to be the controlling motor parameter below 8 lb/sec. At higher mass-flow rates, improvements in efficiency are obtained by increasing L*. From these tests it was impossible to detect if any improvement in efficiency was obtained by use of the 15 degree nozzle approach. In addition, some potential
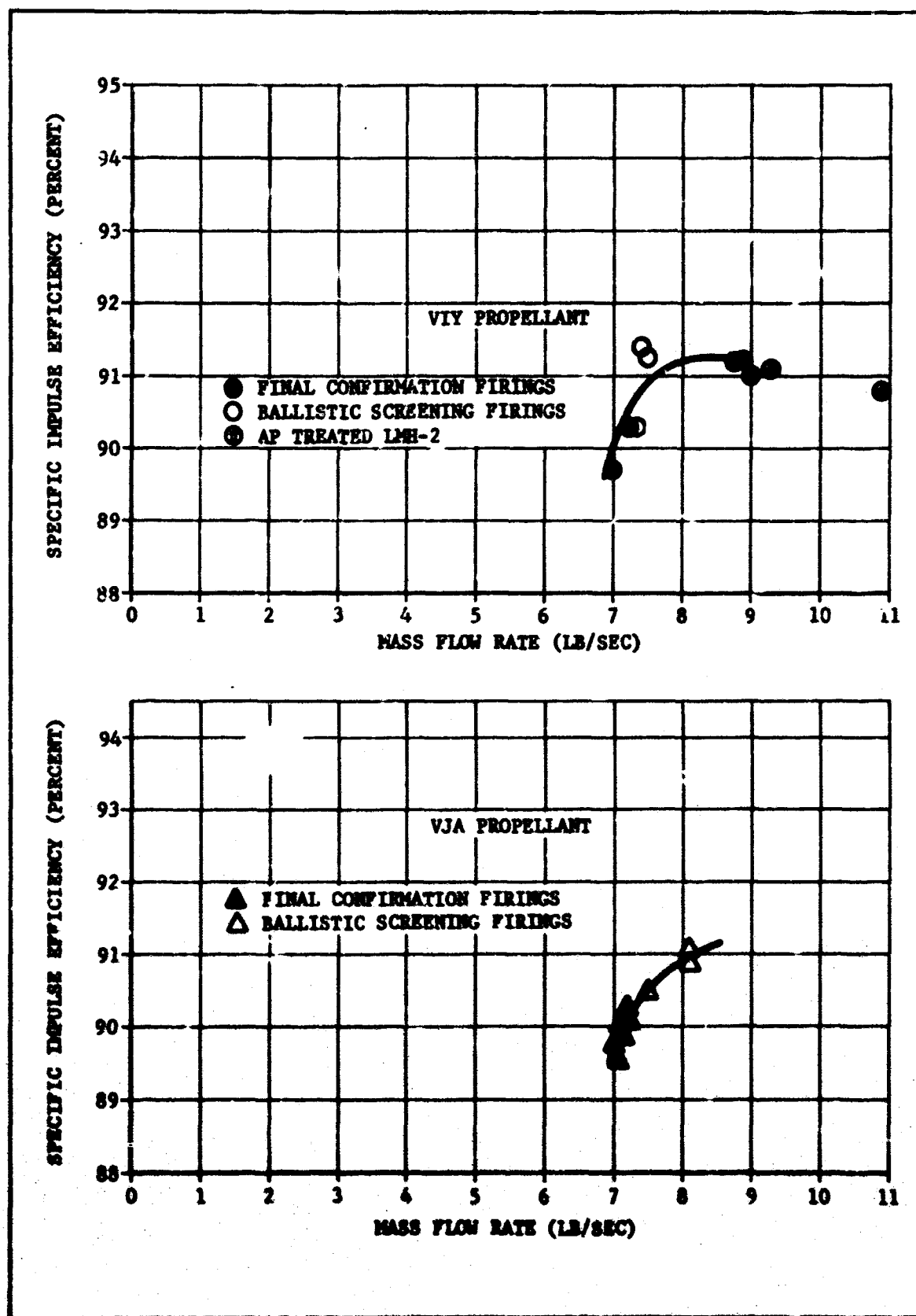
Figure 3 . Impulse Efficiency as a Function of Mass-Flow Rate for VIY and VJA Propellants
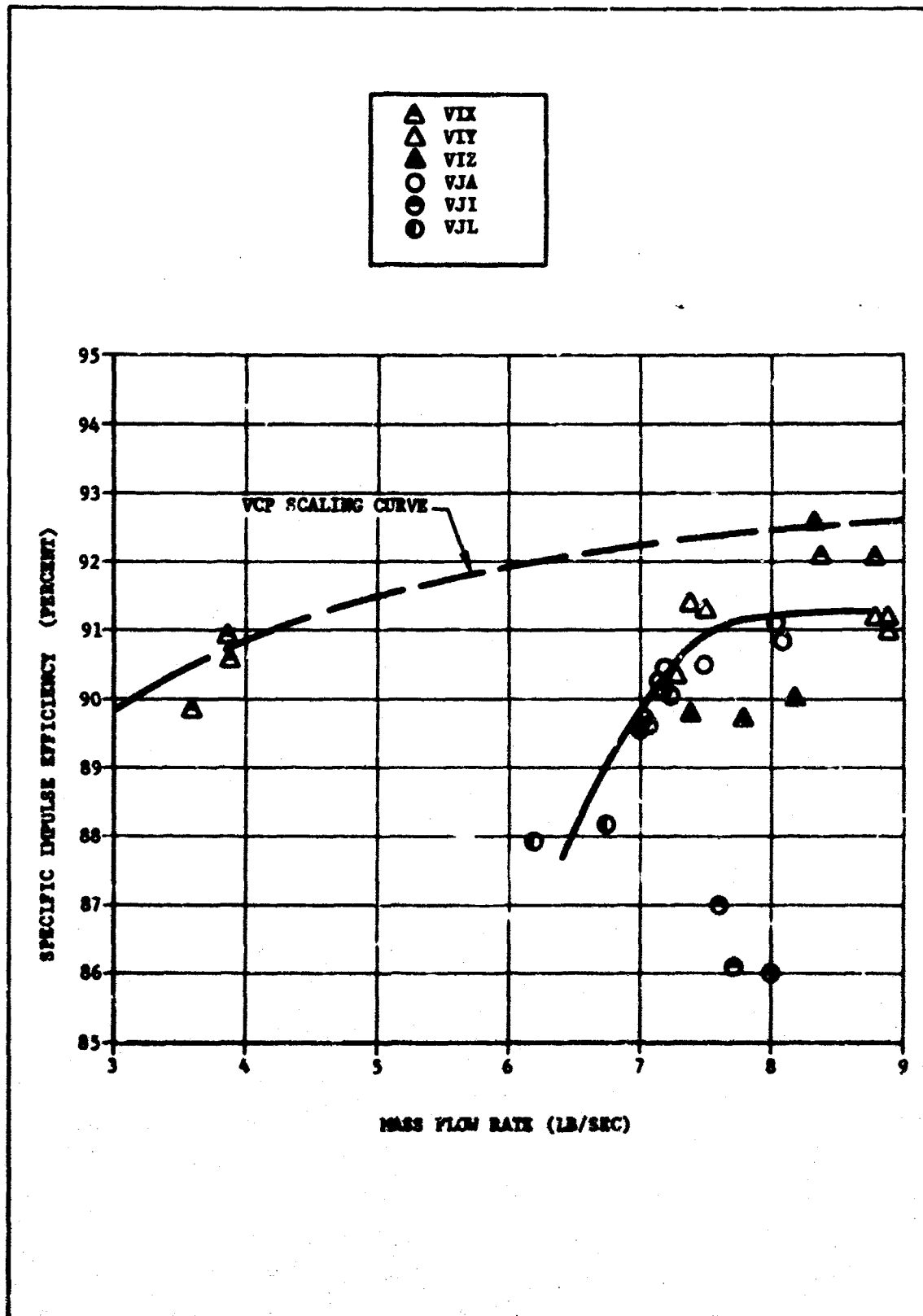
Figure 36. Impulse Efficiency as a Function of Mass-Flow Rate
for LMH-2 Propellants

CONFIDENTIAL

performance gains may be lost by using propellants which show higher performance at less favorable motor conditions in place of propellants with higher theoretical performance which give lower performance in small motors.

4.  **LMH-2 Performance Losses**

The previous analysis and correlations have allowed optimization of propellant and motor parameters to a large extent and corresponding attainment of the program goal. However, the limitations of this semi-empirical approach in leading to a better understanding of losses observed with Be and LMH-2 propellants is acknowledged. The apparent rapid drop in efficiency at high LMH-2 loadings limits the attainment of the ultimate performance potential for LMH-2 propellants, and a clearer understanding of this phenomenon is particularly important. An attempt was thus made to further isolate the factors affecting impulse efficiency.

The basic behavior of LMH-2 in nitrasol propellants has been explored by other recent programs.

Under Contracts AF 04(611)-9097 and AF 04(611)-11219, Lockheed Propulsion Company[10] has used, with some success, the nonequilibrium flame temperature (T*), assuming fuel pyrolysis only, in predicting LMH-2 propellant efficiencies. Fundamental combustion studies have shown that metals such as Be that form protective oxide coatings require temperatures close to their oxide melting points for particle ignition. According to Lockheed, T* values should be in the neighborhood of 2500° to 2600° K, approximating the melting point of BeO (2820° K), for efficient LMH-2 combustion at LMH-2 loadings above 15 percent. Deviations at low LMH-2 loadings and low T* values, where high efficiencies were obtained, were explained in terms of the basic decomposition mechanism. For low LMH-2 loadings, it is suspected that the hydride was ejected into the gas stream; whereas for higher LMH-2 loadings, surface decomposition and metal agglomeration is a favored assumption. T* calculations were performed on six LMH-2 propellants tested and are shown correlated with impulse efficiency in Figure 37. A sharp drop in efficiency at low T* values is observed as predicted.

Under Contract AF 04(611)-10742, Hercules' Allegany Ballistics Laboratory[11] (ABL) has extensively explored the combustion behavior of LMH-2 using combustion-bomb and window-bomb techniques. Results of this work indicate agglomeration is the main cause of observed combustion-bomb inefficiencies. Limited data suggest flame temperature and oxidation ratio influence combustion efficiency by affecting agglomerate combustion rather than agglomerate formation.

A series of closed-bomb tests were also performed on selected Be and LMH-2 propellants tested in this program. Combustion-bomb tests for residue analysis and micro-window-bomb tests for agglomerate size data were performed at ABL using techniques previously employed under Contract AF 04(611)-10742. Heat-of-explosion tests were performed at Bacchus in a standard Parr bomb. Results of these tests are summarized in Table IX.

10,11 Refer to List of References

61
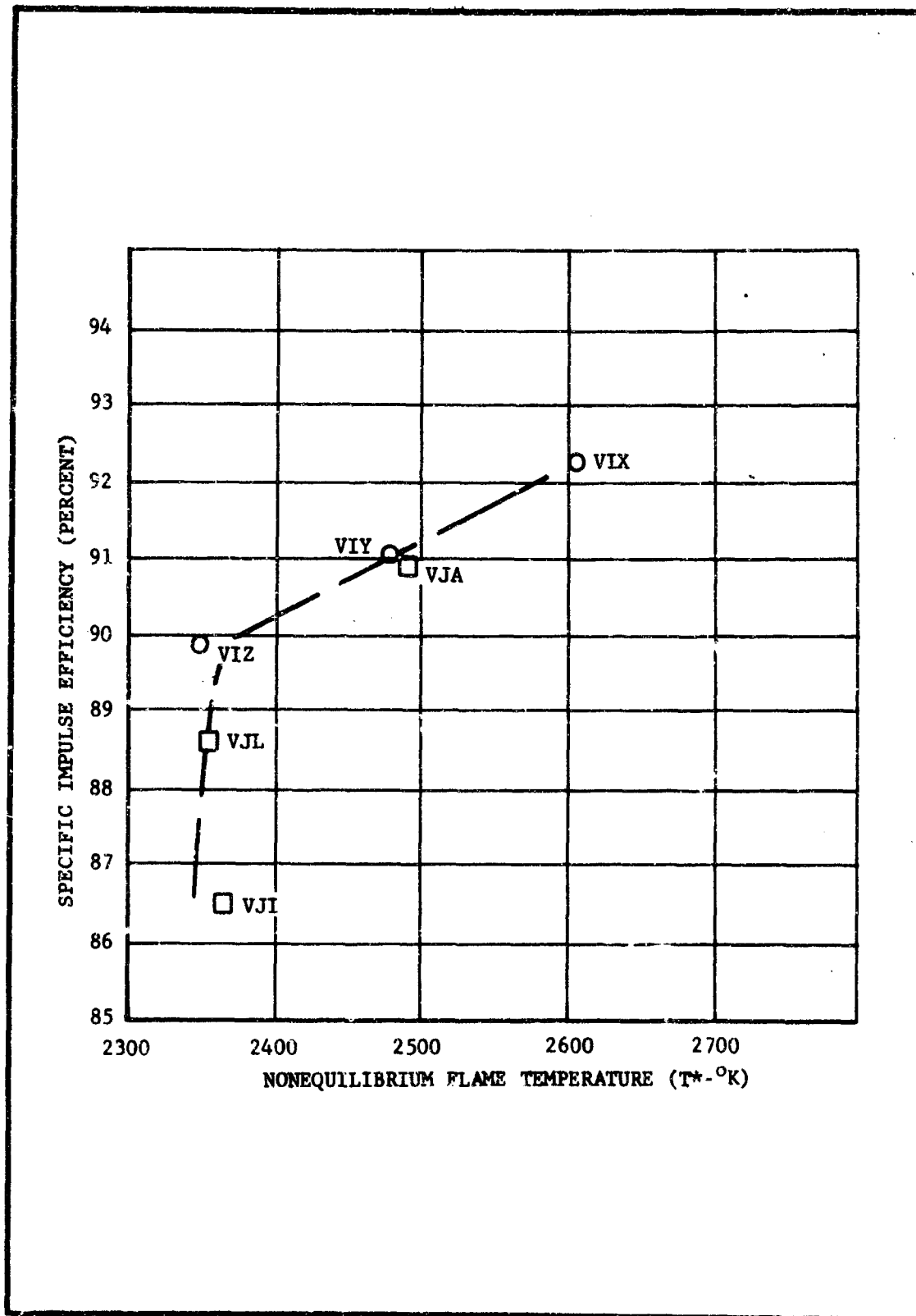
CONFIDENTIAL

Figure 37.   Effect of T* on Efficiency of LMH-2 Propellants

TABLE IX

CLOSED BOMB DATA

| | Beryllium Propellants | | | | | | | | | | LMB-2 Propellants | | | | | | | | | |
|---|---|---|---|---|---|---|---|---|---|---|---|---|---|---|---|---|---|---|---|---|
| | VIH (45μAP) | VII (90μAP) | VLI (45μAP) | VLI (90μAP) | VLI (180μAP) | IIK (-5μAP) | VIL (45μAP) | VIH | VIH | IID (45μAP) | VIX | VIX(1) | VIX | VIX(2) | VIX(1) | VIX(3) | VJA | VJI | VJL |
| Mix No. | 37-40 | 69-41 | | 37-95 | 83-100 | 27-96 | 37-99 | 70-73 | 70-87 | | 37-97, 83-2 | 83-31 | 83-52 | 83-52 | 83-31 | 83-56 | | | |
| Residue analysis(4) | | | | | | | | | | | | | | | | | | | |
| Pressure (psia) | | | | | | | | | | | | | | | | | | | |
| 1000 | 100 | 97.5 | 99.7 | 100 | 98.5 | 99.8 | 100 | 77.0 | 83.3 | 99.8 | 100, 100 | 98.2 | | 93.0 | 96.4 | | 96.0 | 89.0 | |
| 400 | 99.7 | 90.8 | 99.6 | 100 | 82.6 | 99.4 | 100 | 43.8 | 50.9 | 99.5 | 96.4, 97.5 | 93.3 | | 95.8 | 89.4 | | 94.0 | 84.0 | |
| Window bomb agglomerate size (mils) | | | | | | | | | | | | | | | | | | | |
| Pressure (psia) | | | | | | | | | | | | | | | | | | | |
| 1000 | <2 | <2 | <1 | 2.8 | 2.3 | 1.0 | <2 | 8.0 | 6.5 | <2 | 2.7, 3.4 | 3.6 | | 4.1 | 4.0 | | 3.5 | 4.1 | |
| 400 | <2 | 2.5 | <1 | 4.6 | 3.3 | 1.0 | <2 | 15.8 | 14.1 | <2 | 3.3, 4.7 | 4.3 | | 4.5 | 5.2 | | 4.1 | 4.8 | |
| 200 | Small flaking | - | - | Flaking | - | | <2 | - | 12.8 | - | 4.5, 4.3 | 4.6 | | - | - | | - | - | |
| Heat of explosion(5) (cal/gm) experiment | | | | 2628, 2606 | | | | 2172 | 1992, 2024 | 1955 | 2311, 2280 | 2324, 2296 | 2320 | 2333, 2330 | 2303 | 1866, 2337 | 2001, 2142, 2158 | 2068 | 2235 |
| Heat of explosion(5) (cal/gm) theoretical | | | | 2654 | | | | 2331 | 2205 | 1867 | 2270 | 2270 | 2384 | 2384 | 2384 | 2500 | 2217 | 2305 | 2385 |
| Percent of theoretical | | | | 98.3 to 99.2(6) | | | | 93.2 | 90.5 to 91.6 | 105 | 101 to 102 | 101 to 102 | 97.3 | 97.7 to 98.7 | 96.6 | 74.6 to 93.5 | 96.2 to 97.5 | 89.7 | 93.7 |

Notes:

(1) Contains AP treated LMB-2

(2) Contains 0.5 percent urea on LMB-2

(3) Contains 0.5 percent urea over-coat on AP treated LMB-2

(4) Percent beryllium converted to BeO

(5) Heat of explosion values refer to formulation but not necessarily mix numbers

(6) Values were obtained on VLI (45μAP) and VLI (180μAP) respectively

Analysis of the data in Table IX indicates the following:

(a) Beryllium propellants--VIH, VII, VIJ, VIK, VIL and VIO --all showed good combustion efficiency at 1000 psia, with maximum impulse losses of 0.5 percent predicted for VII and VIJ (180$\mu$AP). VII and VIJ (180$\mu$AP) formulations showed combustion inefficiencies at 400 psia with an impulse loss of 1.5 percent predicted for VII and 3.0 percent for VIJ (180$\mu$AP). Based on agglomerate size, VIJ (90$\mu$AP) could also show efficiency losses at low pressures.

The VIM and VIN data show AN-oxidized systems to have a significantly lower efficiency than AP-oxidized systems. Based on these data, only a limited number of AN firings were made to confirm the combustion-bomb results.

(b) LMH-2 propellants, VIX and VIY formulations, gave good combustion-bomb efficiencies at high pressures with a trend toward lower efficiencies at lower pressures. The use of AP-treated LMH-2 also decreased efficiency. Of the remaining two formulations tested in the combustion bomb (VJA and VJI), both were HMX oxidized and were significantly less efficient than AP-oxidized propellants. As shown, heat-of-explosion data appeared to follow the same trend as the combustion-bomb data. Also of significance is the larger agglomerate size of LMH-2 propellants compared to efficient Be propellants.

Although decreasing combustion-bomb efficiencies imply lower impulse efficiencies, a direct relation remains to be established. Some insight may be gained, however, by calculating the impulse efficiency loss based on unburned Be and also by a direct comparison of closed-bomb data with observed impulse efficiencies. Table X contains calculated impulse losses assuming fixed percentages of unburned LMH-2 for VIY and VJI formulations. These data show a maximum calculated loss of 2 percent based on combustion-bomb efficiency for the VJI formulation. However, the impulse efficiency of VJI was 6 percent lower than that of the VIX formulation showing no unburned Be. This large discrepancy precludes the estimation of impulse losses from combustion-bomb data directly. However, Figures 38 and 39 show a definite trend toward lower impulse efficiences with lower combustion-bomb and heat-of-explosion efficiencies, although other effects are obvious. In addition, Figure 40 illustrates a trend toward lower motor efficiencies with increasing agglomerate size, as determined from window-bomb firings; although, again, a large variance is present. These trends support the agglomeration theory for the observed inefficiencies at high LMH-2 loading and low oxidation ratios. Data are too limited to determine the interaction of $T_c$, $P^*$, or oxidation ratio on the

agglomerate formation. However, ABL has made the following observations relating to the effect of agglomerate formation on LMH-2 combustion efficiency:

(a) At constant flame temperature and oxidation ratio, combustion efficiency is inversely proportional to the agglomerate size.

(b) For constant agglomerate size, combustion efficiency increases with increasing flame temperature and oxidation ratio.

(c) Agglomerate size increases with increasing LMH-2 loadings and particle size.

(d) Agglomerate size increases with increasing AP particle size.

These observations, coupled with the developed flame-temperature and oxidation-ratio correlations, may be used as guides in optimizing LMH-2 performance. However, the determination of the interaction between agglomerate growth and the propellant environment appears necessary before the ultimate potential of LMH-2 propellants can be projected. The large differences between the observed efficiency losses and those predicted from combustion-bomb efficiency also warrants additional consideration. Because of the lower flame temperature of LMH-2 propellants, coupled with the high melting points of BeO, nozzle losses may be partially responsible for the discrepancy. Figure 13 shows that both Be and LMH-2 propellants show efficiency losses with increasing expansion ratio. If, as has been suggested, these losses are connected with supercooling phenomena, the lower flame temperature Be and LMH-2 propellants should exhibit these losses early in the expansion process. Calculations were performed on the VIY formulation to determine the magnitude of the losses to be expected from supercooling and are summarized in Table XI. As shown, a 1-percent loss is calculated for VIY at an expansion ratio of 10:1, whereas no loss is calculated for the high-temperature Be propellants at this expansion ratio. In addition, Table X shows that for 10-percent unburned Be in the VJI matrix, a flame temperature decrease of approximatley $200^\circ$ K could reduce impulse efficiency by an additional 1 percent, assuming supercooling.

In summary, the performance losses associated with Be and LMH-2 propellants appear due to a combination of both combustion and expansion losses. The combustion losses appear due to agglomeration, which is improved mainly by higher flame temperatures and oxidation ratios. Nozzle losses also are probably a function of the combustion efficiency and flame temperature. Additional testing and analysis are needed to better define the interaction between the combustion process and the resultant impulse efficiency.

## TABLE X

### EFFECT OF UNBURNED Be ON THEORETICAL
### IMPULSE FOR LMH-2 PROPELLANTS

| Wt % Unburned LMH-2* | Theoretical Isp(1000/14.7) | Calculated Efficiency | $T_c$ ($^\circ K$) | O.R. |
|---|---|---|---|---|
| VIY | | | | |
| 0 | 308.9 | 100 | 3679 | 1.22 |
| 5 | 306.6 | 99.3 | 3595 | 1.26 |
| 10 | 303.8 | 98.4 | 3503 | 1.30 |
| 20 | 297.3 | 96.2 | 3294 | 1.36 |
| 50 | 279.8 | 90.6 | 3020 | 1.73 |
| VJI | | | | |
| 0 | 314.0 | 100 | 3623 | 1.06 |
| 5 | 311.2 | 99.1 | 3537 | 1.09 |
| 10 | 307.9 | 98.1 | 3440 | 1.12 |
| 20 | 301.2 | 95.9 | 3217 | 1.19 |
| 50 | 282.6 | 90.0 | 2959 | 1.45 |

*Calculations assume pyrolysis of LMH-2 to Be
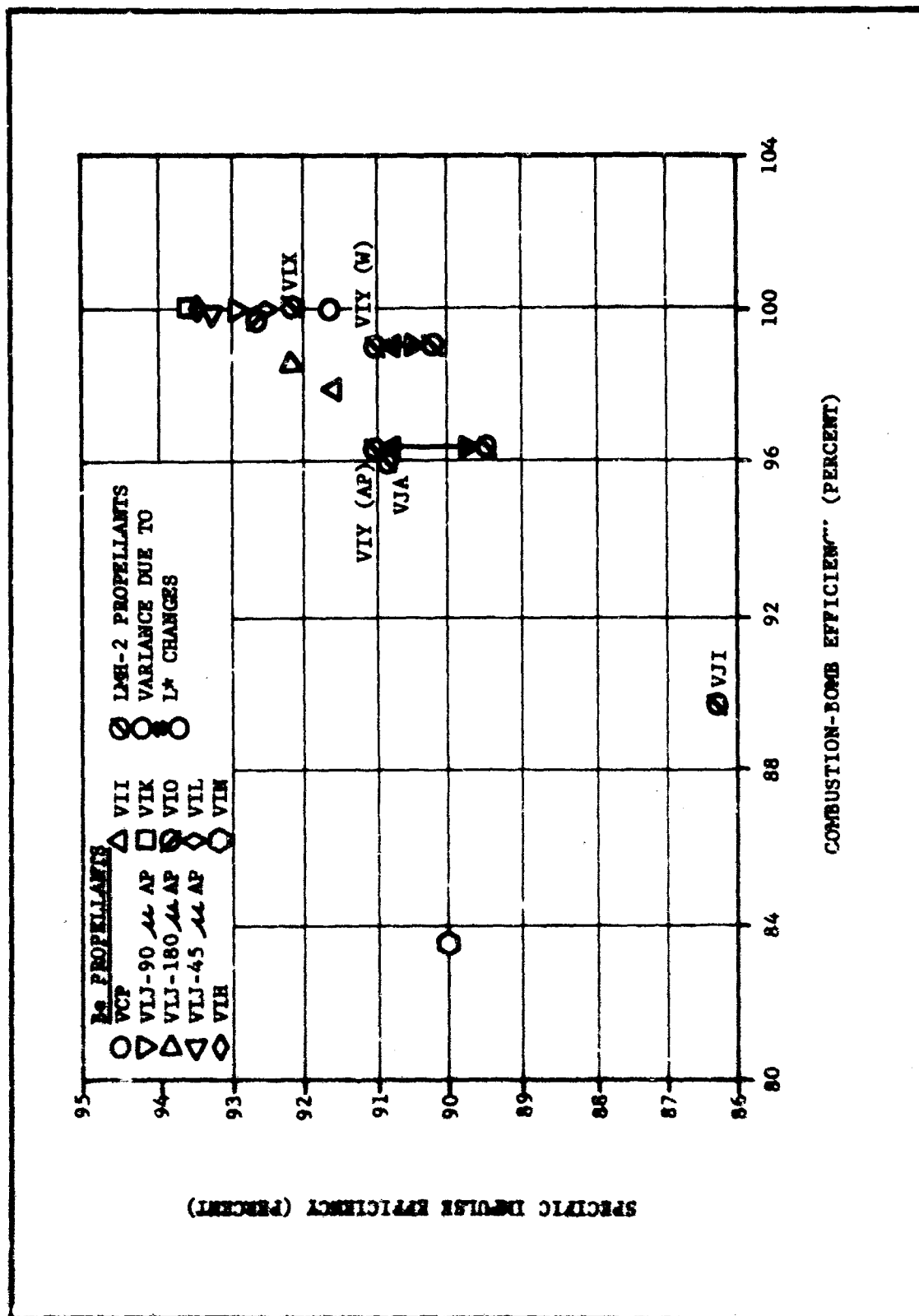
Figure 38. Impulse Efficiency as a Function of Combustion-Bomb Efficiency
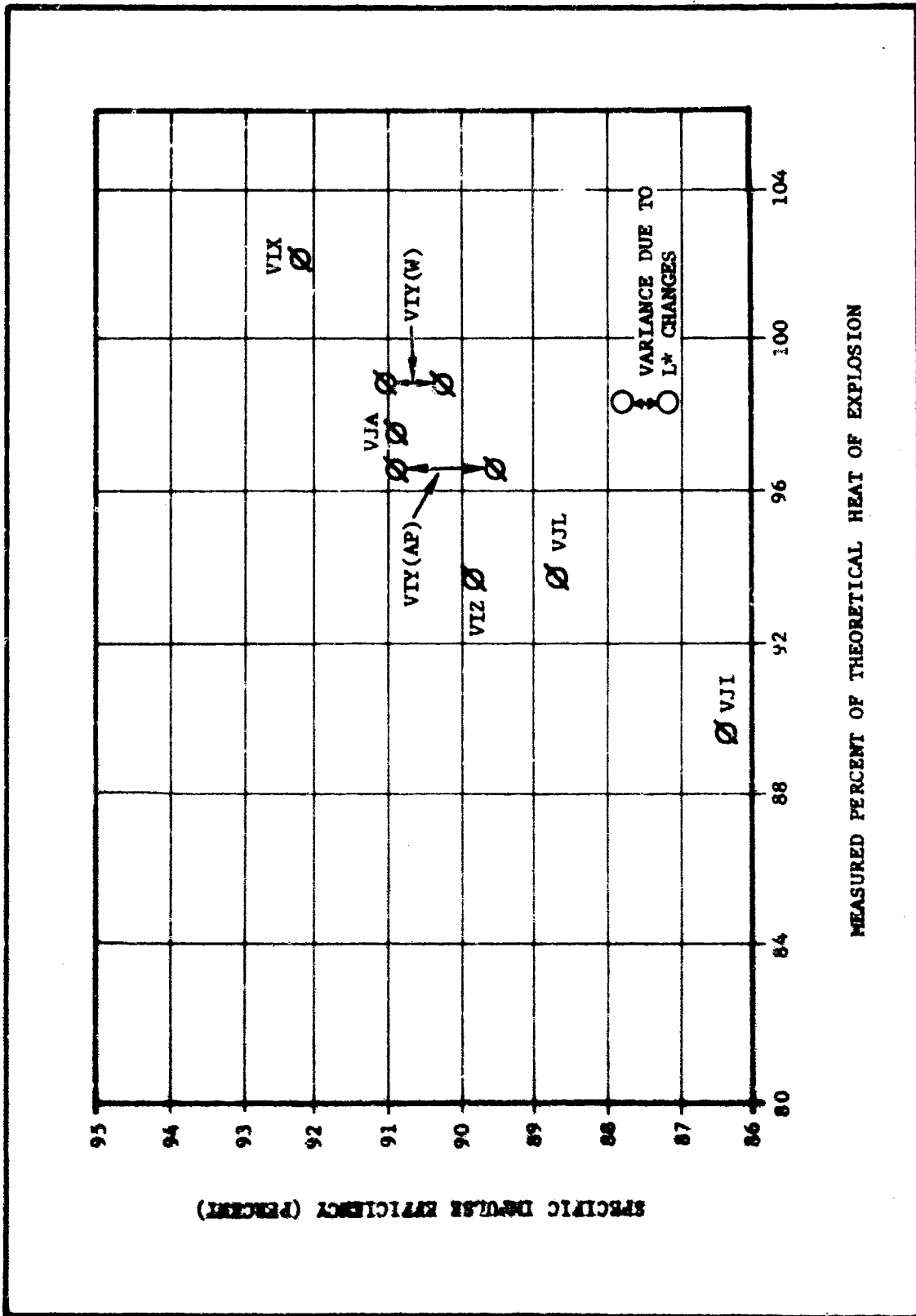
Figure 39. Impulse Efficiency as a Function of Heat-of-Explosion Efficiency for LMH-2 Propellants
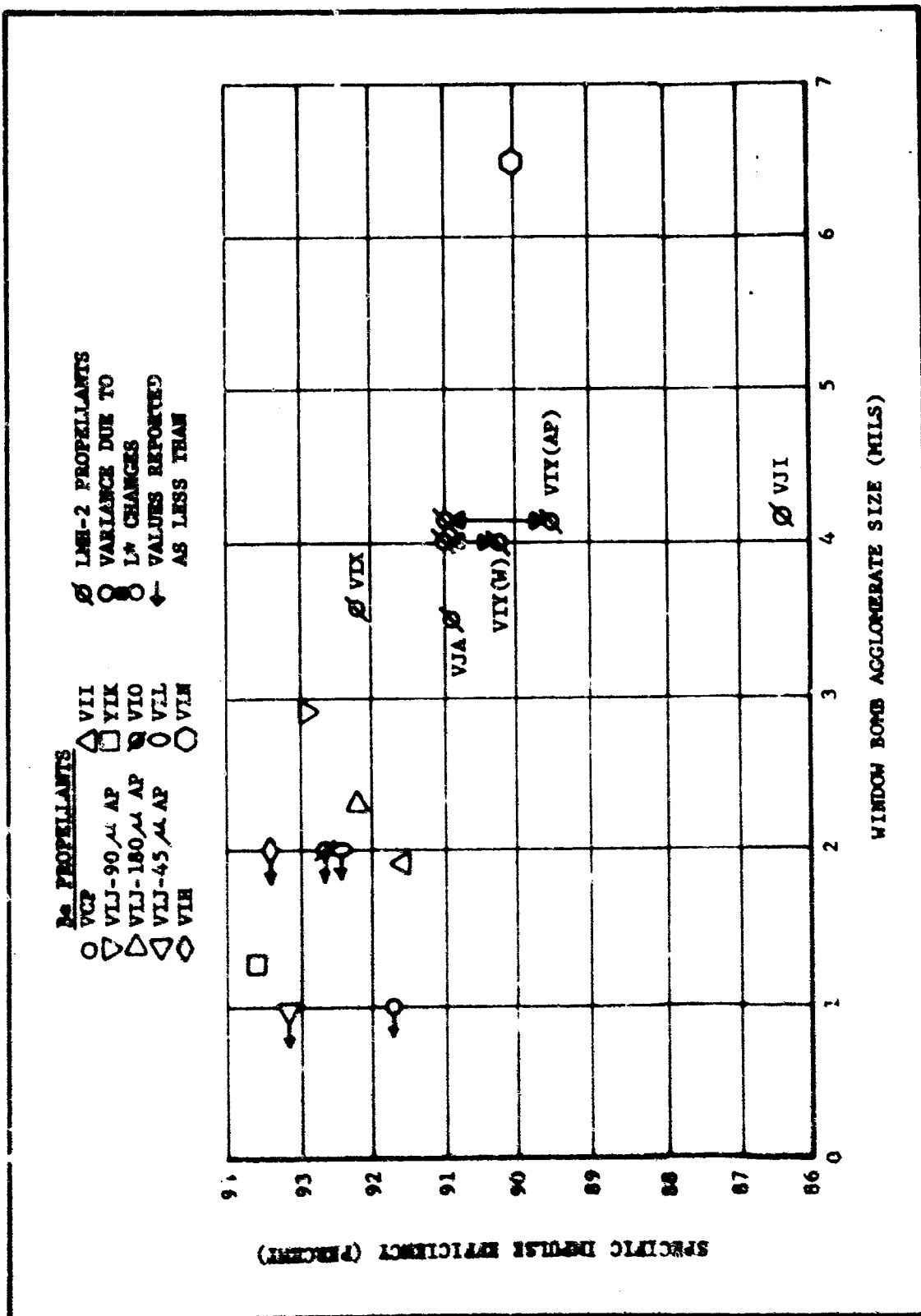
Figure 40. Impulse Efficiency as a Function of Agglomerate Size

TABLE XI

CALCULATED EFFECT OF SUPERCOOLING FOR
THE VIY FORMULATION

| Expansion Ratio | Equilibrium Exit Temp (°K) | Equilibrium Vacuum Isp | Supercooled Exit Temp (°K) | Supercooled Vacuum Isp | Efficiency (%) |
|---|---|---|---|---|---|
| 3.5 | 2820 | 297.8 | 2764 | 297.8 | 100 |
| 5.0 | 2820 | 311.6 | 2623 | 310.8 | 99.7 |
| 7.5 | 2740 | 326.4 | 2471 | 324.0 | 99.3 |
| 10.0 | 2638 | 335.8 | 2367 | 332.4 | 99.0 |
| 30.0 | 2256 | 366.1 | 1994 | 359.3 | 98.1 |
| 50.0 | 2083 | 377.5 | 1836 | 369.5 | 97.9 |

F.   ULTIMATE LMH-2 PERFORMANCE POTENTIAL

It should be emphasized that the high delivered impulses obtained
for LMH-2 propellants in this program were achieved mainly by the use
of a high-energy binder (16.4 NC/82.0 HG). The energy level of this binder
is felt to be close to the maximum within the present state-of-the-art. As
higher energy plasticizers and oxidizers become available, higher performance
levels from LMH-2 propellants can be reasonably projected. Of particular
interest are the advanced perchlorate oxidizers and difluoramino compounds.

Consideration must also be given to the effect of motor scaling on
LMH-2 performance. Some estimate of the effect of motor scaling is available
by considering data generated on L* and mass-flow rate effects for LMH-2
propellants tested to date. Figure 32 shows that additional improvements
in efficiency can be expected by increasing L* levels above 300. Because of
the increased heat loss to the high L* motor, improvements in addition to
those shown can also be expected for a low-heat-loss motor. Data obtained
from Task II firings indicate an increase of efficiency of 0.5 percent can
be obtained by decreasing the nozzle approach angle from 30 to 15 degrees.
Combining these effects, efficiencies as high as 97.5 percent can reason-
ably be projected for VIY, giving a delivered impulse of approximately
285 sec in PFC motors.

Although density was not a consideration in formulation of the initial LMH-2 propellants, it is now interesting to explore the optimum performance potential of LMH-2 propellants based on impulse-density considerations. To give some basis for comparison, a density exponent of 0.25 was arbitrarily selected as being representative of possible upper stage applications for LMH-2 propellants. Using this density exponent, a performance comparison of the four high performance propellants tested to date is presented in Table XII. The highest performance is obtained with VJA (HMX oxidized) formulation.

## TABLE XII

### Isp DENSITY POTENTIAL OF CANDIDATE LMH-2 PROPELLANTS

| Propellant Type | VIX | VIY | VIZ | VJA |
|---|---|---|---|---|
| Theoretical Performance | | | | |
| Isp (1000/14.7) | 303.7 | 308.9 | 313.8 | 30⁰.3 |
| $\rho$ (gm/cc) | 1.356 | 1.319 | 1.284 | 1.355 |
| Isp x $\rho^{0.25}$ | 329 | 331 | 334 | 334 |
| Delivered Performance | | | | |
| $Isp^{15}_{1000}$ | 290 | 281 | 282 | 281 |
| Isp x $\rho^{0.25}$ | 302 | 301 | 300 | 303 |

Consideration was also given to the effect of solids loading and the use of mixed metal systems on theoretical impulse density using the same density exponent of 0.25. The effect of increasing solids loading from approximately 60 to 70 volume percent by increasing solid oxidizer loading for the formulations explored in this program is presented in Table XIII. Processing considerations would probably limit this increase to approximately 65 volume percent solids. Only a marginal increase in Isp x $\rho^{0.25}$ was obtained by increasing the solid oxidizer loading for either the AP or HMX systems. It should be pointed out that the VJI formulation (17-percent LMH-2/HMX) with an Isp x $\rho^{0.25}$ of 337 is nearly the maximum obtainable. There is little evidence to indicate increased solids oxidizer loading in place of NG would be beneficial for LMH-2 combustion, and this does not appear to be a desirable approach.

The effect of the addition of Be, Al, and Zr on impulse density is presented in Table XIV. The addition was made by replacing either solid oxidizer or liquid. The addition of any of these three metals is detrimental to the LMH-2/AP system performance over that presently available with the VIZ formulation. For the HMX system, calculations were performed on Be addition only. These calculations show that essentially equivalent performance is obtained by Be addition to that presently available.

TABLE XIII

EFFECT OF SOLIDS LOADING ON Isp $\rho$

| Formulation* | | | | Theo Isp | $\rho$ (gm/cc) | $T_c$ ($^\circ$K) | O.R.** | Ispx $\rho^{0.25}$ |
|---|---|---|---|---|---|---|---|---|
| LMH-2 | AP | HMX | NG | | | | | |
| 12 | 26 | 0 | 50 | 295.7 | 1.415 | 3663 | 1.57 | 323 |
| 15 | 23 | 0 | 50 | 303.7 | 1.356 | 3678 | 1.34 | 328 |
| 17 | 21 | 0 | 50 | 308.9 | 1.319 | 3679 | 1.22 | 331 |
| 19 | 19 | 0 | 50 | 313.8 | 1.284 | 3672 | 1.11 | 334 |
| 21.45 | 16.55 | 0 | 50 | 319.0 | 1.244 | 3626 | 1.00 | 337 |
| 15 | 38 | 0 | 35 | 301.0 | 1.387 | 3680 | 1.43 | 328 |
| 17 | 36 | 0 | 35 | 307 | 1.341 | 3680 | 1.30 | 330 |
| 19 | 34 | 0 | 35 | 312 | 1.313 | 3680 | 1.17 | 334 |
| 22.30 | 30.7 | 0 | 35 | 319.3 | 1.258 | 3628 | 1.00 | 338 |
| 12 | 0 | 27 | 50 | 301.7 | 1.415 | 3602 | 1.29 | 329 |
| 15 | 0 | 24 | 50 | 309.3 | 1.355 | 3621 | 1.15 | 334 |
| 17 | 0 | 22 | 50 | 314.0 | 1.319 | 3623 | 1.06 | 337 |
| 18.7 | 0 | 20.3 | 50 | 317.3 | 1.290 | 3590 | 1.00 | 3_ |
| 15 | 0 | 39 | 35 | 310.3 | 1.384 | 3560 | 1.05 | 337 |
| 17 | 0 | 37 | 35 | 314.5 | 1.346 | 3530 | 1.00 | 339 |

*All calculations were made with 10 percent NC and 2 percent stabilizers
for the AP system or 1 percent stabilizer for the HMX system

**Oxidation ratio

## TABLE XLV

### EFFECT OF ADDITIVES ON $Isp \, \rho$

| Formulation* | | | | Theoretical Isp | $\rho$ (gm/cc) | Tc (°K) | O.R.** | $Isp \times \rho^{0.25}$ |
|---|---|---|---|---|---|---|---|---|
| LMH-2 | AP | Be | NC | | | | | |
| 12 | 26 | 0 | 50 | 295.7 | 1.415 | 3663 | 1.57 | 323 |
| 12 | 26 | 3 | 47 | 299.0 | 1.422 | 3779 | 1.32 | 327 |
| 12 | 26 | 6 | 44 | 300.9 | 1.427 | 3870 | 1.13 | 330 |
| 14 | 24 | 0 | 50 | 301.1 | 1.375 | 3675 | 1.41 | 326 |
| 14 | 24 | 3 | 47 | 304.0 | 1.382 | 3778 | 1.20 | 330 |
| 14 | 24 | 6 | 44 | 305.5 | 1.387 | 3837 | 1.0~ | 332 |
| 16 | 22 | 0 | 50 | 306.3 | 1.337 | 3679 | 1.28 | 330 |
| 16 | 22 | 2 | 48 | 308.2 | 1.342 | 3741 | 1.15 | 332 |
| 16 | 22 | 4 | 46 | 309.3 | 1.345 | 3779 | 1.05 | 333 |
| 12 | 24 | 2 | 50 | 298.3 | 1.413 | 3742 | 1.39 | 326 |
| 12 | 22 | 4 | 50 | 300.3 | 1.412 | 3813 | 1.24 | 327 |
| 12 | 20 | 6 | 50 | 301.8 | 1.411 | 3869 | 1.11 | 329 |
| 14 | 22 | 2 | 50 | 303.5 | 1.374 | 3746 | 1.26 | 329 |
| 14 | 20 | 4 | 50 | 305.2 | 1.373 | 3804 | 1.13 | 331 |
| 14 | 18 | 6 | 50 | 306.2 | 1.372 | 3830 | 1.02 | 332 |
| 16 | 20 | 2 | 50 | 308.4 | 1.336 | 3740 | 1.15 | 332 |
| 16 | 18 | 4 | 50 | 309.8 | 1.335 | 3774 | 1.03 | 333 |
| 16 | 16 | 6 | 50 | 308.4 | 1.334 | 3706 | 0.94 | 331 |
| | HMX | | | | | | | |
| 12 | 27 | 0 | 50 | 301.7 | 1.415 | 3602 | 1.29 | 329 |
| 12 | 25 | 2 | 50 | 304.7 | 1.415 | 3689 | 1.17 | 332 |
| 12 | 23 | 4 | 50 | 306.7 | 1.414 | 3760 | 1.06 | 334 |
| 14 | 25 | 0 | 50 | 306.8 | 1.376 | 3616 | 1.19 | 332 |
| 14 | 23 | 2 | 50 | 309.4 | 1.375 | 3692 | 1.09 | 335 |
| 12 | 27 | 2 | 48 | 304.9 | 1.419 | 3682 | 1.16 | 333 |
| 12 | 27 | 4 | 46 | 307.3 | 1.422 | 3742 | 1.05 | 336 |
| 14 | 25 | 2 | 48 | 309.6 | 1.379 | 3684 | 1.08 | 336 |

*, ** Refer to end of table for legend

TABLE XIV (Cont)

EFFECT OF ADDITIVES ON Isp $\rho$

| Formulation* | | | | Theoretical Isp | $\rho$ (gm/cc) | Tc (°K) | O.R.** | Isp x $\rho^{0.25}$ |
|---|---|---|---|---|---|---|---|---|
| IMH-2 | AP | Al | NG | | | | | |
| 12 | 26 | 0 | 50 | 295.7 | 1.415 | 3663 | 1.57 | 323 |
| 12 | 26 | 3 | 47 | 295.6 | 1.433 | 3719 | 1.42 | 323 |
| 12 | 26 | 6 | 44 | 295.3 | 1.449 | 3773 | 1.29 | 324 |
| 14 | 24 | 0 | 50 | 301.1 | 1.375 | 3675 | 1.41 | 326 |
| 14 | 24 | 3 | 47 | 300.8 | 1.392 | 3717 | 1.29 | 327 |
| 14 | 24 | 6 | 44 | 300.2 | 1.407 | 3756 | 1.17 | 327 |
| 16 | 22 | 0 | 50 | 306.3 | 1.337 | 3679 | 1.28 | 329 |
| 16 | 22 | 3 | 47 | 305.7 | 1.353 | 3701 | 1.17 | 330 |
| 16 | 22 | 6 | 44 | 304.7 | 1.367 | 3717 | 1.07 | 329 |
| 12 | 24 | 2 | 50 | 295.8 | 1.420 | 3698 | 1.46 | 323 |
| 12 | 22 | 4 | 50 | 296.0 | 1.426 | 3738 | 1.36 | 324 |
| 12 | 20 | 6 | 50 | 296.1 | 1.432 | 3772 | 1.27 | 324 |
| 14 | 22 | 2 | 50 | 301.1 | 1.380 | 3699 | 1.32 | 326 |
| 14 | 20 | 4 | 50 | 301.1 | 1.386 | 3730 | 1.23 | 327 |
| 14 | 18 | 6 | 50 | 300.1 | 1.391 | 3753 | 1.15 | 326 |
| 16 | 20 | 2 | 50 | 306.1 | 1.343 | 3689 | 1.20 | 330 |
| 16 | 18 | 4 | 50 | 305.9 | 1.347 | 3707 | 1.12 | 330 |
| 16 | 16 | 6 | 50 | 305.4 | 1.352 | 3710 | 1.05 | 329 |
| | | Zr | | | | | | |
| 12 | 26 | 0 | 50 | 295.7 | 1.415 | 3663 | 1.57 | 323 |
| 12 | 26 | 3 | 47 | 293.7 | 1.446 | 3697 | 1.49 | 322 |
| 12 | 26 | 6 | 44 | 291.6 | 1.476 | 3726 | 1.42 | 321 |
| 14 | 24 | 0 | 50 | 301.1 | 1.375 | 3675 | 1.41 | 326 |
| 14 | 24 | 3 | 47 | 297.0 | 1.433 | 3733 | 1.28 | 325 |
| 14 | 24 | 6 | 44 | | | | | |
| 16 | 22 | 0 | 50 | 306.3 | 1.337 | 3679 | 1.28 | 330 |
| 16 | 22 | 3 | 47 | 304.3 | 1.365 | 3711 | 1.22 | 329 |
| 16 | 22 | 6 | 44 | 302.2 | 1.392 | 3731 | 1.16 | 328 |

*, ** Refer to end of table for legend

TABLE XIV (Cont)

EFFECT OF ADDITIVES ON Isp $\rho$

| Formulation* | | | | Theoretical Isp | $\rho$ (gm/cc) | Tc (°K) | O.R.** | Isp x $\rho^{0.25}$ |
|---|---|---|---|---|---|---|---|---|
| LMH-2 | AP | Zr | NG | | | | | |
| 12 | 24 | 2 | 50 | 294.6 | 1.429 | 3687 | 1.50 | 322 |
| 12 | 22 | 4 | 50 | 293.5 | 1.444 | 3706 | 1.44 | 322 |
| 12 | 20 | 6 | 50 | 292.3 | 1.459 | 3724 | 1.38 | 321 |
| 14 | 22 | 2 | 50 | 300.0 | 1.388 | 3698 | 1.35 | 326 |
| 14 | 20 | 4 | 50 | 298.9 | 1.402 | 3714 | 1.30 | 325 |
| 14 | 18 | 6 | 50 | 297.7 | 1.416 | 3730 | 1.24 | 325 |
| 16 | 20 | 2 | 50 | 305.3 | 1.350 | 3702 | 1.23 | 329 |
| 16 | 18 | 4 | 50 | 304.1 | 1.363 | 3715 | 1.18 | 329 |
| 16 | 16 | 6 | 50 | 302.9 | 1.376 | 3727 | 1.13 | 328 |

*All calculations were made with 10-percent NC and 2-percent stabilizer for AP formulations or 1-percent stabilizer for the HMX formulations

**Oxidation ratio

It is concluded that any consideration of increased solids loading or the use of mixed-metal systems must be based on improved impulse efficiency.

In summary, four areas of investigation appear particularly attractive to obtain additional increases in performance of LMH-2 above those obtained to date on this program. They are as follows:

(1) Additional combustion studies to determine the interaction between closed-bomb data and motor performance

(2) Motor scaleup of selected high-energy LMH-2 propellants with close attention to motor design parameters

(3) Additional emphasis on those propellant ingredients which can appreciably improve the propellant combustion environment as represented by flame temperature and oxidation ratio

(4) Investigation of the potential of mixed metals to improve combustion efficiency in conjunction with higher solids loadings

## SECTION III

### TASK II, FORMULATION AND BALLISTIC EVALUATION

A. SCOPE

Task II comprised the majority of the program effort. The objective of this task was to formulate and test candidate high-performance propellant systems selected under Task I. This task utilized both Be control and analog formulations as well as LMH-2 formulations. Under this task, 35 LMH-2 and 70 Be motors were evaluated. The test motors contained a nominal 10- to 15-lb propellant charge and exhibited mass-flow rates of 5 lb/sec or greater. The task was divided into two phases. In phase A, formulation screening was conducted, with the bulk of the motors fired at approximately 1000 psia exhausted to Bacchus ambient pressure ($\sim$ 12.2 psia) with optimum expansion ratio. Phase B more extensively characterized selected high-performance LMH-2 formulations. Table XV contains a breakdown of various areas investigated under Task II.

### TABLE XV

### TASK II, FORMULATION SCREENING

| Subtask | Purpose | No. Firings (Be) | No. Firings (LMH-2) |
|---------|---------|------------------|---------------------|
| **Phase A** | | | |
| II-6 | Efficiency correlations with Be propellants | 43 | -- |
| II-7 | Oxidizer particle size studies with Be propellants | 8 | -- |
| II-8 | Optimum nozzle geometry | 11 | -- |
| II-9 | Increased L* studies | 4 | 9 |
| II-10 | LMH-2/AP propellants | -- | 6 |
| II-11 | LMH-2/AN or HMX propellants | -- | 9 |
| **Phase B** | | | |
| II-12 | Characterization of selected Be and LMH-2 propellants | 4 | 11 |

B. LABORATORY FORMULATION AND PROCESSING STUDIES

1. **Beryllium Propellants**

Based on the results of Task I, laboratory formulation studies were performed on Be analog formulations of proposed LMH-2 propellants presented in Table II.

The VIH propellant was designed to have the same metal level, oxidation ratio as the proposed 19-percent LMH-2 formulation. The VII propellant was formulated to demonstrate the effect on efficiency due to decreasing oxidation ratio in a high-metal-level propellant. The VLJ propellant was designed to show the effect on efficiency of oxygen source (5 percent more AP for NG than the VIH formulation) at a constant metal level and oxidation ratio. VLJ was also formulated with 45, 90, and 180 μ AP to determine the effect of AP particle size on efficiency. The VIK, VIL, VIM, and VIN propellants represented the Be analogs of the 17-percent LMH-2/AP; 15-percent LMH-2/AP/HMX; 19-percent LMH-2/AN; and 17-percent LMH-2/AN, respectively, in both metal level and oxidation ratio. The VIO propellant was designed to determine the effect of oxidation ratio on efficiency at a low metal level, and VIG was formulated to evaluate $TAGNO_3$ as an oxidizer.

Processing studies were conducted to determine the tradeoff between liquid level and oxidizer particle size on processibility. In conjunction, a review was made of past processing experience with Be propellants. Consideration was given to weight and volume percent solids loading, solids particle size, particle size ratio, and overall composition. Figure 41 shows propellant viscosity as a function of the weight ratio of fine to coarse particles, based on the total solids content. Although the data are scattered due to ingredient and composition differences, the effect of increasing fines on viscosity was normally predictable.

For propellants containing 10 to 15 μ PNC and 12 μ Be, little effect on viscosity is noted by decreasing the oxidizer particle size down to 90μ, or a particle size ratio of approximately 6:1. However, for particle sizes less than 90μ, viscosity rapidly increased even at moderate solids loadings. This effect is further illustrated in Figure 42 for the VIH and VLJ formulations containing 57- and 61-percent-by-volume solids loading, respectively.

Using Figure 42 as a guide, formulation work was completed on the Be analog formulations with little processing difficulty. Table XVI shows the rheological criteria and Table XVII the pertinent propellant data for the analog formulations.

2. **LMH-2 Propellants**

Laboratory formulation screening and processing studies were conducted on six candidate LMH-2 propellants selected from the Task I correlations, which were predicted to meet the program objective of a delivered impulse in excess of 280 lbf-sec/lbm.
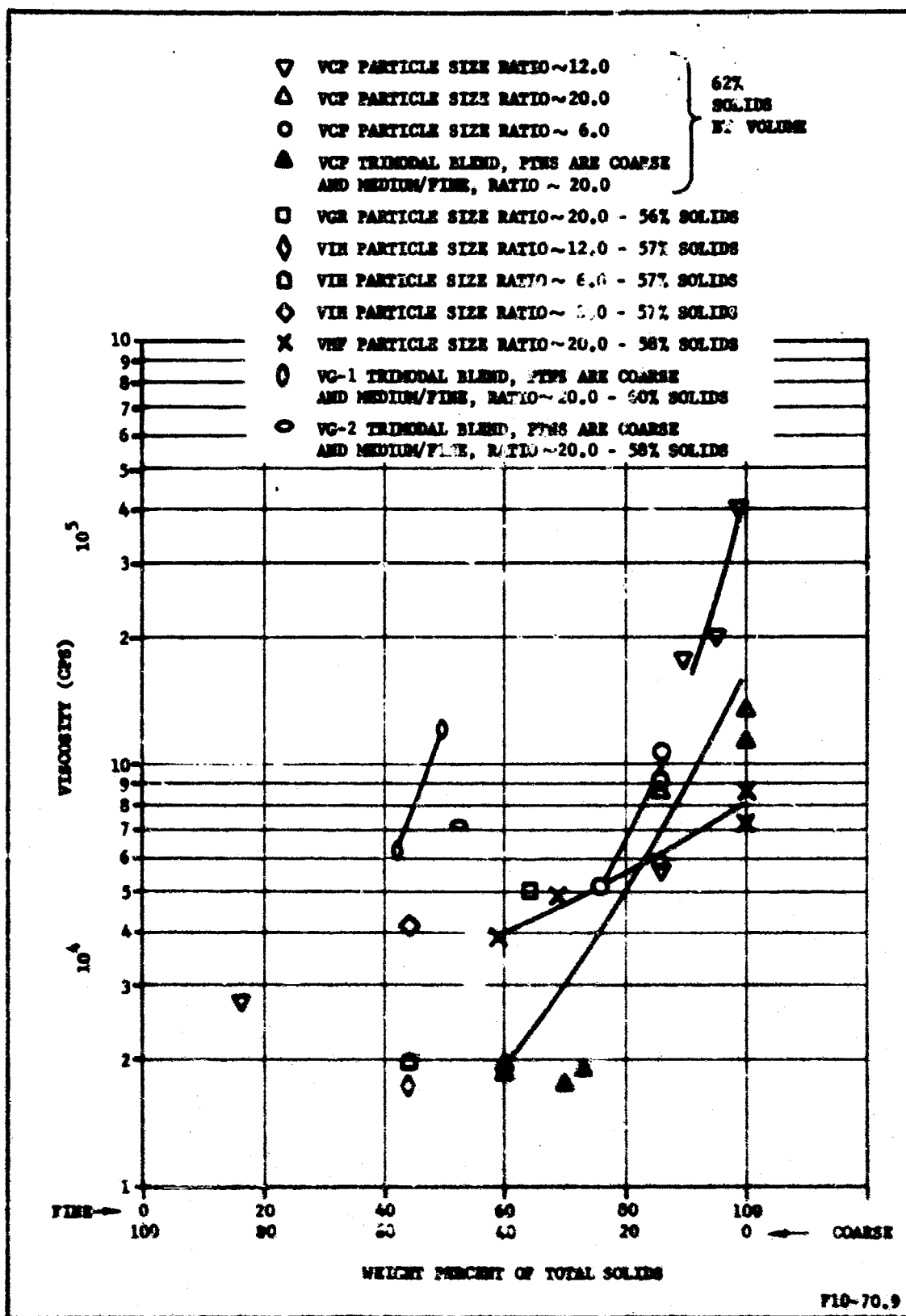
Figure 41. Viscosity as a Function of Percent Fine/Coarse Particles for Be Double-Base Propellants
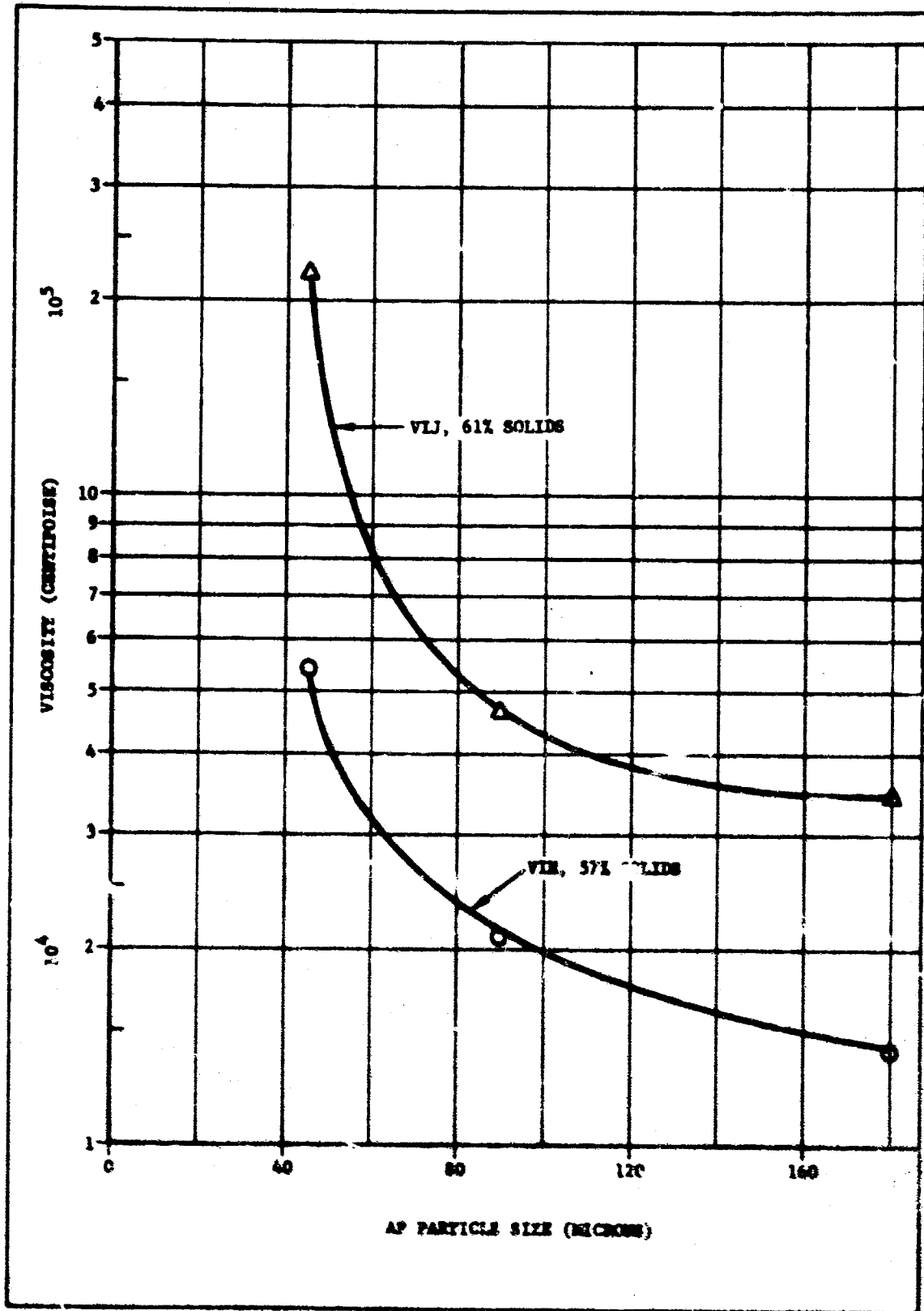
Figure 42. Viscosity as a Function of AP Particle Size

TABLE XVI

BERYLLIUM PROPELLANTS - RHEOLOGICAL CRITERIA

| | Propellant Type | | | | | | | | | |
|---|---|---|---|---|---|---|---|---|---|---|
| | VIH | VII | VIJ | VIJ | VIJ | VIK | VIL | VIH | VIO | VIG |
| Volume percent solids | 56.6 | 60.2 | 61.4 | 61.4 | 61.4 | 56.4 | 56.4 | 63.0 | 59.8 | 63.5 |
| Weight percent solids | 60.0 | 60.0 | 65.0 | 65.0 | 65.0 | 60.0 | 60.0 | 65.0 | 63.5 | 65.0 |
| Percent coarse solids | 54.1 | 57.7 | 57.7 | 57.7 | 57.7 | 56.7 | 60.0* | 60.0 | 68.5* | 60.0* |
| Particle size oxidizer (microns) | 45 | 90 | 45 | 90 | 180 | 45 | 45/180 | 300 | 45/180 | -- |
| Particle size ratio | 3 | 6 | 3 | 6 | 12 | 3 | 3-12 | 20 | 3-12 | -- |
| Viscosity (centipoise) at 3 rm and 80°F | 54,000 | 45,000 | 220,000 | 46,000 | 35,000 | 66,000 | 22,000 | 46,400 | 22,000 | -- |

*These formulations have a trimodal distribution of oxidizer and fuel

TABLE XVII

BERYLLIUM PROPELLANTS FOR IMPULSE EFFICIENCY STUDIES

a. <u>Binder Selection</u>

Because of the apparent dependency of the efficiency of LMH-2 propellants on flame temperature and oxidation ratio, it was necessary to formulate with a highly energetic binder. A 10-percent-NC level was selected as being the lower limit which would give adequate physical properties without crosslinking techniques. Based on predicted impulse values and projected processibility criteria, formulations containing up to 50-percent NG were considered. A series of 10-gm LMH-2 mixes were made with varying liquid compositions and AP, AP + HMX, and AN as primary oxidizers. At the 50-percent liquid level, the following liquid compositions were investigated for their effect on uncured sensitivity:

(1)   99-percent NG + 1-percent 2-NDPA

(2)   95-percent NG + 4-percent TA + 1-percent 2-NDPA

(3)   97-percent NG + 2-percent TDI + 1-percent 2-NDPA

Table XVIII contains the matrix compositions and the range of values obtained for the uncured sensitivities. The lower range of impact and friction sensitivity values obtained compared to conventional double-base propellants indicated an additional degree of hazard was involved in processing with these liquid compositions. There appeared to be no significant difference in the sensitivity levels of any of the three liquid compositions considered. Additional sensitivity tests were also run with a 90-percent NG, 9-percent-TA solvent, which showed only a marginal improvement in the sensitivity levels. These tests indicated the total amount of NG in the formulations was a major contributor to the lower uncured sensitivity values and that little advantage was gained by small coplasticizer dilutions.

Because of the increased sensitivity of the proposed LMH-2 propellants due to the high-energy solvent, additional sensitivity testing was performed to determine the hazards from thin propellant films. The test (thin film propagation) consisted of measuring the potential of thin propellant films to propagate in the uncured state from impact. The test apparatus utilized the standard impact apparatus modified for a thin propellant film ribboned out to 4 in. long and containing two intermediate breakwires. In a complete propagation, both breakwires fire. In a partial propagation, only one breakwire fires. Conventional double-base propellants show no tendency to propagate in this test. The LMH-2 candidate formulations containing both 90- and 99-percent-NG solvents were tested. The resulting data are the following:

| VIY (99-percent NG) | VJA (99-percent NG) |
|---|---|
| 7 complete propagations | 10 complete propagations |
| 3 partial propagations | |

TABLE XVIII

LMH-2 PROPELLANTS FOR SENSITIVITY EVALUATION

| | Propellant Designation* | | | | |
|---|---|---|---|---|---|
| | BAP-15 | BAP-17 | BH-15 | BNA-15 | BNF-17 |
| **Formulation (wt %)** | | | | | |
| NC | 10.0 | 10.0 | 10.0 | 10.0 | 10.0 |
| NG | 48-50 | 48-50 | 48-50 | 48-50 | 48-50 |
| AP | 23.0 | 21.0 | -- | 11.5 | -- |
| HMX | -- | -- | 24.0 | 11.5 | -- |
| AN | -- | -- | -- | -- | 21.0 |
| LMH-2 | 15.0 | 17.0 | 15.0 | 15.0 | 17.0 |
| Res | 1.0 | 1.0 | -- | 1.0 | 1.0 |
| 2-NDPA | 1.0 | 1.0 | 1.0 | 1.0 | 1.0 |
| TA + TDI | 0-2 | 0-2 | 0-2 | 0-2 | 0-2 |
| **Theoretical** | | | | | |
| $I_{sp}$ (sec) | 304 | 309 | 309 | 307 | 309 |
| $T_c$ (°K) | 3620-3678 | 3620-3679 | 3564-3261 | 3578-3636 | 3469-3529 |
| O.R.** | 1.31-1.34 | 1.18-1.22 | 1.13-1.15 | 1.19-1.23 | 1.21-1.25 |
| **Sensitivity - Uncured** | | | | | |
| Impact (cm/2Kg) | 1.0-6.9 | 1.0-6.9 | 1.0-6.9 | 3.5 | 3.5-6.9 |
| Friction (lb @ ft/sec) | 40/3-18/8 | 17/4-50/8 | 13/4-72/8 | 100/6-50/8 | 72/8-100/8 |
| ESD*** (Joules) | 0.025->6.25 | 0.25->6.25 | 0.05->6.25 | 0.050-1.25 | 0.0125-0.025 |
| Auto Ignition (°C) | 200-226 | 205-231 | 210-230 | 196-210 | 194-204 |
| Talliani (mm Hg) | 19-43 | 38 | 12-26 | 17-73 | 117-141 |

*Legend:  B  - LMH-2 Fuel
AP - Ammonium Perchlorate Oxidizer
H  - HMX Oxidizer
NA - Ammonium Perchlorate Oxidizer
NF - Ammonium Nitrate Oxidizer
15 - 15% LMH-2
17 - 17% LMH-2

**Oxidation Ratio
***Electrostatic discharge

| VIY (90-percent NG) | VJA (90-percent NG) |
|---|---|
| 10 partial propagations | 7 partial propagations |
| | 3 nonpropagations |

Although a trend toward improved thin film propagations results when the lower NG solvents is evident, it is of such a magnitude as to be of questionable significance in indicating a reduced hazard.

Based on results of the propagation and standard sensitivity tests, modifications were made to the production facility to allow complete remote handling through castings of the 15PC motors. Of particular significance was the instigation of remote cleaning procedures to eliminate hazards from thin films during cleanup.

Using these added precautions, it was anticipated that the following binder could be processed safely:

Candidate LMH-2 propellant binder

| Ingredient | Weight (percent) |
|---|---|
| NG (Plastisol NC 10 to 15μ) | 16.4 |
| NG | 82.0 |
| 2-NDPA | 1.6 |

Because of the anticipated problems with the incorporation of high percentages of LMH-2 (19 percent), the binder level was fixed at 61 percent by weight for all formulations representing between 57- and 60-percent-volume solids loading for those formulations under consideration.

b. Solid Oxidizer Considerations

The three primary oxidizers, AP, HMX, and AN, were originally considered for the LMH-2 propellants. Because of efficiency considerations, AN was subsequently eliminated. Of the final six formulations, three contained AP, two HMX, and one AP and HMX.

Oxidizer particle size selection for the candidate formulations was based on both processibility and impulse efficiency considerations. Since the ingredient types, particle size distributions, and volume solids loadings for the LMH-2 propellants were similar to the Be analog formulations, similar process considerations could be employed. Figure 42 shows viscosity is relatively insensitive to AP particle size down to 90μ but increases rapidly for decreasing particle sizes below this level. Figures 24 and 32 show the effect of AP particle size on the efficiency of

Al, Be, and LMH-2 double-base propellants. These data show an almost linear relation exists between AP particle size and impulse efficiency. Thus, some additional performance gains could be expected for formulations containing AP particle size less than $90\mu$. Because of the rapid viscosity increase with AP particle sizes less than $90\mu$, and the necessity to formulate up to 60-percent-solids loading at high LMH-2 loadings, $90\mu$ AP was selected as the best compromise for the three all-AP oxidized LMH-2 propellants. For the HMX formulations, advantage was taken of the lack-of-efficiency loss with increasing HMX particle size, and Class A HMX ($180\mu$) was used. This also allowed the incorporation of the fine AP ($15\mu$) in the mixed AP/HMX propellant.

It should be pointed out that lower void volumes resulting in lower viscosities could have been obtained by the use of a bimodal or a trimodal oxidizer blend. A bimodal distribution is present with NO and LMH-2 considered in addition to the $90\mu$ AP. However, little increase in packing is obtained by the addition of a third particle size until a particle size ratio of approximately 20 to 1 is exceeded. This would require a large percentage of the solid oxidizer to be in excess of $200\mu$ and was felt to be prohibitive from efficiency considerations.

c. LMH-2 Incorporation

Work prior to the start of Contract AF 04(611)-10754 had shown that processibility of LMH-2 propellants became marginal at LMH-2 loadings above 15 percent (58-percent-volume-solids loading). Even at these low LMH-2 levels it was usually necessary to use ground LMH-2. This limitation was felt to be due to a combination of low bulk densities, a poor shape factor, and surface anomalies. Considerable effort was expended to improve the processibility and rheological properties to allow increased LMH-2 loadings. Primary emphasis was placed on the development of post-treatment methods to improve LMH-2 bulk density and shape factor and to mask surface effects. Of the various methods tried, the following were the most successful.

1) Grinding

All LMH-2 lots were ball-milled by the Ethyl Corporation for 30 min. This normally increased bulk density from 0.30 to 0.38 gm/cc, although variations in specific surface, particle size, and bulk density between lots was apparent.

2) Wax Treating

A 1-percent coating of CEC high vacuum wax was placed on the LMH-2 by stripping from a volatile solvent.

### 3; AP Treating

AP was recrystallized in the presence of LMH-2 from a saturated AP/LMH-2 water dispersion.

In addition, various LMH-2 lots exhibited a tendency to gas during cure, resulting in porous propellant. Two posttreatments were used to eliminate this gassing. These posttreatments consisted of an elevated temperature vacuum baking cycle or a room-temperature water-wash cycle.

Complete details of the characterization of LMH-2 and the developed posttreatments are contained in Section IV.

### d. Propellant Selection

Based on the efficiency correlations, binder and oxidizer particle size studies, and the developed LMH-2 posttreatments, the six propellants listed in Table XIX were selected for ballistic screening. The VIX, VIY, and VIZ propellants were selected to explore the tradeoff between LMH-2 loadings and delivered impulse for an all-AP oxidized system. The VJA and VJI propellants were selected to explore an all-HMX oxidized system. It was also desirable to explore the use of fine AP in a mixed AP/HMX system from efficiency considerations. Several mixes were made to determine the effect on processibility due to substituting fine AP for HMX in the VJI matrix. These results are listed in the following tabulation:

| Percent 15 $\mu$ AP | 0 | 5 | 8 |
|---|---|---|---|
| Viscosity @ 3 rpm (cps) | 77,000 | 160,000 | 393.000 |

Because of the marginal processibility with greater than 5-percent fine AP, VJL was chosen for ballistic evaluation.

Table XIX also contains a summary of pertinent data obtained on the six candidate LMH-2 formulations. As previously discussed, uncured sensitivity data was satisfactory for processing, although impact and friction values were lower than conventional double-base propellants. Cured sensitivity values were comparable to conventional double-base. Thermal stability was excellent, as evidenced by autoignition tests. Physical properties were more than adequate for subscale and some large motor applications. The lower tensile strength of 75 psi for VJA compared to 100 to 120 psi for VIX, VIY, and VIZ is due to the large Class A HMX particle used in VJA. Improvements in physical properties could be made in these formulations by cross-linking techniques. Experimental densities were greater than 98 percent of theoretical in all cases, confirming the adequacy of the posttreatments used.

# TABLE XIX

## PROPERTIES OF LMH-2 PROPELLANTS

| Propellant Type | VLX | VIY | VLZ | VJA | VJI | VJL |
|---|---|---|---|---|---|---|
| **Formulation (wt %)** | | | | | | |
| NC (PNC, 10 μ) | 10.0 | 10.0 | 10.0 | 10.0 | 10.0 | 10.0 |
| NG | 50.0 | 50.0 | 50.0 | 50.0 | 50.0 | 50.0 |
| AP | 23.0 (90μ) | 21.0 (90μ) | 19.0 (90μ) | -- | -- | 5.0 (15μ) |
| RDX (Class A) | -- | -- | -- | 24.0 | 22.0 | 16.7 |
| LMH-2 (Ground) | 15.0 | 17.0 | 19.0 | 15.0 | 17.0 | 17.0 |
| Res | 1.0 | 1.0 | 1.0 | -- | -- | 1.0 |
| 2-NDPA | 1.0 | 1.0 | 1.0 | 1.0 | 1.0 | 1.0 |
| **Theoretical** | | | | | | |
| Isp (1000/14:7) | 303.7 | 308.9 | 313.8 | 309.3 | 314.0 | 312.7 |
| Tc (°K) | 3678 | 3679 | 3672 | 3621 | 3623 | 3614 |
| ρ (lb/in.$^3$) | 0.0490 | 0.0477 | 0.0464 | 0.0490 | 0.0477 | 0.0476 |
| Oxidation ratio | 1.342 | 1.219 | 1.113 | 1.146 | 1.062 | 1.082 |
| **Sensitivity*** | | | | | | |
| Impact (cm/2Kg) | 3.5 (21) | 3.5 (33) | 3.5 (26) | 3.5 (21) | 3.5 (26) | 3.5 (26) |
| Friction (lbf at ft/sec) | 23 @6 (90 @8) | 17 @6 (90 @8) | 23 @6 (90 @8) | 50 @6 (154 @8) | 46 @8 (61 @8) | 30 @6 (156 @8) |
| Electrostatic discharge (joules) | 1.25 (1.25) | 1.25 (1.25) | >1.00 (>.250) | 0.625 (1.25) | >5.00 (>5.00) | >5.00 (1.25) |
| Autoignition (°C) | 205 (230) | 203 (208) | 211 (223) | 227 (235) | 238 (212) | 224 (215) |
| Differential thermal analysis, ignition (°C) | 178 (178) | 170 (178) | 165 (172) | 181 (178) | -- (184) | 167 (167) |

*First number is for uncured propellant, number in parentheses is for cured propellant

TABLE XIX (Cont)

## PROPERTIES OF LMH-2 PROPELLANTS

| Propellant Type | VIX | VIY | VIZ | VJA | VJI | VJL |
|---|---|---|---|---|---|---|
| Physical Properties | | | | | | |
| Tensile (psi) | 110 | 100 | 120 | 75 | -- | -- |
| Elongation (%) | 22 | 20 | 20 | 22 | -- | -- |
| Modulus (psi) | 480 | 600 | 490 | 420 | -- | -- |
| Density (lb/in.3) | 0.0485 | 0.0472 | 0.0457 | 0.0485 | 0.0473 | 0.0473 |
| (% theoretical) | 99.0 | 99.0 | 98.4 | 99.0 | 99.2 | 99.3 |
| Burning Rate** | | | | | | |
| γ @1000 psia | 1.03 | 0.97 | 0.90 | 0.76 | 0.76 | 0.88 |
| Exponent | -- | 0.332 | -- | 0.485 | -- | -- |

**Motor data

88

e. **Process Studies**

Table XX shows the rheological criteria for the LMH-2 formulations. The VIZ formulation with 60-percent-volume solids and 19-percent LMH-2, and the VJL formulation with 59-percent-volume solids, 17-percent LMH-2, and 5-percent 15μ AP were the most difficult formulations to be processed in the program. The following techniques were used to facilitate mixing and casting of these formulations:

(1) Use of wax-treated or AP-treated LMH-2

(2) A heated mix cycle

(3) Agitation and vibration during casting

Figure 43 shows the effect of LMH-2 loadings (from 15 to 19 percent) on viscosity for two LMH-2 lots evaluated (99 and 97). Lot 99 gave significantly higher viscosities than lot 97 at both 15- and 19-percent LMH-2 loadings. The effect of wax treating and AP treating on lot 99 is also shown in Figure 43. Use of wax treatment for lot 99 decreased viscosity from 120,000 to 70,000 cps in VIX (15-percent LMH-2) formulation. The AP treatment further decreased viscosity from 300,000 to 240,000 cps in VIZ (19-percent LMH-2) formulation with lot 99. Viscosity reduction obtained with the wax-treated material was considered adequate and because of its simplicity was selected over AP treatment. For lot 97, significant improvements in solids loading over lot 99 could be made at loadings up to 19-percent LMH-2. This viscosity variance observed between LMH-2 lots becomes increasingly significant as higher density LMH-2 propellants are sought. Control of the LMH-2 lot variance is discussed in detail in Section IV.

The decrease of viscosity with increasing mix temperature is illustrated in Figure 44 for the VIX and VJA formulations. This same trend was apparent for all formulations and, as a result, elevated mixing cycles were employed. To determine the limit to which an elevated temperature cycle could be used, a pot-life study was run on the VJL formulation. Results obtained are listed in the following tabulation:

| Mix Temperature (°F) | Mixing Time (min) | Viscosity @ 3 rpm (cps) |
|---|---|---|
| 110 | 13 | 160,000 |
| 108 | 45 | 293,000 |
| 111 | 68 | >333,000 |

From the pot-life study it is apparent a definite tradeoff exists between viscosity, mixing temperature, and mixing time. For the 15PC castings, a progressive temperature mix cycle was used with the final 15 min of a 45-min cycle at 100° to 110° F.

**TABLE XX**

**IMB-2 PROPELLANTS-RHEOLOGICAL CRITERIA**

| | Propellant Type | | | | | |
|---|---|---|---|---|---|---|
| | VIX | VIY | VIZ | VJA | VJI | VJL |
| Volume percent solids | 57.6 | 58.8 | 59.9 | 57.6 | 58.8 | 58.8 |
| Weight percent solids | 50.0 | 50.0 | 50.0 | 50.0 | 50.0 | 50.0 |
| Percent coarse solids | 46.0 | 42.0 | 38.0 | 48.0 | 44.0 | 32.0 |
| Particle size oxidizer (microns) | 90 | 90 | 90 | 180 | 180 | 15-180 |
| Particle size ratio | 6 | 6 | 6 | 12 | 13 | 1-13 |
| Viscosity (centipoise at 3 rpm and 100° F) | 70,000 | 120,000 | 300,000 | 50,000 | 80,000 | 160,000 |
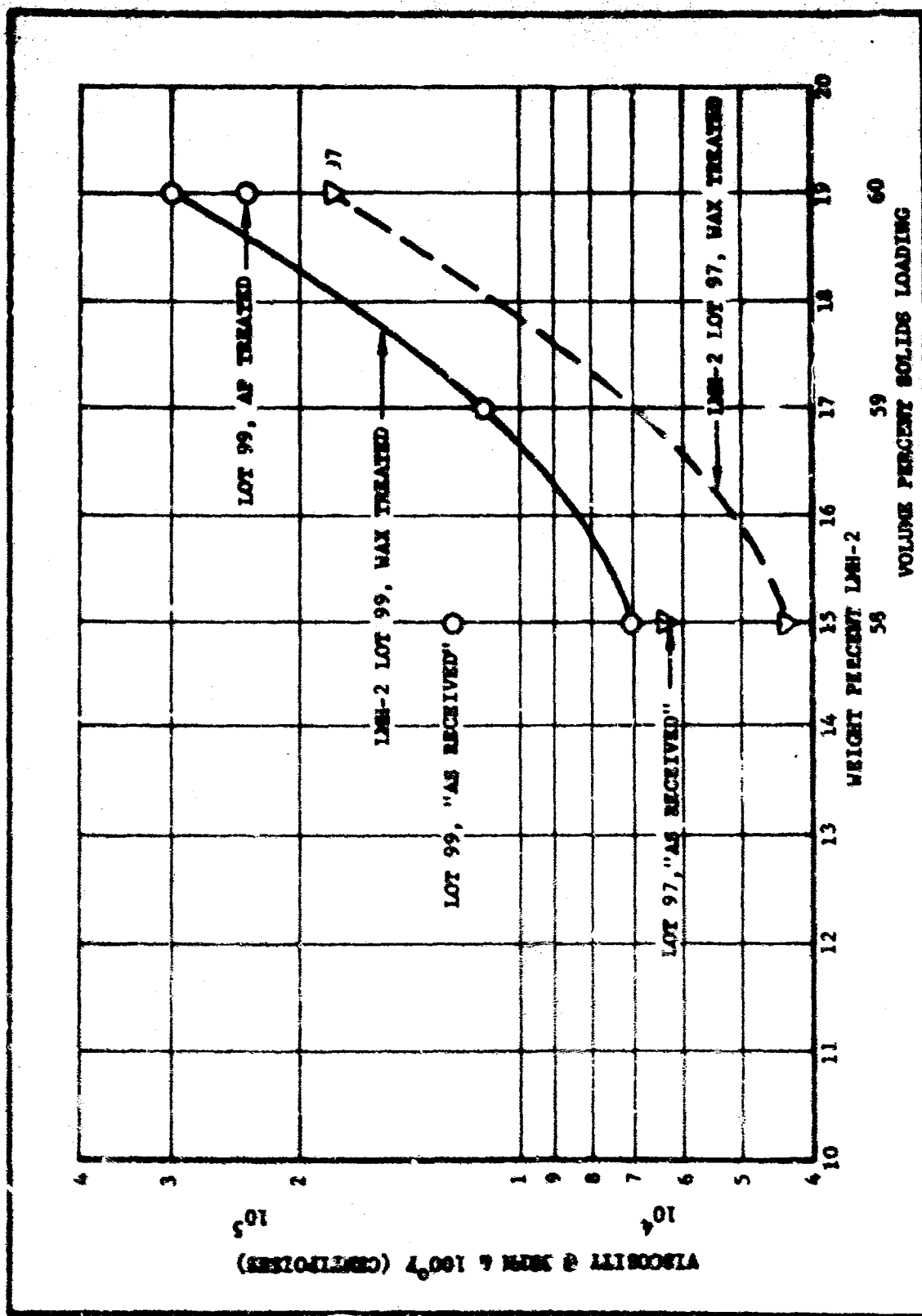
Figure 43. Viscosity as a Function of LMH-2 Loading
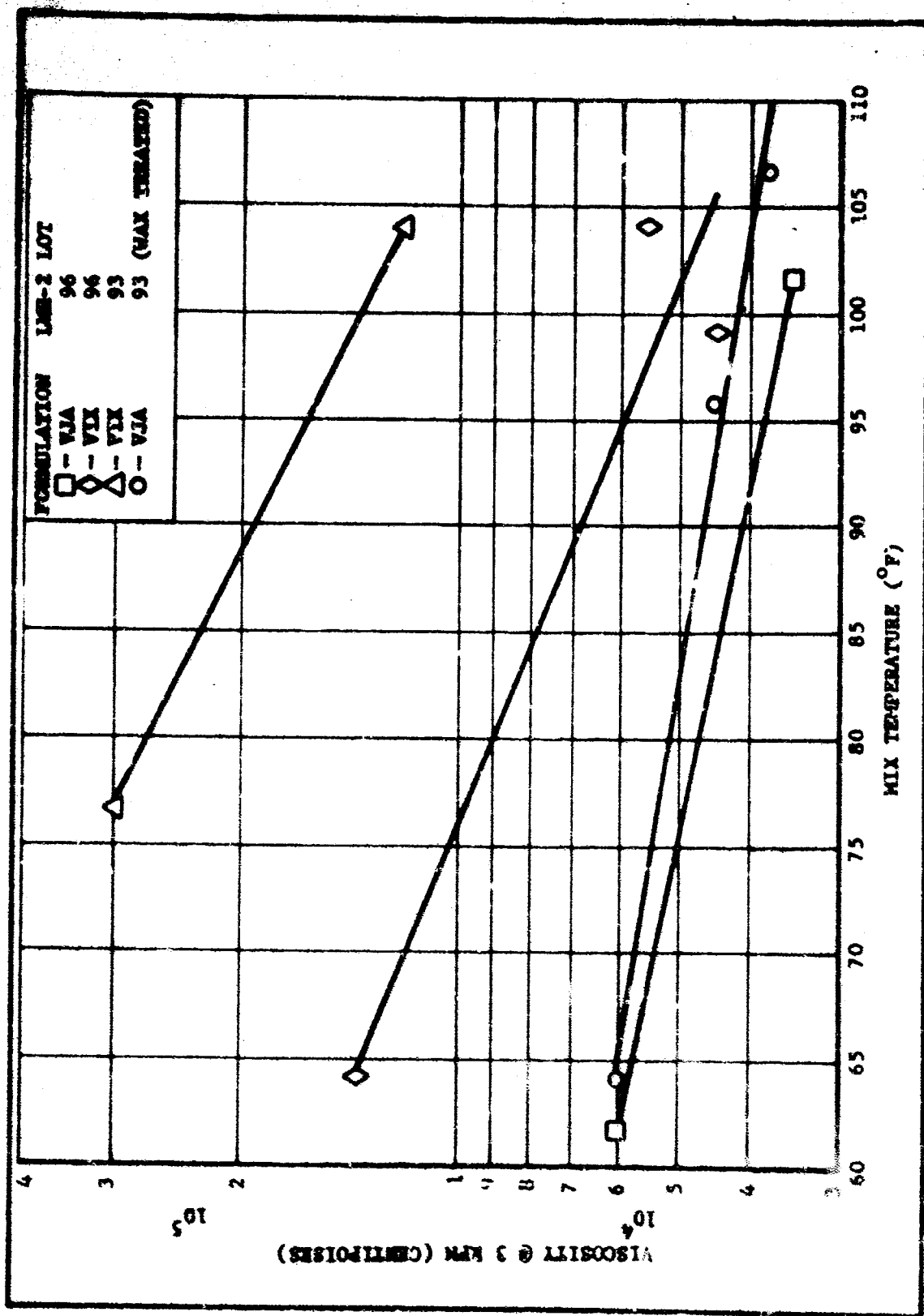
Figure 44. Viscosity as a Function of Temperature

Figure 45 shows viscosity as a function of shear rate for the VIZ and VJL formulations showing the typical thixotropic nature of LMH-2 formulations. To take advantage of this effect, all formulations were cast through the bottom dump valve of the mixer with the agitator rotating at 6 to 8 rpm. For the thicker mixes, some vibration was also applied to the mixing bowl.

## C.   BALLISTIC TESTING

### 1.   Motor Design Studies

#### a.   Grain Design

The basic motor configuration selected for motor firings on the Task II effort was the 15PC (nominal 15PC for a propellant density of 0.062 lb/in.$^3$). This motor was designed and developed under Contract AF 04(611)-9062 (Be/Taz).

The 15PC motor gave excellent results with VCP propellant; however, only a limited mass-flow range was covered ( > 6 lb/sec). This range was extended under Contract AF 04(694)-127 to approximately 5 lb/sec. With this background, it was felt necessary to keep mass-flow rates on the current program above 5 lb/sec. Because of this requirement, coupled with anticipated low burning rates and low densities, it was necessary to modify the basic grain design. In reviewing new grain designs the following items were considered as desirable:

(1)   No major alterations to existing hardware from implementation of the design

(2)   A neutral pressure-time trace

(3)   A minimum chance for propellant sliver at burnout

(4)   A maximum propellant weight of 15 lb with VCP propellant

(5)   Ease of propellant consolidation

It was decided to use a cylindrical, center-perforated grain with the standard 15PC inhibitor in order to maximize the use of existing hardware and minimize slivering.

In order for the initial burning surface (Si) to equal the final burning surface (Sf) for a center-perforated grain burning on both ends and the center core, the length (L) must equal 1.5 x OD + 0.5 x ID of the grain. The larger the web, the less neutral the burning surface is between Si and Sf. Conversely, a small web means a long grain and more difficult consolidation of high-viscosity mixes.
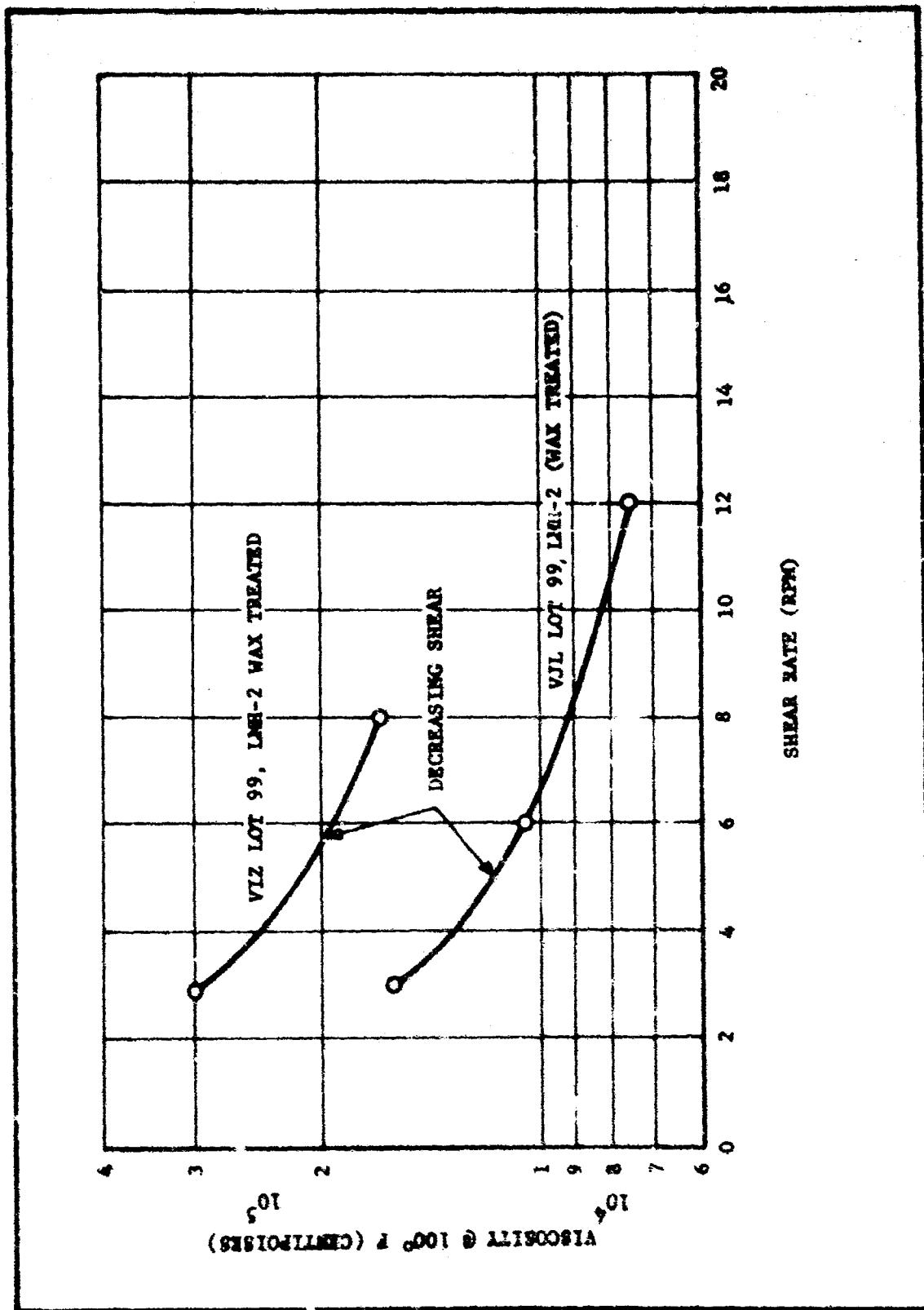
Figure 45. Viscosity as a Function of Shear Rate

Figure 46 shows a plot of grain design parameters for a single grain. The present 15PC design, which will be used for many of the firings, is almost on the intersection of the line where Si = Sf and the line where propellant weight is 15 lb for VCP propellant. In order to maintain the 5 lb/sec mass-flow rate with a reasonable web thickness, grain length must be increased at a considerable loss of neutrality. However, a single grain was selected from this grid which should provide a good compromise design. This grain (Mod-1 design) was 14 in. long with a web of 1.0 in. Although slightly progressive, it will maintain mass flows of 5 lb/sec down to burning rates of 0.45 in./sec and densities of 0.047 lb/in.³.

It was expected that rates somewhat lower than 0.45 in./sec might be observed. For these tests, a single grain is not suitable, so a two-grain concept was reviewed. Figure 47 shows a plot of grain design parameters for a double grain. In order to avoid excessive case-bond area and yet accommodate rates as low as 0.3 in./sec, a combined length of 18 in. was chosen as a second alternate design. This design (Mod-2) is only slightly regressive. Figure 48 shows the predicted pressure-versus-time curves for the alternate designs.

The basic and two alternate grain designs gave a high degree of flexibility in matching burning rates and density-to-mass-flow rate. Figure 49 shows the standard 15PC compared with the Mod-2 configuration. Note the chamber extension added to accommodate the Mod-2 grain. By removal of the chamber extension, the chamber can be used for standard 15PC firings. Figure 50 shows the configuration for the Mod-1 grain design.

b. Residence Time Effects

Fourteen 15PC firings were scheduled to study the effect of L* on efficiency. The standard 15PC motor with VCP at K of 140 (1000 psi) has an L* of 160. In order to provide a larger free volume, the same chamber extension made with Mod-2 grain design was employed. By using this chamber extension and a standard grain design (Figure 50), an L* of 400 is achieved with VCP at a K of 140.

c. Optimum Nozzle Geometry Firings

Twelve 15PC firings were scheduled for evaluation of approach angle effect on efficiency. Both 15 and 5 degree approach cones were required for these tests. The 15 degree approach cones were fired in a standard 15PC altitude chamber, and the 5 degree approach cones were fired in the high L* chamber. (See Figure 51.) Table XXI compares the ballistic design criteria for the various test motors used on this program.

2. Control Propellant

Control firings of a well-characterized, efficient Be propellant were dispersed throughout the motor testing program to provide checks on data validity. Additional firings of the control propellant were also made
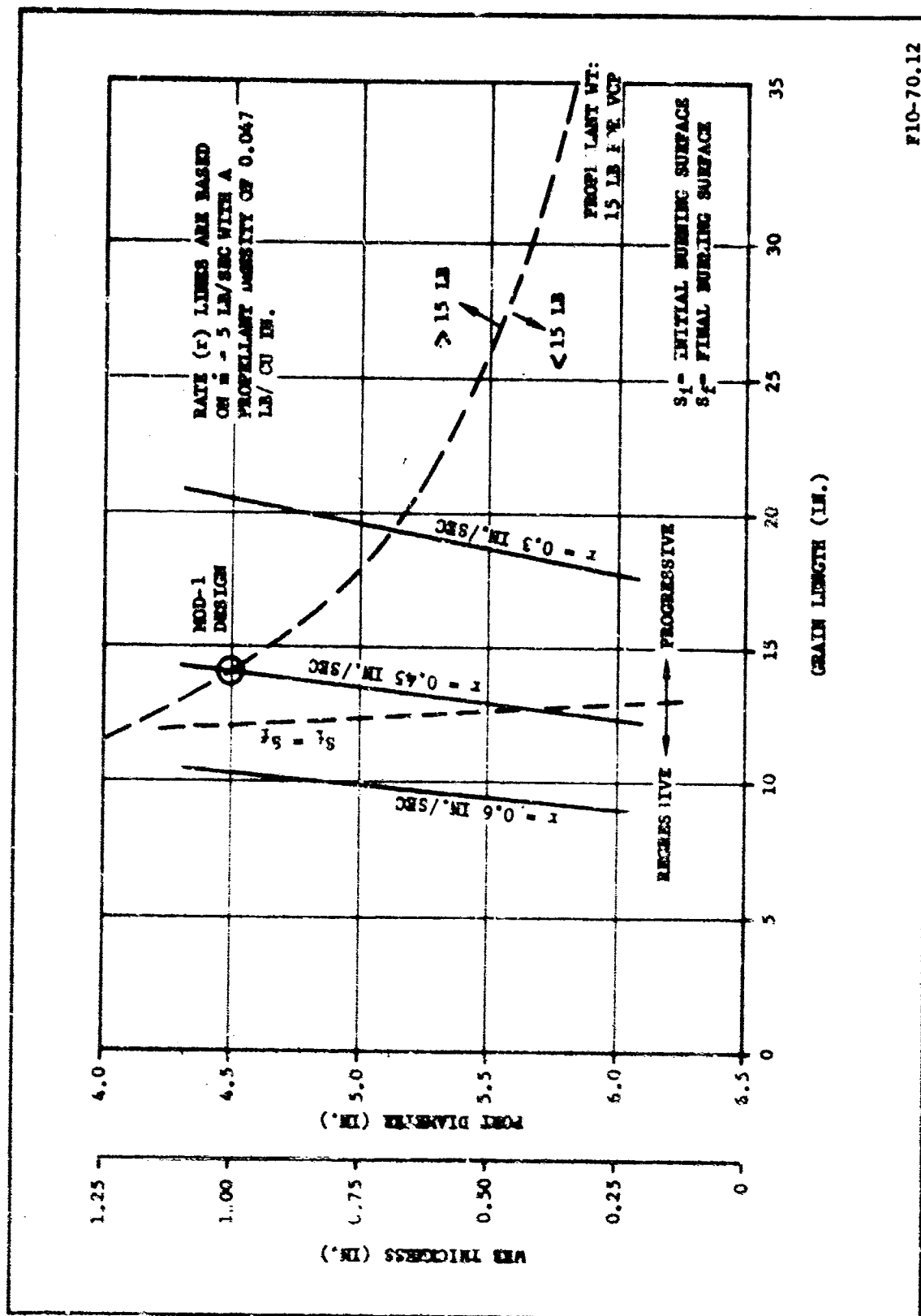
Figure 46. Grain Design Tradeoffs for Single-Length 15PC Motor at a Constant Mass Flow of 5 lb/sec
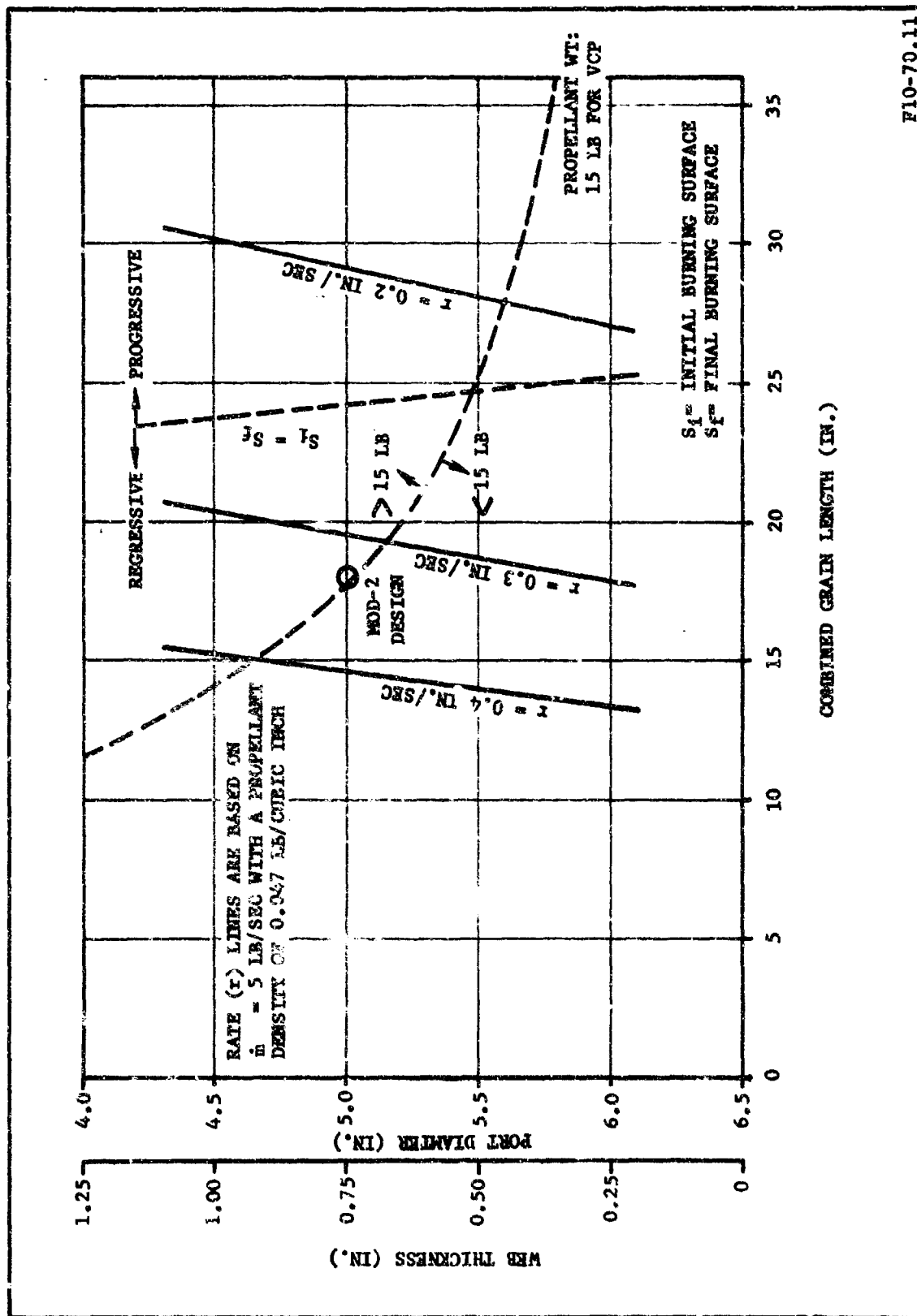
Figure 47. Grain Design Tradeoffs for Double-Length 15PC Motor
as a Constant Mass Flow of 5 lb/sec

F10-70.11

97

MOD-1 GRAIN DESIGN
BASED ON VCP
PROPELLANT
$\bar{K}$ = 150

MOD-2 GRAIN DESIGN
BASED ON VCP
PROPELLANT
$\bar{K}$ = 150

PRESSURE (PSI)

TIME (SEC)

F10-70.13

98

Figure 49. Motor Configurations for Standard 15PC Motor and Mod-2 Grain

MOD-1 15PC
SINGLE GRAIN FOR INTERMEDIATE RATF PROPELLANT
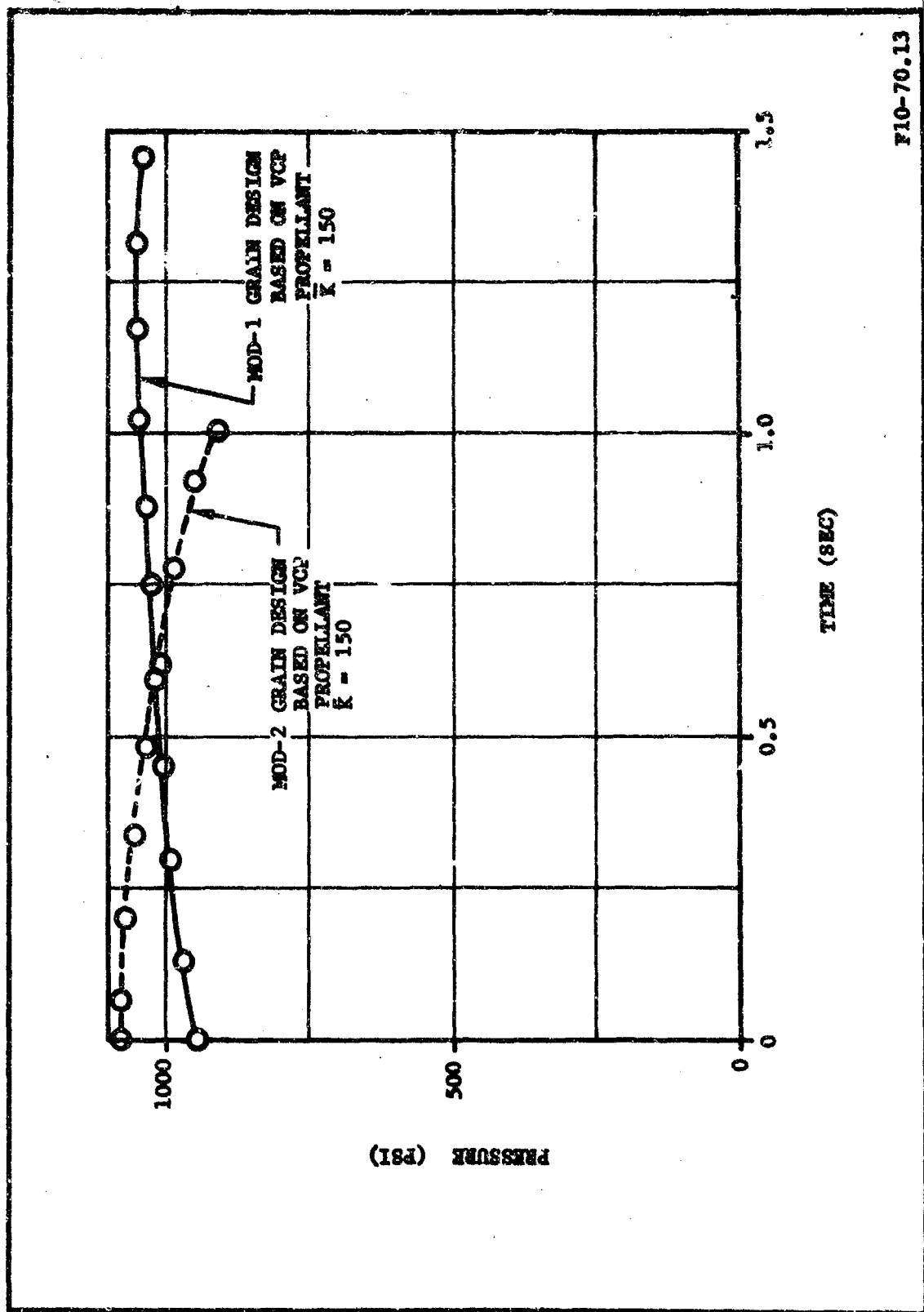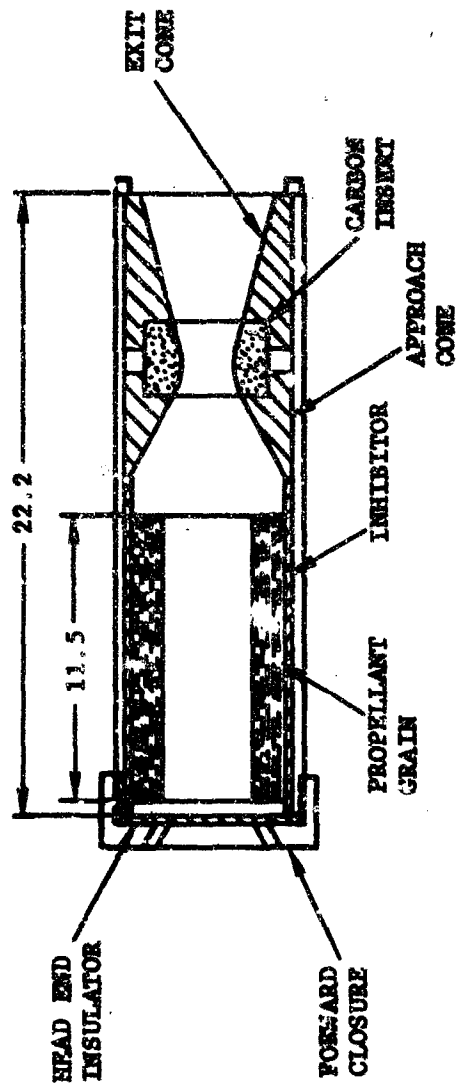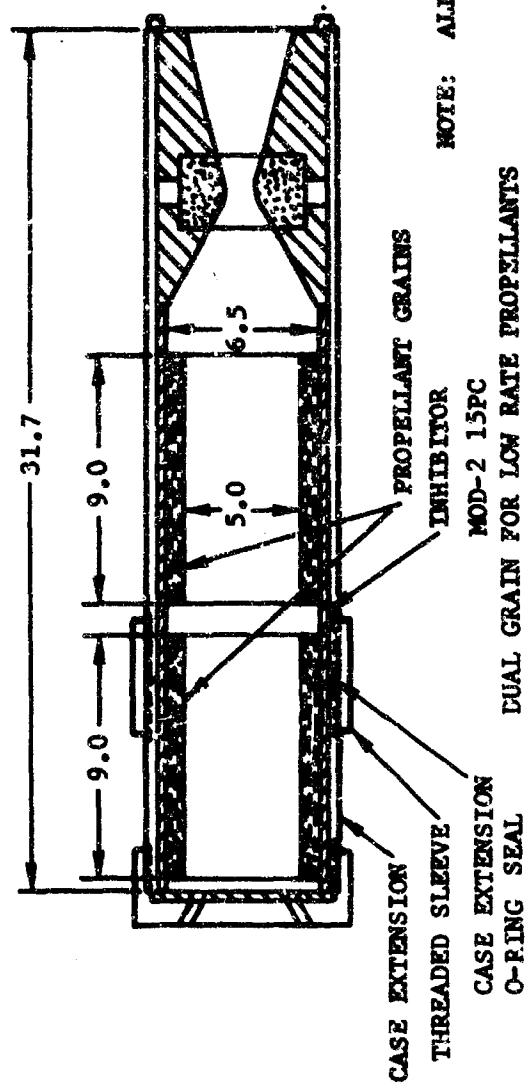
HIGH L* 15PC

Figure 50. Motor Configurations for L* Firings
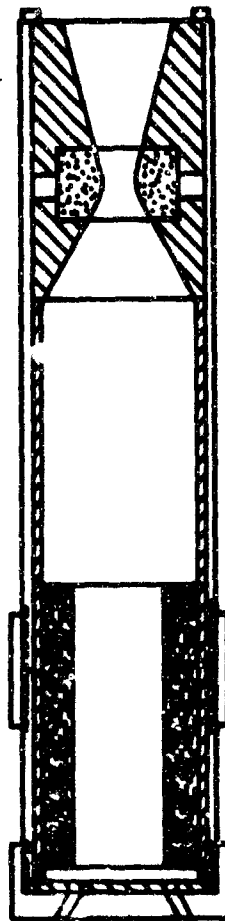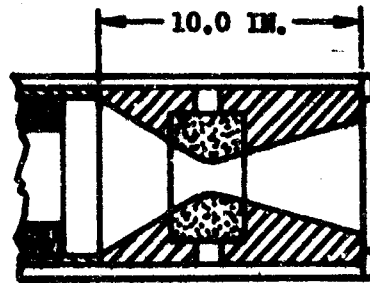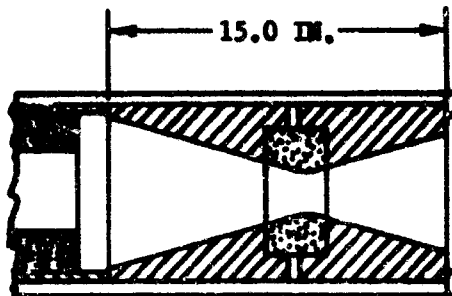
NOTE: ALL DIMENSIONS IN IN.

F10-70.1

100
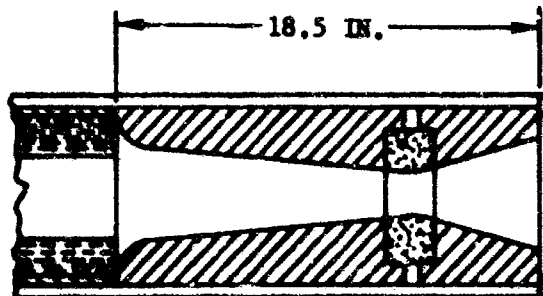
Figure 31. Comparison of 15PC Motor Nozzle Configurations

101

TABLE XXI

COMPARISON OF BALLISTIC DESIGN CRITERIA FOR
AF 04(611)-10754 EVALUATION MOTORS

| Motor Designation | 5PC | Standard 15PC | Mod-1 15PC | Mod-2 15PC |
|---|---|---|---|---|
| Grain Dimensions | | | | |
| OD (in.) | 4.51 | 6.50 | 6.50 | 6.50 |
| ID (in.) | 2.6 | 3.9 | 4.5 | 5.0 |
| No. grains per motor | 1 | 1 | 1 | 2 |
| Length (in.) | 8.0 | 11.5 | 14.0 | 9.0 |
| Web (in.) | 0.95 | 1.3 | 1.0 | 0.75 |
| S (in$^2$) | 89.0 | 189 | 242 | 325 |
| Volume of propellant (in$^3$) | 84.5 | 246 | 242 | 244 |
| Weight of propellant (lb @ 0.062 lb/in$^3$) | 5.2 | 15.2 | 15.0 | 15.1 |
| Free volume ($V_F$-in$^3$) | 77.0 | 242 | 297.3 | 510 |
| Throat area (1) ($A_t$) | 0.594 | 1.26 | 1.61 | 2.17 |
| $L^* = V_F/A_t$ | 130 | 192 | 184 | 277 |
| $\frac{P_{mi}/P_b/P_{max}}{P_p/P_b/P_b}$ | 0.96/1.0/1.08 | 0.92/1.00/1.08 | 0.92/1.00/1.04 | 0.90/1.00/1.02 |
| Divergence angle (°) | 15 | 15 | 15 | 15 |
| Expansion Ratio | 4.8 | 3.7 to 30 | 3.7 to 30 | 3.7 to 30 |

(1) Based on VCP, K = 150 @ 1000 psi

in the nozzle approach contouring and high L* studies to provide a firm basis for determining the effect of these motor parameters on motor efficiency. The control propellant selected was the VCP formulation which had previously been extensively characterized in 5PC, 15PC, and 400-lb motor firings over a wide pressure range and at high expansion ratios. A summary of properties for the VCP formulation is presented in Table XXII.

TABLE XXII

SUMMARY OF PROPERTIES FOR VCP

| Propellant Type | VCP Control Propellant |
|---|---|
| Formulation (Wt %) | |
| NC | 15.0 |
| NG | 32.4 |
| AP | 9.0 |
| HMX | 29.0 |
| Be | 10.0 |
| Res | 1.0 |
| 2-NDPA | 1.0 |
| TA | 2.6 |
| | |
| Theoretical Performance | |
| Isp(1000/14.7)(sec) | 283.0 |
| Tc ($^\circ$K) | 3850.0 |
| Oxidation ratio | 1.22 |
| $\rho$ (lb/in.$^3$) | 0.062 |

3.   Beryllium Castings and Firings

A total of 76 Be 15PC motors were cast and 70 were fired. A summary of the subtask castings and firings is presented in Table XXIII. All but six of the castings were completed successfully.

Processing problems were observed in manufacturing VIJ (45$\mu$ AP) and VIN compositions. Due to thick, highly viscous mixes the compositions were difficult to cast and consolidate. One grain of each composition was found to be discrepant because of poor propellant consolidation resulting from the marginal processibility. One mix of each formulation was also lost during attempts to reduce viscosity by use of an elevated temperature mixing cycle. Later mixes of the VIN formulation were successfully processed with 25 percent of the fines removed from the AN. Careful control of the heated mix cycle was successful for the completion of the VIJ (45$\mu$ AP) castings.

TABLE XXIII

SUMMARY OF Be CASTINGS AND FIRINGS

| Purpose | Propellant Type | Grain Design | No. Castings | No. Firings |
|---|---|---|---|---|
| Be efficiency studies | VCP | Standard | 3 | 3 |
| | | Mod-1 | 3 | 3 |
| | VIG | Standard | 4 | 3 |
| | VIH | Standard | 3 | 3 |
| | VII | Mod-1 | .3 | 3 |
| | | Mod-2 | 3 | 3 |
| | VIJ | Standard | 4 | 3 |
| | | Mod-1 | 3 | 3 |
| | VIK | Standard | 3 | 3 |
| | | Mod-1 | 3 | 3 |
| | VIL | Standard | 3 | 3· |
| | | Mod-1 | 2 | 2 |
| | | Mod-2 | 1 | 1 |
| | VIN | Mod-2 | 6 | 4 |
| | VIO | Mod-1 | 3 | 3 |
| Oxidizer particle size | VIJ (45$\mu$ AP) | Standard | 4 | 2 |
| | VIJ (90$\mu$ AP) | Standard | 3 | 3 |
| | VIJ (180$\mu$ AP) | Mod-1 | 3 | 3 |
| Optimum nozzle geometry | VCP | Standard | 4 | 4 |
| | VIJ | Standard | 7 | 7 |
| Increased L* | VCP | Standard | 2 | 2 |
| | VII | Mod-1 | 2 | 2 |
| Characterization of selected propellants | VCP | Standard | 2 | 2 |
| | | Mod-2 | 2 | 2 |
| Total | | | 76 | 70 |

All firings except one were successful. One VIJ firing (LM 2-18) with a 15-degree nozzle approach cone suffered a burnthrough in the forward end of the motor. The burnthrough resulted from leakage in a pressure takeoff fitting, which allowed the chamber gasses to escape the forward end of the motor.

A problem with poor efficiency, resulting in apparent unstable burning, occurred with the VIN formulation containing AN. Figure 52 shows p-K-r data based on four VIN firings. As noted, an apparent slope change occurred in the p-r and p-K curves above 430 psia. This anomalous behavior is also apparent in a change in the discharge coefficients from 0.0078 $sec^{-1}$ for the low pressure firings to 0.0064 $sec^{-1}$ for the high pressure firings and is consistent with combustion-bomb data showing AN formulations to be significantly less efficient than AP or HMX formulations.

Firings made for optimum nozzle studies were observed to have greater nozzle erosion as the approach angle was reduced. Also VIJ firings were observed to have greater nozzle erosion than VCP. These results are shown in Figure 53.

A complete ballistic summary of the individual Be firings is given in Appendix B (Tables B-3 through B-7).

4. LHM-2 Castings and Firings

A total of twenty-six LMH-2 15PC mixes were made and twenty-four 15PC motors fired for ballistic screening of the six candidate LMH-2 propellants. A summary of the subtask castings and firings is presented in Table XXIV. As noted, all but two of the mixes resulted in acceptable grains with mixes containing up to 19-percent LMH-2 at 60-percent-volume solids loading successfully manufactured. Special procedures used for the LMH-2 castings have been described under laboratory formulation studies.

One VIY (containing AP-treated LMH-2) mix was not completed because of an abnormally high viscosity. When the LMH-2 was added to the solvent for this mix, the resulting material had the consistency of sand. A laboratory evaluation of the remaining AP-treated LMH-2 used for this mix was made and found to also give extremely high viscosities. A check of the process cycle showed the AP-treated material was allowed to stand for approximately 3 days in an alcohol slurry before stripping. It is believed that the LMH-2 and AP rearranged to give an abnormally low bulk density, resulting in the higher mix viscosity. Because of the higher delivered impulse obtained with initial firings of wax-treated LMH-2 in the VIY formulation, a wax-treated casting was substituted for the final AP-treated casting. The first VJL mix was also uncastable. The resultant mix was extremely tacky, indicating the pot life had been exceeded. Better mixing action of the larger mixer, coupled with the elevated temperature, appears to have resulted in a shorter pot life than was experienced in the laboratory. The remaining VJL grains were cast at a lower temperature and with a shorter elevated temperature mix cycle.

105

Figure 52. Burning Rate and K for VIN Propellant
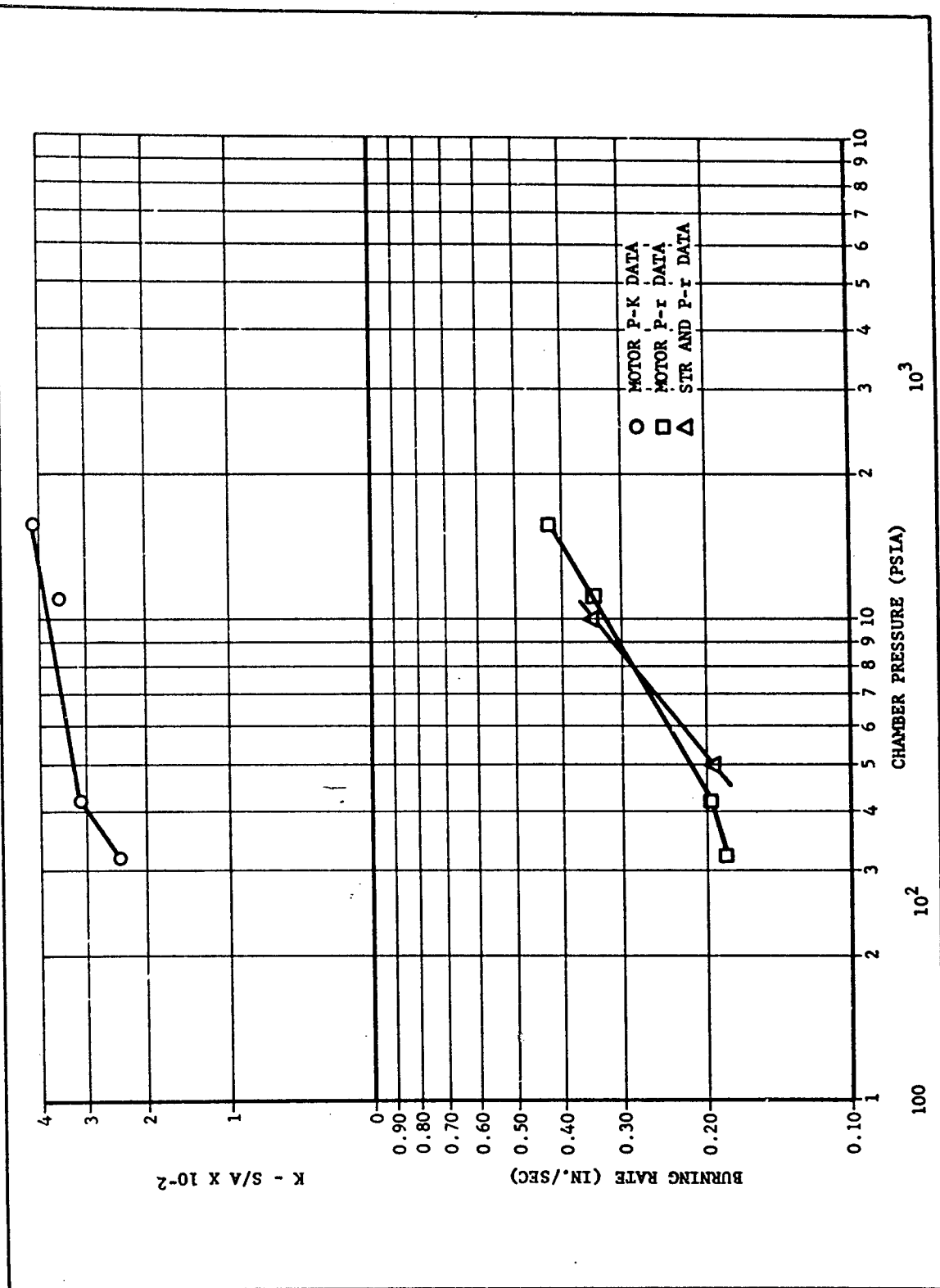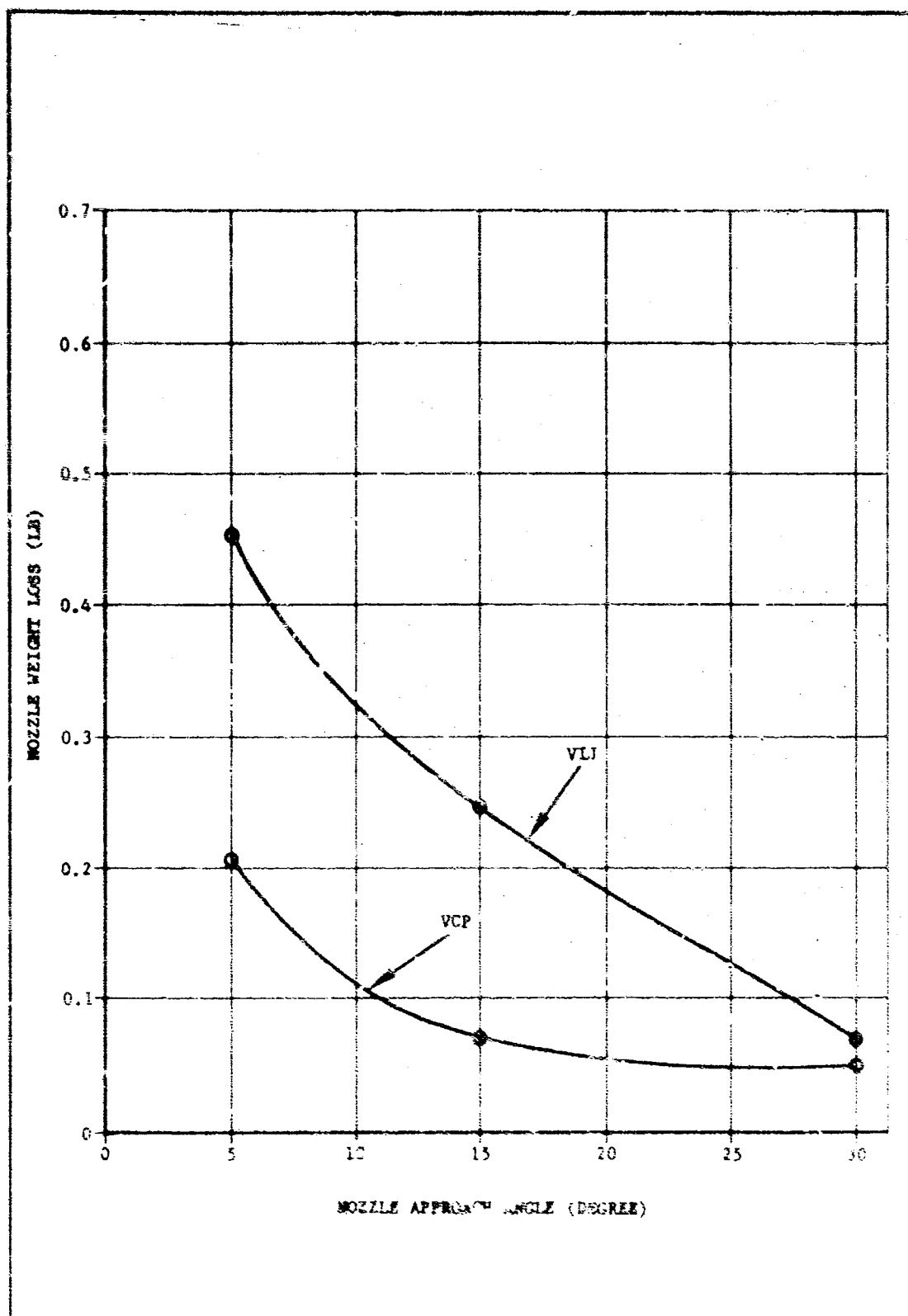
Figure 53. Nozzle Erosion Weight Loss vs Approach Angle

TABLE XXIV

SUMMARY OF LMH-2 CASTINGS AND FIRINGS

| Purpose | Propellant Type | Grain Design | No. Castings | No. Firings |
|---|---|---|---|---|
| Increased L* | VIY (wax-treated LMH-2) | Standard | 5 | 5 |
| | VIY (AP-treated LMH-2) | Standard | 5 | 4 |
| LMH-2/AP Propellants | VIX | Standard | 3 | 3 |
| | VIZ | Standard | 3 | 3 |
| LMH-2/HMX Propellants | VJA | Mod-1 | 3 | 3 |
| | VJI | Standard | 3 | 3 |
| | VJL | Standard | 4 | 3 |
| Final Characterization | VJA | Standard | 3 | 3 |
| | | Mod-1 | 3 | 3 |
| | VIY | Standard | 5 | 5 |
| Total | | | 37 | 35 |

All LMH-2 firings were successful. Figure 54 shows a typical pressure-time curve for the VIY formulation. A complete ballistic summary of the individual firings is given in Appendix B (Tables B-8 through B-10), and a detailed analysis of the resulting data is given in Section II. A summary of performance data obtained from the ballistic screening firings made at high L* values with wax-treated LMH-2 is contained in the following tabulation:

| Formulation | VIX | VIY | VIZ | VJA | VJI | VJL |
|---|---|---|---|---|---|---|
| Percent LMH-2 | 15 | 17 | 19 | 15 | 17 | 17 |
| Oxidizer | AP | AP | AP | HMX | HMX | AP/HMX |
| Isp (1000/14.7) | 303.7 | 308.9 | 313.8 | 309.3 | 314.0 | 312.7 |
| Tc ($^{\circ}$K) | 3678 | 3679 | 3672 | 3621 | 3623 | 3614 |
| O.R. | 1.34 | 1.22 | 1.11 | 1.15 | 1.06 | 1.08 |
| $\rho$ (gm/cc) | 0.049 | 0.0477 | 0.0464 | 0.049 | 0.0477 | 0.0476 |
| Efficiency | 92.24 | 91.01 | 89.81 | 90.83 | 86.37 | 88.57 |
| $Isp^{15}_{1000}$ | 280.1 | 281.1 | 281.8 | 280.9 | 271.2 | 277.0 |

As shown, the first four formulations all exceeded the target impulse goal. Based on these data the VJA and VIY formulations were chosen for the final characterization firings. VJA has the highest impulse-density and lowest burn rate. VIY offers almost equivalent performance with some advantage in mechanical properties.

### 5. Characterization of Selected Propellants

Five 15PC castings and firings of VIY and six 15PC castings and firings of VJA were ma   to further characterize these formulations. Four 15PC VCP control firings were also made. Ballistic data from individual firings are summarized in Appendix B (Tables B-11 and B-12). Analysis of the data is given in Section II.

Figures 55 and 56 show the resulting p-K-r data for VIY and VJA, respectively. The VIY formulation gave a burning rate of 0.97 in./sec at 1000 psia with a pressure exponent of 0.332. VJA gave a burning rate of 0.77 in./sec at 1000 psia with a pressure exponent at 0.485.

### 6. Explosive Classification

Phase I testing of "Military Explosive Hazard Classification Procedure" was performed on VIY and VJA. The results are presented in Table XXV. These tests indicate VIY and VJA are ICC Class A explosives.
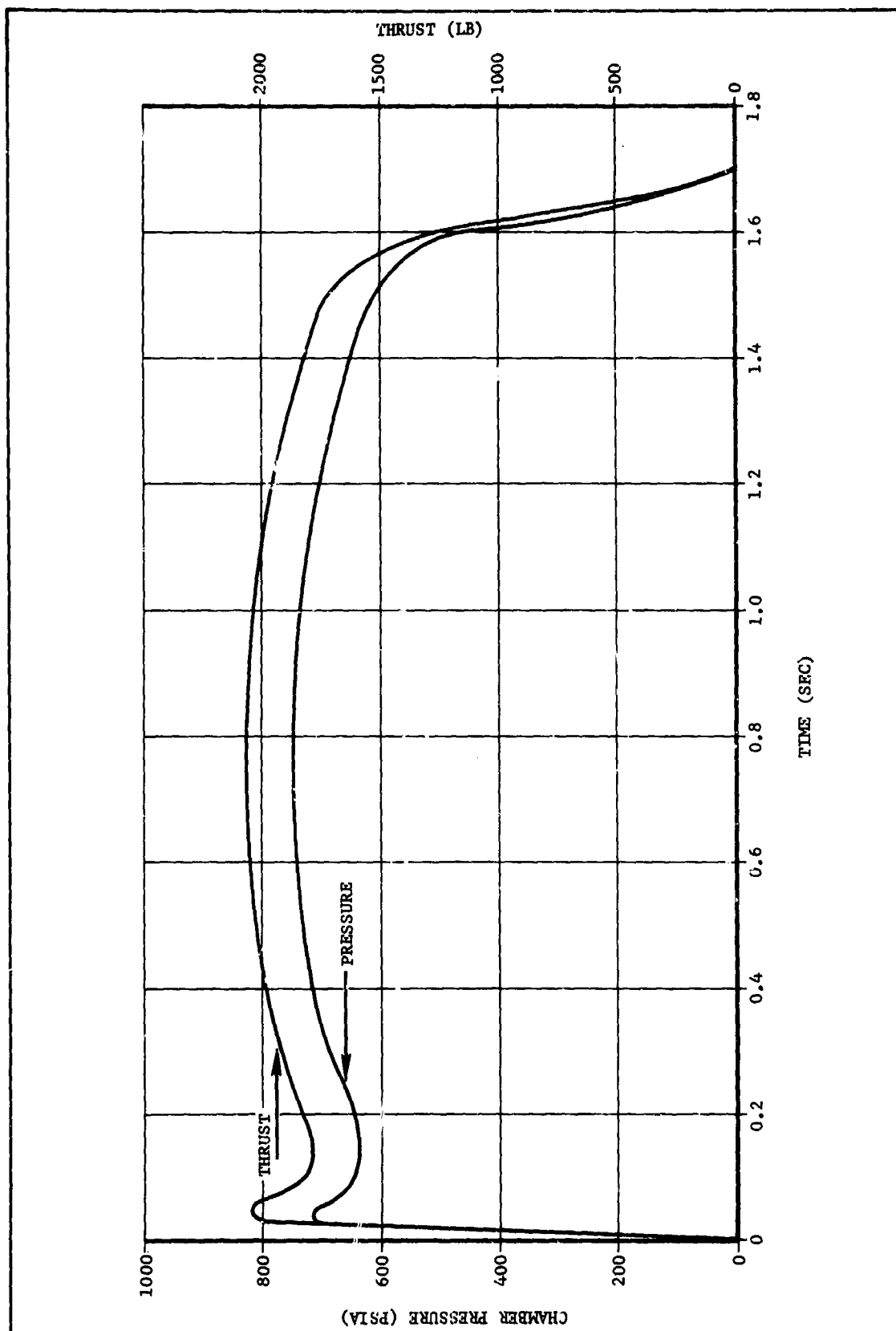
Figure 54. Pressure and Thrust-Time Curves for VIY Propellant
Containing Waxed LMH-2

110
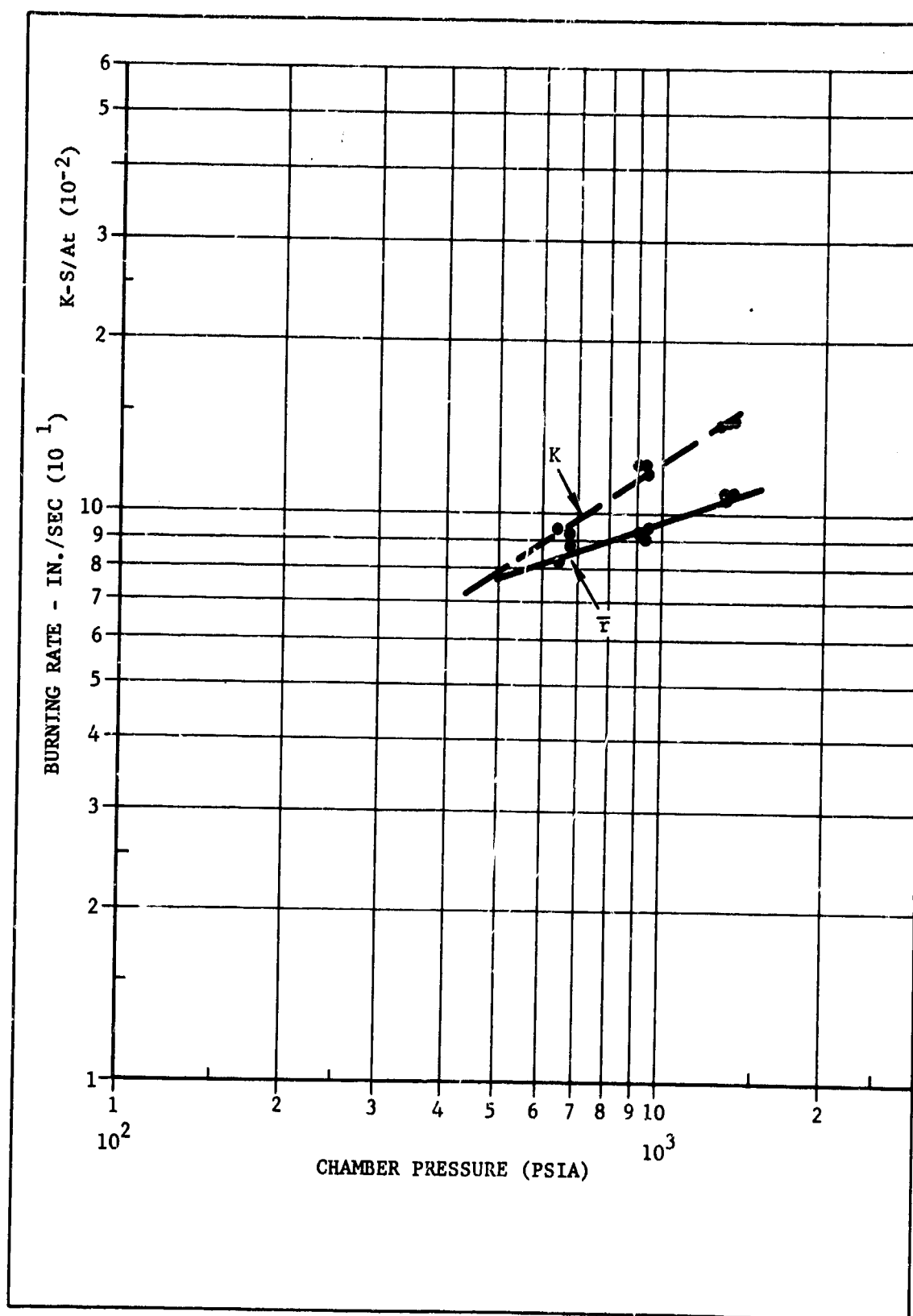
Figure 55.  Burning Rate and K as a Function of
Chamber Pressure for VIY

111
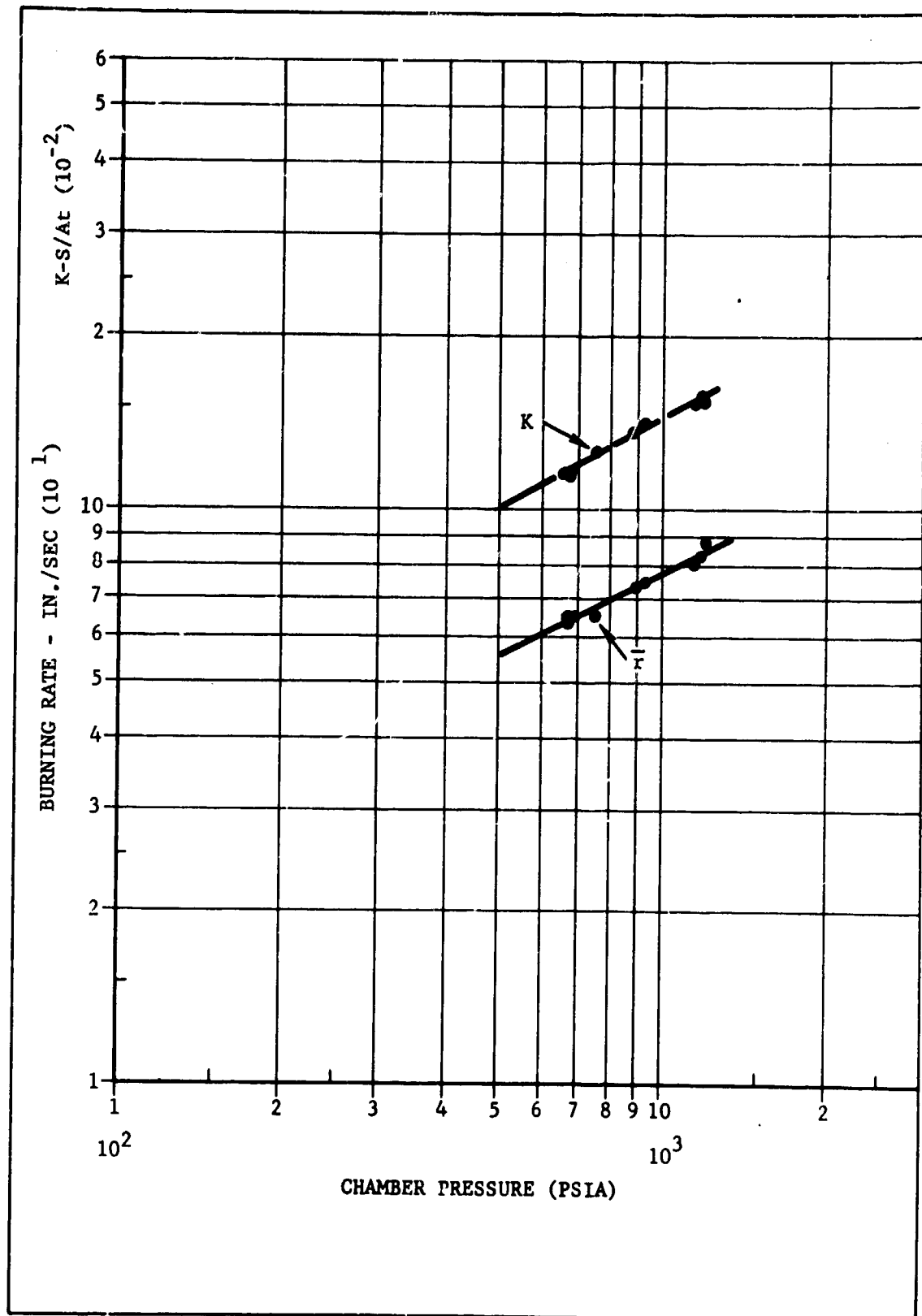
Figure 56. Burning Rate and K as a Function of
Chamber Pressure for VJA

112

TABLE XXV

MILITARY EXPLOSIVE HAZARD CLASSIFICATION RESULTS

| Test | VIY | VJA |
|------|-----|-----|
| Detonation Test | | |
| (1)  No. 8 blasting cap | Detonated | No. detonation |
| (2)  No. 8 blasting cap | | Detonated |
| | | |
| Ignition and Unconfined Burning | | |
| (1)  One 1-in. cube | Burned without detonation | Burned without detonation |
| (2)  One 2-in. cube | Burned without detonation | Burned without detonation |
| (3)  One 2-in. cube | Burned without detonation | Burned without detonation |
| (4)  Four 2-in. cubes | Burned without detonation | Burned without detonation |
| Thermal Stability | | |
| (1)  One 1-in. cube, 48 hr @ 75° C | No ignition | No ignition |
| Impact Sensitivity | | |
| (1)  20 tests without ignition, 2 kg wt | 21 cm | 21 cm |
| Differential Thermal Analysis | | |
| (1)  20 mg sample, temp at which exothermic reaction of sample occurs | 175° C | 182° C |

113

CONFIDENTIAL

SECTION IV

TASK III, ADVANCED CONCEPTS

A.  SCOPE

The objective of Task III was to use advanced formulation or motor
techniques to study and improve LMH-2 combustion.  Six LMH-2, two Be, and
one Al 5PC motors were fired.  The experiments in this task were designed
to evaluate the effect of the propellant combustion mode on performance.
The task included the following three major areas of effort: ·

(1)  Characterization of LMH-2

(2)  Modification of LMH-2

(3)  Fluorine addition

B.  BACKGROUND

Based on the Task I correlations and theoretical calculations, two
means of promoting higher efficiencies for LMH-2 propellants were originally
selected for investigation under this task.  The correlations showed that
both decreasing the AP particle size and grinding LMH-2 would increase
LMH-2 propellant efficiencies.  This led to the belief that more intimate
contact between the oxidizer and fuel might lead to additional performance
gains.  One means investigated was the pressing of LMH-2/AP binary mixtures.
Work in the first quarter[12] showed pressing to be unattractive because of
the poor physical properties of the pressed material and the corresponding
high pressures required for consolidation.  Another means of achieving
intimate contact, developed under independent research and development
funding, was the recrystallization of LMH-2/AP from an AP-saturated water
dispersion.  Initial attempts at incorporating the AP-treated material in
propellant showed a marked improvement in processibility over "as received"
LMH-2.  As a result, emphasis was transferred from pressing LMH-2/AP
mixtures to AP treatment of LMH-2.  Other methods of surface treating LMH-2
were also investigated.

In addition to more intimate contact to improve LMH-2 performance,
theoretical calculations showed that in LMH-2 fluorine systems, significant
amounts of $BeF_2$ gas are formed, which may improve thrust efficiency by re-
ducing particle lag effects.  The possibility also exists that a fluorine
environment may improve LMH-2 combustion efficiency.  To study these
possibilities, means of introducing fluorine into LMH-2 propellants were
investigated.

[12]Refer to List of References

114

CONFIDENTIAL

To provide support to Tasks II and III efforts, a limited amount of work was also scheduled to characterize the chemical and physical properties of LMH-2 being used on this and associated contracts. However, because of difficulties experienced with variable processing and apparent incompatibility problems with LMH-2, extensive laboratory work was required to develop adequate posttreatments to control processibility and eliminate porosity.

## C. CHARACTERIZATION AND MODIFICATION OF LMH-2

### 1. Background

From previous work by Hercules and other propellant formulators, problems were anticipated with the processibility of formulations containing high LMH-2 loadings and with the tendency of certain "as received" LMH-2 lots to produce gassing and porous grains during cure.

The poor processing characteristics of LMH-2 propellants had generally been attributed to the low bulk density of the as-produced LMH-2 (approximately 44 percent of the true density), an unfavorable particle shape, and possibly surface anomalies. Grinding of LMH-2 generally improved processibility although exceptions for some lots were observed. The improved processibility of the ground material could be related to an improvement in bulk density and particle shape. Propellant gassing had been observed for certain LMH-2 lots in double-base propellant by both Hercules and the Atlantic Research Corporation (ARC). No explanation for the gassing apparent, although various test methods for prior screening of LMH-2 lots had been developed by ARC. An elevated temperature and vacuum cycle had been used with some success at Hercules to eliminate gassing.

Since the present production of LMH-2 is confined to 5-lb batches, differences in the LMH-2 purity level, percentages of the various contaminants, and the rheological properties between lots were anticipated on this program. Prior to the shipment of major quantities of LMH-2, several small samples of LMH-2 lots having a wide range of impurities were requested from the Ethyl Corporation. It was hoped evaluation of these samples would provide a clue to the reasons for gassing and subsequently lead to the development of an adequate posttreatment. In addition, samples were requested both unground and ground. The samples were evaluated as follows:

(a) Unground

(b) Ground (ball milled by the Ethyl Corporation for 15 min)

(c) Unground and evacuated 4 hr at $100^\circ$ C

(d) Ground and evacuated 4 to 8 hr at $100^\circ$ C

An analysis of the LMH-2 lots tested is presented in Table XXVI. The samples were incorporated into an LMH-2 formulation containing 12-percent

TABLE XXVI

ANALYSIS OF LMH-2 LOTS FOR EVALUATION

| Sample No. | Composition (Wt %) | | | | | | True Density (g/cc) | Bulk Density (g/cc) |
|---|---|---|---|---|---|---|---|---|
| | LMH-2 | Be Metal | Be Alkyls | Be Alkoxide | Total Chloride | Volatiles | | |
| Lot 80 | 93.7 | 3.5 | 2.1 | 0.12 | 0.28 | Nil | 0.63 | 0.29 |
| B-208 | 96.5 | 2.1 | 1.3 | 0.08 | 0.09 | Nil | 0.64 | 0.26 |
| B222-3 | 94.2 | 1.0 | 1.2 | 0.11 | 0.05 | 0.16 | 0.63 | 0.26 |
| B-249-50 | 92.2 | 2.4 | 2.4 | 0.27 | 0.08 | Nil | 0.56 | 0.25 |
| B253-4 | 93.2 | 4.0 | 1.9 | 0.08 | 0.06 | Nil | 0.58 | 0.27 |
| B270-2 | 94.1 | 2.0 | 1.2 | 0.31 | 1.02 | Nil | 0.65 | 0.26 |
| B273-4 | 91.2 | 6.5 | 3.4 | 0.10 | 0.31 | Nil | 0.64 | 0.28 |
| B297-8 | 94.7 | 1.9 | 1.8 | 0.30 | 1.18 | 0.07 | 0.65 | 0.31 |
| B264-6 | 95.1 | 3.3 | 2.1 | 0.24 | 0.32 | 0.15 | 0.64 | 0.27 |
| B267-9 | 94.5 | 2.5 | 3.0 | 0.22 | 0.37 | Nil | 0.65 | 0.27 |
| B301-2 | 91.9 | 4.9 | 2.5 | 0.08 | 1.04 | 0.01 | 0.64 | 0.30 |
| B275-7 | 94.2 | 2.7 | 5.7 | 0.33 | 0.17 | 0.06 | 0.63 | 0.28 |
| B168-70 | 91.9 | 1.5 | 1.7 | 0.69 | 0.80 | 0.57 | 0.65 | 0.27 |
| 19 | 94.3 | 2.5 | 2.3 | 0.08 | 0.11 | -- | 0.64 | 0.29 |

Analysis as reported by the Ethyl Corp

LMH-2 with 57-percent-volume-solids loading. Ten-gram mixes were cast and cured. All of these samples showed varying degrees of porosity when cured at 140° F for 3 days or longer. However, four different lots cured at a lower temperature (120° F) showed no porosity with this formulation. Estimated viscosities for these mixes ranged from 40,000 to 300,000 centipoises with no apparent correlation between viscosity and porosity. This indicated high viscosities, and resulting poor deaeration was probably not the cause of the porosity. A comparison of viscosities from mixes containing ground versus unground lots showed improvement in processing for only certain lots; however, where no improvement was obtained, photomicrographs of the LMH-2 indicated incomplete grinding.

Based on the results of the above mixes, a second series of mixes was made with a formulation containing 8-percent LMH-2 which had a considerably lower viscosity to eliminate the possibility of poor deaeration as a cause of porosity. Using this formulation and curing at 120° F, void-free grains were consistently obtained with vacuum-baked lots.

Because of a limited supply of material, no additional tests were run with the above lots, and the results shed limited light on the nature of the gassing problem. However, cure temperatures in excess of 120° F were shown to be detrimental and all other LMH-2 propellants were cured at 120° F. Subsequent production lots were requested to be ground for an additional 15 min and vacuum baked for 4 hr at 100° C.

### 2. Modification of LMH-2

Preliminary studies conducted indicated that processing would become marginal at 15- to 17-percent LMH-2 loadings even at moderate total solids loading. A limited amount of work was conducted to determine if other posttreatments such as an acid or water bath or surfactants would improve processing. Neither of these surface treatments improved processing, and other more drastic methods were sought.

It was postulated that deposition of a surface coating might improve both the shape factor and surface character of LMH-2. As a result, preliminary work was conducted to determine if a surface coating could be applied. It was also suggested that a more intimate contact of oxidizer with LMH-2 might enhance combustion efficiency. Consequently, initial attempts for surface coating were made using the primary oxidizer, AP.

#### a. AP Treating

Attempts were made to place a surface coating of AP onto LMH-2 by both temperature recrystallization and crystallization by evaporation.

In the temperature recrystallization method, a saturated aqueous solution of AP containing dispersed LMH-2 was heated to 60° C. The mixture was shaken vigorously to ensure that all AP had dissolved. The

117

mixture was then cooled as rapidly as possible and suction filtered. The
filter cake was washed twice with Freon-TA[1] solvent and dried for 16 hr
under vacuum. A 1-percent addition of Triton X-100 surfactant was then
applied to the AP-treated LMH-2, and the material was vacuum dried for 16 hr
at 120° F. The ratio of AP to LMH-2 was controlled by the temperature-
solubility difference of AP in the aqueous solution.

In the crystallization by evaporation method, a laboratory
rotating evaporator (Rinco) was charged with an aqueous AP/LMH-2 dispersion.
The water was stripped off by heating it at 60° C under 14 mm Hg.

Laboratory batches of the resulting materials were charac-
terized by liquid separation techniques, chemical analysis, particle size
analysis, and photomicroscopy. The AP-treated material was also evaluated
for sensitivity, processing, and combustion characteristics.

1) Sensitivity

Representative runs made by temperature and vacuum
recrystallization are presented in Table XXVII. Sensitivity data show
AP-treated LMH-2 material to be satisfactory for safe handling with impact
values between 40 and 115 cm/2Kg and friction between 10 lb at 6 ft/sec and
40 lb at 8 ft/sec. Sensitivity values show that wax-treated samples are
comparable in sensitivity to AP-treated LMH-2, but isopropanol-wet material
may be more sensitive to impact and electrostatic discharge. (Refer to
paragraph b. for discussion on wax treatment.) No significant difference
in sensitivity resulted from the two different methods of AP-treated LMH-2
preparation.

2) Microscopy

The AP-treated LMH-2 material was examined with a
polarizing microscope under this contract and also under an independent
research and development program. The photomicrographs are presented in
Figure 57. Utilizing the birefringence phenomena of AP, the product was
seen to be an agglomerate with the oxidizer forming the center. The LMH-2
particles appeared to be adhered to the surface of the AP crystal. The
size of the agglomerates appeared to be approximately 75 to 150 microns.

3) Micromerographs

Micromerographs of AP-treated LMH-2 prepared by both
the temperature recrystallization method and by crystallization through
vacuum evaporation (Rinco method) were taken and are presented in
Figure 58. The plots show that the particle size distribution was similar
for the two methods, although dissimilar processing properties in propel-
lants were observed, as discussed in subpara 6). The micromerograph data for
the AP-treated LMH-2 gives a somewhat questionable picture of particle size
distribution, since the material tested consists of free LMH-2, free AP,
and LMH-2 adhered to AP crystals and, consequently, results in variable
composition and density.

---

[1]Azeotrope of Freon TF and acetone

118

TABLE XXVII

AP-TREATED IMH-2 RUNS

| | IMH-2 Lot | Material Balance | | | I (cm/2Kg) | Sensitivity | | Autoignition (°C) |
| --- | --- | --- | --- | --- | --- | --- | --- | --- |
| | | IMH-2 (gm) | AP (gm) | AP/IMH-2 | | F (lb/ft-sec) | ESD (Joules) | |
| **Treated by Temp Recrystallization** | | | | | | | | |
| X-110-50 | 275-76 | 10 | 12.6 | 1.26/1 | >115 | 40/6 | 0.025 | >300 |
| X-110-51 | 90A | 10 | 7.4 | 0.74/1 | >115 | 10/6 | 0.025 | >300 |
| X-110-52-i | 90A | 10 | 6.5 | 0.65/1 | 80 | 21/6 | 0.025 | >300 |
| X-110-54 | 90A | 125 | 127 | 1.03/1 | 41 | 48/8 | 0.025 | >300 |
| **Isopropanol wet** | | | | | | | | |
| X-110-56 | 90A | 75 | 111 | 1.45/1 | 21 | 40/8 | 0.00125 | >300 |
| X-110-58 | 90A | 100 | 81 | 0.81/1 | >115 | 38/6 | -- | 291 |
| 0.5% CEC wax | | | | | 41 | 50/6 | -- | >300 |
| 1.0% CEC wax | | | | | >115 | 38/8 | 0.025 | >300 |
| 2.0% CEC wax | | | | | 80 | 38/8 | -- | >300 |
| X-110-66 | 90A | 250 | 330 | 1.32/1 | | | | |
| X-110-73 | 93-1 | 100 | 120 | 1.20/1 | | | | |
| X-110-74 | 93-1 | 100 | 122 | 1.22/- | | | | |
| **Treated by Vacuum Evaporation** | | | | | | | | |
| X-110-62 R | 90A | 10 | 12.4 | 1.24/1 | >115 | 38/6 | -- | 292 |
| X-110-68 R | 90A | 10 | 12.4 | 1.24/1 | >115 | 40/8 | 0.050 | >300 |
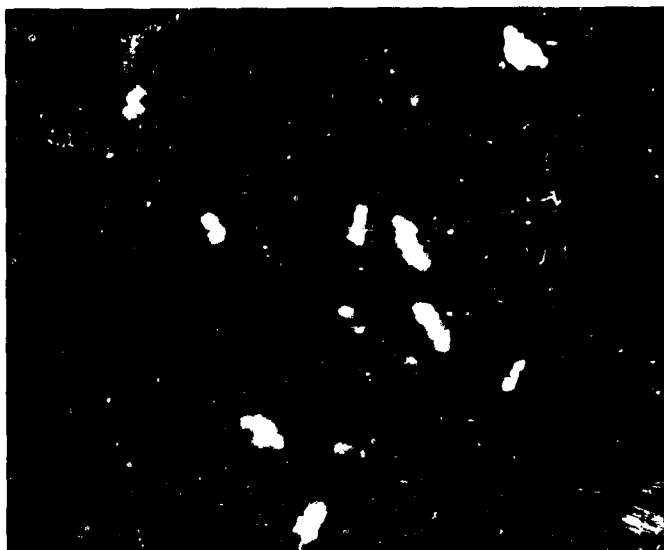
VIEW A. TEMPERATURE RECRYSTALLIZED AP/LMH-2 (100X)



VIEW B. VACUUM CRYSTALLIZED AP/LMH-2 (430X)

Figure 57. AP-Treated LMH-2 Under Polarized Light

120
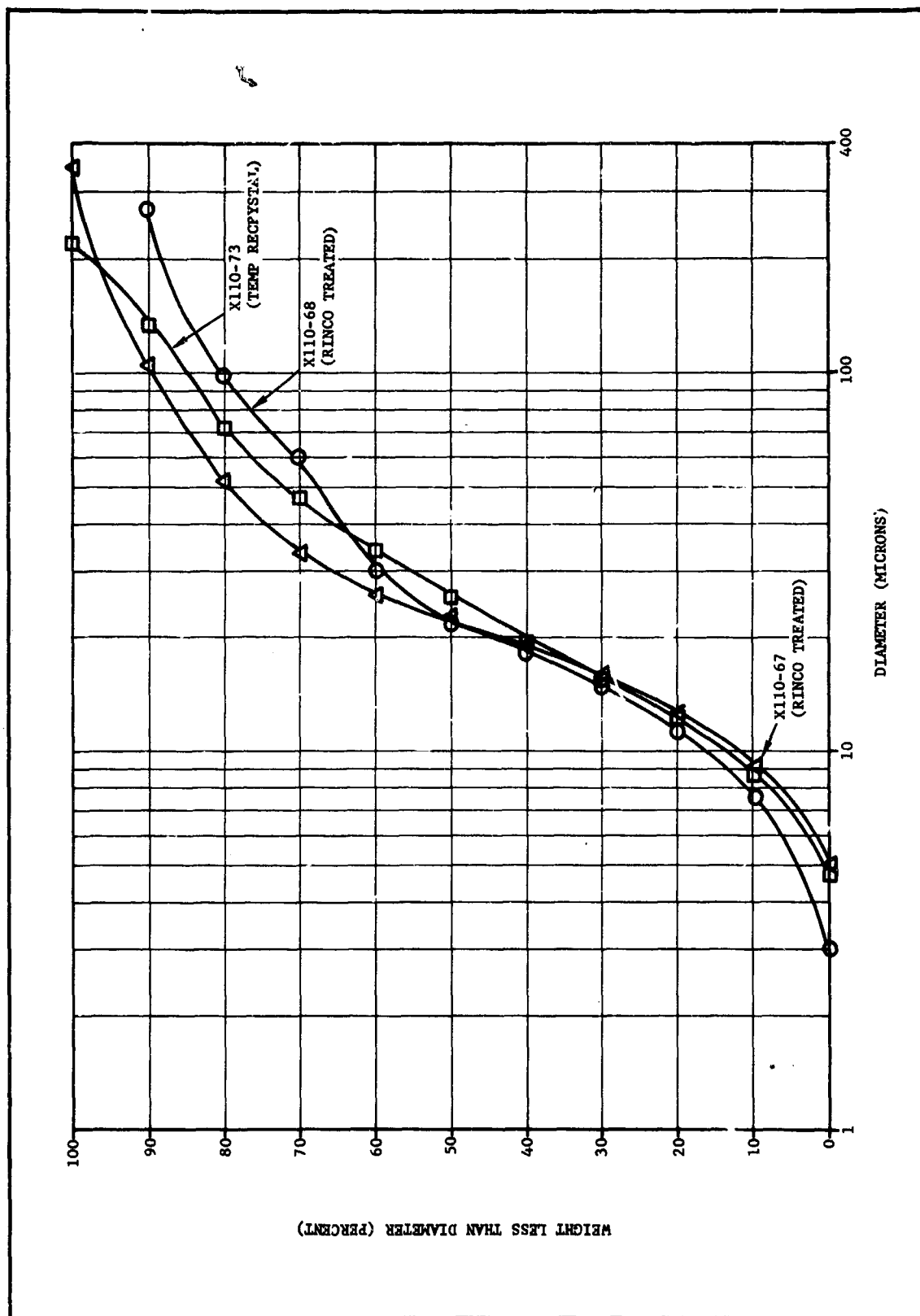
Figure 58. Particle Size Distribution Analysis by Micromerograph

121

### 4) Liquid Separation

Samples of AP-treated LMH-2 were separated with benzene into a light fraction ( < 0.88 g/cc) and a heavy fraction ( > 0.88 g/cc). With the temperatt. recrystallized material, the light fraction contained approximately 98-percent LMH-2, whereas the heavy fraction contained 5- to 8-percent LMH-2. Any LMH-2 in the heavy fraction would have to be adhered to the AP in some manner, since the density of LMH-2 is 0.65 g/cc. Based on the weight and analysis of each fraction, the separation indicated that the AP-treated LMH-2 is primarily free LMH-2 and free AP with only 5 to 10 percent of the total LMH-2 adhering to the surface of the AP. A run was also made in which the light fraction was recycled three times through the crystallization process, but the final combined product still showed only approximately 10-percent LHM-2 in the heavy fraction.

### 5) Chemical Analysis

The AP-treated LMH-2 was analyzed for active hydrogen to determine whether any LMH-2 decomposition had occurred during the crystallization process. The analysis showed the treated LMH-2 had the same active hydrogen content as the untreated LMH-2.

### 6) Processing Studies

Initial attempts at AP treating consisted of preparing a material for use in the VIX formulation by temperature recrystallization. For this formulation the AP-treated material should contain 60.5 percent AP and 39.5 percent LMH-2.

Table XXVIII contains a summary of mixes made with both untreated and treated LMH-2 at approximately 15-percent LMH-2 loadings. Also presented in Table XXVIII is the composition of the various AP-treated LMH-2 runs used. For mixes using the AP-treated material, it is necessary to either adjust them to the exact formulation by adding AP or LMH-2 or to have them suffer some compositional variance. Of particular interest in Table XXVIII is the comparison between the 300-gm mixes--83-2 using untreated LMH-2 and 83-31 using AP-treated LMH-2. As indicated, both viscosity and flow properties were markedly improved with the treated material. Figure 59 shows viscosity as a function of shear rate for these two mixes. This same marked improvement in processing was observed at higher LMH-2 loadings and with all LMH-2 lots investigated.

Only a limited amount of AP-treated material was prepared by vacuum crystallization. These samples failed to show the same process improvements as obtained by temperature recrystallization, and this method was eliminated from further consideration. The lack of improvement in processing was not sufficiently explored to allow a valid explanation to be made for this anomaly.

Based on the results of processing, liquid separation, and microscopy studies with the temperature recrystallized material, it

122

TABLE XXVIII

AP-TREATED LMH-2 PROCESS STUDIES,
15-PERCENT LOADINGS

| Mix No. | Mix Size (gm) | Formulation (%) | | | | | Special Treatment | Viscosity** (Centipoise) | Flow | Heat of Explosion (cal/gm) | Specific Gravity (g/cc) |
|---|---|---|---|---|---|---|---|---|---|---|---|
| | | Binder | Stabilizer | LMH-2 | AP | AP Treated LMH-2* | | | | | |
| 37-77 | 10 | 60 | 2 | 15 | 23 | -- | Ground | 300,000 | None | -- | -- |
| 82-12 | 20 | 60 | 2 | 15 | 23 | -- | Ground | 210,000 | None | 2286 | -- |
| 37-97 | 300 | 60 | 2 | 15 | 23 | -- | Ground | 250,000 | None | -- | 1.334 |
| 83-2 | 300 | 60 | 2 | 15 | 23 | -- | Ground & baked | 166,000 | None | -- | 1.334 |
| 83-4 | 300 | 60 | 2 | 15 | 23 | -- | None | Could not mix | -- | -- | -- |
| 80-28 | 20 | 60 | 2 | 15 | 23 | -- | Ground & benzene washed | -- | None | -- | -- |
| 80-29 | 20 | 60 | 2 | 15 | 23 | -- | Ground, benzene washed, & surfactant applied | -- | None | -- | -- |
| 83-11 | 20 | 60 | 2 | 7.4(15.0)*** | -- | 30.6(1) | -- | 200,000 | Slight | 2297 | -- |
| 83-13 | 20 | 60 | 2 | (15.0) | 12.9 | 25.1(2) | -- | 150,000 | Slight | 2272 | -- |
| 83-14 | 20 | 60 | 2 | (15.0) | -- | 38.0(3) | -- | 200,000 | Slight | 2324 | -- |
| 83-19 | 20 | 60 | 2 | (15.9) | -- | 38.0(4) | Triton added AP treated LMH-2 | 100,000 | none | -- | 1.378 |
| 83-20 | 20 | 60 | 2 | (16.1) | -- | 38.0(5) | -- | 120,000 | None | -- | 1.361 |
| 83-31 | 276 | 60 | 2 | 9.9(15.0) | 1.5 | 26.6(6) | Triton | 66,000 | Good | 2306 | 1.334 |
| 83-34 | 20 | 60 | 2 | (14.4) | -- | 28.0(7) | Ungrouna & Triton | Could not mix | -- | -- | -- |
| 83-35 | 20 | 60 | 2 | (14.3) | -- | 38.0(8) | Unground | Could not mix | -- | -- | -- |

* AP treated LMH-2 compositions (%)

| | (1) | (2) | (3) | (4) | (5) | (6) | (7) | (8) |
|---|---|---|---|---|---|---|---|---|
| LMH-2 | 24.6 | 58.9 | Blend of | 41.9 | 42.3 | 20.0 | 38.0 | 37.6 |
| AP | 75.4 | 41.1 | 56.1(1) | 57.1 | 57.7 | 79.0 | 62.0 | 61.3 |
| Triton X-100 | -- | -- | 43.1(2) | 1.0 | -- | 1.0 | -- | 1.1 |

** Viscosities for 10 and 20 gm mixes are estimated

*** Actual LMH-2 loadings are in parentheses. (15.0)
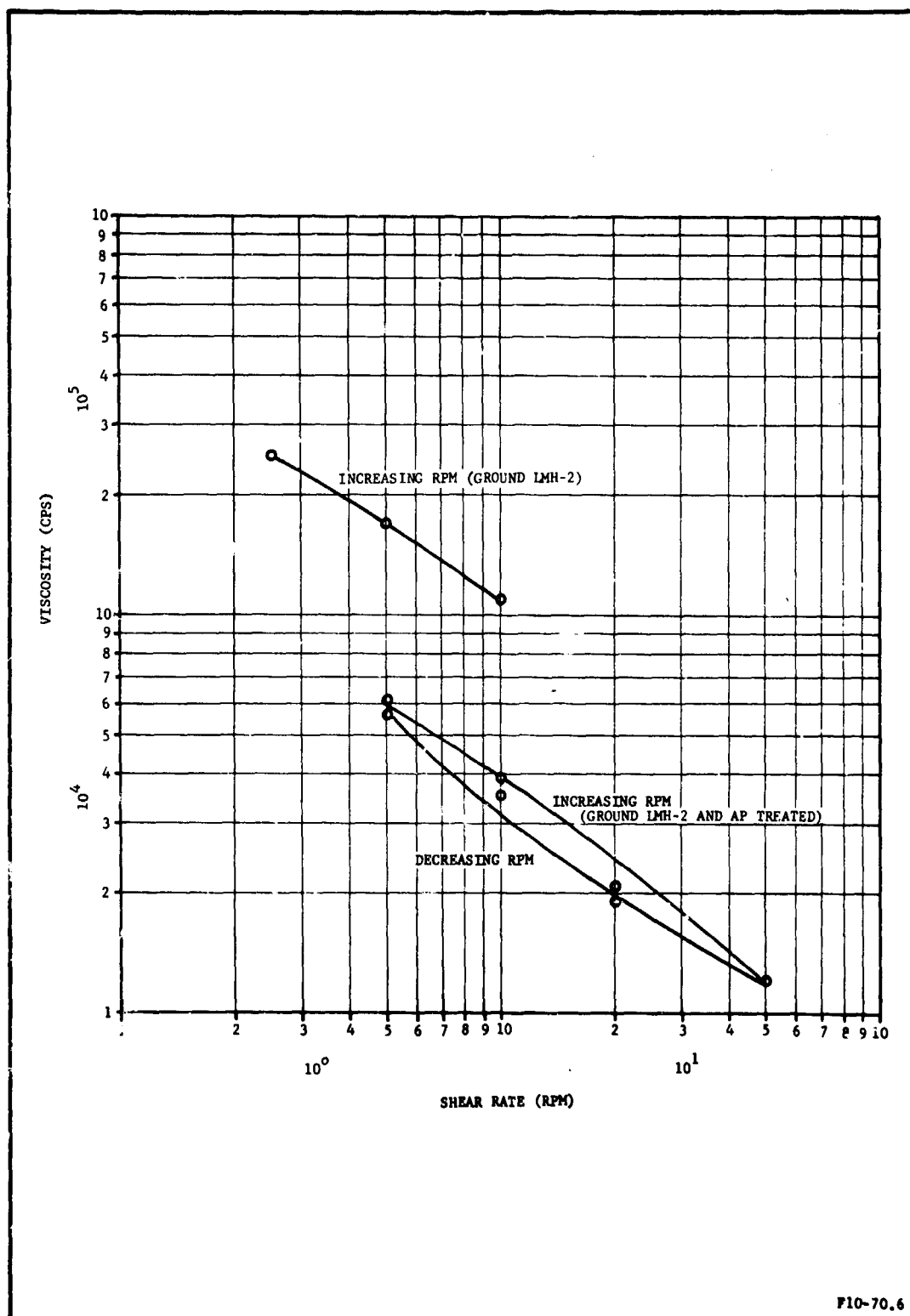
Figure 59. Viscosity as a Function of Shear Rate for the VIX
For      n Containing Nontreated and AP-Treated LMH-2

124

appears the improvements in processing are due to a general improvement in packing and particle shape.

### 7) Closed Bomb Studies

Combustion bomb, window bomb, and heat of explosion tests were conducted on VIX and VIY formulations containing AP-treated LMH-2 and compared to those with untreated LMH-2. These results have been previously given in Table IX and show propellants made with the AP-treated material to be slightly less efficient, contrary to expectations. This lower efficiency was later confirmed in motor firings at low L* values, but at high L* values there was no significant difference in efficiency between AP-treated and non-treated LMH-2. The reasons for the lower efficiency are not readily apparent.

### b. Wax Coating Studies

Coating LMH-2 with a wax obtained from Consolidated Electrodynamics Corporation was also found to improve propellant processing of LMH-2 propellants. Wax coatings were applied to LMH-2 in which the weight percent of wax on LMH-2 was varied from 0.01 to 10.0 percent. Optimum wax content for best processing with "as received" LMH-2 was found to be 1 percent at the 17-percent LMH-2 level.

As-received LMH-2 and vacuum-baked LMH-2 were wax coated by the addition of an acetone-isopropanol solution of the wax, calculated to give the desired percent of wax after the solvent was stripped off. Extended heated vacuum drying times were required to completely remove all traces of solvent which, when present, caused premature gelation of the nitrocellulose and excessively high mix viscosities. As the wax became coated on the LMH-2 surface, a hard outer shell formed that trapped some process solvent, causing solvent removal to be difficult. Heated vacuum drying removed the last traces of acetone-isopropanol solvent.

Figures 60 and 61 show a comparison of the effects of wax treating and AP treating for two LMH-2 lots in the VIY formulation. As shown, the wax treatment reduced the viscosity by approximately a factor of two, whereas the AP treatment reduced viscosity by a factor of three. The viscosity reduction achieved with the waxed material was sufficient to allow incorporation with up to 19-percent LMH-2.

### 3. Final Characterization

Five different LMH-2 lots were received for formulation and motor evaluation on this program. Lot designations and quantities were as follows:

| LMH-2 Lot | Quantity (lb) |
|-----------|---------------|
| 90A | 5 |
| 93 | 20 |
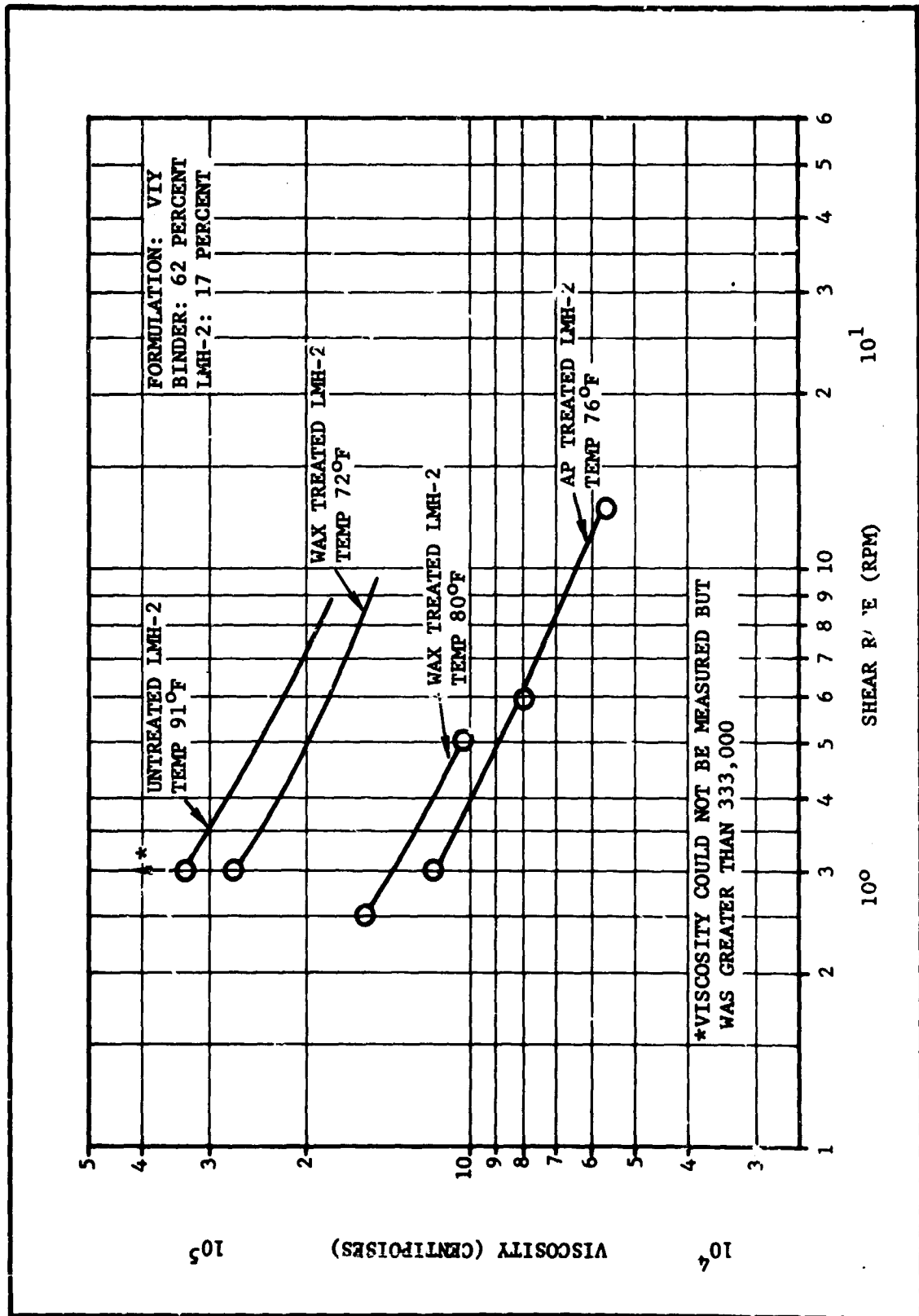
Figure 60.  Viscosity as a Function of Shear Rate For
Posttreated LMH-2, Lot 90A
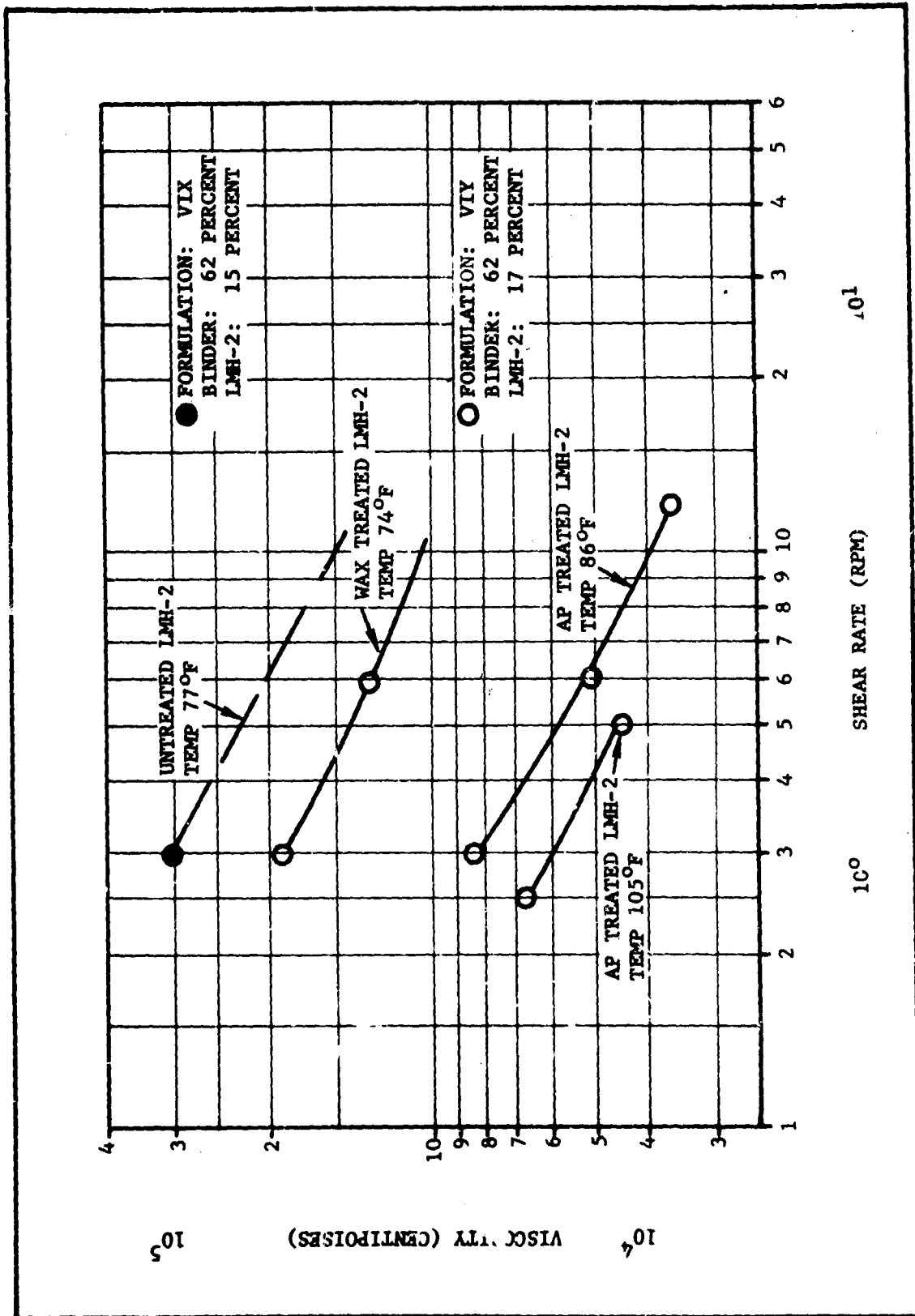
Figure 61. Viscosity as a Function of Shear Rate For
Posttreated IMH-2, Lot 93-1

127

| LMH-2 Lot (Cont) | Quantity (lb) (Cont) |
|------------------|----------------------|
| 96 | 24 |
| 97 | 20 |
| 99 | 40 |

In addition, data was available on lots 95 and 95A from motor evaluation work on Contract AF 04(611)-10742 and on lot 275-7 from a previous IR & D program. Data obtained from testing of these lots is included to provide added information on LMH-2 characterization. Table XXIX summarizes analyses of these lots, and Figure 62 shows the particle size analysis by microrer-graph. The analyses provided by the Ethyl Corporation were run prior to grinding and the 4-hr vacuum bake cycle. All of the lots except lot 95 were ball milled for 30 min. Table XXX contains results of evaluation of these lots with the various candidate LMH-2 formulations. This comparison shows gross differences between lots as to processibility and the extent of the posttreatment required to eliminate porosity. The posttreatments shown are in addition to the 4-hr initial vacuum-bake cycle given all lots by the Ethyl Corporation. In addition, there was a significant difference in the posttreatment required for formulations containing HMX (VJA, VJI) with porosity in these formulations being more severe. As shown for lot 275-7, no additional posttreatment was required. For lots 90A and 93, a 4-hr bake cycle coupled with the wax or AP treatments was sufficient to eliminate porosity in the AP systems but not for the HMX propellants. For lots 95, 95A, 96, and 97, a 16-hr bake cycle was sufficient to eliminate porosity in both the AP and HMX propellants. However, lot 99 required an extended 32-hr vacuum-bake cycle for AP propellants and a water-wash cycle for the HMX systems. In general, the auxilliary wax and AP treatments reduced the amount of time required for the bake cycle, possibly because of the solvent action or the vacuum stripping operation.

Laboratory mixes of VIX, VIZ (AP systems), and VJI (HMX systems) made to evaluate lot 99 are summarized in Table XXXI. The initial evaluation was made with lot 99 vacuum baked for 16 hr at $100^\circ$ C and wax treated. However, mixes 38 through 44 showed that porous grains were obtained in all three formulations with this posttreatment. A series of mixes was then made in which lot 99 was given an elevated temperature and extended baking cycle or a water-wash cycle. The results obtained (Table XXXI) show that nonporous grains in the LMH-2/AP system were produced with a 32-hr, $120^\circ$ C bake cycle with both a 3-mm-Hg and 40-mm-Hg propellant evacuation cycle. Although nonporous at 3 mm Hg, the LMH-2 propellant (VJI) was porous at 40 mm Hg. (The 40-mm Hg evacuation cycle is necessary to prevent foaming during the pilot plant mix cycle.) To eliminate the VJI porosity at 40 mm Hg, lot 99 was given a water-wash cycle. Results obtained using the water-washed material show a 1/2-hr contact time at room temperature was adequate to eliminate porosity for VIX with a 3-mm-Hg evacuation cycle, whereas a 16-hr contact time was necessary for VJI at 3 and 40 mm Hg. Using the extended and elevated temperature vacuum-bake cycle for VIZ and the water-wash cycle for VJI, nonporous 15PC castings were consistently produced.

TABLE XXIX

ANALYSIS OF LMH-2 LOTS

| Analysis (wt %) | 275-7 | 90A | 93 | | 95 | | 95A | 96 | | 97 | | 99 | |
|---|---|---|---|---|---|---|---|---|---|---|---|---|---|
| | (a) | (a) | (a) | (b) | (a) | (b) | (b) | (a) | (b) | (a) | (b) | (a) | (b) |
| LMH-2 | 94.2 | 92.9 | 92.6 | -- | 96.4 | -- | -- | 95.5 | -- | 94.0 | -- | 94.4 | -- |
| Active hydrogen | 17.73 | 17.52 | 17.44 | 16.3 | 17.87 | 17.20 | 18.0 | 17.66 | 17.40 | 17.55 | 18.7 | 17.58 | 17.0 |
| Be metal | 2.7 | 2.2 | 2.3 | -- | 1.0 | -- | -- | 1.1 | -- | 2.0 | -- | 1.5 | -- |
| Be alkyls | 2.6 | 2.5 | 3.1 | 4.7 | 3.2 | -- | 3.8 | 2.3 | 2.4 | 3.3 | 4.8 | 2.5 | 3.7 |
| Be alkoxides | 0.33 | 0.14 | 0.15 | 0.28 | 0.14 | -- | 0.13 | 0.15 | 0.26 | 0.16 | 0.20 | 0.13 | 0.8 |
| Total chlorides | 0.17 | 0.38 | 0.42 | 0.63 | 0.11 | -- | 0.10 | 0.16 | 0.14 | 0.22 | 0.35 | 0.26 | 0.21 |
| Volatiles | 0.06 | 0.23 | 0.09 | 0.4 | 0.01 | -- | 0.20 | Nil | 0.22 | -- | 1.7 | Nil | 0.6 |
| Particle size ($\mu$) | -- | -- | -- | 11 | -- | 37.5 | 28 | -- | 25 | -- | 25 | -- | -- |
| Surface area ($m^2/gm$) | -- | -- | -- | -- | -- | 0.918 | 1.56 | -- | 1.39 | -- | 2.20 | -- | 1.84 |
| Bulk density (gm/cc) (c) | 0.28 | -- | -- | -- | -- | 0.33 | -- | -- | -- | -- | -- | -- | -- |
| Bulk density (gm/cc) (d) | -- | -- | -- | 0.40 | -- | -- | 0.41 | -- | -- | -- | -- | -- | 0.39 |
| True density (gm/cc) | 0.63 | 0.62 | 0.63 | -- | 0.64 | -- | -- | 0.64 | -- | 0.64 | -- | 0.64 | -- |

(a) Analyzed by Ethyl

(b) Analyzed by Bacchus

(c) Unground

(d) Ground
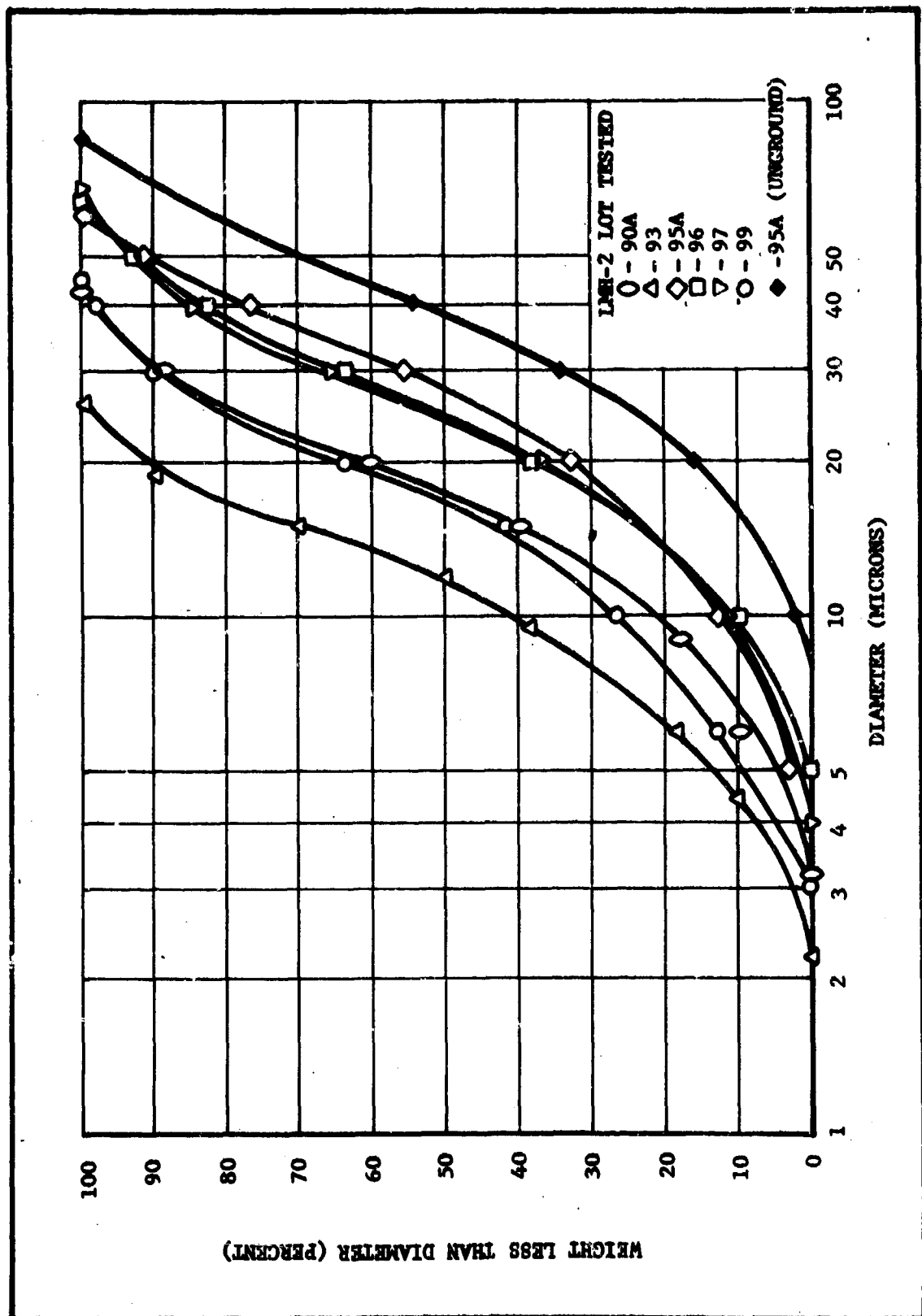
Figure 62. Particle Size Distribution Analysis for LMH-2 Lots by Micromerograph

130

TABLE XXX

EFFECT OF VARIOUS POSTTREATMENTS ON APPARENT COMPATIBILITY
AND PROCESSIBILITY WITH SEVERAL LMH-2 LOTS

| LMH-2 Lot No. | Treatment | Formulation* AP | Formulation* HMX | Specific Surface | Particle Size | Viscosity |
|---|---|---|---|---|---|---|
| 275-7 | None | (1) | | -- | -- | Too thick for mixing |
| 275-7 | Ground | Nonporous(1) | | | | 225,000/76 |
| 275-7 | Ground, ApT | Nonporous(1) | | | | 100,000/78 |
| 90A | Ground | Porous(2) | | -- | 18 | 333,000/91 |
| 90A | Ground, ApT | Nonporous(2) | | | | 116,000/76 |
| 90A | G, 4 hr bake, waxed | Nonporous(2) | | | | 266,000/72 |
| 90A | G, 4 hr bake, waxed | | | | | 51,200/78 |
| 93 | Ground | Porous(1) | Porous(4) | -- | 12 | 303,000/77 |
| | | | | | | 120,000/104 |
| 93 | Ground, ApT | Slight Porosity(2) | | | | 83,000/86 |
| 93 | Ground, 4 hr bake, ApT | Nonporous(2) | | | | 117,000/72 |
| | | | | | | 60,000/105 |
| 93 | Ground, 4 hr bake, waxed | Nonporous(2) | | | | 190,000/74 |
| 93 | Ground, 16 hr bake, waxed | | Porous(4) | | | 250,000/102 |
| 93 | Ground, 4 hr bake, waxed | | Porous(4) | | | 61,000/64 |
| 93 | Ground, 16 hr bake, waxed | | Porous(4) | | | 45,000/96 |
| 93 | Ground, 16 hr bake, waxed and rebaked 8 hr | | Porous(4) | | | 38,000/107 |
| 93 | Ground, 10 hr bake, waxed | Nonporous(1) Slight porosity(5) | | 0.92 | 38 | 58,000/105 |
| 95 | 4 hr bake | | | | | |
| 95 | 18 hr bake | Nonporous(5) | | | | |

*Formulation Key: (1) VIX, (2) VIY, (3) VIZ, (4) VJA, (5) FIQ, (6) VJI

TABLE XXX (Cont)

EFFECT OF VARIOUS POSTTREATMENTS ON APPARENT COMPATIBILITY
AND PROCESSIBILITY WITH SEVERAL LMH-2 LOTS

| LMH-2 Lot No. | Treatment | Formulation* AP | Formulation* EMK | Specific Surface | Particle Size | Viscosity |
|---|---|---|---|---|---|---|
| 95A | Ground, 4 hr bake | Porous(5) | | 1.59 | 28 | |
| 95A | Ground, 8 hr bake | Slight porosity(5) | | | | |
| 95A | Ground, 16 hr bake | Nonporous(5) | | | | 50,000/81 |
| 95A | Ground, water washed | Nonporous(5) | | | | 32,000/83 |
| 95A | Ground | Porous(1) | | | | 140,000/64 |
| 95A | Ground | | Porous(4) | | | 45,000/98 |
| 96 | Ground, 4 hr bake | Porous(1) | | | | 56,000/104 |
| 96 | Ground, 8 hr bake | Porous(1) | | | | 93,000/98 |
| 96 | Ground, 16 hr bake | Nonporous(1) | | 1.4 | 25 | |
| 96 | Ground, 8 hr bake, waxed | Nonporous(2) | | | | |
| 96 | Ground, 8 hr bake, waxed | Nonporous(2) | | | | 32,000/105 |
| 96 | Ground, 4 hr bake | | Porous(4) | | | 61,000/62 |
| 96 | Ground, 16 hr bake | | Nonporous(4) | | | 35,000/102 |
| 97 | Ground, 16 hr bake | Nonporous(1) | | 2.2 | 25 | 65,000/102 |
| 97 | Ground, 16 hr bake, waxed | Nonporous(1) | | | | 43,000/104 |
| 97 | Ground, 16 hr bake | Porous(1) | Nonporous(4) | | | 68,000/100 |
| 99 | Ground, 16 hr bake | Porous(3) | | 1.84 | 17 | 123,000/100 |
| 99 | Ground, 16 hr bake, waxed | | | | | 300,000 |
| 99 | Ground, 16 hr bake, waxed | | Porous(6) | | | 70,000 |

*Formulation Key:  (1) VIX,  (2) VIY,  (3) VIZ,  (4) VJA,  (5) FIQ,  (6) VJA/ 17% LMH-2

TABLE XXXI

POSTTREATMENT EVALUATION FOR LMH-2, LOT 99

| Propellant Type | VIX | VIZ | VLJ | VIX | VIX | VIX | VIX |
|---|---|---|---|---|---|---|---|
| Mix No. | 95-38 | 95-41 | 95-42 | 95-44 | 95-52 | 95-50 | 95-71 |
| Mix size (gm) | 500 | 500 | 500 | 300 | 300 | 300 | 300 |
| LMH-2 lot | 99 | 99 | 99 | 99 | 99 | 99 | 99 |
| Special treatment | Vac baked 16 hr @ 100° C | Vac baked 16 hr @ 100° C, waxed | Vac baked 16 hr @ 100° C, waxed | Vac baked 16 hr @ 100° C, waxed | Vac baked 16 hr @ 120° C, waxed | Vac baked 32 hr @ 120° C, waxed | Vac baked 32 hr @ 120° C, waxed |
| Mixing temperature (°F) | 100 | 109 | 100 | 106 | 106 | 103 | 110 |
| Mix viscosity @ 3 RPM | 123,000 | 300,000 | 70,000 | 40,000 | 83,000 | 70,000 | 73,000 |
| Comments | Quite porous | Porous | Porous | Porous at 3 and 40 mm Hg evacuation | Slight porosity at 3 mm Hg | Nonporous at 3 mm Hg | Nonporous at 3 and 40 mm Hg |

| Propellant Type | VIX | VJI | VIX | VIX | VJI | VJI |
|---|---|---|---|---|---|---|
| Mix No. | 95-47 | 95-54 | 95-48 | 95-49 | 95-51 | 95-56 |
| Mix size (gm) | 300 | 300 | 300 | 300 | 500 | 300 |
| Special treatment | Vac baked 32 hr @ 120° C, 2%, waxed | Vac baked 32 hr @ 120° C, waxed | Water washed 1/2 hr | Water washed 1/2 hr, waxed | Water washed 1/2 hr, waxed | Water washed 16 hr, waxed |
| Mix temperature (°F) | 100 | 104 | 101 | 102 | 101 | 106 |
| Mix viscosity @ 3 RPM | 85,000 | 77,000 | 111,000 | 97,000 | 133,000 | 107,600 |
| Comments | Nonporous at 3 mm Hg | Porous at 40 Nonporous at 3 mm Hg | Nonporous at 3 mm Hg | Nonporous at 3 mm Hg | Porous at 3 mm Hg | Nonporous at 3 and 40 mm Hg |

A study was also conducted on the desorption of gas by LMH-2 under vacuum. This study was initiated because of the large volume increase experienced with propellants during the pot deaeration vacuum cycle. Volume increases of as much as 400 percent were observed.

This large volume increase presented a problem with the pilot-plant mixer which had a free-board limited to approximately 150 percent. It was also felt that the precure gassing might be related to the porous grain problem. As a consequence, a series of tests was run in which various LMH-2 lots were exposed to solvent under vacuum conditions. Results of these tests are summarized in Table XXXII. The test method consisted of placing 50 gm of preevacuated solvent and 12 gm of LMH-2 in a slurry in a vacuum bell jar. Vacuum was then applied and the volume increase observed visually.

In Run No. 1 (Table XXXII) a full vacuum of 4 mm Hg was applied for a period of 40 min to lots 95A and 96 with various posttreatments. A significant volume increase occurred with all samples tested which were exposed to NG solvent. The water-washed lot 95A showed a volume increase of 400 percent, whereas the wax- and AP-treated material both howed approximately 100-percent increases. Lots 95A and 96, with extended baking cycles, showed volume increases intermediate to these extremes. Visual observation of these tests indicated the volume change was the result of gas liberation coupled with a thick (high surface tension) layer of LMH-2 tapping the gas during expansion. Estimates of the volume of gas liberated were made from the volume increases, but this volume could be considerably lower than the actual amount because of gas loss through the film. It was also noted in Run No. 1 that LMH-2 exposed to TA showed no gas evolution.

Because of the apparent solvent differences, a compatibility problem between LMH-2 and NG was indicated. Micro tests were conducted to collect and analyze the off gases by gas chromatography. The resulting analysis showed only air was liberated.

Two additional runs were made (Table XXXII) in which the vacuum was incrementally decreased beginning at 40 mm Hg to see if the amount of air liberated was pressure dependent. None of the materials tested, with the exception of the two "as received" lots, showed any desorption above 20 mm Hg. Possibly, because of the nature of the test, the amount of gas desorbed with a given material was only partially pressure dependent.

Only limited conclusions can be made from the above tests; however, it has been shown that significant amounts of adsorbed air were liberated from LMH-2 under certain conditions. The data in Table XXXII show that between 1 and 8 cc of gas per 100 gm LMH-2 at standard conditions were liberated, depending on the various LMH-2 lot or posttreatment. To obtain more quantitative results, the Ethyl Corporation was contacted, which reported approximately 11 cc of air were desorbed from lot 95A under vacuum at room temperature. To determine the effect of not removing the adsorbed air on cured propellant, FIQ mixes were made at both Bacchus and ABL with

TABLE XXXII

FOAMING STUDIES

| Run No. | Material | LMH-2 Lot | Special Treatment | Vacuum (mm Hg) | Time (min) | Volume Change (%) | Volume Liberated (STP/100 gm) |
|---|---|---|---|---|---|---|---|
| 1 | NG + LMH-2 | 96 | AP treated | 4 | 40 | 100 | 2.1 |
|  | NG + LMH-2 | 96 | Waxed | 4 | 40 | 100 | 2.1 |
|  | NG + LMH-2 | 96 | 16 hr vacuum bake | 4 | 40 | 200 | 4.2 |
|  | NG + LMH-2 | 95A | Water washed | 4 | 40 | 400 | 8.4 |
|  | TA + LMH-2 | 95A | Water washed | 4 | 40 | None | 0 |
|  | NG + LMH-2 | 95A | 12 hr vacuum bake | 4 | 40 | 125 | 2.5 |
|  | NG + LMH-2 | 95A | 16 hr vacuum bake | 4 | 40 | 175 | 3.5 |
| 2 | NG + LMH-2 | 96 | AP treated | 40 | 40 | None | 0 |
|  | NG + LMH-2 | 96 | Waxed | 40 | 40 | None | 0 |
|  | NG + LMH-2 | 96 | 16 hr vacuum bake | 40 | 40 | None | 0 |
|  | NG + LMH-2 | 96 | AP treated | 20 | 20 | 25 | 2.1 |
|  | NG + LMH-2 | 96 | Waxed | 20 | 20 | None | 0 |
|  | NG + LMH-2 | 96 | 16 hr vacuum bake | 20 | 20 | None | 0 |
|  | NG + LMH-2 | 96 | AP treated | 10 | 20 | 40 | 2.1 |
|  | NG + LMH-2 | 96 | Waxed | 10 | 20 | None | 0 |
|  | NG + LMH-2 | 96 | 16 hr vacuum bake | 10 | 20 | 40 | 2.1 |
|  | NG + LMH-2 | 96 | AP treated | 4 | 20 | 50 | 1.1 |
|  | NG + LMH-2 | 96 | Waxed | 4 | 20 | 50 | 1.1 |
|  | NG + LMH-2 | 96 | 16 hr vacuum bake | 4 | 20 | 150 | 3.3 |
| 3 | NG + LMH-2 | 95A | None | 40 | 40 | 25 | 0.8 |
|  | NG + LMH-2 | 96 | None | 40 | 40 | 25 | 0.8 |
|  | NG + LMH-2 | 95A | None | 4 | 20 | 75 | 1.5 |
|  | NG + LMH-2 | 96 | None | 4 | 20 | 100 | 2.0 |

evacuation cycles at 40 mm Hg. The ABL mix was made entirely under vacuum. The Bacchus mix was pot deaerated only prior to casting. The ABL mix was nonporous, and the Bacchus mix showed slight porosity (mix 95-1), which could have resulted from a larger amount of air entrapped during mixing. Both mixes used lot 95A baked for 16 hr. Based on these results, it is questionable whether the porous grain problem is related directly to desorbed air. Additional quantitative work is recommended to determine the amount of adsorbed air present between lots and with various posttreatments.

In an attempt to further define the apparent incompatibility problem, an analysis was made of the gases evolved during cure from propellants containing LMH-2 (lot 99). Analysis of these gases above propellants containing HMX or AP and unbaked LMH-2 showed 500 percent more nitrous oxide and nitric oxide than was found in the same propellant with baked LMH-2. Hydrogen was present in all of the gas samples; however, there did not appear to be a correlation between the concentration of hydrogen and porosity.

Analysis of lot 99 LMH-2 before and after vacuum baking showed that in addition to the adsorbed air of the material being lowered the water content was also decreased 50 percent. The analysis also showed that this particular sample contained above average concentrations of Be chlorides and alkoxides.

Previous experience with various chlorides had shown that they were incompatible with double-base propellants and that water catalyzed the incompatibility. Therefore, a study was initiated to determine if Be chloride and also Be alkoxides were incompatible with double-base propellants or some particular ingredient and if water catalyzed the incompatibility. The test utilized was a microcompatibility test, which consisted of heating the test material with some propellant ingredient and/or double-base propellant at 135° C for 30 min. The gases generated were then analyzed for the presence of decomposition gases. HMX was chosen as the propellant ingredient to test the various compounds against for two reasons: (a) HMX formulations were generally more porous than AP formulations, and (b) HMX alone does not thermally decompose at 135° C in 30 min. The results of this investigation are summarized in the following tabulation:

$CCS/gm$

| Test Compound | $CO_2$ | $N_2O$ | $N_2$ | NO | $NO_2$ |
|---|---|---|---|---|---|
| Be Ethoxide | 1.0 | 3.3 | Trace | 0.0 | 0.0 |
| $BeCl_2$ | 1.0 | 2.3 | 0.3 | 15.9 | 2.3 |
| Be Methoxide | 1.0 | 26.5 | 14.2 | 0.0 | 3.0 |
| LMH-2 unbaked | Trace | 0.2 | 1.6 | 0.0 | 0.0 |
| LMH-2 vacuum baked with water added | Trace | 0.2 | 1.6 | 0.0 | 0.0 |

As was shown by this data, Be chloride and Be alkoxides were to a degree incompatible with HMX. This data also showed that the vacuum-baked LMH-2 with water added to its original concentration generated as much gas as the unbaked LMH-2. It was, therefore, very likely that porosity in LMH-2 propellants was in part due to Be chloride and Be alkoxides.

Of the various lots evaluated there was no apparent trend in contaminants with the observed porosity. However, since the majority of the lots evaluated were composite blends of several pyrolysis runs of varying chemical content, it is likely any trend would be obscured. To overcome this difficulty, several samples of individual pyrolysis runs were obtained from the Ethyl Corporation for evaluation. In Table XXXIII an analysis of these samples is presented. All samples were ground 30 min and given a 4-hr vacuum-bake cycle by the Ethyl Corporation. The samples were subsequently vacuum baked 16 hr at $100^\circ$ C, wax treated at Bacchus, and incorporated in the VIX formulation. All mixes were split into two samples; one was evacuated at 40 mm Hg and one at 3 mm Hg to determine if adsorbed air was a factor. Results of these analyses are presented in Table XXXIV.

Only one sample (357-8) gave serious gassing at 3 mm Hg. This sample had both a high chloride and alkoxide content. (Refer to Table XXXIV.) Several of the other samples showed some porosity with the 40-mm Hg evacuation. This problem is suspected to be due to adsorbed air. There is a definite trend in porosity with the 40-mm Hg evacuation cycle for those samples showing the largest specific surface area and smallest particle size distribution as would be suspected if adsorbed air were a problem. Additional tests are needed to isolate the apparent incompatibility from adsorbed air and to confirm the source of the incompatibility.

Insight into the lot-to-lot variation in processibility can also be obtained from individual LMH-2 pyrolysis runs. A comparison of viscosity with bulk density, specific surface area, and particle size is presented in Table XXXV. Also presented for comparison purposes are lots 93, 95A, and 99, which show extremes in processibility. There was no clear trend apparent of viscosity with either specific surface or particle size. However, Figure 63 shows bulk density of wax-treated material appears to significantly influence processibility. Limited data on as-received LMH-2 indicates factors other than bulk density can drastically alter processibility. These results indicate wax treating may alter the surface character of LMH-2, possibly by filling surface defects, and render the particle more rheologically predictable. Additional studies are needed to further define the process behavior of LMH-2 in plastisol propellants.

D. FLUORINE ADDITION

1. Formulation Screening

There is some basis for believing introduction of fluorine into LMH-2 propellants could improve impulse efficiency. The fluorine environment in itself may improve combustion efficiency, and the formation of

TABLE XXXIII

ANALYSIS OF INDIVIDUAL LMH-2 PYROLYSIS RUNS

| Sample Number | B357-8 | B362-3 | B383-5 | B386-7 | B388-91 | B403-7 | B414-6 |
|---|---|---|---|---|---|---|---|
| Analysis (wt %) | | | | | | | |
| LMH-2 | 92.0 | 92.5 | 96.5 | 95.6 | 94.2 | 96.6 | 94.0 |
| Active hydrogen | 17.14 | 17.14 | 17.87 | 17.63 | 17.41 | 17.75 | 17.50 |
| Be metal | 2.6 | 2.8 | <1.0 | <1.0 | 2.2 | <1.0 | 3.3 |
| Be alkyls | 2.6 | 5.5 | 1.9 | 2.1 | 2.2 | 2.4 | 2.1 |
| Be alkoxides | 1.26 | 0.05 | 0.13 | 0.10 | 0.05 | 0.13 | -- |
| Total chlorides | 0.54 | 0.15 | 0.09 | 0.03 | 0.03 | 0.03 | -- |
| Volatiles | Nil | Nil | 0.01 | Nil | Nil | Nil | -- |
| True density | 0.64 | 0.63 | 0.65 | 0.65 | 0.65 | 0.64 | -- |
| Bulk density | 0.36 | 0.34 | 0.32 | 0.29 | 0.30 | 0.30 | -- |
| Particle size($\mu$)[2] | 19.0 | 23.0 | 20.0 | 18.0 | 21.0 | 22.0 | 21.0 |
| Specific surface[2] ($M^2/gm$) | 2.25 | 1.32 | 1.51 | 2.94 | 1.81 | 1.60 | 1.61 |

Notes: (1) Analysis reported by the Ethyl Corporation before posttreating, except as noted

(2) Analyzed at Bacchus

TABLE XXXIV

EVALUATION OF INDIVIDUAL LMH-2 PYROLYSIS RUNS
IN THE VIX FORMULATION

| Mix No. | 95-73 | 95-74 | 95-64 | 95-66 | 95-75 | 95-65 | 95-67 |
|---|---|---|---|---|---|---|---|
| Mix size (gm) | 300 | 300 | 300 | 300 | 300 | 300 | 300 |
| LMH-2 sample | B357-8 | B362-3 | B383-5 | B386-7 | B388-91 | B403-7 | B414-6 |
| Mix temperature ($^\circ$F) | 111 | 110 | 105 | 106 | 107 | 107 | 107 |
| Mix viscosity at 3 RPM | 95,000 | 78,000 | 110,000 | 100,000 | 77,000 | 133,000 | 143,600 |
| Comments | | | | | | | |
| 40 mm Hg evacuation | Gassed, doming | Nonporous | Nonporous | Slight porosity | Porous | Porous | Porous |
| 3 mm Hg evacuation | Gassed, doming | Nonporous | Nonporous | Nonporous | Nonporous | Nonporous | Nonporous |

TABLE XXXV

COMPARISON OF VISCOSITY WITH PHYSICAL DATA FOR LMH-2 SAMPLES

| LMH-2 Lot | Viscosity (cps) | Bulk Density* (as received) (gm/cc) | Bulk Density* (waxed) (gm/cc) | Specific Surface Area* ($M^2$/gm) | Particle Size* ($\mu$) |
|---|---|---|---|---|---|
| B357-8 | -- | 0.35 | -- | 2.25 | 19 |
| Waxed | 95,000 | | 0.36 | | |
| B362-3 | -- | -- | -- | 1.32 | 23 |
| Waxed | 78,000 | | 0.36 | | |
| B383-5 | -- | -- | -- | 1.51 | 20 |
| Waxed | 110,000 | | -- | | |
| B386-7 | -- | -- | -- | 2.94 | 18 |
| Waxed | 100,000 | | -- | | |
| B388-91 | -- | -- | | 1.81 | 21 |
| Waxed | 77,000 | | 0.36 | | |
| B403-7 | -- | -- | | 1.60 | 22 |
| Waxed | 133,000 | | 0.33 | | |
| B414-6 | -- | -- | | 1.61 | 21 |
| Waxed | 143,000 | | 0.35 | | |
| Lot 93 | 120,000 | 0.40 | | -- | 12 |
| Waxed | 58,000 | | 0.39 | | |
| Lot 95A | 38,000 | 0.41 | | 1.59 | 28 |
| Waxed | -- | | -- | | |
| Lot 99 | 123,000 | 0.39 | | 1.84 | 17 |
| Waxed | 70,000 | -- | 0.37 | -- | -- |

*Analysis performed at Bacchus
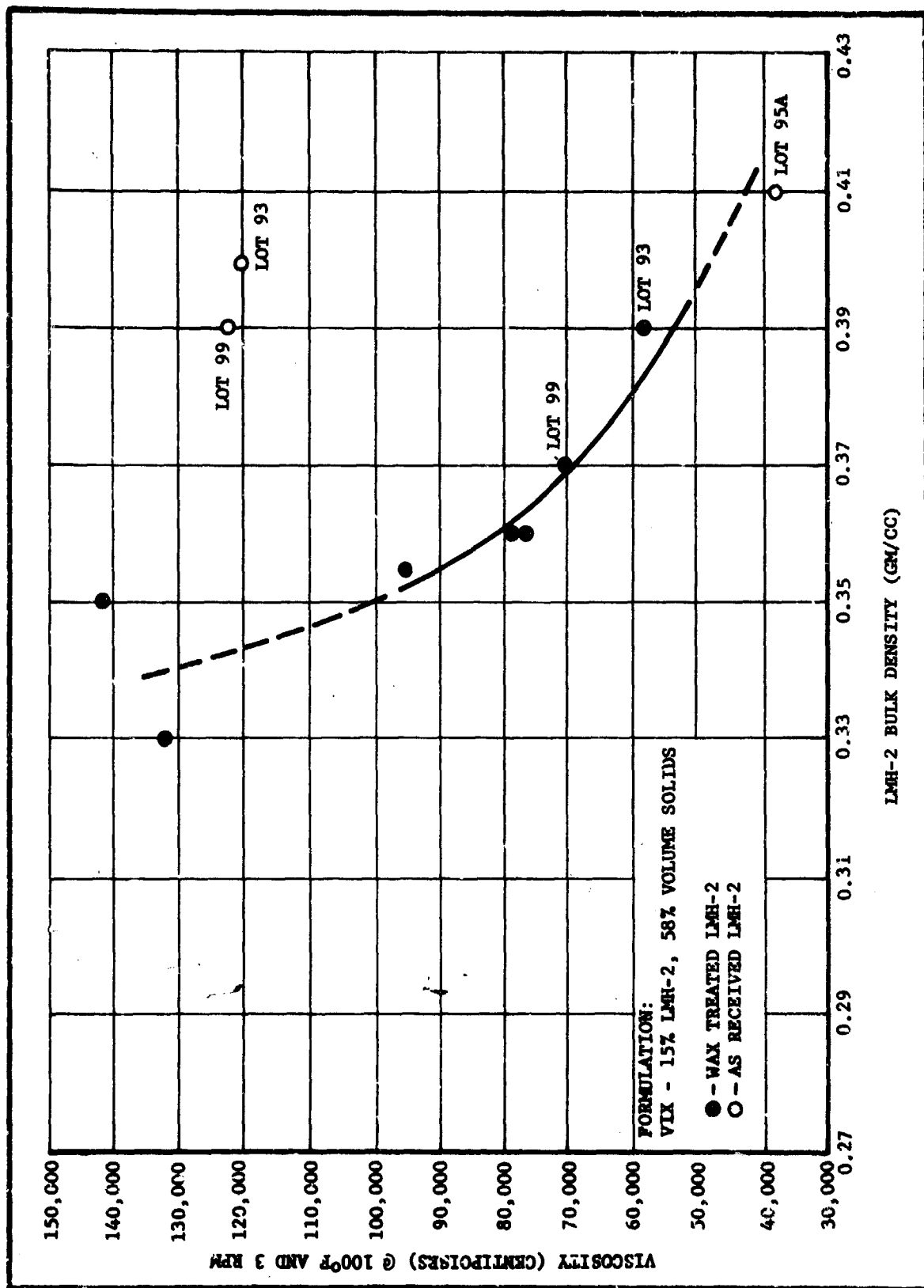
Figure 63. Viscosity as a Function of LMH-2 Bulk Density

significant amounts of the gaseous metal fluoride should reduce particle lag effects. Several means were investigated to incorporate fluorine into an LMH-2 system. The use of the high energy "Domino" compounds was not within the scope of this program, although this would be the most desirable approach. Pressed propellants containing LMH-2/AP and Teflon were investigated experimentally. Because of high compaction pressures required for consolidation, this approach also appeared undesirable at this time. Direct addition of Teflon was not possible because of the low contact angle of Teflon and corresponding propellant segregation. The most promising method investigated was the direct addition of low-molecular-weight Viton-LM. Initial formulation work indicated it was possible to incorporate up to 20-percent-by-weight Viton-LM in double-base propellants while maintaining adequate physical properties. Table XXXVI summarizes theoretical calculations performed on Al, Be, and LMH-2 propellants containing Viton-LM. As shown, at 16- to 20-percent Viton levels, significant amounts of metal fluorides are formed with all three metal fuels.

Because the Viton-LM is a highly viscous thermoplastic, a temperature of approximately $140^{\circ}$ F was required to achieve initial dispersion of the Viton-LM in NG. After dispersion of the Viton-LM the temperature could be lowered to approximately $115^{\circ}$ F and the mix completed while maintaining a good dispersion. At temperatures much below $115^{\circ}$ F, separation occurred. However, at $115^{\circ}$ F a serious pot-life problem existed and mix cycles had to be carefully controlled.

Formulation studies showed the following propellants could be processed adequately:

| Propellant Type | VJE | VJF | VJG |
|---|---|---|---|
| Formulation (wt %) | | | |
| NC | 10.0 | 10.0 | 10.0 |
| NG | 32.5 | 40.0 | 45.0 |
| LMH-2 | -- | -- | 15.0 |
| Be | -- | 12.0 | -- |
| Al | 18.0 | -- | -- |
| Viton-LM | 20.0 | 20.0 | 18.0 |
| AP | 17.5(90 $\mu$) | 16.0(90 $\mu$) | 10.5(90 $\mu$) |
| Res | 1.0 | 1.0 | 0.5 |
| 2-NDPA | 1.0 | 1.0 | 1.0 |

**TABLE XXXVI**

**FLUORINE ADDITION**

| Formulation (%) | LMH-2 | | | | | | | Be | Al | |
|---|---|---|---|---|---|---|---|---|---|---|
| NC | 10.0 | 10.0 | 10.0 | 10.0 | 10.0 | 10.0 | 10.0 | 10.0 | 10.0 | 10.0 |
| NG | 45.0 | 45.0 | 45.0 | 45.0 | 45.0 | 45.0 | 42.5 | 40.0 | 40.0 | 40.0 |
| BeB2 | 14.0 | 14.0 | 16.0 | 15.0 | 15.0 | 12.0 | 15.0 | -- | -- | -- |
| Be | -- | -- | -- | -- | -- | -- | -- | 12.0 | -- | -- |
| Al | -- | -- | -- | -- | -- | -- | -- | -- | 18.0 | 21.6 |
| Viton LM | 20.0 | 16.0 | 16.0 | 20.0 | 18.0 | 20.0 | 20.0 | 20.0 | -- | -- |
| AP | 4.0 | 8.0 | 6.0 | 8.5 | 10.5 | 11.5 | 8.5 | 16.0 | 10.0 | 6.4 |
| TA | 5.0 | 5.0 | 5.0 | -- | -- | -- | 2.5 | -- | -- | -- |
| Res | 1.0 | 1.0 | 1.0 | 0.5 | 0.5 | 0.5 | 0.5 | 1.0 | 1.0 | 1.0 |
| 2NDPA | 1.0 | 1.0 | 1.0 | 1.0 | 1.0 | 1.0 | 1.0 | 1.0 | 1.0 | 1.0 |
| **Theoretical Performance** | | | | | | | | | | |
| $I_{sp}$ (1000/14.7) | 283.4 | 289.6 | 291.4 | 292.9 | 296.5 | 286.7 | 288.9 | 276.2 | 254.7 | 249.6 |
| $T_c$ (°K) | 2820 | 3036 | 2909 | 3117 | 3218 | 2194 | 2950 | 3633 | 3439 | 3377 |
| Oxidation ratio | 0.935 | 0.997 | 0.915 | 0.984 | 1.017 | 1.129 | 0.950 | 1.032 | 1.089 | 0.960 |
| MeO* (moles/100 gm) | 0.907 | 0.969 | 1.124 | 0.975 | 1.058 | 0.893 | 0.977 | 1.034 | 0.282 | 0.253 |
| MeFx* | 0.319 | 0.254 | 0.255 | 0.322 | 0.257 | 0.161 | 0.322 | 0.265 | 0.092 | 0.267 |

\* Concentration of primary metal oxide and metal fluoride at exit conditions

| Propellant Type (Cont) | VJE (Cont) | VJF (Cont) | VJG (Cont) |
|---|---|---|---|
| Theoretical | | | |
| Isp (1000/14.7) | 254.7 | 276.2 | 296.5 |
| $\rho$ (gm/cc) | 1.811 | 1.696 | 1.294 |
| Tc ($^\circ$K) | 3465 | 3633 | 3218 |
| Oxidation ratio | 1.12 | 1.032 | 1.017 |
| MeO* moles/100 gm | 0.292 | 1.034 | 1.058 |
| MeF* | 0.068 | 0.265 | 0.257 |

*Concentration of primary metal oxides and metal fluorides at exit conditions.

Pertinent propellant data for these formulations is presented in Table XXXVII.

## 2. Firings - Task III

The six 5PC grains containing Viton-LM were successfully cast and fired. Table XXXVIII summarizes ballistic data obtained from these firings. Table XXXIX summarizes ballistic data obtained from three 5PC firings of VIX used as the control formulation. A summary of pertinent data from these firings is presented in the following tabulation:

| Formulation | VIX | VJE | VJF | VJG |
|---|---|---|---|---|
| Al | -- | 18.0 | -- | -- |
| Be | -- | -- | 12.0 | -- |
| LMH-2 | 15.0 | -- | -- | 15.0 |
| Viton LM | -- | 20.0 | 20.0 | 18.0 |
| Tc ($^\circ$K) | 3678 | 34.5 | 3633 | 3218 |
| Oxidation Ratio (with Fluorine) | -- | 1.12 | 1.03 | 1.02 |
| Oxidation Ratio (Oxygen only) | 1.34 | 0.98 | 0.91 | 0.91 |
| MeO* | 1.25 | 0.292 | 1.034 | 1.058 |
| MeF* | -- | 0.068 | 0.265 | 0.257 |

*Concentration of primary metal oxide and metal fluorides at exit conditions

## TABLE XXXVII

## VITON-LM FORMULATION DATA

| Propellant Type | VJE | VJF | VJG |
|---|---|---|---|
| **Process Data** | | | |
| Viscosity (cps @ °F) | 10,600 @ 106 | 24,642 @ 114 | 76,360 @ 113 |
| Castability time (max) | 35 - 45 min | 35 - 45 min | 30 - 40 min |
| **Sensitivity Data*** | | | |
| Impact (cm/2kg) | 3.5 (26) | 6.9 (33) | 3.5 (33) |
| Sliding friction (lb$_f$ @ ft/sec) | 88 @ 8 (700 @ 8) | 23 @ 8 (200 @ 8) | 156 @ 8 (500 @ 8) |
| Electrostatic discharge (joules) | 1.25 (0.625) | 0.075 (0.625) | 0.625 (0.625) |
| Autoignition (°C) | 226 (245) | 210 (212) | 219 (223) |
| Differential thermal analysis, ignition (°C) | 173 (169) | 171 (166) | 171 (170) |
| Taliani ($\Delta$P mm @ 93.3°C/ 23 hr) | 10 (4) | 6 (16) | 12 (5) |
| **Ballistic Data** | | | |
| **Strand Rates** | | | |
| 500 psi | 0.334 | 0.332 - 0.338 | 0.541 |
| 750 psi | 0.434 | 0.474 - 0.477 | 0.568 - 0.576 |
| 1000 psi | 0.541 | 0.560 - 0.566 | 0.614 - 0.616 |
| 1500 psi | -- | -- | -- |
| **Physical Properties (Instron Uniaxial Properties)** | | | |
| Tensile strength (psi) | 36 | 27 | -- |
| Elongation (%) | 34.1 | 30.5 | -- |
| Modulus of elasticity (psi) | 186 | 112 | -- |

*First No. is for uncured propellant; No. in parenthesis is for cured propellant

| Formulation (Cont) | VIX (Cont) | VJE (Cont) | VJF (Cont) | VJG (Cont) |
|---|---|---|---|---|
| ṁ (lb/sec) | 3.8 | 1.5 | 1.9 | 1.7 |
| Efficiency | 90.47 | 89.10 | 85.43 | 84.78 |
| Efficiency Adjusted** | 86.9 | 89.4 | 85.3 | 84.8 |

**Adjusted to a mass flow rate of 1.7 lb/sec

As shown, the efficiencies of the Be and LMH-2 fluorine systems were approximately 85 percent. A direct comparison between the fluorine propellants and VIX is not possible because of widely varying mass-flow rates. However, by use of the VCP scaling curve a comparison is possible. Figure 64 shows efficiency as a function of mass-flow rate for VCP in 5PC, 15PC, and FPC motors. Superimposed on this scaling curve are the VIX 5PC and 15PC firings. As shown, VIX appears to fit the curve, and an estimate of the efficiency of VIX at mass-flow rates comparable to the Viton firings can be made. This comparison shows that VIX is approximately 2 percent more efficient than the VJF or VJG formulations. However, the 15PC firings of the low-oxidation-ratio VJI propellant were 6 percent below VIX. (Refer to Section II.) It should be noted that both VJF and VJG had oxidation ratios (including fluorine) well below VJI, and thus some improvement in efficiency could be attributed to the use of fluorine in Be or LMH-2 systems.

Figure 64 also shows the VCP scaling curve correlates 5PC data for the efficient aluminum propellant, DDP. Using the scaling curve as a basis for comparison for the Al/fluorine system indicates an increase in efficiency was also obtained over DDP.

It is also interesting to note at this time that recent data reported by ARC (1966 ICPRG Bulletin) in which a formulation containing LMH-2/TVOPA/NFPA with an oxidation ratio (including fluorine) of 0.98 gave an efficiency of 91 percent in 5PC firings. This data supports the findings of this program.

Only limited conclusions can be made from the data generated on this and other programs as to the effect of fluorine substitution. However, there is a strong indication that fluorine may improve combustion efficiency at low oxidation ratios, and additional testing appears warranted.

TABLE XXXVIII

VITON-IM 5PC FIRINGS

| Propellant Type | VJE | VJF | VJF | VJG | VJG | VJG |
|---|---|---|---|---|---|---|
| Motor Design | N5PC | N5PC | N5PC | N5PC | N5PC | N5PC |
| Grain No. | S731 | S732B | S733B | S739BH | S738BH | S739BH |
| Firing No. | 2-501 | 2-505 | 2-506 | 2-509 | 2-507 | 2-508 |
| Propellant wt (lb) | 5.32 | 4.86 | 3.46 | 3.97 | 3.90 | 3.92 |
| Powder wt (lb) | 0.03 | 0.03 | 0.03 | 0.03 | 0.02 | 0.02 |
| $K$ $(S/A_t)$ | 143.3 | 140.6 | 171.0 | 151.0 | 180.0 | 181.4 |
| $t_a$ (sec) | 3.460 | 2.603 | 5.152 | 2.514 | 2.122 | 2.164 |
| $t_b$ (sec) | 3.047 | 2.243 | 4.483 | 2.387 | 2.008 | 2.023 |
| $\bar{P}_a$ (psia) | 380 | 487 | 351 | 558 | 800 | 800 |
| $\bar{P}_b$ (psia) | 410 | 518 | 382 | 572 | 823 | 807 |
| $\bar{P}max$ (psia) | 474 | 630 | 450 | 656 | 938 | 904 |
| $\bar{P}amb$ (psia) | 12.32 | 12.41 | 12.29 | 12.26 | 12.24 | 12.26 |
| $\bar{r}$ (in./sec) | 0.302 | 0.406 | 0.205 | 0.387 | 0.453 | 0.450 |
| $\dot{m}$ (lb/sec) | 1.54 | 1.87 | 0.67 | 1.58 | 1.84 | 1.81 |
| $C_d$ (sec$^{-1}$) | 0.00637 | 0.00603 | 0.00517 | 0.00479 | 0.00465 | 0.00474 |
| $\epsilon$ $(A_e/A_t)$ | 9.269 | 9.275 | 5.834 | 8.321 | 8.129 | 8.388 |
| $\bar{F}_a$ (lb$_f$) | 313 | 412 | 145 | 378 | 463 | 456 |
| Isp del $\left(\dfrac{lb_f\text{-sec}}{lbm}\right)$ | 203.9 | 221.3 | 215.3 | 239.8 | 252.4 | 252.2 |
| Theoretical Isp at firing conditions | 227.9 | 258.2 | 249.0 | 284.6 | 294.7 | 294.2 |
| Efficiency | 89.46 | 85.70 | 86.47 | 84.26 | 85.65 | 85.72 |
| $Isp^{15}_{1000}$ | 228.0 | 236.7 | 238.8 | 249.8 | 254.0 | 254.1 |
| Isp del (c)* | 203.0 | 219.8 | 213.5 | 238.3 | 251.3 | 251.1 |
| Efficiency (c)* | 89.1 | 85.12 | 85.74 | 83.73 | 85.27 | 85.35 |
| $Isp^{15}_{1000}$ (c)* | 226.9 | 235.1 | 236.8 | 248.3 | 252.8 | 253.1 |

*Values corrected for powder embedment

Notes: All efficiency values were calculated at the actual firing conditions.

$Isp^{15}_{1000}$ and $Isp^{15}_{1000}$ (c) values were calculated by multiplying efficiency times the theoretical Isp at standard conditions.

TABLE XXXIX

VIX 5PC FIRINGS

| Propellant Type | VIX | VIX | VIX |
|---|---|---|---|
| Motor Design | N5PC | N5PC | N5PC |
| Grain No. | S728BH | S730BH | S729BH |
| Firing No. | 2-502 | 2-503 | 2-504 |
| Propellant wt (lb) | 3.93 | 3.88 | 3.69 |
| Powder wt (lb) | 0.02 | 0.03 | 0.03 |
| $K$ $(S/A_t)$ | 111.5 | 108.9 | 106.4 |
| $t_a$ (sec) | 1.003 | 1.001 | 1.020 |
| $t_b$ (sec) | 0.931 | 0.928 | 0.946 |
| $\bar{P}_a$ (psia) | 928 | 909 | 861 |
| $\bar{P}_b$ (psia) | 964 | 941 | 895 |
| $\bar{P}max$ (psia) | 1022 | 1010 | 958 |
| $\bar{P}amb$ (psia) | 12.17 | 12.30 | 12.28 |
| $\bar{r}$ (in./sec) | 0.994 | 0.997 | 0.973 |
| $\dot{m}$ (lb/sec) | 3.92 | 3.88 | 3.62 |
| $C_d$ $(sec^{-1})$ | 0.00527 | 0.00523 | 0.00524 |
| $\epsilon$ $(A_e/A_t)$ | 9.758 | 9.537 | 9.957 |
| $\bar{F}_a$ $(lb_f)$ | 1087 | 1045 | 989 |
| Isp del $\left(\dfrac{lb_f\text{-sec}}{lbm}\right)$ | 278.4 | 279.0 | 275.1 |
| Theoretical Isp at firing conditions | 305.0 | 305.0 | 304.0 |
| Efficiency | 90.98 | 91.48 | 90.49 |
| $IspP^{15}_{1000}$ | 276.3 | 277.8 | 274.8 |
| Isp del (c)* | 277.3 | 277.3 | 273.2 |
| Efficiency (c)* | 90.62 | 90.92 | 89.87 |
| $IspP^{15}_{1000}$ (c)* | 275.2 | 276.1 | 272.9 |

*Values corrected for powder embedment.

Notes: All efficiency values were calculated at the actual firing conditions.

$IspP^{15}_{1000}$ and $IspP^{15}_{1000}$ (c) values were calculated by multiplying efficiency times the theoretical Isp at standard conditions.
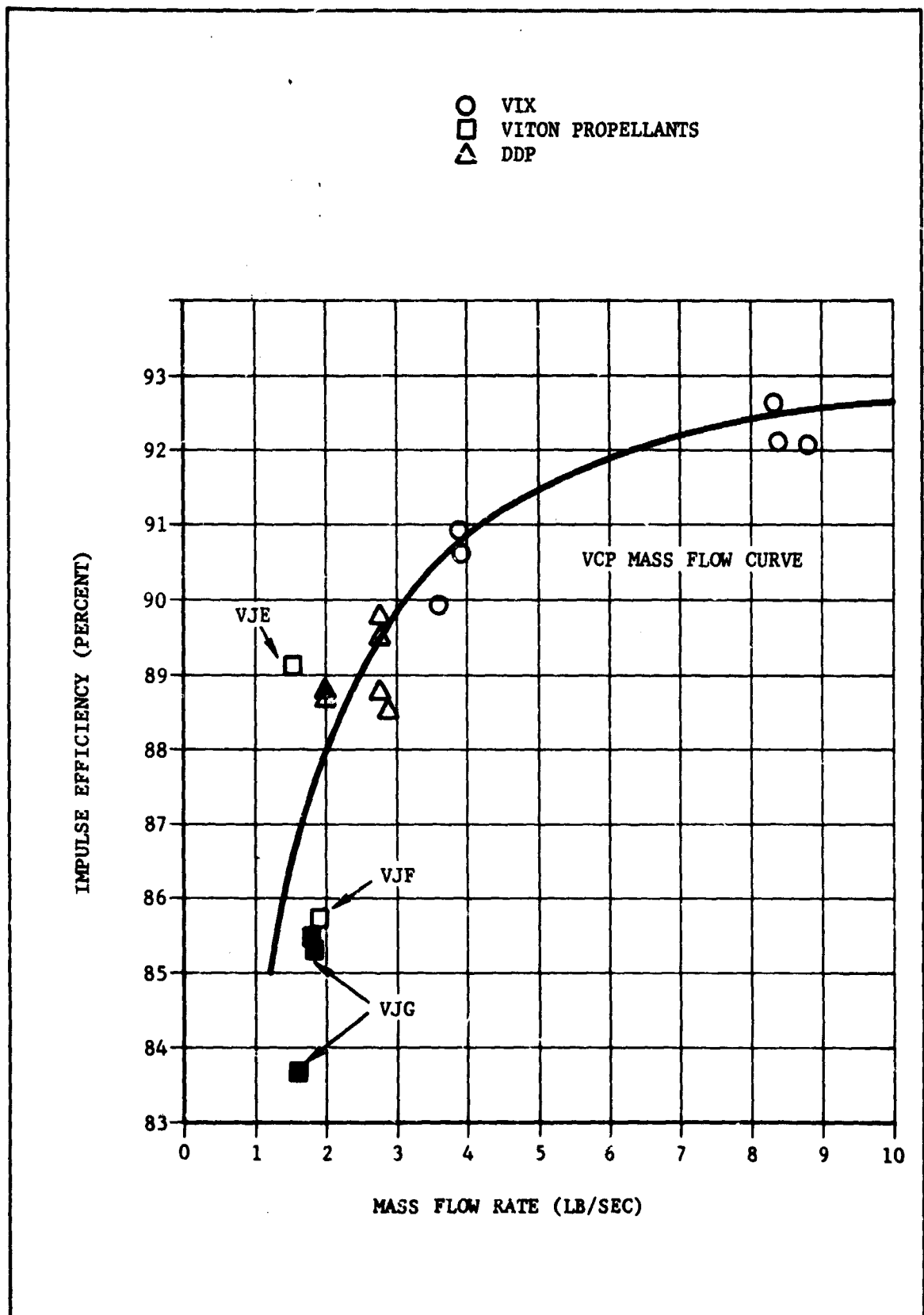
Figure 64. Impulse Efficiency as a Function of Mass-Flow Rate for Viton Propellants

# SECTION V

## INDUSTRIAL HYGIENE

All personnel associated with this contract who worked with Be or Be compounds were examined by the medical department physicians prior to this assignment and reexamined every 3 months thereafter. There were no suspected exposures, and all personnel were found to be free of symptoms associated with Be exposure.

An air-monitoring program was conducted throughout the contract period. Air samples were obtained at the worker breather zone in all areas where Be materials were used on an 8-hr shift basis and analyzed as soon thereafter as possible. The recommended maximum acceptable concentration for Be was never exceeded.

A total of 10 air samplers are strategically located at the plant periphery and operate continually. The samples are not routinely analyzed, but are stored for future reference. Periodic spot-check analyses have indicated no change in the background level of Be.

A total of 10 air samplers are located off the plant property in populated areas and are controlled through a telephone network. These samplers do not operate on a shift or continual basis, but can be activated through the plant telephone switchboard. The system will be activated in the event of a fire or explosion in the plant area. The system is activated at least 1 day per month and checked by the Instrument Calibration Group personnel.

The 16-meter meteorological tower and the continuous recording equipment (W/D, W/S, $\Delta$ T) are routinely checked and calibrated by the Instrument Calibration Group personnel. All subscale motor static testing operations are scheduled with and monitored by the Utah State Health Department. All test firings are accomplished in the scrubber facility.

All propellant mixing and testing operations involving Be were performed during periods of favorable meteorological conditions. There were no unusual incidents during the period of this contract relating to industrial hygiene problems.

Air sampling analysis data will be forwarded to AFRPL under separate cover.

## SECTION VI

### CONCLUSIONS AND RECOMMENDATIONS

Conclusions reached as a result of work on this contract are:

(1) Delivered Isp values in excess of the 280 lbf-sec/lbm, ARPA Project PRINCIPIA goal, have been achieved at density levels of 0.046 to 0.049 lb/in.$^3$ in 15PC motors. Allowing for motor scaling, delivered impulses of 285 lbf-sec/lbm now appear state-of-the-art. These high values were obtained by using an energetic binder consisting of 16.4 NC/82.0 NG/ 1.6 2-NDPA.

(2) The Isp efficiency of both Be and LMH-2 propellants was found to depend on flame temperature, oxidation level (and/or metal level), and motor residence time. Highest efficiencies are obtained by keeping all three of these parameters as high as possible.

(3) The Isp efficiency of propellants having LMH-2 concentrations in excess of 15 percent is particularly sensitive to oxidation ratio. Agglomerate growth appears to control the combustion efficiency at these high fuel concentrations. The temperature before metal combustion (T*) may be a significant parameter in determining combustion efficiency.

(4) Limited testing indicates that a fluorine environment improves the combustion efficiency of LMH-2 propellants at low-oxidation ratios.

(5) Analyses of "off gases" obtained from propellants during cure indicate an incompatibility problem exists between one or more LMH-2 contaminants and plastisol binder ingredients. This incompatibility, coupled with desorption of air from the LMH-2 during cure, is believed responsible for the low-density grains obtained with some LMH-2 lots.

The demonstrated high-performance gains of LMH-2 propellants have not been achieved without some sacrifice in other important propellant properties. Some of these are:

(1) The high energy binder results in increased sensitivity and increased processing hazards as evidenced by the low impact and friction values obtained for the uncured propellants. Cured propellants exhibit sensitivity values comparable to conventional double-base propellants.

(2) The high energy binder results in higher burning rates (0.77 to 0.97 in./sec @ 1000 psi) than are desirable for upper stage applications.

    (3)   The volumetric solids loading is currently limited to
        60 percent, with a corresponding density penalty.

Based on these results, the following recommendations are made to further extend the performance level of LMH-2 propellants and improve the properties of the high performance propellants developed in this program:

    (1)   The influence of the propellant environment, as represented
        by flame temperature, oxidation ratio, and nonequilibrium
        flame temperatures, on combustion and impulse efficiency is
        not entirely clear and warrants further investigation.
        Investigation of the effect of mixed metals in high perform-
        ance systems, therefore, appears worthwhile.  A demonstra-
        tion of motor scaling effects, with close attention to motor
        design parameters, for high performance propellants of the
        VIY type also appears worthwhile at this time.

    (2)   Further investigation of the effect of fluorine addition to
        improve LMH-2 performance efficiency appears worthwhile.
        To minimize theoretical performance losses, the direct
        addition of small percentages of TVOPA to double-base pro-
        pellants having high theoretical impulses (VJI, VIZ type)
        seems a best first approach.

    (3)   Prior to the scale-up of LMH-2 propellants to larger demon-
        stration motors, additional studies should be performed
        which include development of a wider range of available
        burning rates, density improvements, optimization of mechani-
        cal properties, and further development of methods to ensure
        uniformity of LMH-2 lots.  These studies should be combined
        with (1) above.

# LIST OF REFERENCES

1. <u>Combustion of High Energy Solid Propellants</u>, First Quarterly Report, Volume II, Report No. RPL-TCI-65-142, Contract AF 04(611)-10742, Hercules Powder Company (ABL), July 1965

2. <u>Proceedings of the Second Beryllium Propellant Symposium</u>, Technical Documentary Report No. RTD-TDR-63-1091, Air Force Rocket Propulsion Laboratory, October 1963

3. <u>High Energy Solid Propellant Efficiency Investigation</u>, Second Quarterly Progress Report, Report No. RPL-TDR-64-126, Contract AF 04(611)-9709, Atlantic Research, September 1964

4. <u>Rocket Motor Performance - Nozzle Configuration Effects</u>, Preprint 2E, 53rd Meeting AIChE, Pittsburg, Pa, B. Brown, May 17-20, 1964

   Proceedings of First Meeting ICPRG Working Group on Thermo Chemistry, B. Brown, June 1964

5. <u>ABL-AGC Motor Interchange</u>, Reference Report, 10 March 1961

6. <u>JPL Space Programs Summary No. 37-30, Volume V</u>

7. <u>Preliminary Data for Aerojet General Corporation</u> obtained from AFRPL

8. <u>Performance of Propellants Containing Beane</u>, Bulletin of the 21st ISP Meeting, CPIA Pub. No. 71, Volume 1, June 1965

9. <u>Third Stage Minuteman Production Support Program Final Report</u>, HPC-MTD-22-IV, January 1966, Hercules Incorporated, Magna, Utah

10. <u>Characterization and Evaluation of Light Metal Hydrides</u>, AFRPL-TR-66-48, March 1966, Lockheed Propulsion Co., Redlands, California

11. <u>Combustion of High Energy Solid Propellants</u>, Preliminary Final Report, AF 04(611)-10742, Hercules Incorporated, Cumberland, Md

12. <u>Development and Test of High Energy Solid Propellants</u>, HPC-230-12-5-1, 28 October 1965, Hercules Incorporated, Magna, Utah

153

APPENDIX A

## THEORETICAL SPECIFIC IMPULSE CALCULATIONS

Theoretical Isp calculations for LMH-2 and Be containing propellant systems were made with a variety of binders and oxidizers. Nitrate, hydrocarbon, and fluorocarbon binders were investigated. Oxidizers included ammonium perchlorate (AP), ammonium nitrate (AN), cyclotetramethylene tetranitramine (HMX), mixtures of AP/HMX, triaminoguanidine nitrate (TAGN), and, to a lesser extent, hydrazinium diperchlorate (HDP) and nitronium perchlorate (NP). In addition, additives to improve theoretical LMH-2 combustion included the metals Al, Be, Li, Mg, Si, and Zr and lithium perchlorate (LIP) and triaminoguanidine azide (TAZ).

### A.  PRESENTATION OF RESULTS

Since calculations for the most part involve systematic treatment of three and four variable systems, the results are best presented in tabular form in Tables A-1 through A-5. Three dimensional grid network graphs (ternary systems within specified limits of the variables) are also presented, as are the usual binary systems on a common graph. The tables, however, show general characteristics of Isp, chamber temperature ($T_c$) and oxidation ratio (O.R.) and may be used to form many more grid networks and binary lines for comparison.

### B.  RESULTS OF THEORETICAL CALCULATIONS

#### 1.  Double-Base Systems - LMH-2

Tables A-1 through A-5 represent the LMH-2 calculations performed with various oxidizers. These oxidizers are AN, AP, HMX, AP/HMX mixtures, and TAGN. LMH-2, double-base propellants optimize at high Isp values (315 to 325 sec) but at relatively low temperatures ($3600^\circ \pm 100^\circ$ K). Table A-6 illustrates the comparitive results of all oxidizers in the 10 NC, 50 NG, 1 NDPA, 1 RES, LMH-2 system. The data is presented in tabular form for more accurate comparisons. Graphical presentation of these results shows considerable overlapping. The oxidizers are arranged in the order of their oxidizing potential. For these calculations, oxidation ratio is defined as O.R. $= \dfrac{O}{C + Be}$ when oxygen is the only oxidizing element present. If fluorine is also present, O.R. $= \dfrac{O + 1/2F}{C + Be}$.

Nitronium perchlorate, with the highest oxidizing potential and a positive heat of formation (+8.0 kcal/mole), produces the high temperatures desirable with LMH-2; however, its incompatibility with double base and poor combustion characteristics make it an unlikely candidate. The similarity of HDP and AP with molecular weights in almost exact 2:1 ratios accounts for the fact that the impulse results are similar for those two oxidizers regardless of the binder system.

Figures A-1, A-2, and A-3 show the basic grid networks in graphical form for the oxidizers AN, AP, and HMX. The basic networks contain no triacetin (TA). Peak impulse values are usually found at OMOX (OMOX condition implies an oxidation ratio = 1.0) or slightly in the fuel rich area, whereas peak $T_c$ values occur on the oxygen rich side of OMOX, with very rapid decrease in $T_c$ occurring on the negative (fuel rich) side of OMOX. The rate of climb of Isp is also very steep for LMH-2 systems, often rising 3 to 4 Isp units per 1-percent hydride addition.

The magnitude of peak impulse has been found to generally follow the oxygen level of the oxidizer. The order is AN, AP, HMX, TAGN, with a fairly large gap between AP and HMX. AP/HMX mixtures fill this gap. Temperatures do not follow the same order, however. From a temperature standpoint, the AP system gives fairly constant $T_c$ values at all NG levels. HMX exceeds $3600^\circ$ K only at the higher NG levels. The TAGN system does not appear promising in LMH-2 systems because of its very low $T_c$ values $(3400^\circ$ K max).

## 2. Double-Base Systems - Be

All LMH-2 systems have been repeated with Be metal replacing the hydride. The calculations are represented in Tables A-7 through A-11. With Be systems, the maximum Isp values are 280 to 290, whereas $T_c$ values are usually very high $(3900^\circ$ to $4200^\circ$ K). In general, the effect of oxidizers on Isp is reversed for Be systems as compared to LMH-2 systems. For example, HMX and TAGN (the lower oxygen level ingredients) give higher Isp values than AP and AN. Highest temperatures, however, are shown by the latter ingredients. TAGN gives the highest Isp values within the range studied ($\sim$ 293 sec), but again TAGN does not produce the high temperature values with Be as do the other oxidizers.

## 3. Effect of Additives on LMH-2/AP, Double-Base Systems

The effect of addition of up to 6 percent of certain additives on impulse of the propellant system 10 NC, 50 NG, 1 NDPA, 1 RES, LMH-2/AP is summarized in Table A-12. The additives considered are the metals Al, Be, Li, Mg, Si, and Zr; the oxidizer lithium perchlorate (LIP); and the fuel triaminoguanidine azide (TAZ). Selected data from this table is plotted in Figure A-4 to show the comparison when LMH-2 is 16 percent. In general, only Be, Li, and TAZ show an Isp potential of greater than 308 sec, and Be is the only additive showing an increasing $T_c$ value with increasing Isp. TAZ, being a nonmetal fuel, has the advantage of maintaining low metal content.

## 4. Hydrocarbon and Fluorocarbon Binders

The basic ternary LMH-2, AP, binder systems are presented in Figures A-5 through A-7. The binders included a hydrocarbon binder (HC) and two fluorocarbons. The fluorocarbon binders were FAAV (a mixture of 20-percent C7A, 60-percent C7M, and 20-percent Viton) and pure Teflon (TFLN). The ingredients in FAAV are fluorinated acrylates and methacrylates.

In general, low fluorocarbon binder levels, viz, 10 to 15 percent, are required for peak performance at any constant hydride level. Chamber temperatures drop rapidly with increasing binder level. It should be noted that a binder level of zero represents the basic LMH-2/AP binary system, which would necessarily be a pressed charge propellant. This binary system is basic to all three graphs. The performance of the hydrocarbon binder HC (polybutadiene type) is shown to peak sharply at about 10 percent binder level. Chamber temperature and Isp drop very rapidly within this system from peak levels. This system is also representative of the type whose peak performance is not at, or near, OMOX.

5. **Thermochemical Ingredient Data**

The thermochemical ingredient data used in the theoretical impulse calculations are presented in Table A-13.

TABLE A-1

THEORETICAL $I_{sp}$ OF LMH-2, AN, DOUBLE-BASE SYSTEMS

| NG (Wt %) | AN (Wt %) | LMH-2 (Wt %) | $I_{sp}$ (Sec) | $T_c$ (°K) | O.R.* | NG | AN | LMH-2 | $I_{sp}$ | $T_c$ | O.R.* | NG | AN | LMH-2 | $I_{sp}$ | $T_c$ | O.R.* |
|---|---|---|---|---|---|---|---|---|---|---|---|---|---|---|---|---|---|
| | | | | | | | | | TA = 0 Wt % | | | | | | | | |
| 30 | 44 | 14 | 298.5 | 3341 | 1.62 | 40 | 34 | 14 | 299.8 | 3417 | 1.53 | 50 | 24 | 14 | 301.1 | 3492 | 1.45 |
| 30 | 42 | 16 | 304.3 | 3373 | 1.45 | 40 | 32 | 16 | 305.5 | 3446 | 1.38 | 50 | 22 | 16 | 306.6 | 3518 | 1.31 |
| 30 | 40 | 18 | 310.0 | 3402 | 1.31 | 40 | 30 | 18 | 311.0 | 3471 | 1.25 | 50 | 20 | 18 | 312.0 | 3540 | 1.19 |
| 30 | 38 | 20 | 315.4 | 3427 | 1.18 | 40 | 28 | 20 | 316.3 | 3492 | 1.13 | 50 | 18 | 20 | 317.1 | 3555 | 1.09 |
| 30 | 34.38 | 23.62 | 324.2 | 3428 | 1.00 | 40 | 25.25 | 22.75 | 322.7 | 3472 | 1.00 | 50 | 16.11 | 21.89 | 321.2 | 3530 | 1.00 |
| | | | | | | | | | TA = 2 Wt % | | | | | | | | |
| 30 | 42 | 14 | 297.9 | 3290 | 1.54 | 40 | 32 | 14 | 299.3 | 3367 | 1.46 | 50 | 22 | 14 | 300.7 | 3444 | 1.39 |
| 30 | 40 | 16 | 303.9 | 3324 | 1.38 | 40 | 30 | 16 | 305.2 | 3398 | 1.32 | 50 | 20 | 16 | 306.4 | 3471 | 1.26 |
| 30 | 38 | 18 | 309.7 | 3354 | 1.25 | 40 | 28 | 18 | 310.8 | 3424 | 1.20 | 50 | 18 | 18 | 311.8 | 3494 | 1.15 |
| 30 | 36 | 20 | 315.2 | 3381 | 1.14 | 40 | 26 | 20 | 316.2 | 3446 | 1.09 | 50 | 16 | 20 | 317.0 | 3506 | 1.05 |
| 30 | 33.18 | 22.82 | 322.2 | 3380 | 1.00 | 40 | 24.04 | 21.96 | 320.7 | 3430 | 1.00 | 50 | 14.91 | 21.09 | 319.2 | 3484 | 1.00 |
| | | | | | | | | | TA = 4 Wt % | | | | | | | | |
| 30 | 40 | 14 | 297.2 | 3237 | 1.48 | 40 | 30 | 14 | 298.7 | 3315 | 1.40 | 50 | 20 | 14 | 300.2 | 3393 | 1.33 |
| 30 | 38 | 16 | 303.4 | 3273 | 1.33 | 40 | 28 | 16 | 304.7 | 3348 | 1.27 | 50 | 18 | 16 | 306.1 | 3222 | 1.21 |
| 30 | 36 | 18 | 309.3 | 3305 | 1.20 | 40 | 26 | 18 | 310.5 | 3376 | 1.15 | 50 | 16 | 18 | 311.6 | 3446 | 1.11 |
| 30 | 34 | 20 | 314.9 | 3333 | 1.10 | 40 | 24 | 20 | 315.9 | 3397 | 1.05 | 50 | 14 | 20 | 316.8 | 3447 | 1.01 |
| 30 | 31.98 | 22.02 | 320.0 | 3330 | 1.00 | 40 | 22.84 | 21.16 | 318.6 | 3382 | 1.00 | 50 | 13.71 | 20.29 | 317.3 | 3435 | 1.00 |

*Oxidation Ratio

Percentage Limits of Variables:

LMH-2 14-20% & OMOX
NG 30-50%
TA 0-4%
AN Difference

Sum = 88%

Percentage of Constants:

NC 10%
NDPA 1%
RES 1%

TABLE A-2

THEORETICAL $I_{sp}$ OF LMH-2, AP, DOUBLE-BASE SYSTEMS

**Block 1 (NG = 30 Wt %)**

| NG (Wt %) | AP (Wt %) | LMH-2 (Wt %) | $I_{sp}$ (Sec) | $T_c$ (°K) | O.R.* |
|---|---|---|---|---|---|
| *TA = 0 Wt %* | | | | | |
| 30 | 44 | 14 | 298.6 | 3679 | 1.54 |
| 30 | 42 | 16 | 303.9 | 3685 | 1.38 |
| 30 | 40 | 18 | 309.0 | 3685 | 1.25 |
| 30 | 38 | 20 | 313.8 | 3675 | 1.13 |
| 30 | 35.33 | 22.67 | 319.4 | 3628 | 1.00 |
| *TA = 2 Wt %* | | | | | |
| 30 | 42 | 14 | 298.9 | 3626 | 1.47 |
| 30 | 40 | 16 | 304.2 | 3631 | 1.33 |
| 30 | 38 | 18 | 309.6 | 3629 | 1.20 |
| 30 | 36 | 20 | 314.1 | 3616 | 1.09 |
| 30 | 34.10 | 21.90 | 318.0 | 3579 | 1.00 |
| *TA = 4 Wt %* | | | | | |
| 30 | 40 | 14 | 298.9 | 3568 | 1.41 |
| 30 | 38 | 16 | 304.3 | 3573 | 1.27 |
| 30 | 36 | 18 | 309.4 | 3570 | 1.16 |
| 30 | 34 | 20 | 314.3 | 3553 | 1.05 |
| 30 | 32.87 | 21.13 | 316.5 | 3528 | 1.00 |

**Block 2 (NG = 50 Wt %)**

| NG | AP | LMH-2 | $I_{sp}$ | $T_c$ | O.R.* |
|---|---|---|---|---|---|
| *TA = 0 Wt %* | | | | | |
| 50 | 24 | 14 | 299.9 | 3677 | 1.47 |
| 50 | 22 | 16 | 305.1 | 3682 | 1.33 |
| 50 | 20 | 18 | 310.2 | 3680 | 1.20 |
| 50 | 18 | 20 | 315.0 | 3668 | 1.10 |
| 50 | 16.55 | 22.06 | 319.2 | 3627 | 1.00 |
| *TA = 2 Wt %* | | | | | |
| 50 | 22 | 14 | 300.0 | 3622 | 1.41 |
| 50 | 20 | 16 | 305.3 | 3626 | 1.28 |
| 50 | 18 | 18 | 310.4 | 3623 | 1.16 |
| 50 | 16 | 20 | 315.2 | 3607 | 1.06 |
| 50 | 15.32 | 21.29 | 317.8 | 3577 | 1.00 |
| *TA = 4 Wt %* | | | | | |
| 50 | 20 | 14 | 299.9 | 3563 | 1.36 |
| 50 | 18 | 16 | 305.3 | 3569 | 1.23 |
| 50 | 16 | 18 | 310.5 | 3563 | 1.12 |
| 50 | 14 | 20 | 315.2 | 3539 | 1.02 |
| 50 | 14.09 | 20.52 | 316.2 | 3524 | 1.00 |

**Block 3 (NG = 50 Wt %)**

| NG | AP | LMH-2 | $I_{sp}$ | $T_c$ | O.R.* |
|---|---|---|---|---|---|
| *TA = 0 Wt %* | | | | | |
| 50 | 24 | 14 | 301.1 | 3675 | 1.41 |
| 50 | 22 | 16 | 306.3 | 3679 | 1.28 |
| 50 | 20 | 18 | 311.4 | 3677 | 1.16 |
| 50 | 18 | 20 | 316.1 | 3661 | 1.06 |
| 50 | 16.55 | 21.45 | 319.0 | 3626 | 1.00 |
| *TA = 2 Wt %* | | | | | |
| 50 | 22 | 14 | 301.1 | 3618 | 1.36 |
| 50 | 20 | 16 | 306.4 | 3622 | 1.23 |
| 50 | 18 | 18 | 311.5 | 3618 | 1.12 |
| 50 | 16 | 20 | 316.3 | 3596 | 1.03 |
| 50 | 15.32 | 20.68 | 317.5 | 3575 | 1.00 |
| *TA = 4 Wt %* | | | | | |
| 50 | 20 | 14 | 301.0 | 3558 | 1.30 |
| 50 | 18 | 16 | 306.4 | 3561 | 1.19 |
| 50 | 16 | 18 | 311.6 | 3557 | 1.09 |
| 50 | 14 | 20 | 315.9 | 3518 | 0.996 |
| 50 | 14.09 | 19.91 | 315.8 | 3522 | 1.00 |

*Oxidation Ratio

Percentage Limits of Variables:

LMH-2 12-18% & OMOX
NG 30-50%
TA 0-4%
AP/HMX Difference
50/50

Sum = 88%

Percentage of Constants:

NC 10%
NDPA 1%
RES 1%

TABLE A-3

THEORETICAL $I_{sp}$ OF LMH-2, AP AND HMX, DOUBLE-BASE SYSTEMS

| NG (Wt %) | 50/50 AP/HMX (Wt %) | LMH-2 (Wt %) | $I_{sp}$ (Sec) | $T_c$ (°K) | O.R.* | NG | 50/50 AP/HMX | LMH-2 | $I_{sp}$ | $T_c$ | O.R.* | NG | 50/50 AP/HMX | LMH-2 | $I_{sp}$ | $T_c$ | O.R.* |
|---|---|---|---|---|---|---|---|---|---|---|---|---|---|---|---|---|---|
| | | | | | | | | TA = 0 Wt % | | | | | | | | | |
| 30 | 46 | 12 | 298.8 | 3591 | 1.40 | 40 | 36 | 12 | 298.8 | 3606 | 1.40 | 50 | 26 | 12 | 298.7 | 3621 | 1.40 |
| 30 | 44 | 14 | 304.1 | 3601 | 1.27 | 40 | 34 | 14 | 304.0 | 3617 | 1.28 | 50 | 24 | 14 | 304.0 | 3632 | 1.28 |
| 30 | 42 | 16 | 309.1 | 3604 | 1.16 | 40 | 32 | 16 | 309.1 | 3621 | 1.17 | 50 | 22 | 16 | 309.0 | 3638 | 1.18 |
| 30 | 40 | 18 | 313.9 | 3596 | 1.07 | 40 | 30 | 18 | 313.9 | 3615 | 1.07 | 50 | 20 | 18 | 313.8 | 3634 | 1.08 |
| 30 | 38.50 | 19.50 | 316.9 | 3567 | 1.00 | 40 | 28.27 | 19.73 | 317.3 | 3582 | 1.00 | 50 | 18.00 | 20.00 | 317.9 | 3596 | 1.00 |
| | | | | | | | | TA = 2 Wt % | | | | | | | | | |
| 30 | 44 | 12 | 298.1 | 3532 | 1.36 | 40 | 34 | 12 | 298.1 | 3548 | 1.36 | 50 | 24 | 12 | 298.1 | 3564 | 1.36 |
| 30 | 42 | 14 | 303.5 | 3542 | 1.24 | 40 | 32 | 14 | 303.5 | 3559 | 1.24 | 50 | 22 | 14 | 303.5 | 3575 | 1.24 |
| 30 | 40 | 16 | 308.7 | 3546 | 1.13 | 40 | 30 | 16 | 308.7 | 3564 | 1.14 | 50 | 20 | 16 | 308.7 | 3581 | 1.14 |
| 30 | 38 | 18 | 313.5 | 3534 | 1.04 | 40 | 28 | 18 | 313.6 | 3555 | 1.05 | 50 | 18 | 18 | 313.6 | 3575 | 1.05 |
| 30 | 37.15 | 18.85 | 315.1 | 3514 | 1.00 | 40 | 26.92 | 19.08 | 315.7 | 3530 | 1.00 | 50 | 16.65 | 19.35 | 316.2 | 3545 | 1.00 |
| | | | | | | | | TA = 4 Wt % | | | | | | | | | |
| 30 | 42 | 12 | 297.3 | 3470 | 1.31 | 40 | 32 | 12 | 297.3 | 3486 | 1.32 | 50 | 22 | 12 | 297.4 | 3502 | 1.32 |
| 30 | 40 | 14 | 302.9 | 3481 | 1.20 | 40 | 30 | 14 | 302.9 | 3498 | 1.20 | 50 | 26 | 14 | 302.9 | 3514 | 1.21 |
| 30 | 38 | 16 | 308.2 | 3485 | 1.10 | 40 | 28 | 16 | 308.2 | 3503 | 1.10 | 50 | 18 | 16 | 308.2 | 3521 | 1.11 |
| 30 | 36 | 18 | 312.9 | 3464 | 1.01 | 40 | 26 | 18 | 313.0 | 3488 | 1.02 | 50 | 16 | 18 | 313.1 | 3511 | 1.03 |
| 30 | 35.81 | 18.19 | 313.2 | 3458 | 1.00 | 40 | 25.58 | 18.42 | 313.8 | 3475 | 1.00 | 50 | 15.31 | 18.69 | 314.4 | 3491 | 1.00 |

*Oxidation Ratio

Percentage Limits of Variables:

LMH-2 12-18% & ONOX
NG 30-50%
TA 0-4%
AP/HMX Difference
50/50

Sum = 88%

Percentage of Constants:

NC 10%
NDPA 1%
RES 1%

TABLE A-4

THEORETICAL $I_{sp}$ OF LMH-2, HMX, DOUBLE-BASE SYSTEMS

| NG (Wt %) | HMX (Wt %) | LMH-2 (Wt %) | $I_{sp}$ (Sec) | $T_c$ (°K) | O.R.* | NG | HMX | LMH-2 | $I_{sp}$ | $T_c$ | O.R.+ | NG | HMX | LMH-2 | $I_{sp}$ | $T_c$ | O.R.* |
|---|---|---|---|---|---|---|---|---|---|---|---|---|---|---|---|---|---|
| | | | | | | | | TA = 0 Wt % | | | | | | | | | |
| 30 | 47 | 12 | 303.2 | 3526 | 1.18 | 40 | 37 | 12 | 302.5 | 3565 | 1.24 | 50 | 27 | 12 | 301.7 | 3602 | 1.29 |
| 30 | 45 | 14 | 308.6 | 3538 | 1.09 | 40 | 35 | 14 | 307.8 | 3578 | 1.14 | 50 | 25 | 14 | 306.8 | 3616 | 1.19 |
| 30 | 43 | 16 | 313.4 | 3520 | 1.01 | 40 | 33 | 16 | 312.7 | 3581 | 1.06 | 50 | 23 | 16 | 311.7 | 3624 | 1.10 |
| 30 | 41 | 18 | 312.0 | 3368 | 0.934 | 40 | 31 | 18 | 315.2 | 3517 | 0.979 | 50 | 21 | 18 | 316.2 | 3612 | 1.02 |
| 30 | 42.81 | 16.19 | 313.7 | 3512 | 1.00 | 40 | 31.58 | 17.42 | 315.6 | 3552 | 1.00 | 50 | 20.34 | 18.66 | 317.3 | 3590 | 1.00 |
| | | | | | | | | TA = 2 Wt % | | | | | | | | | |
| 30 | 45 | 12 | 302.0 | 3465 | 1.16 | 40 | 35 | 12 | 301.4 | 3506 | 1.21 | 50 | 25 | 12 | 300.7 | 3545 | 1.26 |
| 30 | 43 | 14 | 307.5 | 3478 | 1.07 | 40 | 33 | 14 | 306.8 | 3521 | 1.12 | 50 | 23 | 14 | 306.0 | 3560 | 1.17 |
| 30 | 41 | 16 | 311.3 | 3437 | 0.987 | 40 | 31 | 16 | 311.9 | 3522 | 1.03 | 50 | 21 | 16 | 311.0 | 3569 | 1.08 |
| 30 | 39 | 18 | 310.0 | 3279 | 0.916 | 40 | 29 | 18 | 312.7 | 3420 | 0.961 | 50 | 19 | 18 | 315.5 | 3546 | 1.01 |
| 30 | 41.34 | 15.66 | 311.5 | 3457 | 1.00 | 40 | 30.10 | 16.90 | 313.7 | 3500 | 1.00 | 50 | 18.86 | 18.14 | 315.6 | 3540 | 1.00 |
| | | | | | | | | TA = 4 Wt % | | | | | | | | | |
| 30 | 43 | 12 | 300.6 | 3401 | 1.13 | 40 | 33 | 12 | 300.2 | 3444 | 1.18 | 50 | 23 | 12 | 299.6 | 3485 | 1.23 |
| 30 | 41 | 14 | 306.3 | 3416 | 1.05 | 40 | 31 | 14 | 305.8 | 3461 | 1.09 | 50 | 21 | 14 | 305.1 | 3502 | 1.14 |
| 30 | 39 | 16 | 308.6 | 3338 | 0.968 | 40 | 29 | 16 | 311.0 | 3458 | 1.01 | 50 | 19 | 16 | 310.2 | 3512 | 1.06 |
| 30 | 37 | 18 | 307.9 | 3229 | 0.900 | 40 | 27 | 18 | 310.0 | 3322 | 0.943 | 50 | 17 | 18 | 313.6 | 3466 | 0.987 |
| 30 | 39.87 | 15.13 | 305.1 | 3399 | 1.00 | 40 | 28.62 | 16.38 | 311.6 | 3445 | 1.00 | 50 | 17.38 | 17.62 | 313.8 | 3488 | 1.00 |

*Oxidation Ratio

Percentage Limits of Variables:

LMH-2 12-18% & OMOX
NG 30-50%
TA 0-4 %
HMX Difference

Sum = 89%

Percentage of Constants:

NC 10%
NDPA 1%

TABLE A-5

THEORETICAL $I_{sp}$ OF LMH-2, TAGN, DOUBLE-BASE SYSTEMS

**NG = 30 Wt %**

| NG (Wt %) | TAGN (Wt %) | LMH-2 (Wt %) | $I_{sp}$ (Sec) | $T_c$ (°K) | O.R.* |
|---|---|---|---|---|---|
| | | | | | **TA = 0 Wt %** |
| 30 | 50 | 8 | 283.5 | 2948 | 1.41 |
| 30 | 48 | 10 | 291.4 | 3015 | 1.27 |
| 30 | 46 | 12 | 298.8 | 3076 | 1.15 |
| 30 | 44 | 14 | 305.7 | 3129 | 1.05 |
| 30 | 42.93 | 15.07 | 309.0 | 3140 | 1.00 |
| | | | | | **TA = 2 Wt %** |
| 30 | 48 | 8 | 281.3 | 2890 | 1.37 |
| 30 | 46 | 10 | 289.4 | 2961 | 1.24 |
| 30 | 44 | 12 | 297.0 | 3024 | 1.12 |
| 30 | 42 | 14 | 304.1 | 3079 | 1.03 |
| 30 | 41.43 | 14.57 | 305.9 | 3084 | 1.00 |
| | | | | | **TA = 4 Wt %** |
| 30 | 46 | 8 | 279.0 | 2830 | 1.33 |
| 30 | 44 | 10 | 287.4 | 2904 | 1.20 |
| 30 | 42 | 12 | 295.2 | 2972 | 1.10 |
| 30 | 40 | 14 | 302.4 | 3024 | 1.003 |
| 30 | 39.93 | 14.07 | 302.6 | 3024 | 1.00 |

**NG = 40 Wt %**

| NG | TAGN | LMH-2 | $I_{sp}$ | $T_c$ | O.R.* |
|---|---|---|---|---|---|
| | | | | | **TA = 0 Wt %** |
| 40 | 40 | 8 | 285.8 | 3102 | 1.48 |
| 40 | 38 | 10 | 293.1 | 3160 | 1.33 |
| 40 | 36 | 12 | 300.0 | 3213 | 1.21 |
| 40 | 34 | 14 | 306.3 | 3259 | 1.11 |
| 40 | 31.52 | 16.48 | 313.4 | 3285 | 1.00 |
| | | | | | **TA = 2 Wt %** |
| 40 | 38 | 8 | 283.8 | 3046 | 1.43 |
| 40 | 36 | 10 | 291.4 | 3108 | 1.30 |
| 40 | 34 | 12 | 298.4 | 3164 | 1.18 |
| 40 | 32 | 14 | 305.0 | 3213 | 1.08 |
| 40 | 30.02 | 15.98 | 310.8 | 3236 | 1.00 |
| | | | | | **TA = 4 Wt %** |
| 40 | 36 | 8 | 381.7 | 2989 | 1.39 |
| 40 | 34 | 10 | 289.5 | 3054 | 1.26 |
| 40 | 32 | 12 | 296.8 | 3113 | 1.16 |
| 40 | 30 | 14 | 303.5 | 3165 | 1.06 |
| 40 | 28.52 | 15.48 | 308.0 | 3193 | 1.00 |

**NG = 50 Wt %**

| NG | TAGN | LMH-2 | $I_{sp}$ | $T_c$ | O.R.* |
|---|---|---|---|---|---|
| | | | | | **TA = 0 Wt %** |
| 50 | 30 | 8 | 287.5 | 3250 | 1.54 |
| 50 | 28 | 10 | 294.2 | 3300 | 1.39 |
| 50 | 26 | 12 | 300.5 | 3346 | 1.27 |
| 50 | 24 | 14 | 306.4 | 3386 | 1.17 |
| 50 | 20.11 | 17.89 | 316.4 | 3417 | 1.00 |
| | | | | | **TA = 2 Wt %** |
| 50 | 28 | 8 | 285.7 | 3198 | 1.49 |
| 50 | 26 | 10 | 292.7 | 3251 | 1.36 |
| 50 | 24 | 12 | 299.2 | 3299 | 1.24 |
| 50 | 22 | 14 | 305.2 | 3342 | 1.14 |
| 50 | 19.61 | 17.39 | 314.2 | 3373 | 1.00 |
| | | | | | **TA = 4 Wt %** |
| 50 | 26 | 8 | 283.9 | 3144 | 1.45 |
| 50 | 24 | 10 | 291.0 | 3201 | 1.32 |
| 50 | 22 | 12 | 297.7 | 3252 | 1.21 |
| 50 | 20 | 14 | 304.0 | 3297 | 1.12 |
| 50 | 17.11 | 16.89 | 311.9 | 3326 | 1.00 |

*Oxidation Ratio

Percentage Limits of Variables:

LMH-2 8-14% & OMOX
NG 30-50%
TA 0-4%
TAGN Difference

Sum = 88%

Percentage of Constants:

NC 10%
NDPA 1%
RES 1%

TABLE A-6

COMPARATIVE PERFORMANCE OF VARIOUS LMH-2, OXIDIZER SYSTEMS

| BeH2 (wt. %) | NP Tc (°K) | NP Isp (sec) | NP O.R.* | AM Tc (°K) | AM Isp (sec) | AM O.R. | HDP Tc (°K) | HDP Isp (sec) | HDP O.R. | AP Tc (°K) | AP Isp (sec) | AP O.R. | HMX Tc (°K) | HMX Isp (sec) | HMX O.R. | TAGN Tc (°K) | TAGN Isp (sec) | TAGN O.R. |
|---|---|---|---|---|---|---|---|---|---|---|---|---|---|---|---|---|---|---|
| 10 | 3896 | 288.5 | 1.858 | -- | -- | -- | 3712 | 290.3 | 1.756 | 3641 | 290.1 | 1.752 | -- | -- | -- | 3300 | 294.2 | 1.392 |
| 12 | 3938 | 294.7 | 1.657 | 3461 | 295.3 | 1.610 | 3735 | 295.8 | 1.570 | 3663 | 295.7 | 1.567 | 3602 | 301.7 | 1.290 | 3346 | 300.5 | 1.270 |
| 14 | 3951 | 300.3 | 1.487 | 3492 | 301.1 | 1.447 | 3743 | 301.2 | 1.414 | 3675 | 301.1 | 1.411 | 3616 | 306.8 | 1.191 | 3386 | 306.4 | 1.156 |
| 16 | 3943 | 305.5 | 1.343 | 3518 | 306.6 | 1.309 | 3741 | 306.3 | 1.281 | 3679 | 306.3 | 1.278 | 3624 | 311.7 | 1.103 | 3420 | 311.3 | 1.075 |
| 18 | 3920 | 310.5 | 1.219 | 3540 | 312.0 | 1.190 | 3732 | 311.3 | 1.166 | 3677 | 311.4 | 1.164 | 3612 | 316.2 | 1.024 | 3349 | 315.5 | 0.760 |
| 20 | 3883 | 315.3 | 1.111 | 3555 | 317.1 | 1.086 | 3709 | 316.0 | 1.066 | 3661 | 316.1 | 1.064 | 3493 | 316.2 | 0.954 | -- | -- | -- |
| 22 | 3818 | 319.6 | 1.016 | 3524 | 321.3 | 0.995 | 3641 | 319.5 | 0.979 | 3598 | 319.5 | 0.997 | -- | -- | -- | -- | -- | -- |
| rmax | 3800 | 320.2 | 1.000 | 3530 | 321.2 | 1.000 | 3667 | 319.0 | 1.000 | 3626 | 319.0 | 1.000 | 3590 | 317.3 | 1.000 | 3417 | 316.4 | 1.000 |
| BeH2 at rmax | | 22.35 | | | 21.89 | | | 21.49 | | | 21.45 | | | 18.66 | | | 17.89 | |

Percentage of Constants

BC   10%
BC   50%
HDPA  1%
HMX   1% (HMX contains no HMS)

*Oxidation Ratio

TABLE A-7

THEORETICAL $I_{sp}$ OF Be, AN, DOUBLE-BASE SYSTEMS

| NG (Wt %) | AN (Wt %) | Be (Wt %) | $I_{sp}$ (Sec) | $T_c$ (°K) | O.R.* | NC | AN | Be | $I_{sp}$ | $T_c$ | O.R.* | NG | AN | Be | $I_{sp}$ | $T_c$ | O.R.* |
|---|---|---|---|---|---|---|---|---|---|---|---|---|---|---|---|---|---|
| | | | | | | | | | TA = 0 Wt % | | | | | | | | |
| 30 | 46 | 12 | 276.7 | | 1.61 | 40 | 36 | 12 | 277.2 | 3799 | 1.52 | 50 | 26 | 12 | 277.8 | 3879 | 1.44 |
| 30 | 44 | 14 | 278.3 | 3835 | 1.42 | 40 | 34 | 14 | 279.0 | 3914 | 1.35 | 50 | 24 | 14 | 279.9 | 3996 | 1.29 |
| 30 | 42 | 16 | 280.1 | 3940 | 1.26 | 40 | 32 | 16 | 281.0 | 4020 | 1.21 | 50 | 22 | 16 | 281.9 | 4100 | 1.16 |
| 30 | 40 | 18 | 282.0 | 4032 | 1.13 | 40 | 30 | 18 | 282.8 | 4103 | 1.09 | 50 | 20 | 18 | 283.4 | 4167 | 1.05 |
| 30 | 37.61 | 20.39 | 282.9 | 4066 | 1.00 | 40 | 28.35 | 19.65 | 283.1 | 4112 | 1.00 | 50 | 19.10 | 18.90 | 283.3 | 4160 | 1.00 |
| | | | | | | | | | TA = 2 Wt % | | | | | | | | |
| 30 | 44 | 12 | 277.5 | 3691 | 1.53 | 40 | 34 | 12 | 278.0 | 3771 | 1.45 | 50 | 24 | 12 | 278.5 | 3853 | 1.38 |
| 30 | 42 | 14 | 279.0 | 3302 | 1.36 | 40 | 32 | 14 | 279.6 | 3883 | 1.30 | 50 | 22 | 14 | 280.4 | 3966 | 1.24 |
| 30 | 40 | 16 | 280.6 | 3905 | 1.21 | 40 | 30 | 16 | 281.4 | 3984 | 1.16 | 50 | 20 | 16 | 282.4 | 4063 | 1.12 |
| 30 | 38 | 18 | 282.4 | 3990 | 1.09 | 40 | 28 | 18 | 283.1 | 4054 | 1.05 | 50 | 18 | 18 | 283.5 | 4100 | 1.01 |
| 30 | 36.30 | 19.70 | 283.0 | 4002 | 1.00 | 40 | 27.04 | 18.96 | 283.2 | 4047 | 1.00 | 50 | 17.79 | 18.21 | 283.4 | 4095 | 1.00 |
| | | | | | | | | | TA = 4 Wt % | | | | | | | | |
| 30 | 42 | 12 | 278.1 | 3655 | 1.47 | 40 | 32 | 12 | 278.6 | 3737 | 1.40 | 50 | 22 | 12 | 279.2 | 3820 | 1.33 |
| 30 | 40 | 14 | 279.8 | 3764 | 1.30 | 40 | 30 | 14 | 280.2 | 3846 | 1.25 | 50 | 20 | 14 | 280.9 | 3930 | 1.19 |
| 30 | 38 | 16 | 281.2 | 3865 | 1.17 | 40 | 28 | 16 | 281.9 | 3943 | 1.12 | 50 | 18 | 16 | 282.7 | 4019 | 1.08 |
| 30 | 36 | 18 | 282.7 | 3939 | 1.05 | 40 | 26 | 18 | T. N. Result | | | 50 | 16 | 18 | 282.4 | 4004 | 0.977 |
| 30 | 34.99 | 19.01 | 282.9 | 3936 | 1.00 | 40 | 25.73 | 18.27 | 283.0 | 3981 | 1.00 | 50 | 16.48 | 17.52 | 283.3 | 4028 | 1.00 |

*Oxidation Ratio

Percentage Limits of Variables:
Be 12-18% & OMOX
NG 30-50%
TA 0-4%
AP Difference

Sum = 88%

Percentage of Constants:
NC 10%
NLPA 1%
RES 1%

TABLE A-8

THEORETICAL $I_{sp}$ OF Be, AP, DOUBLE-BASE SYSTEMS

| NG (Wt %) | AP (Wt %) | Be (Wt %) | $I_{sp}$ (Sec) | $T_c$ (°K) | O.R.* | NG | AP | Be | $I_{sp}$ | $T_c$ | O.R.* | NG | AP | Be | $I_{sp}$ | $T_c$ | O.R.* |
|---|---|---|---|---|---|---|---|---|---|---|---|---|---|---|---|---|---|
| | | | | | | | | TA = 0 Wt % | | | | | | | | | |
| 30 | 46 | 12 | 271.8 | 4003 | 1.53 | 40 | 36 | 12 | 273.7 | 4024 | 1.46 | 50 | 26 | 12 | 275.6 | 4045 | 1.40 |
| 30 | 44 | 14 | 274.1 | 4116 | 1.35 | 40 | 34 | 14 | 276.0 | 4135 | 1.30 | 50 | 24 | 14 | 277.9 | 4154 | 1.25 |
| 30 | 42 | 16 | 276.0 | 4210 | 1.20 | 40 | 32 | 16 | 277.9 | 4225 | 1.16 | 50 | 22 | 16 | 279.7 | 4240 | 1.13 |
| 30 | 40 | 18 | 277.3 | 4274 | 1.08 | 40 | 30 | 18 | 279.0 | 4281 | 1.05 | 50 | 20 | 18 | 280.7 | 4282 | 1.02 |
| 30 | 38.50 | 19.50 | 277.6 | 4291 | 1.00 | 40 | 29.03 | 18.97 | 279.1 | 4286 | 1.00 | 50 | 19.55 | 18.45 | 280.7 | 4280 | 1.00 |
| | | | | | | | | TA = 2 Wt % | | | | | | | | | |
| 30 | 44 | 12 | 273.0 | 3982 | 1.46 | 40 | 34 | 12 | 274.8 | 3999 | 1.40 | 50 | 24 | 12 | 276.5 | 4017 | 1.35 |
| 30 | 42 | 14 | 275.2 | 4086 | 1.30 | 40 | 32 | 14 | 277.0 | 4101 | 1.25 | 50 | 22 | 14 | 278.8 | 4117 | 1.21 |
| 30 | 40 | 16 | 277.1 | 4170 | 1.16 | 40 | 30 | 16 | 273.8 | 4181 | 1.12 | 50 | 20 | 16 | 280.6 | 4192 | 1.09 |
| 30 | 38 | 18 | 278.2 | 4219 | 1.04 | 40 | 28 | 18 | 280.0 | 4217 | 1.02 | 50 | 18 | 18 | 281.1 | 4206 | 0.990 |
| 30 | 37.17 | 18.84 | 278.2 | 4223 | 1.00 | 40 | 27.69 | 18.31 | 279.7 | 4217 | 1.00 | 50 | 18.21 | 17.79 | 281.2 | 4210 | 1.00 |
| | | | | | | | | TA = 4 Wt % | | | | | | | | | |
| 30 | 42 | 12 | 273.9 | 3953 | 1.40 | 40 | 32 | 12 | 275.6 | 3966 | 1.35 | 50 | 22 | 12 | 277.3 | 3981 | 1.30 |
| 30 | 40 | 14 | 276.2 | 4049 | 1.25 | 40 | 30 | 14 | 277.8 | 4061 | 1.21 | 50 | 20 | 14 | 279.5 | 4073 | 1.17 |
| 30 | 38 | 16 | 277.9 | 4123 | 1.12 | 40 | 28 | 16 | 279.6 | 4129 | 1.09 | 50 | 18 | 16 | 281.2 | 4134 | 1.06 |
| 30 | 35 | 18 | 278.7 | 4154 | 1.01 | 40 | 26 | 18 | 280.0 | 4139 | 0.980 | 50 | 16 | 18 | 280.6 | 4106 | 0.960 |
| 30 | 35.82 | 18.18 | 278.7 | 4153 | 1.00 | 40 | 26.35 | 17.65 | 280.1 | 4145 | 1.00 | 50 | 16.87 | 17.13 | 281.4 | 4136 | 1.00 |

*Oxidation Ratio

Percentage Limits of Variables:

Be 12-18% & OMOX
NG 30-50%
TA 0-4%
AP Difference

Sum = 88%

Percentage of Constants:

NC 10%
NDPA 1%
RES 1%

TABLE A-9

THEORETICAL $I_{sp}$ OF Be, AP AND HMX, DOUBLE-BASE SYSTEMS

**NG = 30 Wt %**

| NG (Wt %) | AP/HMX (Wt %) | Be (Wt %) | $I_{sp}$ (Sec) | $T_c$ (°K) | O.R.* |
|---|---|---|---|---|---|
| 30 | 50 | 8 | 277.2 | 3806 | 1.59 |
| 30 | 48 | 10 | 279.14 | 3922 | 1.41 |
| 30 | 46 | 12 | 281.1 | 4026 | 1.26 |
| 30 | 44 | 14 | 282.9 | 4111 | 1.13 |
| 30 | 41.43 | 16.57 | 283.8 | 4157 | 1.00 |
| 30 | 48 | 8 | 277.6 | 3773 | 1.53 |
| 30 | 46 | 10 | 279.6 | 3883 | 1.36 |
| 30 | 44 | 12 | 281.3 | 3982 | 1.22 |
| 30 | 42 | 14 | 283.0 | 4059 | 1.10 |
| 30 | 39.99 | 16.01 | 283.7 | 4087 | 1.00 |
| 30 | 46 | 8 | 277.8 | 3732 | 1.48 |
| 30 | 44 | 10 | 280.0 | 3838 | 1.32 |
| 30 | 42 | 12 | 281.6 | 3932 | 1.19 |
| 30 | 40 | 14 | 283.0 | 4002 | 1.08 |
| 30 | 38.55 | 15.45 | 283.4 | 4015 | 1.00 |

**NG = 40 Wt %**

| NG | AP/HMX | Be | $I_{sp}$ | $T_c$ | O.R.* | | |
|---|---|---|---|---|---|---|---|
| | | | | | | **TA = 0 Wt %** | |
| 40 | 40 | 8 | 277.0 | 3817 | 1.59 | | |
| 40 | 38 | 10 | 278.9 | 3935 | 1.41 | | |
| 40 | 36 | 12 | 280.9 | 4026 | 1.26 | | |
| 40 | 34 | 14 | 282.8 | 4132 | 1.14 | | |
| 40 | 31.24 | 16.76 | 283.8 | 4184 | 1.00 | | |
| | | | | | | **TA = 2 Wt %** | |
| 40 | 38 | 8 | 277.4 | 3785 | 1.53 | | |
| 40 | 36 | 10 | 279.4 | 3899 | 1.36 | | |
| 40 | 34 | 12 | 281.2 | 3999 | 1.23 | | |
| 40 | 32 | 14 | 282.9 | 4082 | 1.11 | | |
| 40 | 29.79 | 16.21 | 283.7 | 4114 | 1.00 | | |
| | | | | | | **TA = 4 Wt %** | |
| 40 | 36 | 8 | 277.6 | 2746 | 1.48 | | |
| 40 | 34 | 10 | 279.8 | 3854 | 1.32 | | |
| 40 | 32 | 12 | 281.4 | 3951 | 1.19 | | |
| 40 | 30 | 14 | 283.0 | 4026 | 1.08 | | |
| 40 | 28.35 | 15.65 | 283.5 | 4042 | 1.00 | | |

**NG = 50 Wt %**

| NG | AP/HMX | Be | $I_{sp}$ | $T_c$ | O.R.* |
|---|---|---|---|---|---|
| 50 | 30 | 8 | 276.8 | 3829 | 1.58 |
| 50 | 28 | 10 | 278.7 | 3948 | 1.41 |
| 50 | 26 | 12 | 280.8 | 4058 | 1.27 |
| 50 | 24 | 14 | 282.7 | 4153 | 1.15 |
| 50 | 21.04 | 16.96 | 283.8 | 4211 | 1.00 |
| 50 | 28 | 8 | 277.2 | 3798 | 1.53 |
| 50 | 26 | 10 | 279.1 | 3912 | 1.37 |
| 50 | 24 | 12 | 281.0 | 4017 | 1.23 |
| 50 | 22 | 14 | 282.9 | 4104 | 1.12 |
| 50 | 19.60 | 16.40 | 283.8 | 4121 | 1.00 |
| 50 | 26 | 8 | 277.5 | 3760 | 1.48 |
| 50 | 24 | 10 | 279.6 | 3870 | 1.32 |
| 50 | 22 | 12 | 281.2 | 3980 | 1.20 |
| 50 | 20 | 14 | 282.9 | 4050 | 1.09 |
| 50 | 18.16 | 15.84 | 283.6 | 4070 | 1.00 |

*Oxidation Ratio

Percentage Limits of Variables:

Be 8-14% & OMOX
NG 30-50%
TA 0-4%
AP/HMX Difference
50/50

Sum = 88%

Percentage of Constants:

NC 10%
NDPA 1%
RES 1%

TABLE A-10

THEORETICAL $I_{sp}$ OF Be, HMX, DOUBLE-BASE SYSTEMS

| NC (Wt %) | HMX (Wt %) | Be (Wt %) | $I_{sp}$ (Sec) | $T_c$ (°K) | O.R.* | NG | HMX | Be | $I_{sp}$ | $T_c$ | O.R.* | NG | HMX | Be | $I_{sp}$ | $T_c$ | O.R.* |
|---|---|---|---|---|---|---|---|---|---|---|---|---|---|---|---|---|---|
| | | | | | | | | | **TA = 0 Wt %** | | | | | | | | |
| 30 | 51 | 8 | 285.4 | 3819 | 1.31 | 40 | 41 | 8 | 28.39 | 3842 | 1.37 | 50 | 31 | 8 | 282.1 | 3858 | 1.42 |
| 30 | 49 | 10 | 287.6 | 3926 | 1.18 | 40 | 39 | 10 | 285.7 | 3952 | 1.23 | 50 | 29 | 10 | 283.7 | 3973 | 1.29 |
| 30 | 47 | 12 | 288.9 | 4010 | 1.07 | 40 | 37 | 12 | 287.2 | 4049 | 1.12 | 50 | 27 | 12 | 285.4 | 4077 | 1.17 |
| 30 | 45 | 14 | 288.0 | 4002 | 0.980 | 40 | 35 | 14 | 288.4 | 4101 | 1.03 | 50 | 25 | 14 | 286.9 | 4157 | 1.07 |
| 30 | 45.45 | 13.55 | 289.1 | 4020 | 1.00 | 40 | 34.41 | 14.59 | 288.2 | 4093 | 1.00 | 50 | 23.38 | 15.62 | 287.0 | 4165 | 1.00 |
| | | | | | | | | | **TA = 2 Wt %** | | | | | | | | |
| 30 | 49 | 8 | 284.8 | 3765 | 1.28 | 40 | 39 | 8 | 283.5 | 3794 | 1.33 | 50 | 29 | 8 | 281.9 | 3816 | 1.39 |
| 30 | 47 | 10 | 287.3 | 3871 | 1.15 | 40 | 37 | 10 | 285.6 | 3902 | 1.21 | 50 | 27 | 10 | 283.7 | 3928 | 1.26 |
| 30 | 45 | 12 | 288.7 | 3949 | 1.05 | 40 | 35 | 12 | 286.9 | 3995 | 1.10 | 50 | 25 | 12 | 285.1 | 4029 | 1.15 |
| 30 | 43 | 14 | 287.1 | 3899 | 0.961 | 40 | 33 | 14 | 287.7 | 4029 | 1.01 | 50 | 23 | 14 | 286.5 | 4100 | 1.05 |
| 30 | 43.89 | 13.11 | 288.7 | 3949 | 1.00 | 40 | 32.85 | 14.15 | 287.5 | 4025 | 1.00 | 50 | 21.82 | 15.18 | 286.5 | 4099 | 1.00 |
| | | | | | | | | | **TA = 4 Wt %** | | | | | | | | |
| 30 | 47 | 8 | 284.0 | 3707 | 1.25 | 40 | 37 | 8 | 282.8 | 3740 | 1.30 | 50 | 27 | 8 | 281.5 | 3768 | 1.36 |
| 30 | 45 | 10 | 286.8 | 3811 | 1.13 | 40 | 35 | 10 | 285.3 | 3848 | 1.18 | 50 | 25 | 10 | 283.6 | 3878 | 1.23 |
| 30 | 43 | 12 | 288.5 | 3882 | 1.03 | 40 | 33 | 12 | 286.8 | 3938 | 1.08 | 50 | 23 | 12 | 285.0 | 3977 | 1.12 |
| 30 | 41 | 14 | 285.5 | 3779 | 0.944 | 40 | 31 | 14 | 286.7 | 3944 | 0.988 | 50 | 21 | 14 | 286.1 | 4037 | 1.03 |
| 30 | 42.33 | 12.67 | 288.4 | 3876 | 1.00 | 40 | 31.29 | 13.71 | 287.1 | 3955 | 1.00 | 50 | 20.25 | 14.75 | 285.9 | 4030 | 1.00 |

*Oxidation Ratio

Percentage Limits of Variables:

Be 8-14% & OMOX
NG 30-50%
TA 0-4%
HMX Difference

Sum = 89%

Percentage of Constants:

NC 10%
NDPA 1%

A-13

TABLE A-11

THEORETICAL $I_{sp}$ OF Be, TAGN, DOUBLE-BASE SYSTEMS

| NG (Wt %) | TAGN (Wt %) | Be (Wt %) | $I_{sp}$ (Sec) | $T_c$ (°K) | O.R.* | NG | TAGN | Be | $I_{sp}$ | $T_c$ | O.R.* | NG | TAGN | Be | $I_{sp}$ | $T_c$ | O.R.* |
|---|---|---|---|---|---|---|---|---|---|---|---|---|---|---|---|---|---|
| | | | | | | | | | **TA = 0 Wt %** | | | | | | | | |
| 30 | 52 | 6 | 277.2 | 3159 | 1.48 | 40 | 42 | 6 | 278.7 | 3315 | 1.54 | 50 | 32 | 6 | 279.4 | 3455 | 1.59 |
| 30 | 50 | 8 | 284.2 | 3309 | 1.29 | 40 | 40 | 8 | 284.5 | 3455 | 1.36 | 50 | 30 | 8 | 283.9 | 3588 | 1.41 |
| 30 | 48 | 10 | 289.5 | 3444 | 1.15 | 40 | 38 | 10 | 288.7 | 3583 | 1.21 | 50 | 28 | 10 | 287.0 | 3713 | 1.27 |
| 30 | 46 | 12 | 293.2 | 3553 | 1.03 | 40 | 36 | 12 | 291.4 | 3696 | 1.09 | 50 | 26 | 12 | 288.0 | 3926 | 1.15 |
| 30 | 45.41 | 12.59 | 293.7 | 3558 | 1.00 | 40 | 34.24 | 13.76 | 292.3 | 3740 | 1.00 | 50 | 23.06 | 14.94 | 289.3 | 3916 | 1.00 |
| | | | | | | | | | **TA - 2 Wt %** | | | | | | | | |
| 30 | 50 | 6 | 275.2 | 3100 | 1.43 | 40 | 40 | 6 | 277.0 | 3261 | 1.49 | 50 | 30 | 6 | 277.9 | 3410 | 1.55 |
| 30 | 48 | 8 | 282.6 | 3255 | 1.26 | 40 | 38 | 8 | 283.2 | 3406 | 1.32 | 50 | 28 | 8 | 282.9 | 3546 | 1.38 |
| 30 | 46 | 10 | 288.3 | 3395 | 1.12 | 40 | 36 | 10 | 287.7 | 3538 | 1.18 | 50 | 26 | 10 | 286.2 | 3672 | 1.24 |
| 30 | 44 | 12 | 292.3 | 3494 | 1.01 | 40 | 34 | 12 | 290.7 | 3651 | 1.07 | 50 | 24 | 12 | 288.3 | 3787 | 1.12 |
| 30 | 43.83 | 12.17 | 292.3 | 3493 | 1.00 | 40 | 32.66 | 13.34 | 291.6 | 3681 | 1.00 | 50 | 21.48 | 14.52 | 288.9 | 3860 | 1.00 |
| | | | | | | | | | **TA = 4 Wt %** | | | | | | | | |
| 30 | 48 | 6 | 273.1 | 3039 | 1.38 | 40 | 38 | 6 | 275.1 | 3205 | 1.44 | 50 | 28 | 6 | 276.4 | 3360 | 1.50 |
| 30 | 46 | 8 | 281.0 | 3200 | 1.22 | 40 | 36 | 8 | 281.7 | 3354 | 1.28 | 50 | 26 | 8 | 281.7 | 3500 | 1.34 |
| 30 | 44 | 10 | 287.0 | 3343 | 1.10 | 40 | 34 | 10 | 286.7 | 3490 | 1.15 | 50 | 24 | 10 | 285.5 | 3629 | 1.21 |
| 30 | 42 | 12 | 290.2 | 3417 | 0.987 | 40 | 32 | 12 | 290.0 | 3603 | 1.05 | 50 | 22 | 12 | 287.8 | 3745 | 1.10 |
| 30 | 42.24 | 11.75 | 290.7 | 3425 | 1.00 | 40 | 31.08 | 12.92 | 290.6 | 3620 | 1.00 | 50 | 19.90 | 14.10 | 288.5 | 3803 | 1.00 |

*Oxidation Ratio

Percentage Limits of Variables:

Be 6-12%
NG 30-50%
TA 0-4%
TAGN Difference

Sum = 88%

Percentage of Constants:

NC 10%
NDPA 1%
RES 1%

TABLE A-12

EFFECT OF VARIOUS ADDITIVES ON
THEORETICAL $I_{sp}$ OF LMH-2, AP, DOUBLE-BASE SYSTEMS

**LMH-2 = 12 (Wt %)**

| LMH-2 (Wt %) | AP (Wt %) | "X" (Wt %) | $I_{sp}$ (Sec) | $T_c$ (°K) | O.R.* |
|---|---|---|---|---|---|
| | | | | | |
| 12 | 26 | - | 295.7 | 3663 | 1.57 |
| 12 | 24 | 2 | 295.8 | 3698 | 1.46 |
| 12 | 22 | 4 | 296.0 | 3738 | 1.36 |
| 12 | 20 | 6 | 296.1 | 3772 | 1.27 |
| | | | | | |
| 12 | 26 | - | 295.7 | 3663 | 1.57 |
| 12 | 24 | 2 | 298.3 | 3742 | 1.39 |
| 12 | 22 | 4 | 300.3 | 3813 | 1.24 |
| 12 | 20 | 6 | 301.8 | 3869 | 1.11 |
| | | | | | |
| 12 | 26 | - | 295.7 | 3663 | 1.57 |
| 12 | 24 | 2 | 298.4 | 3556 | 1.43 |
| 12 | 22 | 4 | 298.6 | 3591 | 1.32 |
| 12 | 20 | 6 | 297.8 | 3491 | 1.22 |

**Additive "X" column groups (LMH-2 = 14)**

| LMH-2 | AP | "X" | $I_{sp}$ | $T_c$ | O.R.* |
|---|---|---|---|---|---|
| Additive "X" = AL | | | | | |
| 14 | 24 | - | 301.1 | 3675 | 1.41 |
| 14 | 22 | 2 | 301.1 | 3699 | 1.32 |
| 14 | 20 | 4 | 301.1 | 3730 | 1.23 |
| 14 | 18 | 6 | 301.0 | 3753 | 1.15 |
| Additive "X" = Be | | | | | |
| 14 | 24 | - | 301.1 | 3675 | 1.41 |
| 14 | 22 | 2 | 303.5 | 3746 | 1.26 |
| 14 | 20 | 4 | 305.2 | 3804 | 1.13 |
| 14 | 18 | 6 | 305.2 | 3830 | 1.02 |
| Additive "X" = LI | | | | | |
| 14 | 24 | - | 301.1 | 3675 | 1.41 |
| 14 | 22 | 2 | 303.6 | 3658 | 1.30 |
| 14 | 20 | 4 | 303.6 | 3577 | 1.20 |
| 14 | 18 | 6 | 302.6 | 3459 | 1.11 |

**LMH-2 = 16 column group**

| LMH-2 | AP | "X" | $I_{sp}$ | $T_c$ | O.R.* |
|---|---|---|---|---|---|
| 16 | 22 | - | 306.3 | 3679 | 1.28 |
| 16 | 20 | 2 | 306.1 | 3689 | 1.20 |
| 16 | 18 | 4 | 305.9 | 3707 | 1.12 |
| 16 | 16 | 6 | 305.4 | 3710 | 1.05 |
| | | | | | |
| 16 | 22 | - | 306.3 | 3679 | 1.28 |
| 16 | 20 | 2 | 308.4 | 3740 | 1.15 |
| 16 | 18 | 4 | 309.8 | 3774 | 1.03 |
| 16 | 16 | 6 | 308.4 | 3706 | 0.94 |
| | | | | | |
| 16 | 22 | - | 306.3 | 3679 | 1.28 |
| 16 | 20 | 2 | 308.6 | 3652 | 1.18 |
| 16 | 18 | 4 | 308.5 | 3554 | 1.09 |
| 16 | 16 | 6 | 307.1 | 3415 | 1.02 |

*Oxidation Ratio

Percentage Limits of Variables:

LMH-2 12-16%

Additive "X" 0-6%

AP Difference

Sum = 38%

Percentage of Constants:

NC 10%

NG 50%

NDPA 1%

RES 1%

TABLE A-12 (Cont)

EFFECT OF VARIOUS ADDITIVES ON
THEORETICAL $I_{sp}$ OF LMH-2, AP, DOUBLE-BASE SYSTEMS

| LMH-2 (Wt %) | AP (Wt %) | "X" (Wt %) | $I_{sp}$ (Sec) | $T_c$ (°K) | O.R.* |
|---|---|---|---|---|---|
| **Additive "X" = MG** | | | | | |
| 12 | 26 | - | 295.7 | 3663 | 1.57 |
| 12 | 24 | 2 | 294.4 | 3626 | 1.48 |
| 12 | 22 | 4 | 293.6 | 3584 | 1.39 |
| 12 | 20 | 6 | 293.0 | 3554 | 1.31 |
| **Additive "X" = SI** | | | | | |
| 12 | 26 | - | 295.7 | 3663 | 1.57 |
| 12 | 24 | 2 | 294.1 | 3633 | 1.44 |
| 12 | 22 | 4 | 292.5 | 3598 | 1.32 |
| 12 | 20 | 6 | 290.9 | 3559 | 1.22 |
| **Additive "X" = ZR** | | | | | |
| 12 | 26 | - | 295.7 | 3663 | 1.57 |
| 12 | 24 | 2 | 294.6 | 3687 | 1.50 |
| 12 | 22 | 4 | 293.5 | 3706 | 1.44 |
| 12 | 20 | 6 | 292.3 | 3724 | 1.38 |

| LMH-2 | AF | "X" | $I_{sp}$ | $T_c$ | O.R.* |
|---|---|---|---|---|---|
| **Additive "X" = MG** | | | | | |
| 14 | 24 | - | 301.1 | 3675 | 1.41 |
| 14 | 22 | 2 | 299.7 | 3636 | 1.33 |
| 14 | 20 | 4 | 298.6 | 3593 | 1.26 |
| 14 | 18 | 6 | 297.7 | 3547 | 1.19 |
| **Additive "X" = SI** | | | | | |
| 14 | 24 | - | 301.1 | 3675 | 1.41 |
| 14 | 22 | 2 | 299.6 | 3642 | 1.30 |
| 14 | 20 | 4 | 298.9 | 3606 | 1.20 |
| 14 | 18 | 6 | 296.4 | 3565 | 1.11 |
| **Additive "X" = ZR** | | | | | |
| 14 | 24 | - | 301.1 | 3675 | 1.41 |
| 14 | 22 | 2 | 300.0 | 3698 | 1.35 |
| 14 | 20 | 4 | 298.9 | 3714 | 1.30 |
| 14 | 18 | 6 | 297.7 | 3730 | 1.25 |

| LMH-2 | AP | "X" | $I_{sp}$ | $T_c$ | O.R.* |
|---|---|---|---|---|---|
| **Additive "X" = MG** | | | | | |
| 16 | 22 | - | 306.3 | 3679 | 1.28 |
| 16 | 20 | 2 | 304.9 | 3640 | 1.21 |
| 16 | 18 | 4 | 303.6 | 3597 | 1.15 |
| 16 | 16 | 6 | 302.4 | 3551 | 1.09 |
| **Additive "X" = SI** | | | | | |
| 16 | 22 | - | 306.3 | 3679 | 1.28 |
| 16 | 20 | 2 | 304.9 | 3645 | 1.18 |
| 16 | 18 | 4 | 303.4 | 3606 | 1.10 |
| 16 | 16 | 6 | 301.8 | 3563 | 1.02 |
| **Additive "X" = ZR** | | | | | |
| 16 | 22 | - | 306.3 | 3679 | 1.28 |
| 16 | 20 | 2 | 305.3 | 3702 | 1.23 |
| 16 | 18 | 4 | 304.1 | 3715 | 1.18 |
| 16 | 16 | 6 | 302.9 | 3727 | 1.13 |

*Oxidation Ratio

Percentage Limits of Variables:

LMH-2 12-16%
Additive "X" 0-6%
AP Difference

Sum = 36%

Percentage of Constants:

NC 10%
NG 50%
NDPA 1%
RES 1%

TABLE A-12 (Cont)

EFFECT OF VARIOUS ADDITIVES ON
THEORETICAL $I_{sp}$ OF LMH-2, AP, DOUBLE-BASE SYSTEMS

**LMH-2 = 12 Wt %**

| LMH-2 (Wt %) | AP (Wt %) | "X" (Wt %) | $I_{sp}$ (Sec) | $T_c$ (°K) | O.R.* |
|---|---|---|---|---|---|
| Additive "X" = LIP | | | | | |
| 12 | 26 | -- | 295.7 | 3663 | 1.57 |
| 12 | 24 | 2 | 295.4 | 3678 | 1.56 |
| 12 | 22 | 4 | 294.8 | 3688 | 1.56 |
| 12 | 20 | 6 | 294.2 | 3697 | 1.56 |
| Additive "X" = TAZ | | | | | |
| 12 | 26 | -- | 295.7 | 3663 | 1.57 |
| 12 | 24 | 2 | 296.8 | 3637 | 1.52 |
| 12 | 22 | 4 | 297.8 | 3608 | 1.48 |
| 12 | 20 | 6 | 298.8 | 3577 | 1.44 |

**LMH-2 = 14**

| LMH-2 | AP | "X" | $I_{sp}$ | $T_c$ | O.R.* |
|---|---|---|---|---|---|
| Additive "X" = LIP | | | | | |
| 14 | 24 | -- | 301.1 | 3675 | 1.41 |
| 14 | 22 | 2 | 300.8 | 3690 | 1.41 |
| 14 | 20 | 4 | 300.2 | 3700 | 1.41 |
| 14 | 18 | 6 | 299.6 | 3710 | 1.40 |
| Additive "X" = TAZ | | | | | |
| 14 | 24 | -- | 301.1 | 3675 | 1.41 |
| 14 | 22 | 2 | 302.2 | 3646 | 1.37 |
| 14 | 20 | 4 | 303.3 | 3616 | 1.33 |
| 14 | 18 | 6 | 304.3 | 3585 | 1.30 |

**LMH-2 = 16**

| LMH-2 | AP | "X" | $I_{sp}$ | $T_c$ | O.R.* |
|---|---|---|---|---|---|
| Additive "X" = LIP | | | | | |
| 16 | 22 | -- | 306.3 | 3679 | 1.28 |
| 16 | 20 | 2 | 305.9 | 3694 | 1.28 |
| 16 | 18 | 4 | 305.3 | 3705 | 1.27 |
| 16 | 16 | 6 | 304.7 | 3714 | 1.27 |
| Additive "X" = TAZ | | | | | |
| 16 | 22 | -- | 306.3 | 3679 | 1.28 |
| 16 | 20 | 2 | 307.5 | 3650 | 1.24 |
| 16 | 18 | 4 | 308.6 | 3619 | 1.21 |
| 16 | 16 | 6 | 309.6 | 3587 | 1.18 |

*Oxidation Ratio

Percentage Limits of Variables:

LMH-2 12-16%
Additive "X" 0-6%
AP Difference

Sum = 38%

Percentage of Constants:

NC 10%
NG 50%
NDPA 1%
RES 1%

TABLE A-13
THERMOCHEMICAL INGREDIENT DATA

| Ingred Symbol | Chemical Name | Chemical Formula | $\Delta H_{f298}$ (kcal/mole) | Density (g/cc) |
|---|---|---|---|---|
| Al | Aluminum | $Al$ | | |
| AN | Ammonium Nitrate | $NH_4NO_3$ | -87.27 | 1.725 |
| AP | Ammonium Perchlorate | $NH_4ClO_4$ | -69.42 | 1.950 |
| BE | Beryllium | $Be$ | 0 | 1.816 |
| LMH-2 | Beryllium Hydride | $Be_{8.86}H_{17.38}C_{.293}C_{.002}$ | -5.5 | 0.650 |
| C5A | Pentyl Fluoroalkyl Acrylate | $C_8F_8H_6O_2$ | -492.0 | 1.481 |
| C7A | Fluorinated Acrylate Adhesive | $C_{2.59}F_{3.108}H_{1.55}O_{.518}$ | -177.6 | 1.5 |
| C7M | Fluorinated Acrylate Adhesive | $C_{2.75}F_3H_2O_{.5}$ | -179.4 | 1.5 |
| C9M | Nonylfluoroalkyl Methacrylate | $C_{13}F_{16}H_8O_2$ | -911.1 | 1.606 |
| FAAV | 20 C7A/60C7M/20 Viton | $C_{2.63}H_{1.70}F_{3.17}O_{.403}$ | -143.1 | 1.364 |
| FAV | 23 C5A/67C9M/10 Viton | $C_{2.62}H_{1.65}F_{3.16}O_{.429}$ | -161.6 | 1.487 |
| HC | Polybutadiene Type Rubber (Thiokol) | $C_{7.19}H_{10.982}N_{.042}O_{.124}$ | -2.1 | 0.908 |
| HDP | Hydrazine Diperchlorate | $N_2H_4 \cdot 2HClO_4$ | -92.554 | 1.86 |
| HMX | Cyclotetramethylenetetranitramine | $C_4H_8N_8O_8$ | +25.03 | 1.903 |
| LI | Lithium | $Li$ | 0 | 0.53 |
| LIP | Lithium Perchlorate | $LiClO_4$ | -92.00 | 2.492 |
| MG | Magnesium | $Mg$ | 0 | 1.74 |
| NC | Nitrocellulose | $C_6H_{7.55}N_{2.45}O_{9.9}$ | -159.8 | 1.660 |
| NDPA | 2-Nitrodiphenylamine | $C_{12}H_{10}N_2O_2$ | +30.0 | 1.200 |
| NFPA | 1,2-bis (Difluoramino) Propyl Acetate | $C_5F_4H_6N_2$ | -124.0 | 1.57 |
| NG | Nitroglycerine | $C_3H_5N_3O_9$ | -88.40 | 1.600 |
| NP | Nitronium Perchlorate | $NO_2ClO_4$ | +8.0 | 2.25 |
| RES | Resorcinol | $C_6H_6O_2$ | -85.26 | 1.272 |
| SI | Silicon | $Si$ | 0 | 2.4 |
| TA | Triacetin | $C_9H_{14}O_6$ | -291.0 | 1.150 |
| TAZ | Triaminoguanidine Azide | $CH_9N_9$ | +105.65 | 1.44 |
| TAGN | Triaminoguanidine Nitrate | $CH_9N_7O_3$ | -11.8 | 1.574 |
| TFLN | Teflon | $C_2F_4$ | -196.0 | 2.2 |
| TVOPA | Hexakis (Difluoramino) Vinoxy Propane | $C_9F_{12}H_{14}N_6O_3$ | -202.0 | 1.5 |
| VITON | Viton Rubber | $C_5F_8H_2$ | 0 | 1.0 |
| ZR | Zirconium | $ZR$ | 0 | 6.4 |
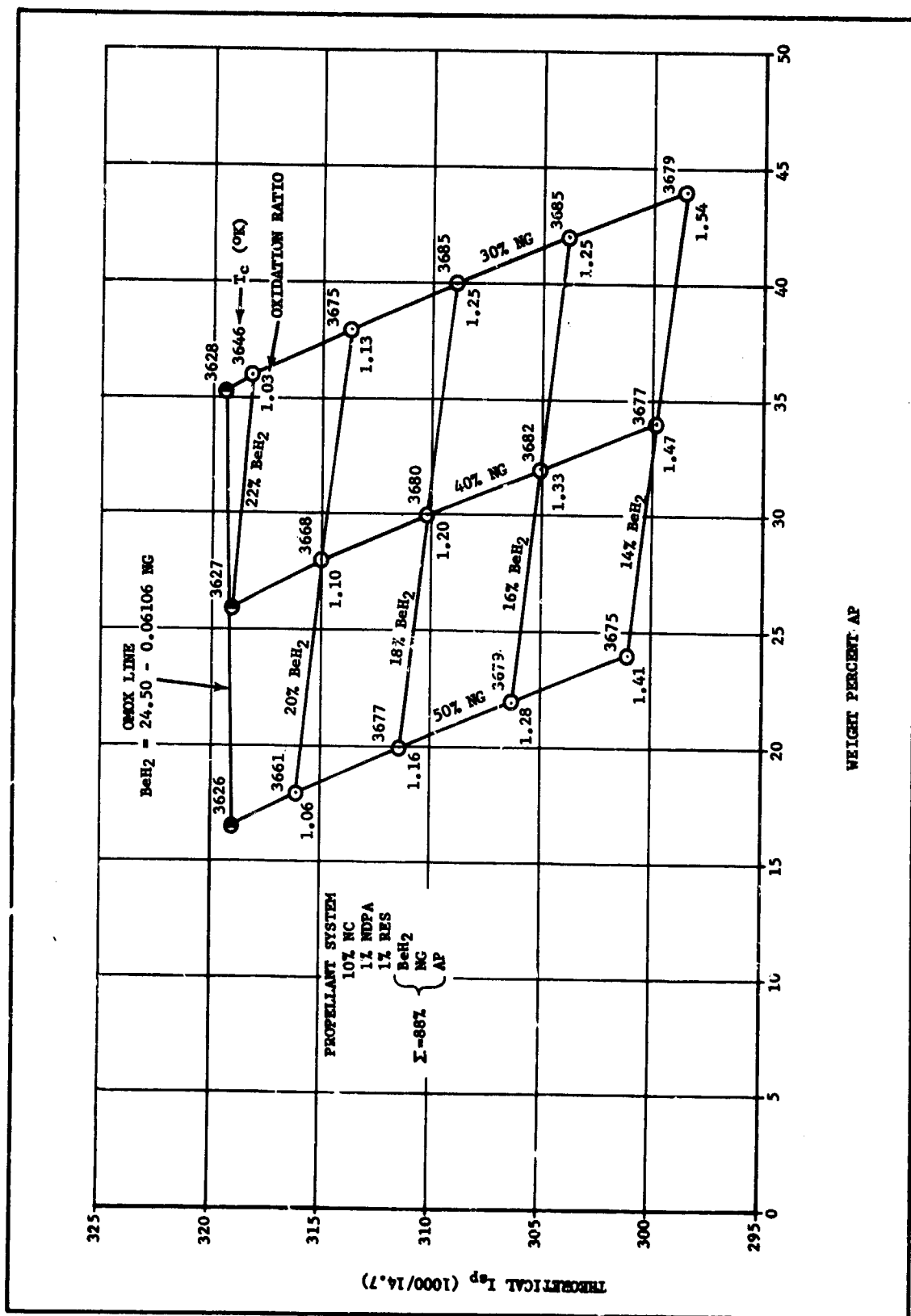
Figure A-1.  Theoretical $I_{sp}$ Potential of a Double-Base, LMH-2, AP System
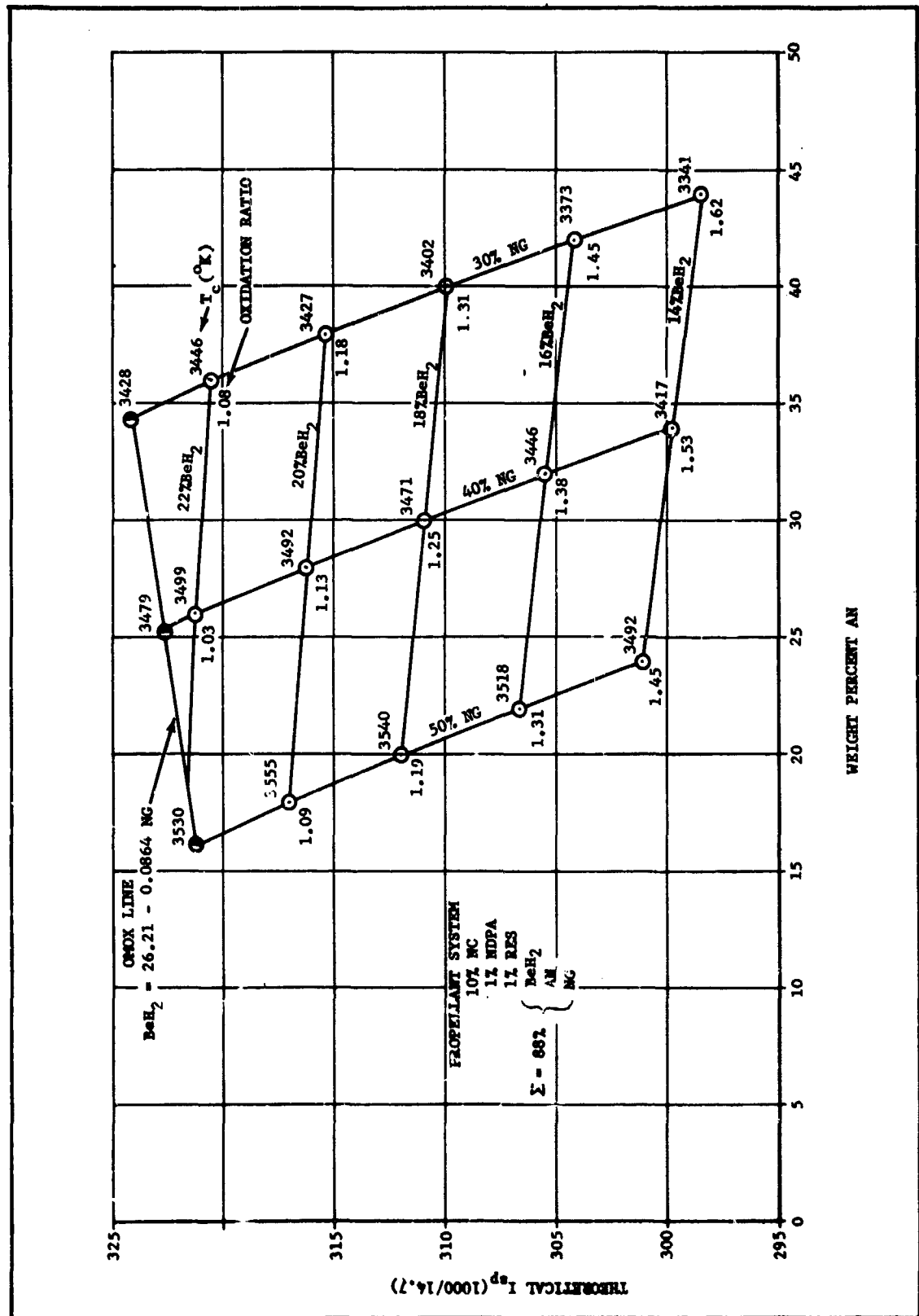
Figure A-2.   Theoretical $I_{sp}$ Potential of a Double-Base, LMH-2
AN System

CONFIDENTIAL
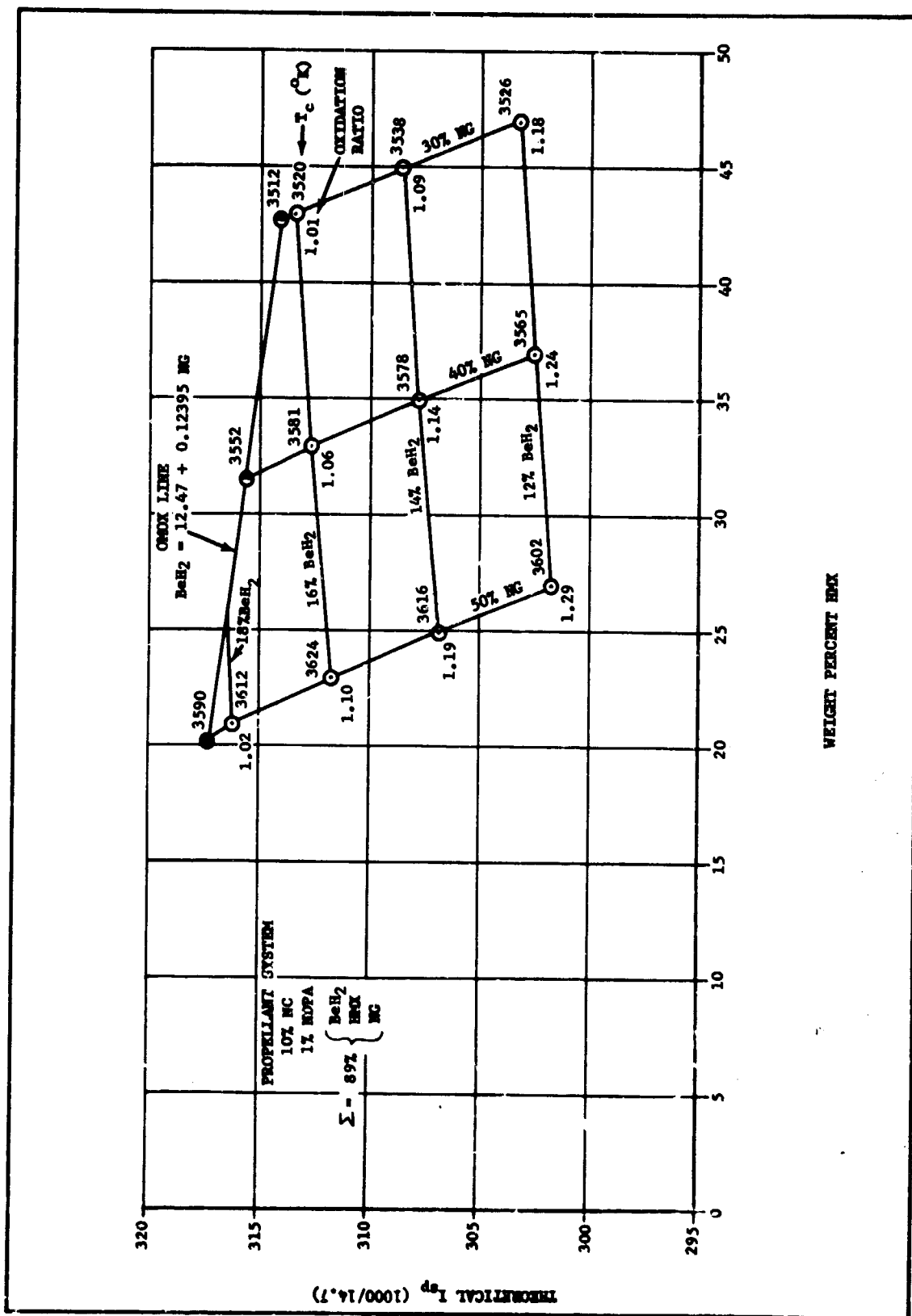


Figure A-3. Theoretical $I_{sp}$ Potential of a Double-Base, LMH-2, HMX System

A-21

CONFIDENTIAL
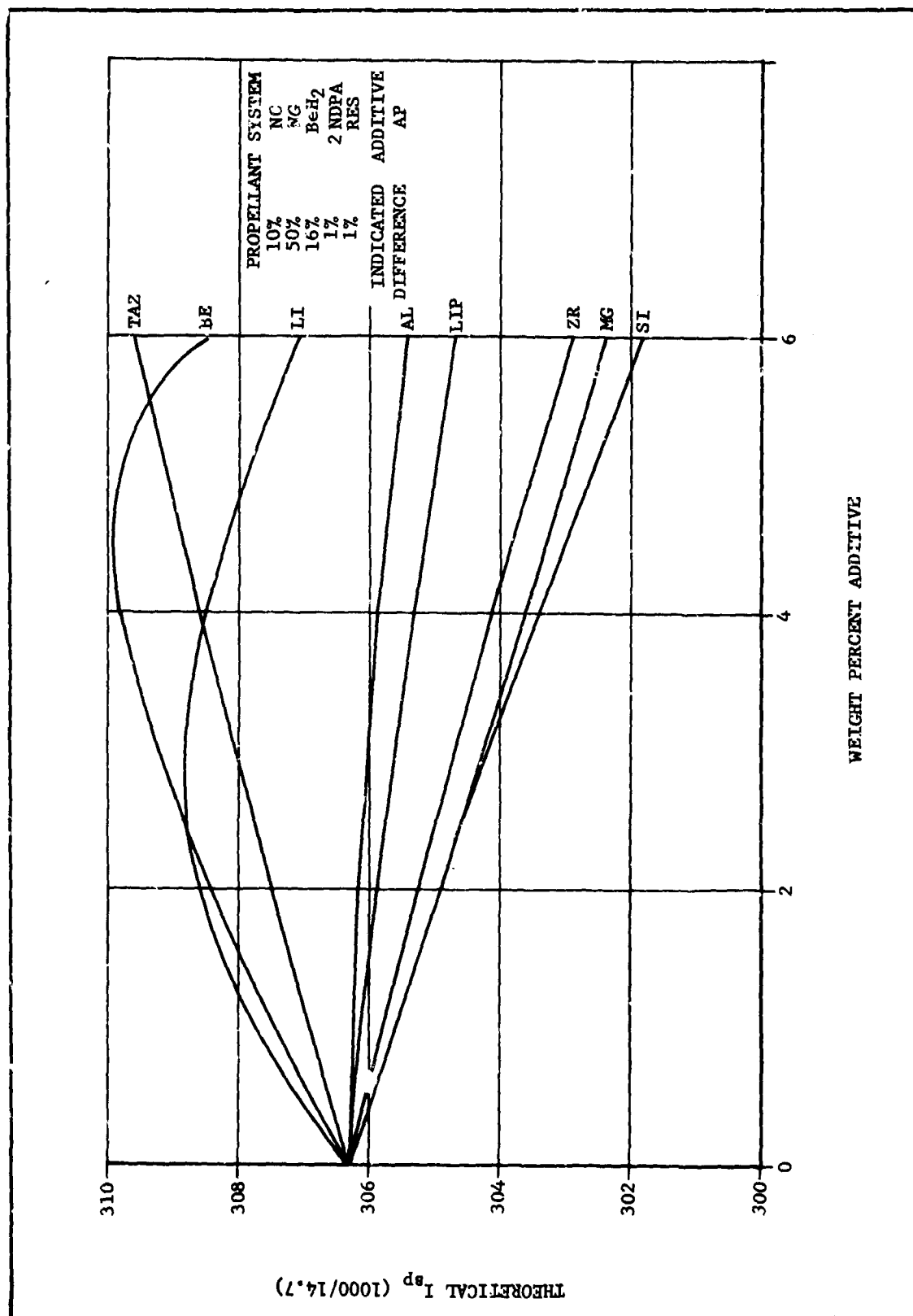
Figure A-4. Effect of Various Additives on a Double-Base, LMH-2, AP System
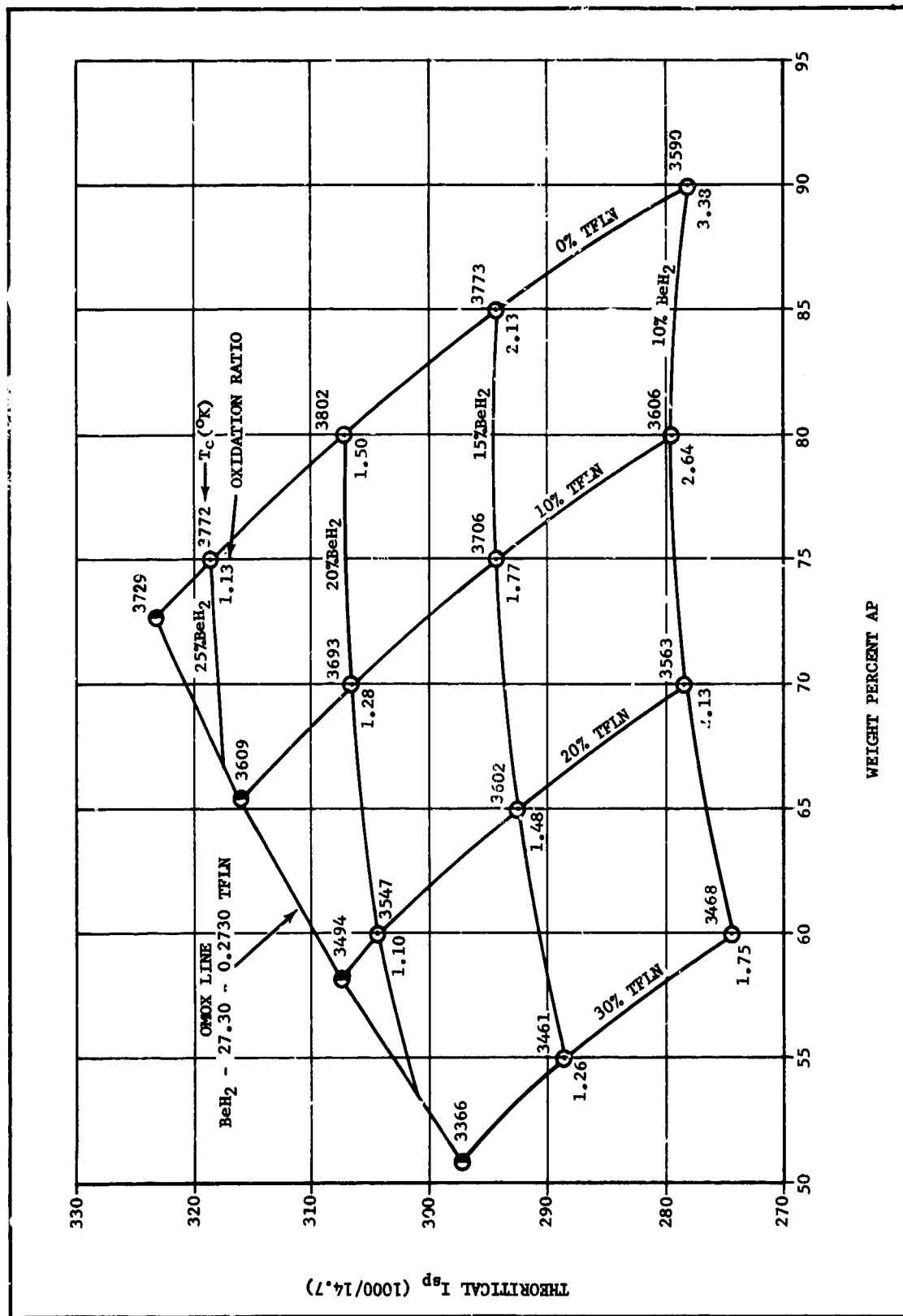
Figure A-5. Theoretical $I_{sp}$ Potential of a LMH-2, AP, TFLN System
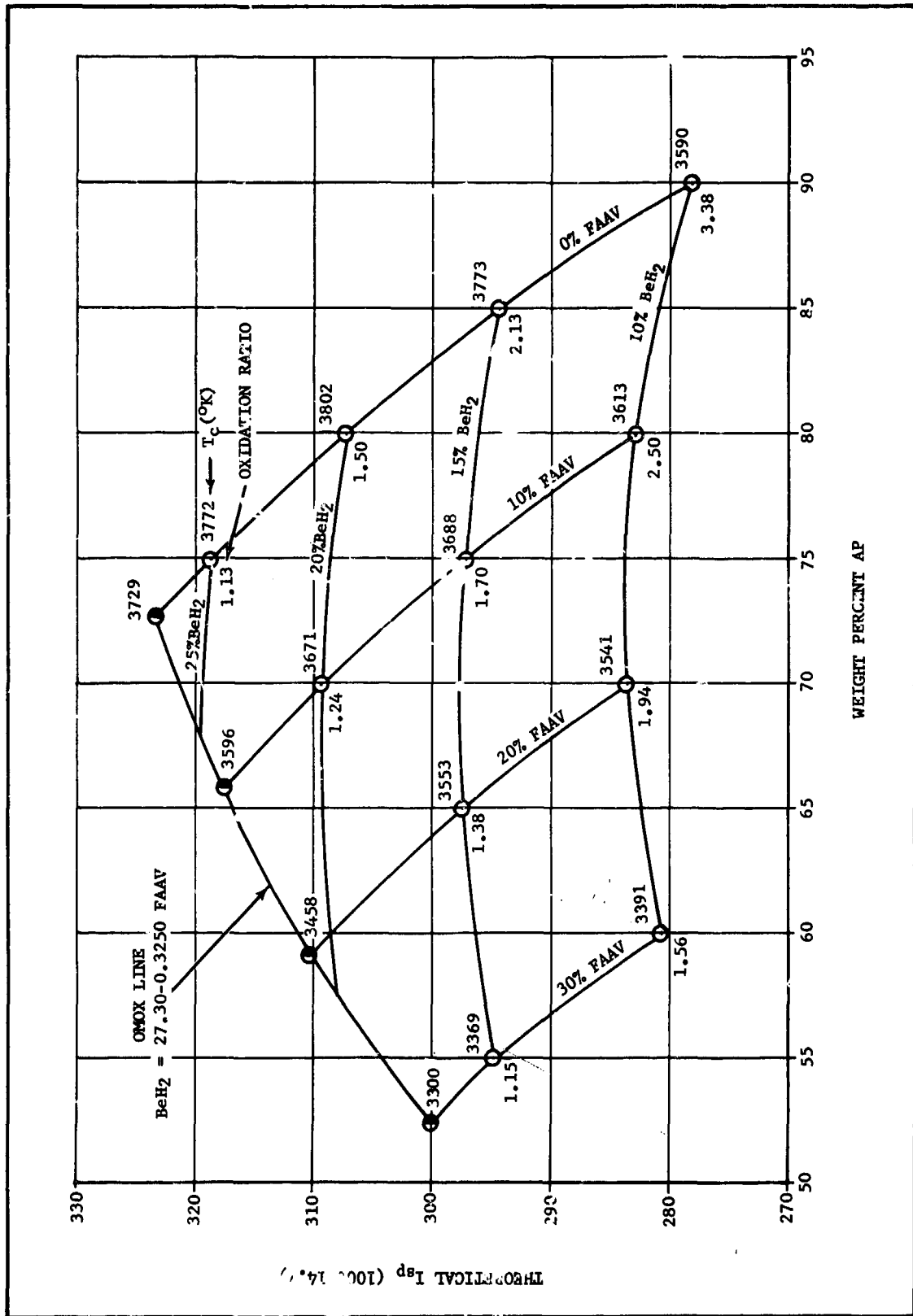
Figure A-6. Theoretical $I_{sp}$ Potential of a LMH-2, AP, FAAV System
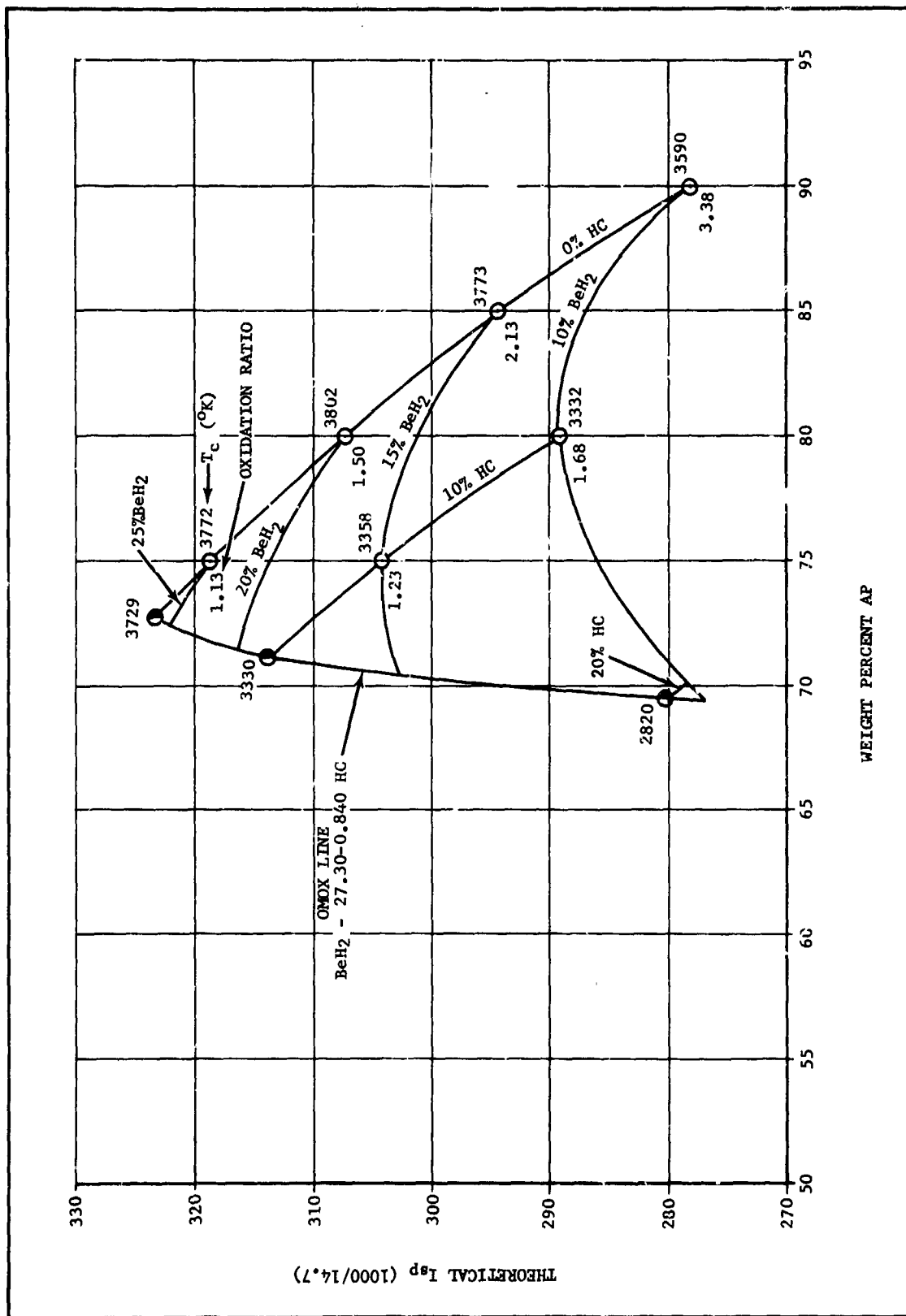
Figure A-7. Theoretical $I_{sp}$ Potential of a LMH-2, AP, HC System

# CONFIDENTIAL

## APPENDIX B

### THEORETICAL PERFORMANCE CALCULATIONS AND
### BALLISTIC DATA SUMMARY

Theoretical performance calculations on Be analog formulations and LMH-2 candidate propellants are summarized in Tables B-1 and B-2. Also included are ballistic summary tables (Tables B-3 through B-12) of individual Be and LMH-2 firings made under the Task II effort.

# CONFIDENTIAL

TABLE B-1

THEORETICAL PERFORMANCE CALCULATIONS FOR
CANDIDATE LMH-2 PROPELLANTS

| Equilibrium Flow | Propellant Type | | | | | |
|---|---|---|---|---|---|---|
| | VIX | VIY | VIZ | VJA | VJI | VJL |
| **Chamber** | | | | | | |
| $P_c$ (psia) | 1000 | 1000 | 1000 | 1000 | 1000 | 1000 |
| $T_c$ ($^\circ$K) | 3678 | 3679 | 3672 | 3620 | 3623 | 3614 |
| $\gamma$ (Heat capacity ratio) | 1.075 | 1.075 | 1.074 | 1.088 | 1.083 | 1.083 |
| Molecular wt gas | 16.35 | 14.82 | 13.83 | 15.40 | 13.87 | 14.01 |
| Total moles* | 5.469 | 5.778 | 6.085 | 5.729 | 5.953 | 6.112 |
| Composition** | | | | | | |
| BeO | 22.5 | 24.4 | 24.8 | 21.9 | 23.8 | 23.8 |
| HCl | 3.0 | 2.5 | 2.0 | -- | -- | 0.5 |
| $N_2$ | 8.7 | 8.1 | 7.6 | 12.2 | 11.2 | 10.2 |
| CO | 17.9 | 17.4 | 16.8 | 22.1 | 21.0 | 20.6 |
| $CO_2$ | 1.0 | 0.6 | 0.3 | 0.5 | 0.2 | 0.2 |
| $H_2$ | 27.0 | 31.3 | 35.3 | 31.8 | 35.4 | 35.1 |
| $H_2O$ | 12.0 | 8.1 | 4.7 | 5.5 | 2.6 | 3.4 |
| H | 4.8 | 5.1 | 5.3 | 4.6 | 4.9 | 4.7 |
| Other | 3.1 | 2.5 | 3.2 | 1.4 | 0.9 | 1.5 |
| **Throat** | | | | | | |
| $C^*$ (ft/sec) | 5896 | 5994 | 6078 | 6000 | 6063 | 6063 |
| $C_d$ ($sec^{-1} \times 10^3$) | 5.46 | 5.37 | 5.30 | 5.37 | 5.31 | 5.31 |
| **Exit** | | | | | | |
| $P_e$ (psia) | 14.7 | 14.7 | 14.7 | 14.7 | 14.7 | 14.7 |
| Teq ($^\circ$K) | 2570 | 2596 | 2619 | 2421 | 2472 | 2474 |
| $I_{sp}$ (1000/14.7) | 303.7 | 308.9 | 313.8 | 309.3 | 314.0 | 312.7 |
| $\gamma$ (Heat capacity ratio) | 1.104 | 1.100 | 1.096 | 1.135 | 1.126 | 1.124 |
| *,**Refer to end of table for footnotes | | | | | | |

TABLE B-1 (Cont)

THEORETICAL PERFORMANCE CALCULATIONS FOR
CANDIDATE LMH-2 PROPELLANTS

| Equilibrium Flow | VIX | VIY | VIZ | VJA | VJI | VJL |
|---|---|---|---|---|---|---|
| Molecular wt gas | 16.47 | 14.91 | 13.43 | 15.39 | 14.04 | 14.14 |
| Total moles* | 5.392 | 5.704 | 6.019 | 5.677 | 5.960 | 5.927 |
| Composition** | | | | | | |
| BeO | 24.2 | 26.0 | 27.6 | 23.1 | 25.0 | 25.1 |
| HCl | 3.5 | 3.0 | 2.5 | -- | -- | 0.7 |
| $N_2$ | 8.9 | 8.2 | 7.7 | 12.4 | 11.4 | 10.4 |
| CO | 17.9 | 17.5 | 17.1 | 22.3 | 21.3 | 20.9 |
| $CO_2$ | 1.3 | 0.7 | 0.3 | 0.7 | 0.2 | 0.3 |
| $H_2$ | 28.9 | 33.5 | 37.7 | 34.5 | 38.2 | 37.8 |
| $H_2O$ | 13.3 | 8.8 | 4.7 | 6.0 | 2.6 | 3.4 |
| H | 1.6 | 1.9 | 2.2 | 0.9 | 1.2 | 1.2 |
| Other | 0.4 | 0.4 | 0.2 | 0.1 | 0.1 | 0.2 |
| Wt % condensibles | | | | | | |
| Frozen Flow | | | | | | |
| $I_{sp}$ (1000/14.7) | 299.4 | 305.1 | 310.3 | 305.1 | 310.1 | 308.8 |
| $T_e$ (°K) | 2257 | 2302 | 2336 | 2157 | 2207 | 2710 |
| $\gamma$ (Heat capacity ratio) | 1.176 | 1.173 | 1.170 | 1.187 | 1.183 | 1.182 |

*Total moles (gas plus solids) per 100 gm propellant

**Mole percent of combustion products

## THEORETICAL PERFORMANCE CALCULATIONS FOR BERYLLIUM PROPELLANTS

| Equilibrium Flow | Propellant Type | | | | | | | | |
|---|---|---|---|---|---|---|---|---|---|
| | VCP | VIG | VIH | VII | VIJ | VIK | VIL | VIN | VIO |
| **Chamber** | | | | | | | | | |
| $P_c$ (psia) | 1000 | 1000 | 1000 | 1000 | 1000 | 1000 | 1000 | 1000 | 1000 |
| $T_c$ (°K) | 3835 | 3633 | 4173 | 3971 | 4145 | 4109 | 4008 | 3744 | 3758 |
| $\gamma$(Heat capacity ratio) | 1.072 | 1.082 | 1.083 | 1.054 | 1.043 | 1.044 | 1.055 | 1.069 | 1.073 |
| Molecular wt gas | 20.78 | 17.10 | 19.86 | 18.60 | 19.82 | 20.78 | 20.74 | 17.94 | 22.10 |
| Total moles* | 4.602 | 5.238 | 4.633 | 4.839 | 4.639 | 4.524 | 4.569 | 4.986 | 4.418 |
| Composition** | | | | | | | | | |
| BeO | 22.7 | 25.1 | 33.6 | 32.2 | 33.5 | 31.4 | 26.9 | 29.9 | 18.7 |
| HCl | 1.2 | 0.8 | 3.4 | 3.2 | 4.0 | 4.0 | 2.2 | -- | 1.6 |
| $N_2$ | 15.4 | 18.8 | 9.3 | 8.1 | 9.0 | 9.6 | 13.4 | 14.6 | 17.1 |
| CO | 27.9 | 21.2 | 18.4 | 22.5 | 17.6 | 18.3 | 23.4 | 17.6 | 26.8 |
| $CO_2$ | 1.7 | 0.1 | 11.0 | 0.5 | 1.0 | 1.6 | 1.7 | 1.2 | 3.2 |
| $H_2$ | 14.8 | 26.8 | 12.7 | 18.6 | 13.3 | 11.3 | 12.7 | 19.1 | 12.0 |
| $H_2O$ | 7.7 | 1.3 | 5.9 | 3.3 | 6.2 | 8.3 | 7.7 | 10.4 | 12.0 |
| H | 4.8 | 4.3 | 7.4 | 6.5 | 7.3 | 6.4 | 6.0 | 4.4 | 3.8 |
| Other | 3.8 | 1.6 | 8.3 | 4.9 | 8.1 | 9.1 | 6.0 | 2.8 | 4.8 |
| **Throat** | | | | | | | | | |
| C* (ft/sec) | 5512 | 5680 | 5391 | 5409 | 5374 | 5358 | 5479 | 5426 | 5464 |
| Cd ($sec^{-1} \times 10^3$) | 5.84 | 5.67 | 5.97 | 5.95 | 5.99 | 6.00 | 5.88 | 5.93 | 5.89 |
| **Exit** | | | | | | | | | |
| $P_e$ (psia) | 14.7 | 14.7 | 14.7 | 14.7 | 14.7 | 14.7 | 14.7 | 14.7 | 14.7 |
| Teq (°K) | 2690 | 2531 | 3015 | 2820 | 2992 | 2959 | 2820 | 2780 | 2569 |
| $I_{sp}$ (1000/14.7) | 283.0 | 290.7 | 278.0 | 278.7 | 277.4 | 276.5 | 281.1 | 280.1 | 281.1 |
| $\gamma$ (Heat capacity ratio) | 1.046 | 1.115 | 1.046 | 1.045 | 1.067 | 1.049 | 1.072 | 1.074 | 1.115 |
| Molecular wt gas | 21.20 | 17.21 | 20.18 | 20.28 | 20.12 | 21.43 | 23.86 | 18.07 | 22.67 |
| Total moles* | 4.520 | 5.185 | 4.555 | 4.587 | 4.585 | 4.413 | 4.143 | 4.946 | 4.319 |
| Composition** | | | | | | | | | |
| BeO | 24.3 | 26.7 | 36.8 | 32.3 | 36.7 | 34.4 | 24.0 | 31.1 | 20.3 |
| HCl | 1.5 | 1.2 | 4.6 | 4.9 | 5.4 | 5.1 | 3.2 | -- | 1.9 |
| $N_2$ | 15.8 | 19.0 | 9.7 | 8.5 | 9.3 | 10.1 | 15.0 | 14.8 | 17.7 |
| CO | 27.9 | 21.5 | 18.4 | 23.8 | 17.6 | 18.1 | 25.0 | 17.4 | 26.2 |
| $CO_2$ | 2.4 | 1.0 | 1.3 | 0.5 | 1.3 | 2.3 | 2.6 | 1.5 | 13.1 |
| $H_2$ | 16.3 | 29.3 | 13.9 | 22.3 | 14.5 | 11.8 | 15.0 | 19.9 | 4.6 |
| $H_2O$ | 9.1 | 0.8 | 7.3 | 2.9 | 7.5 | 10.8 | 10.5 | 11.7 | 14.4 |
| H | 1.9 | 1.3 | 4.9 | 3.4 | 4.7 | 3.9 | 3.0 | 2.8 | 1.1 |
| Other | 0.8 | 0.1 | 3.1 | 1.4 | 3.0 | 3.5 | 1.7 | 0.8 | 0.7 |
| Wt % Condensibles | | | | | | | | | |
| **Frozen Flow** | | | | | | | | | |
| $I_{sp}$ (1000/14.7) | 275.0 | 287.3 | 273.5 | 276.1 | 273.0 | 272.3 | 277.7 | 278.6 | 275.6 |
| $T_e$ (°K) | 2347 | 2261 | 2820 | 2791 | 2820 | 2820 | 2823 | 2577 | 2186 |
| $\gamma$(Heat capacity ratio) | -- | 1.177 | 1.135 | 1.143 | 1.202 | 1.238 | 1.158 | 1.145 | 1.188 |

\* Total moles (gas plus solids) per 100 gm propellant

\*\* Mole percent of combustion products

TABLE B-3

BERYLLIUM EFFICIENCY STUDIES

| | | | | | | | | | | | | | | |
|---|---|---|---|---|---|---|---|---|---|---|---|---|---|---|
| Propellant type | VCP | VCP | VCP | VCP | VCP | VCP | VIH | VIH | VII | VII | VII | VII | VII | VII |
| Motor design | 15PC-1 | 15PC-1 | 15PC-1 | 15PC | 15PC | 15PC | 15PC | 15PC | 15PC | 15PC-2 | 15PC-2 | 15PC-2 | 15PC-1 | 15PC-1 |
| Grain No. | S82B | S87B | S139B | S86B | S76B | S75B | S69B | S81B | S78B | S129B | S130B | S131B | S132B | S133B |
| Firing No. | LM2-1 | LM2-6 | LM2-55 | LM2-16 | LM2-25 | LM2-7 | LM2-3 | LM2-8 | LM2-9 | LM2-36 | LM2-47 | LM2-48 | LM2-39 | LM2-49 |
| Propellant wt (lb) | 14.88 | 14.92 | 14.91 | 15.21 | 15.17 | 15.12 | 15.11 | 15.24 | 15.04 | 14.84 | 14.82 | 14.66 | 14.71 | 14.73 |
| Powder wt (lb) | 0.04 | 0.05 | 0.04 | 0.06 | 0.05 | 0.05 | 0.05 | 0.05 | 0.06 | 0.06 | 0.07 | 0.06 | 0.05 | 0.06 |
| $K$ ($S/A_t$) | 104.0 | 103.3 | 104.0 | 142.5 | 142.5 | 143.2 | 139.8 | 110.5 | 109.2 | 111.1 | 138.1 | 139.0 | 204.9 | 182.2 |
| $t_a$ (sec) | 1.884 | 1.874 | 2.237 | 1.900 | 1.804 | 1.817 | 1.148 | 1.322 | 1.350 | 2.49 | 2.218 | 2.228 | 2.205 | 2.409 |
| $t_b$ (sec) | 1.794 | 1.770 | 2.117 | 1.756 | 1.708 | 1.715 | 1.043 | 1.274 | 1.280 | 2.36 | 2.021 | 2.080 | 2.061 | 2.264 |
| $\bar{P}_a$ (psia) | 578 | 586 | 489 | 1043 | 1069 | 1074 | 1604 | 1121 | 1085 | 337 | 460 | 454 | 903 | 751 |
| $\bar{P}_b$ (psia) | 592 | 600 | 502 | 1085 | 1098 | 1103 | 1695 | 1144 | 1118 | 348 | 484 | 472 | 935 | 775 |
| $P_{max}$ (psia) | 657 | 650 | 545 | 1159 | 1160 | 1175 | 1885 | 1223 | 1202 | 399 | 544 | 527 | 1066 | 881 |
| $\bar{P}amb$ (psia) | 12.41 | 12.12 | 12.29 | 11.94 | 11.85 | 12.10 | 12.41 | 10.20 | 12.19 | 12.17 | 12.22 | 12.307 | 8.141 | 12.15 |
| $\bar{r}$ (in./sec) | 0.557 | 0.565 | 0.477 | 0.751 | 0.773 | 0.764 | 1.246 | 1.028 | 1.023 | 0.317 | 0.371 | 0.373 | 0.490 | 0.446 |
| $\dot{m}$ (lb/sec) | 7.90 | 7.96 | 6.67 | 8.01 | 8.41 | 8.32 | 13.16 | 11.53 | 11.14 | 5.96 | 6.68 | 6.58 | 6.67 | 6.12 |
| $C_d$ ($sec^{-1}$) | 0.00580 | 0.00578 | 0.00583 | 0.00576 | 0.00587 | 0.00581 | 0.00613 | 0.00604 | 0.00603 | 0.00600 | 0.00614 | 0.00614 | 0.00623 | 0.00611 |
| $\epsilon$ ($A_e/A_t$) | 5.615 | 5.616 | 5.717 | 9.640 | 9.590 | 9.607 | 9.576 | 9.624 | 9.607 | 5.627 | 5.623 | 5.604 | 9.477 | .625 |
| $\bar{F}_a$ ($lb_f$) | 1939 | 1995 | 1629 | 2112 | 2227 | 2209 | 3570 | 3088 | 2949 | 1350 | 1586 | 1554 | 1757 | 1530 |
| Isp del $\left(\dfrac{lb_f\text{-sec}}{lbm}\right)$ | 245.6 | 250./ | 244.5 | 263.9 | 265.1 | 265.5 | 272.1 | 267.4 | 264.0 | 226.7 | 237.6 | 236.2 | 263.7 | 250.3 |
| Theoretical Isp at firing conditions | 268.7 | 269.5 | 265.0 | 287.9 | 288.5 | 288.2 | 289.6 | 286.8 | 283.4 | 250.4 | 259.9 | 259.1 | 287.3 | 275.5 |
| Efficiency | 91.40 | 93.02 | 92.26 | 91.66 | 91.89 | 92.1 | 93.96 | 93.48 | 93.44 | 90.54 | 91.42 | 91.16 | 91.79 | 90.86 |
| Isp 1000 | 258.7 | 263.2 | 261.1 | 259.4 | 260.1 | 260.6 | 261.2 | 259.9 | 259.8 | 252.3 | 254.8 | 254.1 | 255.8 | 253.2 |
| Isp del (c)* | 245.0 | 250.0 | 243.9 | 263.1 | 264.4 | 264.9 | 271.4 | 267.4 | 264.0 | 225.9 | 236.6 | 235.4 | 262.7 | 249.5 |
| Efficiency (c)* | 91.18 | 92.76 | 92.04 | 91.39 | 91.65 | 91.92 | 93.71 | 93.24 | 93.16 | 90.22 | 91.04 | 90.85 | 91.44 | 90.56 |
| Isp 1000 (c)* | 258.0 | 262.5 | 260.5 | 258.6 | 259.4 | 260.1 | 260.5 | 259.2 | 259.0 | 251.4 | 253.7 | 253.2 | 254.6 | 252.4 |

Note: Refer to end of table for footnotes

TABLE B-3 (Cont)

BERYLLIUM EFFICIENCY STUDIES

| Propellant type | VII | VLJ | VLJ | VLJ | VLJ | VLJ | VLJ | VIK | VIK | VIK | VIK | VIK | VIK | VIL |
|---|---|---|---|---|---|---|---|---|---|---|---|---|---|---|
| Motor design | 15PC-1 | 15PC-1 | 15PC-1 | 15PC-1 | 15PC | 15PC | 15PC | 15PC-1 | 15PC-1 | 15PC-1 | 15PC | 15PC | 15PC | 15PC-1 |
| Grain No. | 8134B | 884B | 894B | 885B | 891B | 892B | 897B | 888B | 889B | 890B | 872B | 8105B | 8114B | 8116B |
| Firing No. | LM2-50 | LM2-2*** | LM2-12 | LM2-13 | LM2-4 | LM2-5 | LM2-1*** | LM2-14 | LM2-27 | LM2-28 | LM2-10 | LM2-15 | LM2-29 | LM2-26 |
| Propellant wt (lb) | 14.38 | 14.95 | 15.12 | 15.01 | 15.20 | 15.24 | 15.00 | 15.03 | 14.95 | 14.94 | 14.92 | 14.74 | 15.30 | 15.03 |
| Powder wt (lb) | 0.04 | 0.06 | 0.04 | 0.05 | 0.04 | 0.03 | 0.05 | 0.05 | 0.05 | 0.04 | 0.05 | 0.04 | 0.05 | 0.06 |
| $K (S/A_t)$ | 209.3 | 101.8 | 102.9 | 102.5 | 140.5 | 141.3 | 128. | 77.00 | 70.2 | 70.8 | 109.6 | 96.5 | 98.1 | 95.8 |
| $t_a$ (sec) | 1.809 | 1.824 | 1.820 | 1.831 | 1.694 | 1.830 | 1.947 | 1.238 | 1.332 | 1.436 | 1.227 | 1.459 | 1.425 | 1.460 |
| $t_b$-sec | 1.713 | 1.686 | 1.697 | 1.720 | 1.593 | 1.72 | 1.875 | 1.164 | 1.246 | 1.368 | 1.165 | 1.413 | 1.357 | 1.363 |
| $\bar{P}_a$ (psia) | 1135 | 566 | 576 | 568 | 1103 | 1019 | 892 | 621 | 534 | 491 | 1182 | 879 | 925 | 680 |
| $\bar{P}_b$ (psia) | 1167 | 595 | 597 | 587 | 1141 | 1054 | 907 | 640 | 552 | 503 | 1216 | 895 | 950 | 703 |
| Pmax (psia) | 1291 | 671 | 647 | 639 | 1245 | 1145 | 999 | 696 | 595 | 537 | 1303 | 959 | 1022 | 762 |
| Pamb (psia) | 12.303 | 12.41 | 11.97 | 11.92 | 12.11 | 12.10 | 12.00 | 12.09 | 12.18 | 12.14 | 12.08 | 11.44 | 10.33 | 11.54 |
| $\bar{r}$ (in./sec) | 0.590 | 0.593 | 0.589 | 0.581 | 0.822 | 0.761 | 0.693 | 0.859 | 0.797 | 0.731 | 1.116 | 0.927 | 0.965 | 0.737 |
| $\dot{m}$ (lb/sec) | 7.95 | 8.20 | 8.31 | 8.20 | 8.97 | 8.33 | 7.78 | 12.14 | 11.22 | 10.40 | 12.81 | 10.10 | 10.74 | 10.29 |
| $C_d$ (sec$^{-1}$) | 0.00603 | 0.00611 | 0.00611 | 0.00614 | 0.00608 | 0.00612 | 0.00610 | 0.00619 | 0.00606 | 0.00614 | 0.00606 | 0.00606 | 0.00606 | 0.00597 |
| $\varepsilon (A_e/A_t)$ | 9.742 | 5.591 | 5.616 | 5.644 | 9.595 | 9.609 | 9.022 | 5.555 | 5.489 | 5.631 | 9.653 | 9.478 | 9.425 | 5.528 |
| $\bar{F}_a$ (lb$_f$) | 2082 | 1979 | 2031 | 1996 | 2367 | 2180 | 1991 | 3000 | 2725 | 2495 | 3221 | 2638 | 2839 | 2605 |
| Isp del $\left(\dfrac{lb_f\text{-sec}}{lbm}\right)$ | 262.1 | 244.2 | 244.6 | 243.7 | 263.9 | 261.9 | 255.8 | 247.3 | 243.1 | 240.0 | 265.1 | 261.5 | 264.8 | 253.3 |
| Theoretical Isp at firing conditions | 284.6 | 262.9 | 264.1 | 263.9 | 283.1 | 281.6 | 280.6 | 264.6 | 261.1 | 259.4 | 283.7 | 278.5 | 279.8 | 271.9 |
| Efficiency | 92.09 | 92.89 | 92.62 | 92.35 | 93.22 | 93.00 | 91.17 | 93.46 | 93.11 | 92.52 | 93.44 | 93.90 | 94.64 | 93.16 |
| Isp $\dfrac{15}{1000}$ | 256.7 | 257.7 | 256.9 | 256.2 | 258.6 | 258.0 | 252.9 | 258.4 | 257.5 | 255.8 | 258.4 | 259.6 | 261.7 | 261.9 |
| Isp del (c)* | 261.5 | 243.4 | 244.1 | 243.0 | 263.4 | 261.5 | 255.1 | 246.6 | 242.4 | 239.5 | 264.4 | 260.9 | 263.8 | 252.5 |
| Efficiency (c)* | 91.88 | 92.58 | 92.43 | 92.08 | 93.04 | 92.86 | 90.91 | 93.20 | 92.84 | 92.33 | 93.20 | 93.68 | 94.28 | 92.87 |
| Isp $\dfrac{15}{1000}$ (c)* | 256.1 | 256.8 | 256.4 | 255.4 | 258.1 | 257.6 | 252.2 | 257.7 | 256.7 | 255.3 | 257.7 | 259.0 | 260.7 | 261.1 |

Note: Refer to end of table for footnotes

## TABLE B-3 (Cont)

## BERYLLIUM EFFICIENCY STUDIES

| Propellant type | VIL | VIL | VIL | VIL | VIL | VIN**** | VIN | VIN | VIN | VIO | VIO | VIO | VIG | VIG | VIG |
|---|---|---|---|---|---|---|---|---|---|---|---|---|---|---|---|
| Motor design | 15PC-2 | 15PC-1 | 15PC | 15PC | 15PC | 15PC-2 | 15PC-2 | 15PC-2 | 15PC-2 | 15PC-1 | 15PC-1 | 15PC-1 | 15PC-1 | 15PC-1 | 15PC-1 |
| Grain No. | S109B | S117B | S110B | S111B | S115B | S112B | S144B | S142B | S143B | S120B | S121B | S122 | S135B | S136B | S137B |
| Firing No. | LM2-40 | LM2-41 | LM2-42 | LM2-43 | LM2-44 | LM2-30 | LM2-58 | LM2-56 | LM2-73 | LM2-31 | LM2-51 | LM2-52 | LM2-38 | LM2-45 | LM2-46 |
| Propellant wt (lb) | 15.14 | 14.96 | 15.13 | 15.15 | 15.24 | 14.66 | 14.00 | 14.12 | 14.12 | 15.07 | 14.93 | 15.00 | 14.09 | 14.11 | 14.12 |
| Powder wt (lb) | 0.06 | 0.04 | 0.06 | 0.04 | 0.03 | 0.06 | 0.06 | 0.06 | 0.06 | 0.06 | 0.05 | 0.05 | 0.04 | 0.04 | 0.04 |
| $K\ (S/A_t)$ | 86.6 | 81.4 | 114.8 | 115.0 | 115.5 | 245.0 | 308.3 | 414.0 | 359.0 | 162.4 | 119.6 | 119.8 | 179.7 | 207.1 | 206.0 |
| $t_a$ (sec) | 1.261 | 1.648 | 1.578 | 1.565 | 1.582 | 4.931 | 4.203 | 1.900 | 2.282 | 1.163 | 1.725 | 1.866 | 2.310 | 2.032 | 2.047 |
| $t_b$ -sec | 1.109 | 1.536 | 1.509 | 1.507 | 1.522 | 4.184 | 3.885 | 1.734 | 2.084 | 1.071 | 1.636 | 1.767 | 2.192 | 1.953 | 1.966 |
| $\bar{P}_a$ (psia) | 538 | 526 | 983 | 998 | 952 | 296 | 398 | 1482 | 1085 | 1472 | 749 | 698 | 772 | 969 | 936 |
| $\bar{P}_b$ (psia) | 569 | 545 | 1008 | 1020 | 1013 | 324 | 421 | 1567 | 1142 | 1532 | 778 | 717 | 794 | 990 | 1010 |
| Pmax (psia) | 611 | 585 | 1077 | 1124 | 1097 | 406 | 576 | 1817 | 1381 | 1639 | 873 | 801 | 848 | 1096 | 1052 |
| Pamb (psia) | 12.16 | 12.18 | 12.16 | 12.24 | 12.13 | 12.27 | 12.35 | 12.28 | 12.22 | 12.14 | 12.21 | 12.17 | 12.26 | 12.21 | 12.21 |
| $\bar{r}$ (in./sec) | 0.630 | 0.657 | 0.875 | 0.876 | 0.861 | 0.792 | 0.193 | 0.421 | 0.350 | 0.943 | 0.618 | 0.574 | 0.456 | 0.512 | 0.509 |
| $\dot{w}$ (lb/sec) | 12.01 | 9.08 | 9.59 | 9.68 | 9.63 | 2.97 | 3.33 | 7.43 | 6.19 | 12.96 | 8.66 | 8.04 | 6.10 | 7.22 | 7.18 |
| $C_d$ (sec$^{-1}$) | 0.00591 | 0.00596 | 0.00598 | 0.00594 | 0.00593 | 0.00752 | 0.00786 | 0.00638 | 0.00629 | 0.00586 | 0.00569 | 0.00572 | 0.00582 | 0.00609 | 0.00609 |
| $\varepsilon\ (A_c/A_t)$ | 5.609 | 5.568 | 9.546 | 9.565 | 9.493 | 9.648 | 9.633 | 6.631 | 7.029 | 9.621 | 9.476 | 9.463 | 9.507 | 9.542 | 9.400 |
| $\bar{F}_a$ (lb$_f$) | 3008 | 2237 | 2523 | 2549 | 2548 | 597 | 710 | 1903 | 1570 | 3516 | 2223 | 2038 | 1562 | 1810 | 1740 |
| Isp del $\left(\dfrac{lb_f\text{-sec}}{lbm}\right)$ | 250.8 | 246.7 | 263.6 | 263.5 | 264.7 | 200.0 | 213.1 | 256.6 | 254.2 | 271.9 | 258.3 | 254.7 | 256.3 | 260.9 | 258.5 |
| Theoretical Isp at firing conditions | 268.1 | 265.7 | 284.5 | 284.6 | 284.7 | 235.3 | 252.4 | 282.4 | 280.0 | 291.9 | 277.8 | 275.9 | 288.0 | 293.5 | 292.8 |
| Efficiency | 93.55 | 92.85 | 92.65 | 92.59 | 92.98 | 85.3 | 84.43 | 90.80 | 90.79 | 93.15 | 92.98 | 92.32 | 88.99 | 88.89 | 88.25 |
| Isp 1000 | 263.0 | 261.0 | 260.4 | 260.3 | 261.4 | 238.9 | 236.5 | 254.4 | 254.3 | 261.9 | 261.4 | 259.5 | 258.7 | 258.4 | 256.7 |
| Isp del (c)* | 250.0 | 246.2 | 262.8 | 263.0 | 264.3 | 200.0 | 212.2 | 255.7 | 253.4 | 271.1 | 257.4 | 254.1 | 255.8 | 260.3 | 257.9 |
| Efficiency (c)* | 93.25 | 92.66 | 92.37 | 92.41 | 92.83 | 85.00 | 84.07 | 90.55 | 90.50 | 92.87 | 92.73 | 92.10 | 88.82 | 88.69 | 88.08 |
| Isp 1000 (c)* | 262.1 | 260.5 | 259.7 | 259.8 | 261.0 | 238.1 | 235.5 | 253.6 | 253.5 | 261.1 | 260.7 | 258.9 | 258.2 | 257.8 | 256.0 |

Notes: All efficiency values were calculated at the actual firing conditions.
Isp 1000 and Isp 1000 (c) values were calculated by multiplying efficiency times the theoretical Isp at standard conditions

\* Values corrected for powder embedment
** 4 second hangfire
*** Poor thrust-time trace data is questionable
**** All impulse data questionable because of possible flow separation

TABLE B-4

NOZZLE APPROACH STUDY

| | VCP | VCP | VCP | VCP | VIJ | VIJ | VIJ | VIJ | VIJ | VIJ |
|---|---|---|---|---|---|---|---|---|---|---|
| Propellant type | 15PC | 15PC | 15PC | 15PC | 15PC | 15PC | 15PC | 15PC | 15PC | 15PC |
| Motor Design | S96B | S100B | S101B | S119B | S93B | S98B | S99B | S108B | S140B | S141B |
| Grain No. | | | | | | | | | | |
| Firing No. | LM2-19* | LM2-24* | LM2-22** | LM2-37** | LM2-17* | LM2-21* | LM2-23* | LM2-20** | LM2-53** | LM2-54 |
| Propellant wt (lb) | 15.15 | 15.09 | 15.25 | 15.25 | 15.14 | 15.22 | 15.10 | 15.36 | 15.23 | 15.33 |
| Powder wt (lb) | 0.05 | 0.03 | 0.05 | 0.05 | 0.04 | 0.05 | 0.04 | 0.04 | 0.05 | 0.03 |
| $K$ (S/$A_t$) | 141.3 | 140.0 | 140.2 | 139.9 | 139.3 | 137.7 | 136.2 | 141.3 | 142.4 | 142.8 |
| $t_a$ (sec) | 1.953 | 1.975 | 1.837 | 1.890 | 1.815 | 1.903 | 1.961 | 1.833 | 1.760 | 1.784 |
| $t_b$ (sec) | 1.850 | 1.881 | 1.745 | 1.817 | 1.646 | 1.822 | 1.859 | 1.737 | 1.690 | 1.695 |
| $P_a$ (psia) | 974 | 957 | 1057 | 1046 | 1022 | 962 | 939 | 1044 | 1050 | 1055 |
| $P_b$ (psia) | 1001 | 979 | 1089 | 1068 | 1053 | 984 | 968 | 1074 | 1074 | 1088 |
| Pmax (psia) | 1054 | 1019 | 1153 | 1146 | 1138 | 1080 | 1060 | 1173 | 1198 | 1388 |
| $\bar{P}_b$ (psia) | 11.69 | 11.64 | 11.43 | 12.26 | 11.93 | 7.29 | 11.59 | 7.61 | 12.26 | 12.32 |
| $\bar{r}$ (in./sec) | 0.708 | 0.702 | 0.756 | 0.721 | 0.796 | 0.719 | 0.705 | 0.754 | 0.775 | 0.779 |
| $\dot{m}$ (lb/sec) | 7.76 | 7.64 | 8.30 | 8.07 | 8.34 | 8.00 | 7.70 | 8.38 | 8.65 | 8.59 |
| $c^*_d$ (sec$^{-1}$) | 0.00595 | 0.00592 | 0.00583 | 0.00568 | 0.00611 | 0.00612 | 0.00604 | 0.00600 | 0.00611 | 0.00613 |
| $\varepsilon$ ($A_e/A_t$) | 9.626 | 9.599 | 9.555 | 9.507 | 9.633 | 9.411 | 9.551 | 9.544 | 9.451 | 9.414 |
| $F_a$ (lb$_f$) | 2056 | 2022 | 2204 | 2162 | 2200 | 2168 | 2029 | 2278 | 2261 | 2268 |
| Isp del $\left(\dfrac{\text{lb}_f\text{-sec}}{\text{lbm}}\right)$ | 265.2 | 265.0 | 265.7 | 267.8 | 264.0 | 271.5 | 263.7 | 272.2 | 261.6 | 264.2 |
| Theoretical Isp at firing conditions | 286.9 | 286.6 | 288.9 | 287.3 | 281.9 | 288.0 | 280.6 | 288.8 | 281.7 | 281.8 |
| Efficiency | 92.44 | 92.46 | 91.97 | 93.21 | 93.65 | 94.27 | 93.98 | 94.25 | 92.87 | 93.75 |
| Isp 15 1000 | 261.6 | 261.7 | 260.3 | 263.8 | 259.8 | 261.5 | 260.7 | 261.5 | 257.6 | 260.1 |
| Isp del (c)* | 264.6 | 264.6 | 265.0 | 267.2 | 263.5 | 270.8 | 263.2 | 271.7 | 260.9 | 263.8 |
| Efficiency (C)* | 92.23 | 92.32 | 91.72 | 93.00 | 93.47 | 94.03 | 93.80 | 94.08 | 92.62 | 93.61 |
| Isp 15 1000 (c)* | 261.0 | 261.3 | 259.6 | 263.2 | 259.3 | 260.8 | 260.2 | 261.0 | 256.9 | 259.7 |

Notes:   *5° Approach
**15° Approach
Firing LM2-18 suffered a case burnthrough and all data was lost.
All efficiency values were calculated at the actual firing conditions.
Isp 15 1000 and Isp 15 1000 (c) values were calculated by multiplying efficiency times the theoretical Isp at standard conditions.

## TABLE B-5

## AP PARTICLE SIZE STUDY

| Propellant type | VIJ-5021 | VIJ-5021 | VIJ-5021 | VIJ-5061 | VIJ-5061 |
|---|---|---|---|---|---|
| Motor Design | 15PC-1 | 15PC-1 | 15PC-1 | 15PC | 15PC |
| Grain No. | S123B | S124B | S125B | S126B | S128B |
| Firing No. | LM2-32 | LM2-33 | LM2-34 | LM2-35 | LM2-59 |
| Propellant wt (lb) | 15.10 | 15.07 | 15.16 | 15.36 | 14.27 |
| Powder wt (lb) | 0.05 | 0.05 | 0.05 | 0.04 | 0.05 |
| $K$ $(S/A_t)$ | 167.2 | 179.7 | 181.5 | 97.3 | 109.4 |
| $t_a$ (sec) | 2.343 | 2.053 | 2.305 | 1.717 | 1.427 |
| $t_b$ (sec) | 2.224 | 1.902 | 2.305 | 1.649 | 1.314 |
| $\bar{P}_a$ (psia) | 736 | 896 | 785 | 756 | 968 |
| $\bar{P}_b$ (psia) | 757 | 932 | 811 | 774 | 1014 |
| $\bar{P}max$ (psia) | 846 | 1065 | 911 | 838 | 1117 |
| $\bar{P}amb$ (psia) | 12.22 | 12.27 | 12.27 | 12.16 | 12.32 |
| $\bar{r}$ (in./sec) | 0.450 | 0.531 | 0.465 | 0.800 | 0.997 |
| $\dot{m}$ (lb/sec) | 6.45 | 7.34 | 6.58 | 8.95 | 10.0 |
| $C_d$ (sec $^{-1}$) | 0.00602 | 0.00607 | 0.00620 | 0.00609 | 0.00605 |
| $\epsilon$ $(A_e/A_t)$ | 9.573 | 9.527 | 9.555 | 9.243 | 9.520 |
| $\bar{F}_a$ $(lb_f)$ | 1637 | 1892 | 1659 | 2279 | 2637 |
| Isp del $\left(\dfrac{lb_f\text{-sec}}{lbm}\right)$ | 254.2 | 257.9 | 252.1 | 255.0 | 264.0 |
| Theoretical Isp at firing conditions | 273.2 | 278.3 | 275.0 | 274.2 | 281.0 |
| Efficiency | 92.98 | 92.67 | 91.67 | 93.00 | 93.95 |
| Isp $^{15}_{1000}$ | 257.9 | 257.1 | 254.3 | 258.0 | 260.6 |
| Isp del (c)* | 253.5 | 257.2 | 251.4 | 254.4 | 263.3 |
| Efficiency (c)* | 92.72 | 92.42 | 91.42 | 92.78 | 93.70 |
| Isp $^{15}_{1000}$ (c)* | 257.2 | 256.4 | 253.6 | 257.4 | 259.9 |

Notes: VIJ-5021 contains $180\mu$ AP, VIJ-5061 contains $45\mu$ AP
All efficiency values were calculated at the actual firing conditions.

Isp$^{15}_{1000}$ and Isp $^{15}_{1000}$ (c) values were calculated by multiplying efficiency times the theoretical Isp at standard conditions.
*Values corrected for powder embedment

TABLE B-6

HIGH L* BERYLLIUM FIRINGS

| Propellant Type | VCP | VCP | VII | VII |
|---|---|---|---|---|
| Motor Design | 15PC | 15PC | 15PC-1 | 15PC-1 |
| Grain No. | S118B | S113B | S160B | S161B |
| Firing No. | LM2-57 | LM2-66 | LM2-67 | LM2-68 |
| Propellant wt (lb) | 15.17 | 15.38 | 14.63 | 14.62 |
| Powder wt (lb) | 0.04 | 0.04 | 0.03 | 0.03 |
| K (S/A) | 142.2 | 143.9 | 203.2 | 206.5 |
| $L*$ $(V_F/A_t)$ | 440 | 450 | 390 | 390 |
| $t_a$ (sec) | 1.885 | 1.955 | 2.190 | 2.173 |
| $t_b$ (sec) | 1.787 | 1.834 | 2.071 | 1.970 |
| $\overline{P}_a$ (psia) | 1063 | 1013 | 895 | 945 |
| $\overline{P}_b$ (psia) | 1094 | 1049 | 922 | 992 |
| $\overline{P}max$ (psia) | 1165 | 1154 | 1043 | 1142 |
| $\overline{P}amb$ (psia) | 12.29 | 12.24 | 12.04 | 12.23 |
| $\overline{r}$ (in./sec) | 0.738 | 0.714 | 0.488 | 0.513 |
| $\dot{m}$ (lb/sec) | 8.05 | 7.87 | 6.68 | 6.73 |
| $C_d$ $(sec^{-1})$ | 0.0057 | 0.00585 | 0.00624 | 0.00605 |
| $\epsilon$ $(A_e/A_t)$ | 9.631 | 9.586 | 9.274 | 9.386 |
| $\overline{F}_a$ $(lb_f)$ | 2136 | 2065 | 1719 | 1733 |
| Isp del $\left(\dfrac{lb_f\text{-sec}}{lbm}\right)$ | 265.6 | 262.8 | 258.0 | 257.8 |
| Theoretical Isp at firing conditions | 287.7 | 286.8 | 280.0 | 280.9 |
| Efficiency, Eff | 92.32 | 91.63 | 92.14 | 91.78 |
| $Isp^{15}_{1000}$ | 261.3 | 259.3 | 256.8 | 255.8 |
| Isp del (c)* | 265.1 | 262.3 | 257.6 | 257.4 |
| Efficiency (c)* | 92.14 | 91.46 | 92.00 | 91.63 |
| $Isp^{15}_{1000}$ (c)* | 260.8 | 258.8 | 256.4 | 255.4 |

*Values corrected for powder embedment

Notes:  All efficiency values were calculated at the actual firing conditions.

$Isp^{15}_{1000}$ and $Isp^{15}_{1000}$ (c) values were calculated by multiplying efficiency times the theoretical Isp at firing conditions.

TABLE B-7

VCP FINAL CHARACTERIZATION FIRINGS

| Propellant Type | VCP | VCP | VCP | VCP |
|---|---|---|---|---|
| Motor Design | 15PC-1 | 15PC-1 | 15PC | 15PC |
| Grain No. | S83B | S145B | S138B | S77B |
| Firing No. | LM2-90 | LM2-91 | LM2-88 | LM2-89 |
| Propellant wt (lb) | 14.79 | 14.99 | 15.27 | 15.09 |
| Powder wt (lb) | 0.04 | 0.04 | 0.04 | 0.05 |
| $K$ $(S/A_t)$ | 103.6 | 103.8 | 141.6 | 141.7 |
| $t_a$ (sec) | 1.886 | 2.172 | 1.972 | 1.794 |
| $t_b$ (sec) | 1.793 | 2.076 | 1.878 | 1.709 |
| $\bar{P}_a$ (psia) | 571 | 509 | 989 | 1064 |
| $\bar{P}_b$ (psia) | 583.5 | 515 | 1013 | 1090 |
| $\bar{P}max$ (psia) | 650 | 570 | 1090 | 1165 |
| $\bar{P}amb$ (psia) | 12.51 | 12.10 | 12.19 | 12.25 |
| $r$ (in./sec) | 0.558 | 0.486 | 0.697 | 0.767 |
| $\dot{m}$ (lb/sec) | 7.84 | 6.90 | 7.74 | 8.41 |
| $C_d$ $(sec^{-1})$ | 0.00582 | 0.00576 | 0.00584 | 0.00586 |
| $\epsilon$ $(A_e/A_t)$ | 5.658 | 5.694 | 9.521 | 9.520 |
| $\bar{F}_a$ $(lb_f)$ | 1961 | 1698 | 2041 | 2220 |
| Isp del $\left(\dfrac{lb_f\text{-sec}}{lbm}\right)$ | 250.2 | 246.1 | 263.8 | 264.2 |
| Theoretical Isp at firing conditions | 268.3 | 266.4 | 286.2 | 287.6 |
| Efficiency, Eff | 93.25 | 92.38 | 92.17 | 91.86 |
| $Isp^{15}_{1000}$ | 263.9 | 261.4 | 260.8 | 260.0 |
| Isp del (c)* | 249.6 | 245.6 | 263.3 | 263.5 |
| Efficiency (c)* | 93.03 | 92.19 | 92.00 | 91.62 |
| $Isp^{15}_{1000}$ (c)* | 263.3 | 260.9 | 260.4 | 259.3 |

*Values corrected for powder embedment

Notes: All efficiency values are calculated at the actual firing conditions.

$Isp^{15}_{1000}$ and $Isp^{15}_{1000}$ (c) values were calculated by multiplying efficiency times the theoretical Isp at firing conditions.

TABLE B-8

L* STUDY FOR LMH-2 PROPELLANTS

| Propellant Type | VIY* | VIY* | VIY* | VIY* | VIY** | VIY** | VIY** | VIY** | VIY** |
|---|---|---|---|---|---|---|---|---|---|
| Motor | 15PC | 15PC | 15PC | 15PC | 15PC | 15PC | 15PC | 15PC | 15PC |
| Grain No. | S152BH | S156BH | S151BH | S157BH | S150BH | S154BH | S153BH | S155BH | S156BH |
| Firing No. | LM2-61 | LM2-64 | LM2-63 | LM2-70 | LM2-50 | LM2-65 | LM2-62 | LM2-69 | LM2-78 |
| Propellant Wt (lb) | 11.79 | 11.44 | 11.48 | 11.39 | 11.34 | 11.32 | 11.56 | 11.40 | 11.45 |
| Powder Wt (lb) | 0.05 | 0.05 | 0.04 | 0.05 | 0.05 | 0.05 | 0.04 | 0.05 | 0.04 |
| $K$ $(S/A_t)$ | 127.3 | 110.8 | 112.4 | 110.6 | 100.2 | 122.1 | 122.1 | 121.9 | 116.9 |
| $L*$ $(V_F/A_t)$ | 133 | 158 | 330 | 294 | 112 | 178 | 325 | 328 | 315 |
| $t_a$ (sec) | 1.199 | 1.163 | 1.052 | 1.229 | 1.690 | 1.595 | 1.561 | 1.567 | 1.521 |
| $t_b$ (sec) | 1.106 | 1.044 | 0.943 | 1.090 | 1.592 | 1.399 | 1.437 | 1.436 | 1.370 |
| $\overline{P}_a$ (psia) | 1192 | 1042 | 1294 | 1033 | 671 | 835 | 873 | 881 | 897 |
| $\overline{P}_b$ (psia) | 1245 | 1100 | 1376 | 1100 | 695 | 884 | 920 | 924 | 946 |
| $\overline{P}$max (psia) | 1355 | 1246 | 1571 | 1241 | 749 | 953 | 1054 | 995 | 1024 |
| $\overline{P}$amb (psia) | 12.29 | 12.08 | 12.24 | 12.25 | 12.27 | 12.07 | 12.01 | 12.25 | 12.22 |
| $\overline{r}$ (in./sec) | 1.166 | 1.254 | 1.389 | 1.183 | 0.823 | 0.936 | 0.912 | 0.905 | 0.949 |
| $\dot{m}$ (lb/sec) | 9.83 | 9.84 | 10.91 | 9.27 | 6.71 | 8.09 | 7.41 | 7.28 | 7.53 |
| $C_d$ $(sec^{-1})$ | 0.00556 | 0.00553 | 0.00546 | 0.00525 | 0.00530 | 0.00552 | 0.00542 | 0.00533 | 0.00519 |
| $\epsilon(A_e/A_t)$ | 9.663 | 9.462 | 9.644 | 9.466 | 7.446 | 9.626 | 9.629 | 9.595 | 9.189 |
| $\overline{F}_a$ $(lb_f)$ | 2778 | 2778 | 3149 | 2647 | 1822 | 1993 | 2097 | 2039 | 2128 |
| Isp del $\frac{lb_f\text{-sec}}{lbm}$ | 283.2 | 282.8 | 289.4 | 286.2 | 271.5 | 279.7 | 283.7 | 280.5 | 283.4 |
| Theoretical Isp at firing conditions | 316.6 | 313.7 | 317.8 | 313.1 | 300.0 | 308.5 | 309.6 | 309.5 | 309.7 |
| Efficiency, Eff | 89.45 | 90.15 | 91.06 | 91.41 | 90.50 | 90.67 | 91.63 | 90.63 | 91.51 |
| $Isp_{1000}^{15}$ | 276.3 | 278.5 | 281.3 | 282.4 | 279.6 | 280.1 | 283.0 | 280.0 | 282.7 |
| Isp del (c)*** | 282.3 | 281.9 | 288.7 | 285.3 | 270.6 | 278.8 | 283.0 | 279.6 | 282.7 |
| Efficiency (c)*** | 89.16 | 89.86 | 90.84 | 91.12 | 90.20 | 90.37 | 91.41 | 90.34 | 91.28 |
| $Isp_{1000}^{15}$ (c)*** | 275.4 | 277.6 | 280.6 | 281.5 | 278.6 | 279.2 | 282.4 | 279.1 | 282.0 |

*Contains AP-treated LMH-2

**Contains Wax-treated LMH-2

***Values corrected for powder embedment

Notes: All efficiency values were calculated at the actual firing conditions.

$Isp_{1000}^{15}$ and $Isp_{1000}^{15}$ (c) values were calculated by multiplying efficiency times the theoretical Isp at firing conditions

TABLE B-9

LMH-2/AP FIRINGS

| Propellant Type | VIX | VIX | VIX | VIZ | VIZ | VIZ |
|---|---|---|---|---|---|---|
| Motor Design | 15PC | 15PC | 15PC | 15PC | 15PC | 15PC |
| Grain No. | S162BH | S163BH | S164BH | S171BH | S172BH | S173BH |
| Firing No. | LM2-71 | 2-72 | 2-75 | LM2-79 | LM2-80 | LM2-81 |
| Propellant Wt (lb) | 11.55 | 11.74 | 11.69 | 10.97 | 11.08 | 11.29 |
| Powder Wt (lb) | 0.05 | 0.05 | 0.05 | 0.05 | 0.05 | 0.05 |
| $K$ $(S/A_t)$ | 117.8 | 120.1 | 121.7 | 144.6 | 140.0 | 135.7 |
| $t_a$ (sec) | 1.309 | 1.404 | 1.401 | 1.480 | 1.430 | 1.384 |
| $t_b$ (sec) | 1.160 | 1.307 | 1.286 | 1.381 | 1.332 | 1.283 |
| $\overline{P}_a$ (psia) | 1055 | 1006 | 1007 | 1016 | 1076 | 1110 |
| $\overline{P}_b$ (psia) | 1121 | 1046 | 1052 | 1060 | 1124 | 1156 |
| $\overline{P}max$ (psia) | 1268 | 1141 | 1138 | 1188 | 1215 | 1250 |
| $\overline{P}amb$ (psia) | 12.23 | 12.29 | 12.16 | 12.22 | 12.26 | 12.22 |
| $\overline{r}$ (in./sec) | 1.112 | 0.995 | 1.011 | 0.941 | 0.976 | 1.021 |
| $\dot{m}$ (lb/sec) | 8.82 | 8.36 | 8.34 | 7.41 | 7.75 | 8.16 |
| $C_d$ $(sec^{-1})$ | 0.00524 | 0.00529 | 0.00531 | 0.00558 | 0.00533 | 0.00528 |
| $\epsilon(A_e/A_t)$ | 9.426 | 9.486 | 9.553 | 9.740 | 9.473 | 9.199 |
| $\overline{F}_a$ $(lb_f)$ | 2509 | 2370 | 2379 | 2122 | 2220 | 2345 |
| Isp del $\dfrac{lb_f\text{-sec}}{lbm}$ | 284.9 | 283.9 | 285.7 | 286.6 | 287.1 | 288.2 |
| Theoretical Isp at firing conditions | 308.5 | 307.4 | 307.7 | 318.2 | 319.1 | 319.4 |
| Efficiency, Eff | 92.35 | 92.38 | 92.85 | 90.07 | 89.97 | 90.23 |
| $Isp^{15}_{1000}$ | 280.5 | 280.5 | 282.0 | 282.6 | 282.3 | 283.1 |
| Isp del (c)* | 284.0 | 283.0 | 284.9 | 285.7 | 286.2 | 287.3 |
| Efficiency (c)* | 92.06 | 92.06 | 92.59 | 89.79 | 89.69 | 89.95 |
| $Isp^{15}_{1000}$ (c)* | 279.6 | 279.6 | 281.2 | 281.8 | 281.5 | 282.3 |

*Values corrected for powder embedment

Notes: All efficiency values were calculated at the actual firing conditions.

$Isp^{15}_{1000}$ and $Isp^{15}_{1000}$ values were calculated by multiplying efficiency times the theoretical Isp at firing conditions.

TABLE B-10

LMH-2/HMX FIRINGS

| Propellant Type | VJA | VJA | VJA | VJI | VJI | VJI | VJL | VJL | VJL |
|---|---|---|---|---|---|---|---|---|---|
| Motor Design | 15PC-1 | 15PC-1 | 15PC-1 | 15PC | 15PC | 15PC | 15PC | 152C | 15PC |
| Grain No. | S165BH | S166BH | S167BH | S176BH | S177BH | S178BH | S180BH | S181BH | S179BH |
| Firing No. | LM2-74 | LM2-76 | LM2-77 | LM2-82 | LM2-83 | LM2-84 | LM2-86 | LM2-87 | LM2-85 |
| Propellant wt (lb) | 11.46 | 11.39 | 11.50 | 11.45 | 11.56 | 11.63 | 11.32 | 11.32 | 11.41 |
| Powder wt (lb) | 0.05 | 0.04 | 0.04 | 0.28 | 0.27 | 0.20 | 0.06 | 0.05 | 0.06 |
| $K$ $(S/A_t)$ | 126.8 | 142.2 | 136.2 | 149.0 | 150.4 | 156.3 | 109.3 | 130.0 | 132.1 |
| $t_a$ (sec) | 1.530 | 1.409 | 1.428 | 1.501 | 1.499 | 1.455 | 1.832 | 1.674 | 1.630 |
| $t_b$ (sec) | 1.515 | 1.328 | 1.342 | 1.391 | 1.416 | 1.355 | 1.549 | 1.552 | 1.500 |
| $\bar{P}_a$ (psia) | 752.4 | 898 | 886 | 842 | 857 | 922 | 683 | 889 | 948 |
| $\bar{P}_b$ (psia) | 759 | 928 | 915 | 879 | 886 | 962 | 724 | 931 | 993 |
| Pmax (psia) | 866 | 1032 | 1015 | 934 | 954 | 1038 | 797 | 1013 | 1090 |
| $\bar{P}_{amb}$ (psia) | 12.23 | 12.17 | 12.32 | 12.19 | 12.23 | 12.18 | 12.26 | 12.22 | 12.18 |
| $\bar{r}$ (in./sec) | 0.647 | 0.745 | 0.738 | 0.719 | 0.706 | 0.738 | 0.794 | 0.844 | 0.867 |
| $\dot{m}$ (lb/sec) | 7.49 | 8.08 | 8.05 | 7.63 | 7.71 | 7.99 | 6.18 | 6.76 | 7.00 |
| $C_d$ $(sec^{-1})$ | 0.00517 | 0.00527 | 0.00507 | 0.00553 | 0.00555 | 0.00555 | 0.00527 | 0.00529 | 0.00519 |
| $\epsilon$ $(A_e/A_t)$ | 9.309 | 9.558 | 0.944 | 9.53 | 9.62 | 9.57 | 9.451 | 9.951 | 8.469 |
| $\bar{F}_a$ $(lb_f)$ | 2074 | 2281 | 2273 | 2080 | 2080 | 2164 | 1667 | 1876 | 1976 |

TABLE B-10 (Cont)

LMH-2/HMX FIRINGS

| Propellant Type | VJA | VJA | VJA | VJI | VJI | VJI | VJL | VJL | VJL |
|---|---|---|---|---|---|---|---|---|---|
| Isp del $\left(\dfrac{lb_f\text{-sec}}{lbm}\right)$ | 277.5 | 282.9 | 282.8 | 272.9 | 270.5 | 271.5 | 270.2 | 277.8 | 282.6 |
| Theoretical Isp at firing conditions | 305.7 | 310.6 | 309.6 | 312.40 | 312.9 | 314.8 | 306.0 | 314.1 | 314.2 |
| Efficiency, Eff | 90.78 | 91.08 | 91.34 | 87.36 | 86.46 | 86.24 | 88.30 | 88.44 | 89.97 |
| $Isp^{15}_{1000}$ | 280.8 | 281.7 | 282.5 | 274.3 | 271.5 | 270.8 | 276.1 | 276.6 | 281.4 |
| Isp del (c)* | 276.7 | 282.2 | 282.1 | 271.9 | 269.4 | 270.6 | 269.1 | 276.9 | 281.6 |
| Efficiency (c)* | 90.51 | 90.86 | 91.12 | 87.04 | 86.10 | 85.96 | 87.94 | 88.16 | 89.62 |
| $Isp^{15}_{1000}$ (c)* | 280.0 | 281.0 | 281.8 | 273.3 | 270.4 | 269.9 | 275.0 | 275.7 | 280.2 |

*Values corrected for powder embedment

Notes: All efficiency values were calculated at the actual firing conditions.

$Isp^{15}_{100}$ and $Isp^{15}_{1000}$ values were calculated by multiplying efficiency times the theoretical Isp at firing conditions.

TABLE 3-11

VIY FINAL CHARACTERIZATION FIRINGS

| Propellant Type | VIY | VIY | VIY | VIY | VIY |
|---|---|---|---|---|---|
| Motor Design | 15PC | 15PC | 15PC | 15PC | 15PC |
| Grain No. | S183BH | S185BH | S184BH | S186BH | S187BH |
| Firing No. | LM2-92 | LM2-94 | LM2-93 | LM2-95 | LM2-96 |
| Propellant wt (lb) | 11.76 | 11.68 | 11.65 | 11.62 | 11.65 |
| Powder wt (lb) | 0.04 | 0.03 | 0.04 | 0.03 | 0.03 |
| $K$ $(S/A_t)$ | 91.0 | 93.6 | 145.7 | 144.6 | 143.5 |
| $t_a$ (sec) | 1.619 | 1.676 | 1.305 | 1.319 | 1.303 |
| $t_b$ (sec) | 1.495 | 1.593 | 1.208 | 1.230 | 1.212 |
| $\bar{P}_a$ (psia) | 655 | 627 | 1305 | 1285 | 1280 |
| $\bar{P}_b$ (psia) | 681 | 645 | 1356 | 1333 | 1328 |
| $\bar{P}max$ (psia) | 743 | 704 | 1474 | 1440 | 1430 |
| $\bar{P}amb$ (psia) | 12.26 | 12.19 | 12.27 | 12.17 | 12.09 |
| $\bar{r}$ (in./sec) | 0.883 | 0.822 | 1.093 | 1.065 | 1.089 |
| $\dot{m}$ (lb/sec) | 7.208 | 6.968 | 8.927 | 8.809 | 8.979 |
| $C_d$ $(sec^{-1})$ | 0.00528 | 0.00533 | 0.00527 | 0.00524 | 0.00530 |
| $\epsilon (A_e/A_t)$ | 5.622 | 5.622 | 9.507 | 9.52 | 9.422 |
| $\bar{F}_e$ $(lb_f)$ | 1929 | 1847 | 2589 | 2555 | 2584 |
| Isp del $\left(\dfrac{lb_f\text{-sec}}{lbm}\right)$ | 267.9 | 265.3 | 290.7 | 290.3 | 289.4 |
| Theoretical Isp at firing conditions | 296.0 | 295.2 | 317.9 | 317.8 | 317.6 |
| Efficiency, Eff | 90.51 | 89.87 | 91.44 | 91.35 | 91.12 |
| $Isp^{15}_{1000}$ | 279.6 | 277.6 | 282.5 | 282.2 | 282.3 |
| Isp del (c)* | 267.2 | 264.8 | 290.0 | 289.8 | 289.0 |
| Efficiency (c)* | 90.27 | 89.70 | 91.22 | 91.19 | 90.99 |
| $Isp^{15}_{1000}$ (c)* | 278.8 | 277.1 | 281.8 | 281.7 | 281.1 |
| L* | 334 | 3 | 318 | 315 | 313 |

*Values corrected for powder emb  ent.

Notes:  All efficiency values were calculated at the actual firing conditions.

$Isp^{15}_{1000}$ and $Isp^{15}_{1000}$ (c) values were calculated by multiplying efficiency times the theoretical Isp at firing conditions.

TABLE B-12

VJA FINAL CHARACTERIZATION FIRINGS

| Propellant Type | VJA | VJA | VJA | VJA | VJA | VJA |
|---|---|---|---|---|---|---|
| Motor Design | 15PC-1 | 15PC-1 | 15PC-1 | 15PC | 15PC | 15PC |
| Grain No. | S188BH | S189BH | S190BH | S191BH | S192BH | S193BH |
| Firing No. | IM2-97 | IM2-98 | IM2-99 | IM2-100 | IM2-101 | IM2-102 |
| Propellant wt (lb) | 11.87 | 11.85 | 11.86 | 12.07 | 12.07 | 12.05 |
| Powder wt (lb) | 0.04 | 0.04 | 0.03 | 0.04 | 0.04 | 0.03 |
| $K$ $(S/A_t)$ | 117.3 | 116.9 | 116.4 | 156.5 | 154.2 | 155.2 |
| $t_a$ (sec) | 1.641 | 1.652 | 1.645 | 1.701 | 1.714 | 1.667 |
| $t_b$ (sec) | 1.523 | 1.540 | 1.577 | 1.587 | 1.643 | 1.572 |
| $\bar{P}_a$ (psia) | 658 | 655 | 658 | 1137 | 1127 | 1156 |
| $\bar{P}_b$ (psia) | 682 | 678 | 672 | 1176 | 1154 | 1191 |
| $\bar{P}max$ (psia) | 75 | 763 | 743 | 1285 | 1270 | 1304 |
| $\bar{P}amb$ (psia) | 12.15 | 11.85 | 12.32 | 12.28 | 12.22 | 12.22 |
| $\bar{r}$ (in./sec) | 0.656 | 0.656 | 0.634 | 0.832 | 0.803 | 0.883 |
| $\dot{m}$ (lb/sec) | 7.233 | 7.173 | 7.209 | 7.09 | 7.042 | 7.228 |
| $C_d$ $(sec^{-1})$ | 0.00530 | 0.00527 | 0.00525 | 0.00517 | 0.00509 | 0.00513 |
| $\epsilon$ $(A_e/A_t)$ | 5.72 | 5.664 | 5.637 | 9.520 | 9.364 | 9.588 |
| $\bar{F}_a$ $(lb_f)$ | 1947 | 1922 | 1933 | 2010 | 1997 | 2055 |
| Isp del $\left(\dfrac{lb_f\text{-sec}}{lbm}\right)$ | 269.5 | 268.2 | 268.3 | 283.6 | 284.1 | 285.0 |
| Theoretical Isp at firing conditions | 297.9 | 297.0 | 297.4 | 315.9 | 315.7 | 316.4 |
| Efficiency, Eff | 90.47 | 90.30 | 90.22 | 89.78 | 89.99 | 90.08 |
| $Isp^{15}_{1000}$ | 279.8 | 279.3 | 279.0 | 277.6 | 278.3 | 278.4 |
| Isp del (c)* | 268.9 | 267.5 | 267.8 | 282.9 | 283.4 | 284.5 |
| Efficiency (c)* | 90.27 | 90.07 | 90.05 | 89.55 | 89.77 | 89.92 |
| $Isp^{15}_{1000}$ (c)* | 279.2 | 278.6 | 278.5 | 277.0 | 277.7 | 278.1 |
| $\Gamma$* | 337 | 336 | 334 | 347 | 342 | 344 |

*Values corrected for powder embedment

Notes: All efficiency values were calculated at the actual firing conditions.

$Isp^{15}_{1000}$ and $Isp^{15}_{1000}$ (c) values were calculated by multiplying efficiency times the theoretical Isp at firing conditions.